August 2020

Thermoelectrics: Ecological Profile and Fundamental Principles for Sustainability

Rakesh Krishnamoorthy Iyer
Clemson University, rakesh.k.iyer.88@gmail.com

THERMOELECTRICS: ECOLOGICAL PROFILE AND FUNDAMENTAL PRINCIPLES FOR SUSTAINABILITY

A Dissertation
Presented to
the Graduate School of
Clemson University

In Partial Fulfillment
of the Requirements for the Degree
Doctor of Philosophy
Automotive Engineering

---

by
Rakesh Krishnamoorthy Iyer
August 2020

Accepted by:
Dr. Srikanth Pilla, Committee Chair
Dr. Zoran Filipi
Dr. Chris Paredis
Dr. Terry M. Tritt
Dr. Michael Carbajales-Dale

ABSTRACT

The need for efficient energy conversion and utilization has magnified on account of global environmental concerns, leading to a dramatic rise in focus on technologies that can accomplish such enhanced efficiencies. In this context, thermoelectrics (TEs) have emerged as a prominent platform on account of rigorous research that has enabled a significant leap in their conversion efficiencies, which enhances their potential to lower fossil fuel consumption. However, the advent of novel TEs has been accompanied by growing concerns about the use of scarce and toxic constituent elements in most of these materials/systems, raising questions about their eco-friendliness. While these concerns must be suitably addressed, the very nature of looking at TEs solely in terms of either benefits during their usage, or at issues with their constituents, confines the notion of sustainability to one or few stages of their life cycle. This creates doubts about the traditional claims of TEs being ecofriendly, since other environmental issues associated with their life cycle, such as impacts caused by their production or end-of-life treatment, remain neglected. These gaps hinder a true assessment of ecological credentials of TEs as an energy harvesting platform, and also make it difficult to provide adequate directions to policymakers and other stakeholders on the nature of steps required to make this platform ecologically suitable and economically viable.

To ameliorate these gaps, this work explores the environmental profile of TEs using life cycle assessment (LCA). TE devices – modules and generators – were evaluated for environmental performance across their life cycle for three applications differing in their nature of waste heat emission and mobility. These were: (a) baseload coal-based power

plant (static, constant emission); (b) peak load natural gas-based power plants (static, periodic emission); and (c) automobiles (mobile, intermittent emission). For all end-uses, TEs were assessed on various impacts. The *first-ever exhaustive inventory analysis to date* was conducted for production of TE devices, while three end-of-life (EOL) scenarios were considered to determine the benefits and pitfalls of recycling TEs as these use scarce constituents. Subsequently, the results from these LCA analyses were used to distill key findings and postulate principles for developing sustainable thermoelectrics.

LCA analysis of TEs showed that both high electricity consumption for TE processing and use of constituent elements that emit toxic waste during their extraction and refining, caused the bulk of their production-related impacts. Further, while TE devices were observed to be environmentally sound for applications involving continuous waste heat emission (coal-based power), they showed ineffectiveness for periodic (gas-based electricity) and intermittent waste heat emission (automobiles) to varying degrees. In addition, recycling of TEs was seen to have moderate influence on their ecological output, with heat exchanger-based components playing a more significant role. Lastly, using the results from LCA analyses, *eight sustainability principles were postulated* for TEs encompassing their entire life cycle, that can guide policymakers to work with other stakeholders on enhancing overall eco-friendliness of this platform.

ACKNOWLEDGMENTS

First, I would like to express my deep sense of gratitude and sincere thanks to my research advisor, Dr. Srikanth Pilla, for providing me valuable and inspiring guidance throughout the duration of my research at CU-ICAR. I am grateful to him for the motivation and encouragement he has shown towards me at every step of my research, without which this work would not have been possible. I would also like to sincerely thank all my committee members – Dr. Chris Paredis, Dr. Michael Carbajales-Dale, Dr. Zoran Filipi and Dr. Terry M. Tritt – for their research insights, support, motivation and encouragement they provided to me throughout the entirety of my research. Also, as I complete this dissertation, I would like to extend my sincere thanks to all responsible here at CU-ICAR and at Clemson University for having financially supported my studies here, without which it would not have been possible for me to pursue research.

Special thanks are also reserved in particular to Kousaalya Bakthavatchalam – my life partner and an ex-research group colleague – and Sai Aditya Pradeep (PhD student under Dr. Pilla) who have been immense sources of support as friends and colleagues. I am especially indebted to Kousaalya who has constantly motivated me throughout my research journey, especially at moments where I have felt quite frustrated on personal or professional fronts and helped me to build a strong foundation for my future. Additionally, I am also thankful to Harikesh Arunachalam – a friend and former PhD graduate from CU-ICAR – who has helped me at critical moments during my stay in the US on personal and professional aspects. I am also grateful to all teachers at CU-ICAR and Clemson University who have helped me in pursuit of knowledge on other aspects related to thermoelectrics and even general life-lessons, which I believe will enable me to become a more strong-footed professional academic in future.

Last, but probably the most important, I wish to take this opportunity to acknowledge my deepest sense of gratitude to those without whom this journey would never have been possible: my family that is currently based in India. I am indebted to both my parents and my sister who have constantly motivated me towards pursuing higher education by making me aware of its importance at a very young age, and I am continuing to bear the good fruits of this approach as I complete this dissertation, and hopefully will continue to do so later in my life.

TABLE OF CONTENTS

LIST OF ABBREVATIONS

Abbreviation	Full Form
1,4-DCB	1,4-Dichlorobenzene
AWG	American wire gage
BT	Bismuth-telluride
CBE	Coal-based electricity
CE-scenario	Circular economy scenario
CL	Clathrates
CHP	Combined heat-and-power
CWS	Compaction-with-sintering
D-scenario	Disposal scenario
EOL	End-of-life
EPA	(United States) Environmental Protection Agency
FE	Fuel economy
FET	Freshwater ecotoxicity
FRS	Fossil resource scarcity
FTP-72	Federal test procedure
GHG	Greenhouse gas(es)
GW	Global warming
HCT	Human carcinogenic toxicity
HH	Half-Heusler
HNT	Human non-carcinogenic toxicity
HWFET	Highway fuel economy test cycle
IPCC	Intergovernmental Panel on Climate Change
ISO	International Organization for Standardization
LAST	Lead antimony silver telluride
LCA	Life cycle assessment

LDE	Leg dicing efficiency
MET	Marine ecotoxicity
MRS	Mineral resource scarcity
MS	Magnesium silicide (Mg_2Si)
NG	Natural gas
ORG	Organic (thermoelectrics)
OX	Oxides
P-scenario	Practical scenario
PT	Lead-telluride
PV	Photovoltaic
SBE	Solar-based electricity
SC	Silicides
SK	Skutterudite
SLS	Selective laser sintering
SPS	Spark plasma sintering
SS	Stainless steel
TAGS	Tellurium antimony germanium silver (Te/Sb/Ge/Ag)
TCRC	Thermal cycling reduction coefficient
TE	Thermoelectric
TEG	Thermoelectric generator
TET	Terrestrial ecotoxicity
TTW	Tank-to-Wheel efficiency
UDDS	Urban dynamometer driving schedule
UNEP	United Nations Environment Programme
US DoE	United States Department of Energy
WBE	Wind-based electricity
ZP	Zintl phases
ZT	Thermoelectric figure of merit

LIST OF TABLES

LIST OF FIGURES

CHAPTER ONE

INTRODUCTION

1. Thermoelectrics: An Introduction & Literature Review

1.1. Thermoelectrics: The Context

Efficient energy conversion and utilization has been a long-held imperative for numerous sectors, principally guided by concerns about substantial energy costs, scarcity of fossil fuels, and notions of energy security[1–7]. These concerns have compounded in recent years with the advent of climate change as a pernicious threat to sustainable and healthy existence of all living forms, an aspect highlighted yet again in the recent IPCC report[8]. This has led to the development, promotion and application of several energy conversion, harvesting and storage technologies[4,5,9–13]. Among these, thermoelectrics (TEs) have surfaced as an important energy harvesting platform, particularly over the past few decades, on account of the large amounts of waste heat generated across multiple sectors[14–19]. Initially discovered in the early 1800s[20], TEs have witnessed immense growth over the past two decades through significant improvement in their ability to convert waste heat into useful electricity[21–24]. Such improvements have been achieved on the back of novel, more efficient TE materials, as well as the execution of strategies designed to enhance their power factor and/or reduce their thermal conductivity[22–28]. This has been closely accompanied by the ever-widening range of their potential applicability. Traditionally, TEs have been developed, tested and evaluated for sectors involving high fossil fuel use and associated waste heat emissions, such as thermal and nuclear power plants, automobiles, and industries like steel and cement, apart from the customary aerospace sector[14,23,24,29–34]. However, recent initiatives have advocated their use for online storage and computing (servers), body-wearables, micro- and nano-electronics, refrigeration, and even temperature or climate control systems, such as in seats for automobiles[24,25,29,30,35–39]. Additionally, TEs have also been evaluated for their electricity generation in conjunction with established renewable energy technologies, such as solar[20,24,40] and geothermal energy[24,41,42]. Apart from high conversion efficiencies, such broadening of applicability for TEs is in part due to their availability in various topologies, expanding from the standard rectangular topology to other alternatives, including in flexible forms[23,43,44]. Moreover, these benefits are complemented by the near-zero emission of both noise and greenhouse gases during their usage, as well as the absence of any moving parts[17,23,43,45–49].

Together, the aforesaid benefits reveal the prime reasons for growing relevance of this platform. Yet, its predominant use is currently limited to space shuttles and some niche sectors[23,48], such as body-wearables for instance. This is despite the emergence of new thermoelectric systems, that have addressed the long-stifling commercial predominance of bismuth-telluride (BT) for several years[44,48–50]. A plethora of reasons explain the low use of TEs on large scale, including low device conversion efficiencies (< 10 %), high costs of raw material and manufacturing, poor mechanical and thermal stability at operational temperatures, and decrease in conversion efficiency with time due to mismatch in component properties[23,43,56,47–49,51–55]. Even as efforts are underway to address these issues, another concern has increasingly gained credence that raises *fundamental questions on ecofriendliness of this platform* – namely, the use of toxic and scarce constituent elements in all major TEs[23,57,58]. However, these concerns also highlight another central challenge with the current framework of evaluating TEs, namely, the analysis of their performance solely in terms of benefits or pitfalls related to a single or few stages of their life cycle, such as fuel saved by their use, or exposure of workers to toxic elements during their production. Such an approach disregards issues that engulf other life cycle stages, such as ecological impacts of extracting and refining various constituent elements, or end-of-life treatment employed for TEs at the end of their life. This starkly increases the probability of the ecological burden of TEs getting shifted to other stakeholders[59–61], especially final consumers, who may be unaware of its consequences. Further, it also impedes the possibilities for truly developing sustainable thermoelectrics that are also commercially viable for large-scale production and application. This in turn impedes possibilities for policymakers to advocate and achieve the successful adoption of this technological platform, both via individual as well as collective actions in coordination with other stakeholders, for lowering environmental risks associated with its use for various commercial applications.

1.2. Life Cycle Assessment: Literature Review & Gaps

An excellent way to overcome all the above-mentioned challenges is to use the life cycle assessment (LCA) methodology to arrive at a set of principles that can guide policymakers and other stakeholders to undertake effective steps for development of sustainable thermoelectrics. LCA has emerged as an extremely powerful tool to estimate the comprehensive environmental impacts of any product or service across its entire life cycle over the past two decades[59,61–65]. Its strong attractiveness stems in part from being effective at mapping major environmental hotspots and critical impact drivers, along with showing the need for multi-stakeholder action to reduce these impacts[61,66]. Further, the use of LCA has been popularized by the standardization of its methodology by the International Organization for Standardization (ISO)[67,68].

With regard to designing and/or developing sustainability principles, the use of life cycle approach – or focusing on various stages of life cycle – has been an important tool for various domains, be it green engineering[69], sustainable chemistry[70], green tribology[71], or batteries in stationary[72] and mobile applications[73]. However, it is only the studies on batteries[72,73] that have used the LCA approach, albeit solely from the perspective of lowering life cycle greenhouse gas (GHG) emissions. These principles, encompassing all stages of life cycle, focus primarily on lowering energy consumption during production, focusing on specific aspects during use – such as on charging patterns for batteries – and extending the life of technologies for various domains. Such principles provide clarity for policymakers on the specific nature of policies and steps that need to be undertaken by them and/or other stakeholders – such as researchers and product manufacturers or technology providers – for ensuring both ecological suitability and economic viability of the concerned domain. Yet, such principles have not been postulated till date for thermoelectrics (TEs), which can prove to be a vital technology in a world where fossil fuels are expected to play a pivotal role in meeting global energy demand even amidst global focus on renewable energy, as outlined in the recent IPCC report[8].

The primary reason behind the lack of such principles for TEs stems from the lack of enough LCA studies on this domain to estimate its ecological gains and drawbacks, despite the vast growth in LCA studies on energy-related technologies (generation, conversion, harvesting and/or storage) over the past three decades[74,75,84–93,76,94,77–83]. Only a few studies have sought to evaluate TEs from the life cycle ecological perspective for a variety of applications[95–99]. Ghojel (2005)[95] estimated the environmental impacts of a TE waste heat recovery system, composed of bismuth-telluride (BT) modules, during its assembly and use phase, as a replacement to alternators in automobiles. Later, Sergienko et. al (2010)[99] conducted gate-to-gate LCA to calculate the material resource requirement for manufacturing a single BT cooling module using MIPS (material input per service unit) analysis. In the same year, Patyk (2010)[97] presented a preliminary analysis on ecological impacts of BT-based thermoelectric generators (TEGs) for use in passenger cars, woodstoves and combined heat-and-power (CHP) production. Subsequently, Patyk (2013)[98] undertook a more detailed analysis of life cycle impacts and costs for TEGs and steam expanders used in natural gas-based power units. Lastly, Kishita et. al (2016)[96] attempted to gauge the economic and environmental viability of BT-based TEGs for automobiles used in Suita city in Japan till the year 2030.

While all these studies provide some useful insights, they also suffer from several prominent issues. Almost all of them focus solely on a single TE material – bismuth-telluride[95–97,99] – which does not represent the diversity of this platform, especially given the numerous and more efficient TEs that have been developed over the past two decades. Further, the dominant focus of these studies[95,97,99] is on energy savings and/or CO_2

emissions (greenhouse gas or GHG emissions) related to the use stage, while either partly or wholly neglecting the energy consumed to process TEs, as well as the effects of their end-of-life (EOL) treatment. Such focus on GHG emissions also ignores aforementioned challenges about toxicity and scarcity of constituent elements. A lone paper[98] that does attempt to focus on these issues, considers silicon-telluride, containing 50 wt. % each of both silicon and tellurium, as thermoelectric material. However, literature[100] shows that this composition cannot exist in solid state at room temperature, and that it must dissociate into two phases for its stable existence, as a result of which its TE properties are likely to be impacted.

But the central lacuna of previous LCA studies is the dearth of detailed inventory for processing TEs and other device components from initial raw materials. Additionally, none of these studies attempt to understand the effect of end-of-life treatment, particularly the possibility and likely effect of recovering and recycling TEs on conserving scarce constituent elements. Moreover, barring one study on automobiles[96], all these studies assume constant availability of waste heat for electricity generation, which is not the case for either automobiles or other applications like power plants that meet peak loads. In such cases, variation in operating temperature leads to thermal cycling that has a deleterious influence on conversion efficiency of TEs (explained in Chapter 2). Yet, the effect of nature of waste heat generation on TE conversion efficiency and thereby, on their life cycle performance for impacts beyond global warming, has not been understood till date.

Together, the aforementioned gaps render it difficult to evaluate the ecological credentials of this energy harvesting platform. This in turn hinders the development of principles that can guide policymakers as well as other stakeholders, particularly researchers, TE device manufacturers and also potential end-users of this technology, on implementing steps to ensure and improve both economic viability and ecological suitability of TEs. Due to the lack of these beneficial developments, the possibilities for enhancement and sustenance in futuristic relevance of TEs is hampered. Any redressal of these issues and the postulation of such sustainability principles for TEs would thus merit a detailed study that addresses the aforementioned gaps by analyzing environmental performance of existing TEs for various applications, while keeping in mind their nature of waste heat emission.

Hence, in line with similar exercises that have been previously undertaken for other domains as pointed earlier, this study uses life cycle assessment (LCA) methodology to initiate discussion on sustainability principles for thermoelectrics. To accomplish this task via redressal of gaps in existing literature, this discussion focuses on four tasks that were undertaken as outlined in subsequent sub-sections, followed by its organization.

1.3. Research Tasks

1.3.1. Task 1: Inventory Development

Since the lack of detailed inventory impedes a thorough life cycle analysis of TEs, the immediate task was to develop the *first-ever exhaustive inventory* for the entire life cycle of TE devices (modules and generators). The primary focus was on detailing all steps involved from raw material extraction till the manufacturing of TE device components and their final assembly, as little is known on inventory of these steps. In addition, end-of-life treatment steps that have hitherto been ignored were also developed for disposal and recycling processes for TEs. The focus of this task and subsequent tasks, was to consider multiple TEs, including but not confined to bismuth-telluride.

1.3.2. Task 2: Environmental Performance Assessment

The second task involved estimating and *evaluating the ecological impacts of TE devices*, both during their production and across their entire life cycle (using LCA methodology), for various applications. Since the potential applications for TEs differ in their nature of waste heat generation, they were classified into three groups (Table 1-1).

For each TE device, major impact contributors and reasons behind their prominent contribution were identified for the production stage. Further, for each of the chosen applications, life cycle assessment (LCA) methodology was used to evaluate the life cycle performance of representative example mentioned in Table 1-1. For all considered applications, TE devices were evaluated not only on global warming, but also on other impacts that look at their toxicity- and scarcity-related performance, while keeping in mind the associated limitations of each analysis.

Table 1-1: Classification of applications and representative examples used in this work

Type of application		**Representative example used**
Nature of waste heat emission	**Mobility status**	
Continuous	Stationary	Coal-based power plant
Periodic/Intermittent	Stationary	Natural gas-based power plant
Periodic/Intermittent	Mobile	Automobiles

1.3.3. Task 3: Effect of End-of-Life (EOL) Scenarios

Since the EOL stage has not been studied in any depth in previous LCA studies on TEs, there is a complete lack of information on ecological gains that can be attained by recycling specific TE device components (including TEs themselves). Hence, three different EOL scenarios were envisaged to understand their capability in shaping the environmental outcomes of TE devices chosen for each considered application (Table 1-1).

To define these EOL scenarios, the 6R-based material flow approach, as envisaged by Jawahir et. al (2016)[101], was deployed, as it describes the practical incorporation of circular economy vision within the life cycle of numerous products and technologies. For EOL treatment, this 6R-based approach was deployed for different components to envision three scenarios that involve three kinds of EOL treatments: most expected, practically possible, and aggressive level of recycling (described in Chapter 2).

1.3.4. Task 4: Principles of Sustainable TEs

Since the ultimate objective of this study was to develop key principles that can enable policymakers and other stakeholders to determine the steps needed for ecological and commercial viability of thermoelectrics, the obtained results from LCA studies were distilled to postulate these principles. As mentioned earlier, the principles were developed on an exercise similar in nature to that undertaken for sustainable chemistry[70,102], green tribology[71], green engineering[69] and batteries[72,73]. These principles were designed to encapsulate key parameters that impact the entire life cycle of TEs, so that they could help the concerned stakeholders in undertaking specific actions to make this platform more ecofriendly, while acknowledging the limitations of this study. Figure 1.1 shows the linkages between the earlier-mentioned gaps and the proposed tasks in this work.

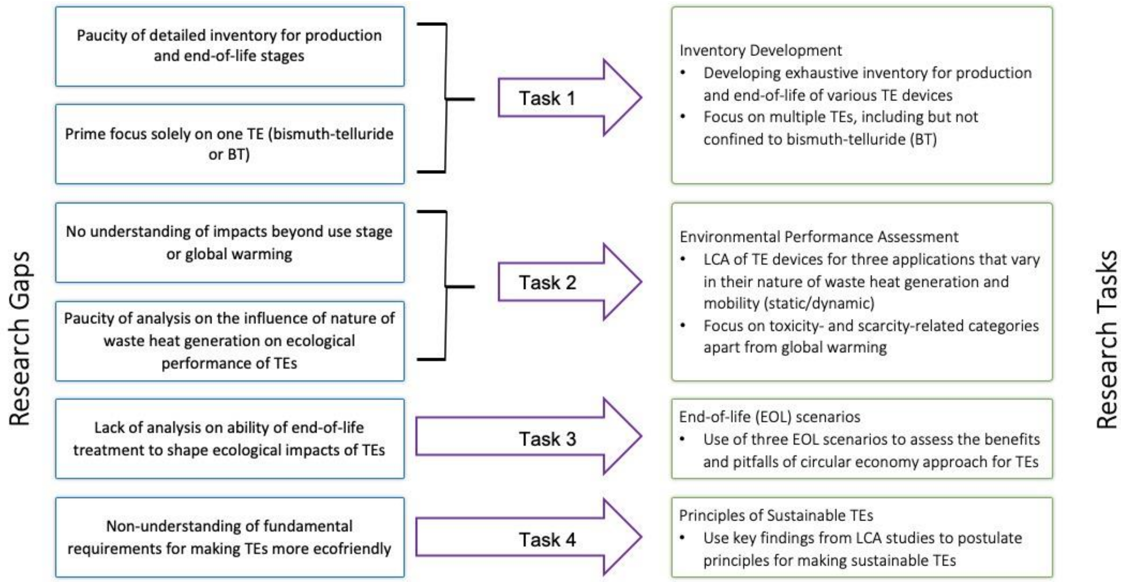

Figure 1.1: Research gaps and corresponding tasks

1.4. Organization of Dissertation

In line with the research gaps and tasks that have been highlighted (Figure 1.1), the rest of this dissertation is organized as follows. Chapter 2 lists the various aspects of LCA – goal and scope (including system boundary), functional unit, inventory development, impact assessment and interpretation – that were used for the three representative examples analyzed in this work. Chapter 3 describes the impact results and presents subsequent discussion on LCA of various TE modules that were considered to harvest waste heat from a baseload coal-based power plant. This evaluates the potential of this platform for stationary applications where waste heat is constantly emitted. Subsequently, Chapter 4 discusses the impact results on LCA of these modules upon use in a peak load natural gas-based power plant, to evaluate their outcomes for stationary applications involving periodic and/or intermittent waste heat generation. Subsequently, to also capture applications that involve mobility, two thermoelectric generators were considered from existing literature, based on some of the modules studied in previous chapters, and were evaluated for their ecological performance in automobiles in Chapter 5. Across these three chapters, the initial three tasks (Tasks 1-3) were completed.

Later, results from Chapters 3-5 were used to arrive at key principles for developing sustainable thermoelectrics. These principles, along with a thorough explanation on their importance as well as specific case studies to further highlight the benefits of their practice, are expounded on in Chapter 6 (Task 4). Finally, Chapter 7 provides a brief summary of the work, and also sheds light on the directions in which future research can be undertaken.

CHAPTER TWO

MATERIALS AND METHODS

2. Materials, Methodology and Assessment

2.1. Materials – Rationale & Choice

As described in Chapter 1, three separate LCA exercises were undertaken in this work, namely, the LCA of TE devices for:

(a) Baseload coal-fired power plants;

(b) Peak load natural gas-based power plants; and

(c) Automobiles

For each exercise, different choices were made for TE devices considered in the specific end-use. Nevertheless, a general description is provided on the nature of TE devices that were considered for this analysis.

Typically, TEs are used as generators, which in turn consist of numerous components that can be assembled in multiple topologies[48,49,103,104]. However, the most common typology used to construct such generators – known as thermoelectric generators or TEGs – is the rectangular topology[48,49,103,104]. Hence, for this work, generators of this topology were considered wherever applicable, with the exact nature of such device used for this work shown in Figure 2.1(a). This generator[103,104] consists of: (a) Plate-fin type heat exchanger, which induces turbulence in waste heat flow to extract its energy and provide it for supply to thermoelectric modules; (b) Thermal grease and insulation, which respectively enable or disable thermal conduction in desired manner to ensure that the waste heat is supplied to thermoelectric modules; and (c) Thermoelectric modules(one module is marked in blue box in Figure 2.1(b)). Thermoelectric modules in turn consist of four components: (a) Thermoelectric (TE) legs – both p- and n-type; (b) Metallic tabs, usually made of copper, that are used to connect these TE legs electrically in series and thermally in parallel; and (c) Ceramic plates, typically made using alumina, that are used to house this entire arrangement between them[103,104].

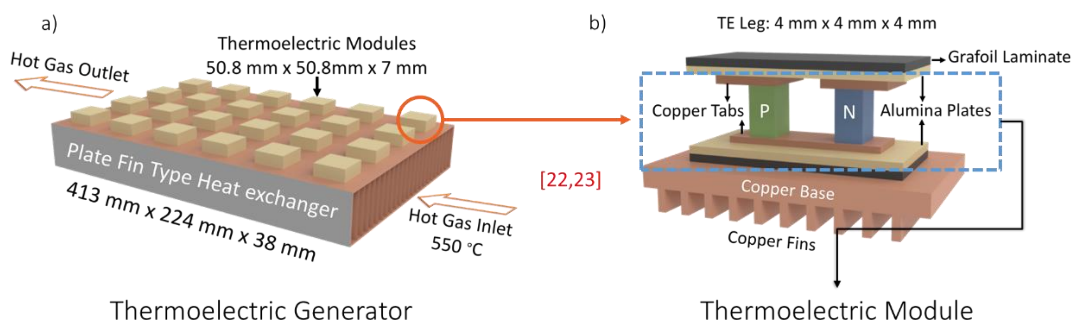

Figure 2.1: (a) Thermoelectric generator and (b) Thermoelectric module – of the kind considered in this work (blue colored box represents the components that constitute modules – p-type and n-type TE legs, metal tabs and ceramic plates)

For this work, commercially produced TE devices were chosen for two reasons. The first was that commercial products typically represent proven technical capability for any technology, as only such products can attain enough commercial viability to generate and meet existing demand[50]. In addition, commercial production for any product is generally optimized for resource and energy consumption, so the use of energy or resource-intensive processing methods for such modules has either already been addressed, or it remains an unresolved issue that can be highlighted through this work.

Regarding TE devices, these are almost entirely produced at the modular level on commercial scale, with generator production typically delegated to the end-user in line with their specific requirements. This hinders the availability of information on commercial TEGs in public domain. At present, more than 50 companies produce TE modules globally[50], of which ~ 30 produce these for power generation applications. However, data on their elemental composition and processing techniques was available for only seven modules produced by six of these companies (with some assumptions). These seven modules – all of the kind shown in Figure 2.1(b) – encompassed five different TEs: two each of bismuth-telluride (BT) and skutterudite (SK) systems; and one each of Half-Heusler (HH), lead-telluride (PT) and silicide (SC) systems.

More information on these modules is provided in Tables 2-1–2-4. Table 2-1 provides all the necessary details about chosen modules – namely, the material system used in TE legs, manufacturing company, and the naming convention used. Table 2-2 provides details on dimensions of each module and/or its TE legs – which were obtained or assumed from concerned journal papers that also discuss the fabrication and/or usage of these modules. Further, Table 2-3 provides data on the mass of individual components of the aforementioned modules – as obtained from calculations undertaken using modular, TE leg and other component-related dimensions, along with the use of specific assumptions for metallic tabs and alumina plates wherever needed. Finally, Table 2-4 gives the values of important TE parameters for the chosen modules, such as: (a) Hot-side (T_H) and cold-side temperatures (T_C); (b) Conversion efficiency (η, %); (c) Amount of both input heat power (Q_{input}) and output power generated by a single module (P_{output}); and (d) Number of modules required for each system to convert 1000 W (or 1 kW) of input waste heat into useful electricity (this number is later used in this study).

Table 2-1: Details about chosen modules

TE Material	**Names**	**Chemical composition of legs**		**Manufacturer**
		p-type leg	**n-type leg**	
Bismuth-Telluride (BT)	BT-1[105]	$Bi_{0.4}Sb_{1.6}Te_3$	$Bi_2Te_{2.4}Se_{0.6}$	II-VI Marlow
	BT-2[106]	$Bi_{0.4}Sb_{1.6}Te_3$	$Bi_2Te_{2.4}Se_{0.6}$	KELK
Skutterudite (SK)	SK-1[103]	$DD_{0.76}Fe_{3.45}Ni_{0.6}Sb_{12}$	$Ba_{0.08}La_{0.05}Yb_{0.04}Co_4Sb_{12}$	II-VI Marlow
	SK-2[107]	$Ce_yFe_xCo_{4-x}Sb_{12}$	$Yb_{0.3}Co_4Sb_{12}$	Shanghai Institute of Ceramics
Half-Heusler (HH)	HH[108,109]	$Hf_{0.5}Zr_{0.5}CoSb_{0.8}Sn_{0.2}$	$Hf_{0.5}Ti_{0.25}Zr_{0.25}NiSn_{0.99}Sb_{0.01}$	Evident Thermoelectrics
Lead-Telluride (PT)	PT[110,111]	PbTe-2 % MgTe, doped with 4 % Na	PbTe, doped with 0.2 % PbI_2	Mottainai Energy Co. Ltd.
Silicide	SC[106,112,113]	$(Mn_{0.98}Mo_{0.02})(Si_{0.9865}Al_{0.0035}Ge_{0.01})_{1.74}$	$Mg_2Si_{0.4}Sn_{0.6}$	KELK

Table 2-2: Dimensions of TE legs and overall module

Module	**Dimensions (mm^3)**	
	Module	**TE legs**
BT-1[104,105]	40.13 × 40.13 × 4	2 × 2 × 2
BT-2[106]	55 × 51.5 × 4.4	2.5 × 2 × 2

SK-1[103]	50.8 × 50.8 × 7	4 × 4 × 4
SK-2[107]	50 × 50 × 10	5 × 5 × 7.5
HH[108,109]	26.5 × 26.5 × 5 (Height is assumed)	1.8 × 1.8 × 2
PT[111]	18 × 15 × 6.8 (Height is obtained via calculations)	2 × 2 × 2.8
SC[112,113]	23.5 × 23.5 × 9.75 (Height is assumed)	4.5 × 4.5 × 6.75

Table 2-3: Mass break-up various components in chosen TE modules (in grams)

Module	**P-type legs**	**N-type legs**	**Ceramic plates**	**Other components**	**Total**
BT-1	6.93	7.67	9.54	0.54	24.69
BT-2	10.98	12.15	24.61	0.15	47.90
SK-1	14.89	15.11	20.39	2.40	52.79
SK-2	45.36	41.53	19.75	0.80	107.44
HH	3.58	3.50	5.55	0.75	13.38
PT	0.73	0.72	2.13	1.65	5.23
SC	5.06	2.89	4.36	0.09	12.41

Table 2-4: Major thermoelectric parameters of chosen TE modules

Module	T_H **(°C)**	T_C **(°C)**	η **(%)**	P_{output} **(W)**	Q_{input} **(W)**	N
BT-1[105]	170	50	4.08	4.17	102.21	9.78
BT-2[114]	250	30	7.00	18.00	257.14	3.89
SK-1[115]	560	100	7.50	11.51	153.44	6.52
SK-2[107]	575	65	7.30	25.08	343.56	2.91
HH[109]	600	100	4.50	15.5	344.44	2.90
PT[111]	600	30	8.80	3.5	39.77	25.14
SC[112,113]	550	30	6.40	4.81	75.20	13.30

Keeping in mind the above-mentioned information on TE modules, the specific type of TE device considered for each end-use, and the background rationale for these choices, are provided in the sub-sections below.

2.1.1. Stationary Applications: Power Plants

Since no data could be obtained on TEGs based on the chosen seven modules – either with their manufacturers or in other literature – and since it was difficult to undertake any analysis on how these modules would perform upon use of heat exchanger due to paucity of time and capability, heat exchanger components were excluded from the purview of analysis for electric power plants. Hence, TE modules were considered as the final TE device for both baseload coal-based and peak load natural gas-based power plants.

In case of coal-based power plants, generally, waste heat is constantly produced throughout the day, so it meets baseload electricity demand (or electricity demand that exists throughout the day). In contrast, natural gas-based power plants are often used to meet peak electricity demand that exists for only a few hours per day. Such waste heat generation in periodic, and sometimes, intermittent manner – all of which is discontinuous – results in thermal cycling of TE modules[19,116]. This causes deterioration in modular conversion efficiency due to two reasons[19,116,117]. First, thermal cycling produces thermal shocks in TE legs and metallic tabs, resulting in defects and mechanical degradation at their interface. Second, it also enhances diffusion of elements across both these components, thereby affecting their purity and resultant TE performance. Hence, TE modules cannot be considered to operate in the same manner for continuous and discontinuous emission of waste heat.

Strikingly, there is no direct data on the extent of decrease in conversion efficiency (or output power) for any of the chosen modules with each thermal cycle – which is defined in this work as "*Thermal Cycling Reduction Coefficient*" or TCRC. While limited data exists in literature for TE systems used in these modules, it poses some challenges. For instance, TCRC data is not available for PT systems at all, while for other TE systems, these values can be calculated only for operating conditions that are different from those considered as optimal for these modules (Table 2-4). Hence, assumptions were made for TCRC values of the remaining six modules based on existing literature, as detailed in Section 2 of Appendix-B. Based on these assumptions, Table 2-5 shows the TCRC values chosen in this work.

Table 2-5: Final TCRC values chosen in this study

Modules	**TCRC (% per cycle)**
BT-1, BT-2	0.0035
SK-1, SK-2	0.0222
HH	0.0050
SC	0.0142

2.1.2. Mobile applications: Automobiles

Apart from thermal cycling, another important factor for TEs in mobile end-uses is their mass, which affects the amount of energy required for mobility (unlike in stationary applications). Hence, unlike in the earlier case of power plants, TEG components beyond modules, particularly heat exchanger-based components, cannot be ignored for the purpose of LCA of TEs in automobiles. Interestingly, literature[103,104] was obtained on TE performance of two automotive TEGs that were composed of two of the aforementioned seven modules – BT-1 and SK-1. While the first generator (TEG-1) was composed of skutterudite (SK-1) modules, the second generator (TEG-2) contained both SK-1 and bismuth-telluride (BT-1) modules that were connected in series[103–105]. Therefore, both due to the availability of information on these TEGs, as well as the influence of mass of TE device on net fuel consumption in mobile applications, coupled with the lack of similar information for other modules, only these TEGs were considered for LCA in this end-use.

More information on both these TEGs is provided in Tables 2-6 and 2-7. While Table 2-6 provides data on dimensions of individual components for these generators, Table 2-7 provides a break-up of their masses in terms of contribution from these components.

Table 2-6: Dimensions of individual components of chosen generators

Components	**TEG-1**	**TEG-2**
Heat Exchanger	Rectangular topology dimensions: 0.413 m × 0.224 m × 0.038 m Rectangular topology volume: 0.003592 m^3	Rectangular topology dimensions: 0.688 m × 0.224 m × 0.023 m Rectangular topology volume: 0.003592 m^3
Copper fins	Number: 22 Thickness: 0.033 m Spacing between fins: 0.00635 m	Number: 22 Thickness: 0.033 m Spacing between fins: 0.00635 m
Thermal grease (Grafoil laminate)	Thickness: 1 mm	Thickness: 1 mm

Thermal insulation (Min-K)	Thickness: 2 mm	Thickness: 2 mm
Thermoelectric legs	Skutterudite leg dimensions: 0.004 m × 0.004 m × 0.004 m	Skutterudite leg dimensions: 0.004 m × 0.004 m × 0.004 m Bismuth-telluride leg dimensions: 0.002 m × 0.002 m × 0.002 m
Electrical wiring	Length: 5.2 m	Length: 7.4 m
Number of thermoelectric modules	48 SK-1 modules	48 SK-1 modules 50 BT-1 modules

Table 2-7: Mass of both TEGs, segregated by individual components

TEG Component	**Sub-component**	**Material Used**	**Amount Used in TEG-1 (kg)**	**Amount Used in TEG-2 (kg)**
Heat exchanger	Copper base	Copper	13.263	22.104
	Side bars	Copper	0.389	0.215
	Copper fins	Copper	7.539	5.981
Thermal grease		Grafoil laminate	0.374	0.624
Thermal insulation layer		Min-K	0.592	0.987
Ceramic plate		Alumina (Aluminum oxide)	6.850	7.265

Skutterudite (SK) thermoelectric legs	n-type legs ($Ba_{0.08}La_{0.05}Yb_{0.04}Co_4Sb_{12}$)	Barium	0.005	0.004
		Lanthanum	0.003	0.002
		Ytterbium	0.003	0.002
		Cobalt	0.099	0.077
		Antimony	0.616	0.475
	p-type legs ($DD_{0.76}Fe_{3.45}Ni_{0.6}Sb_{12}$)	Didymium	0.044	0.034
		Iron	0.077	0.059
		Nickel	0.014	0.011
		Antimony	0.583	0.449
Bismuth-telluride (BT) thermoelectric legs	n-type legs ($Bi_2Te_{2.4}Se_{0.6}$)	Bismuth		0.160
		Tellurium		0.117
		Selenium		0.018
	p-type legs ($Bi_{0.4}Sb_{1.6}Te_3$)	Bismuth		0.032
		Tellurium		0.075
		Antimony		0.147
Copper tabs		Copper	1.101	1.725
Electrical wires			0.243	0.346
Total			**31.794**	**40.908**

2.2. Life Cycle Assessment

2.2.1. Goal, Scope & Functional Unit

The primary goal of this set of analyses was to provide a set of holistic principles that can be used by various stakeholders, particularly policymakers, researchers and device manufacturers, to channelize their actions towards ensuring and enhancing ecological suitability of thermoelectric devices. Hence, these stakeholders, with policymakers playing the prime role in this regard, constitute the primary audience for this work. In order to devise these principles, this work encompasses life cycle assessment (LCA) of TE devices (generators and modules) over cradle-to-grave for each application, beginning with the extraction and processing of their constituent elements, manufacture and assembly of device components, use and post-life treatment. Through a proper capture of all these steps – classified into groups of production, use and end-of-life (EOL) – these analyses identify hot-spots that must be critically focused upon by policymakers and other stakeholders for enhancing environmental credentials of TEs across their entire life cycle.

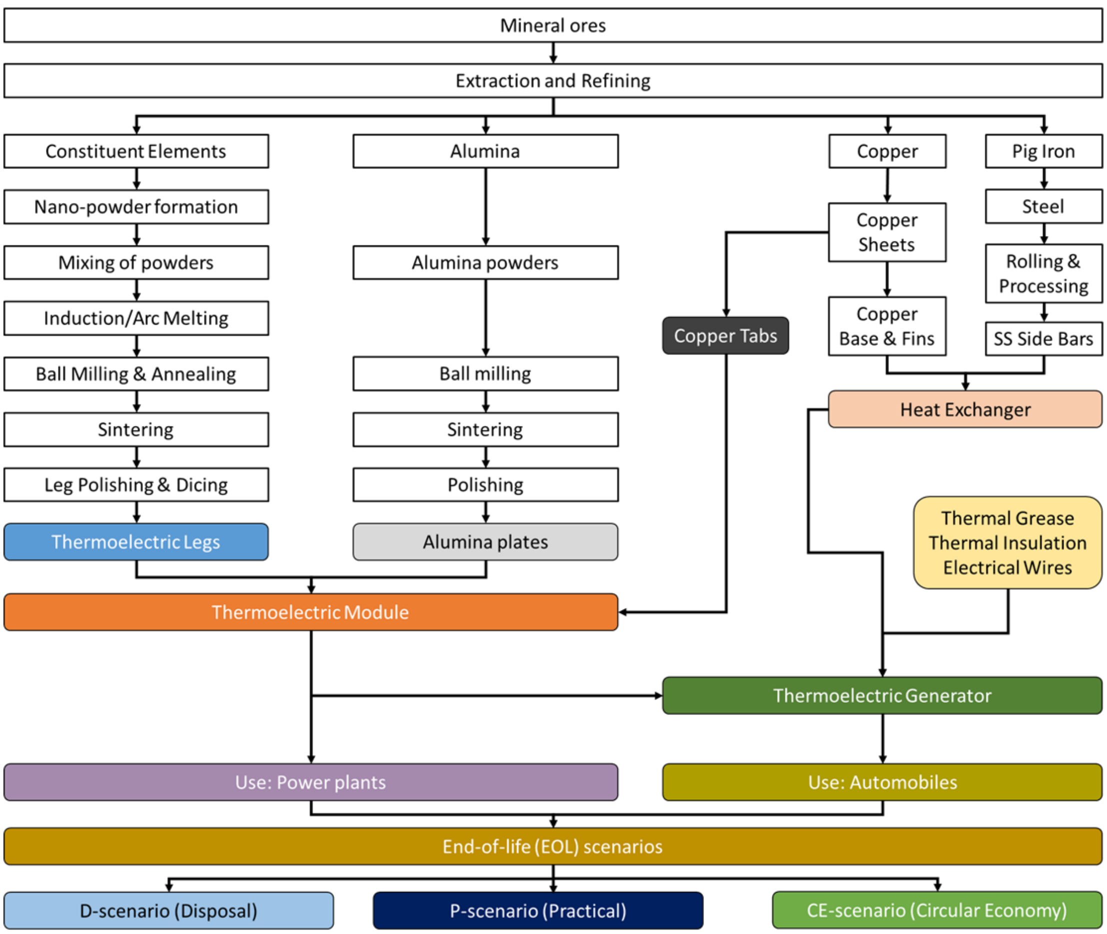

Figure 2.2: Life cycle of TE modules (processing steps and system boundary) for coal- and gas-based power plants

2.2.1.1. Production

For the production stage, irrespective of the considered application, all steps remain the same from raw material extraction till assembling of components to obtain TE modules. In addition, for TE generators (Section 2, Appendix-C), other components – heat exchanger, thermal grease, electrical wires, and thermal insulation – are also incorporated. Hence, their production was also considered.

For TE legs and alumina plates, initial raw materials (constituent elements or alumina, as the case may be) were assumed to be purchased from global market, then jaw-crushed and ball-milled to desired nano-size levels, and subjected to multiple processes to obtain the final component (Figure 2.2 – which shows the system boundary for all LCA analyses of this work). For metallic tabs, metal sheets were considered to be procured from market and cut to desired dimensions. Finally, these components were assembled to produce the final module. On the other hand, for TEGs, thermal grease, electrical wires and thermal insulation were considered to be directly procured from market, while for heat exchanger, it was assumed that plates/rods made of metals (stainless steel or copper, as the case may be) were obtained from market and cut to desired dimensions in-house. Also, upon assembly of all components (including TE modules), the heat exchanger was considered to be in rectangular topology with all modules arranged in longitudinal configuration – as in chosen literature[103,104].

TEG	TE module	P-Type TE	N-Type TE	No. of Couples /Module	No. of Modules /TEG
TEG-1	SK	$DD_{0.76}Fe_{3.45}Ni_{0.6}Sb_{12}$	$Ba_{0.08}La_{0.05}Yb_{0.04}Co_4Sb_{12}$	SK: 32	SK: 48
TEG-2	SK + BT connected in series			SK: 32	SK: 48
		$Bi_{0.4}Sb_{1.6}Te_3$	$Bi_2Te_{2.4}Se_{0.6}$	BT: 127	BT: 50
Functional unit: Conversion efficiency of 3.33 % SK: Skutterudite, BT: Bismuth-telluride					

Figure 2.3: Description and details for various components used in automotive TEGs, with target vehicle of Chevrolet Suburban (blue colored box represents the components that constitute modules – p-type and n-type TE legs, metal tabs and ceramic plates)

Figure 2.2 shows more details on system boundary considered in this work for all the three applications, including some details on the general processing methods employed for TE legs. Specific information on these methods for various modules is given in the sub-sections below, as well as in Figures 2.2 and 2.3. For all in-house processing, unless mentioned otherwise in respective inventory, the average U.S. 2015 electric grid was considered to be used due to paucity of more recent data on this subject in Simapro database.

A. BT-1 Module: TE Legs

For this module, TE legs (both p- and n-type) were assumed to be produced via method described in literature[118]. Under this method, constituent elements are obtained in powder form, thoroughly mixed, and vacuum-sealed in quartz tubes for heating at 850°C for 1.5 h. Subsequently, the heated powders are reduced to nano-size via ball milling, and then cold-pressed and later annealed at 400°C for long duration (10 h). Finally, the annealed samples are polished and diced to legs of desired dimensions (Table 2-2).

B. BT-2 Module: TE Legs

Based on an existing study[119], it was assumed that the elemental composition of TE legs in both BT modules was identical (Table 2-1). For this module, elemental powders are hot-pressed in argon atmosphere. Later, the obtained ingots are polished and diced to final leg dimensions (Table 2-2).

C. SK-1 Module: TE Legs

This module was used from an existing study[103], with both p- and n-type materials considered to be synthesized using procedures established in literature for p-type[120] and n-type legs respectively[121].

For p-type legs, elemental powders (Fe, Ni and Sb) are placed in quartz tubes, melted and then air-quenched. Later, an appropriate amount of DD (didymium, or 95.24 wt. % Nd and 4.76 wt. % Pr) is added to the previous mixture, and the combined powder-set is vacuum-sealed in quartz tubes. These tubes are heated along the following series of steps: (a) At 600°C for 3 days; (b) At 720°C for 2 days; (c) Melted at 950°C; (d) Air-quenched; and (e) At 600°C for 5 days. Subsequently, the powders are ball-milled and uniaxially hot-pressed in argon atmosphere. Cylindrical hot-pressed samples are polished and then diced to desired leg dimensions (Table 2-2).

Regarding n-type legs, elemental powders are mixed and then induction-melted in argon atmosphere. Later, the molten mass is quenched to room temperature and then subjected to the following series of steps: (a) Annealing (750°C, 1 week); (b) Ball milling and then cold pressing of powders to pellets; (c) Annealing (750°C, 1 week); and (d) Ball milling of pellets, followed by re-grounding them to powder form. Afterwards, these powders are processed via spark plasma sintering (SPS) at 50 MPa and 650°C in argon atmosphere. Lastly, the samples are polished and diced to suitable dimensions (Table 2-2).

D. SK-2 Module: TE Legs

For SK-2 module, both TE legs were considered to be synthesized based on the processing methodology provided elsewhere for p-type[122] and n-type legs[123] respectively.

For p-type legs, elemental powders are thoroughly mixed and vacuum-sealed in quartz tubes. Next, these tubes are annealed (1100°C, 30 h, 5°C/min) and then water-quenched. Later, the obtained ingots are ball-milled and cold-pressed into pellets, which are vacuum-sealed again in silica tubes and annealed (700°C, 1 week). Subsequently, the tubes are broken to obtain the pellets, which are ball-milled to powder form. This powder is washed using the combination of hydrochloric and nitric acids (HCl + HNO_3) for the removal of impurity phases (present in small amounts). Finally, the washed powders are sintered using SPS (600°C, 15 min) into cylindrical samples, which are polished and then diced to final leg dimensions (Table 2-2).

Regarding n-type legs, elemental powders are mixed in desired amounts and sealed in quartz tubes in argon atmosphere. These powders are then subjected to the following series of steps: (a) Melting (1100°C, 12 h); (b) Saltwater-quenching; (c) Annealing (660°C, 1 week); and (d) Ball milling to final powders. Later, these powders are hot-pressed in argon atmosphere, and then polished and diced to final leg dimensions (Table 2-2).

E. HH Module: TE Legs

For this module, p- and n-type legs were assumed to be processed based on existing literature[124,125]. For both legs, elemental powders are obtained as ingots via arc melting. Later, these ingots are ball-milled to obtain nano-powders that are hot-pressed (1050°C) to produce bulk cylindrical samples. Lastly, these samples are polished and diced to final leg dimensions (Table 2-2).

F. PT Module: TE Legs

For the PT module, TE legs were considered to be processed based on the method described in an existing study[111]. Appropriate amounts of elemental/compound powders are mixed in glove-box under nitrogen atmosphere, loaded in silica tubes and flame-sealed. Later, these powders are subjected to the following series of steps: (a) Heating from room temperature (RT) to 1050°C (at 70°C/h); (b) Annealing (1050°C, 10 h); (c) Cooling from 1050°C to 600°C (at 11°C/h); and (d) Finally, cooling from 600°C to RT over 15 h.

Subsequently, these powders are ball-milled and placed between the diffusion barrier powders ($Co_{0.8}Fe_{0.2}$). The entire powder mixture (n/p-leg material + $Co_{0.8}Fe_{0.2}$) is hot-pressed in argon atmosphere (500°C, 30 MPa, 1 h), with heating and cooling rates of 15°C/min and 20°C/min respectively employed for this step. Lastly, the obtained samples are polished and diced to desired leg dimensions (Table 2-2).

For module fabrication[111], p- and n-type legs were assumed to be placed alternately onto an insulated alumina substrate that contains both printed copper patterns and a heat-conductive polymer film. Moreover, each pair of TE legs is connected with copper electrodes. The entire arrangement is connected via soldering for structural stability.

G. PT Module: TE Legs

For this module, both p- and n-type materials were assumed to be synthesized based on existing literature[112,113]. For both legs, elemental powders are mixed and melted in induction furnace. The obtained ingots (after cooling) are crushed and ball-milled to nano-powder size. Later, these nano-powders are sintered using SPS to final dimensions, with n-type samples additionally annealed for compound homogenization. Finally, the samples are polished and diced to final leg dimensions (Table 2-2).

H. Ceramic Plates & Metallic Tabs

Typically, while TE legs are connected using metallic tabs to transfer the generated electricity for further use, the entire arrangement is enclosed within ceramic plates for structural stability and to prevent the arrangement from shorting[126]. For most of the aforementioned modules, copper tabs and alumina plates were considered to be respectively used for these purposes. However, for SC module, aluminum tabs were assumed to be used based on existing literature[112,113].

Since the exact dimensions for both these components are not provided for any module barring PT[111], appropriate assumptions were made in this regard. For alumina plates, their length and width were assumed to be the same as those for concerned module. Conversely, the width of each metallic tab was considered to be the same as that for each TE leg, while their length was treated to be the sum of length of two legs plus the space between them. To obtain this inter-leg spacing, TE legs were assumed to be distributed uniformly over the length and width of each module, i.e., equal spacing between any two legs as well as between the end-most leg and the end of ceramic plate (on either side).

For all modules except SC, copper tabs and alumina plates were considered to be connected to TE legs via electrical soldering, while for SC module, thermal spraying was considered the joining technique[127]. However, such technologies are expected to have negligible contribution to overall energy consumed in processing TE modules[96,98]. Hence, neither of these processes were considered in overall inventory calculations for chosen modules. More information regarding various equipment and processing parameters used for individual components of different TE modules is provided in the inventory section (Section 2.2.2).

I. Heat Exchanger Components

As per the studies by Kumar et al.[103,104], the heat exchanger used in both TEG systems is a 'plate-fin heat exchanger' that possesses rectangular topology. It consists of three components: TEG base or parting sheets (on both top and bottom), fins, and two side bars (parallel to the direction in which exhaust gas flows), as shown in Figure 2.1. For the purpose of this study, fins and TEG base are made from copper[103,104], while the side bars were assumed to be made from stainless steel (SS).

The chosen studies[103,104] mention that copper base – which is considered to refer to parting sheets in the plate-fin type heat exchanger – is used to ensure excellent thermal conduction between heat exchanger and the hot side of TE modules. Such conduction results in higher temperature difference between the hot and cold ends of TE modules/legs, thereby improving the TEG conversion efficiency. Since copper base used in chosen studies[103,104] is similar to a small copper sheet, it was assumed that larger-sized copper sheets were used to produce this base.

Between the copper base on either side are placed copper fins[103,104], that generate turbulence in the exhaust gas flowing through it, enabling heat transfer and temperature difference across the TEG for subsequent electricity generation. For both TEGs, these fins were considered to be made from copper sheets. Hence, it is assumed that copper sheets were used as initial material and were then assumed to be cut and subsequently folded in-house using hydraulic cold pressing (that consumes negligible amount of energy and produces inconsequential emissions) to produce the desired copper fins.

Stainless steel (SS) side bars are commonly available in the commercial marketplace, and were assumed to be made from corresponding rods.

J. Thermal Insulation (Min-K)

As per Kumar et al.[103,104], Min-K is used on 20 % surface area of parting plates (on either side) as a thermal insulator to prevent heat leakage and ensure smooth heat transfer from the heat exchanger to hot side of thermoelectric (TE) modules. Min-K is manufactured by Industrial Process Heat Engineering Ltd. (i.e., Improheat Industries Ltd.)[128]. It was assumed that the chemical constituents of Min K[129] – namely, oxides of silicon (SiO_2), aluminum (Al_2O_3), titanium (TiO_2), iron (Fe_2O_3), calcium (CaO), magnesium (MgO), sodium (Na_2O) and potassium (K_2O) – were obtained in powder form and mixed with water to produce Min-K for commercial thermal insulation purposes. Since these chemical constituents (in powder form) are already provided in Ecoinvent 3.5 database, separate inventories were not prepared for them, but were used from existing database. Also, as indicated in company literature[129], evaporation of water due to dry heat results in curing and hardening of Min-K, thereby providing it the desired structure. Hence, it was assumed that no energy consumption takes place during the application of Min-K on parting plate (on top of TEG base).

K. Thermal Grease

The chosen studies[103,104] describe the use of grafoil laminate – or a laminate based on graphitic foil – as a component in TEGs. Due to lack of sufficient data on production of such foils, battery-grade graphite was considered as a substitute in this study.

L. Electrical Wirings

It was assumed that AWG (American wire gage) 10-gage electrical wires (diameter: 2.59 mm; mass per unit length: 46.8 kg/m) are chosen for both TEGs. Assuming a single wire to span across entire length and width of both TEGs, it was calculated that 0.24 kg of electrical wire was required for TEG-1, while 0.31 kg of wire was required for TEG-2.

M. Manufacture & Assembly – TEG

Since existing literature clarifies that negligible energy is used during the assembly of entire generator[96], this assumption was continued with for the purpose of this study.

Table 2-8 lists the major assumptions made with regard to equipment considered for the various processing steps considered for TE device components, while Section 2 of Appendix-A explains some of the other assumptions and parameters that were considered in somewhat greater detail for the production stage. Detailed inventory of components is further provided in Section 2 of Appendix-A and Section 2 of Appendix-C.

Table 2-8: Major assumptions for developing inventory of production stage of TEs

Aspects	Assumptions made
Equipment	• Industrial-level equipment considered
Sintering process parameters	• Processes: Hot pressing, spark plasma sintering • Maximum sample dimensions: 2” diameter; 0.5” height • Hot pressing: Multi-cavity dies • Heating rate: 100 K/min (unless specified otherwise) • Holding time: 10 min (unless given otherwise)
Component assembling	• Negligible energy consumed in assembling step[96,98]
Ball milling	• Volume used per vial: 95 % (4 vials per run) • Fluid used: Ethanol (unless specified otherwise) • Volume of fluid used: 40 % of total vial volume • Ball-to-powder ratio = 10:1 (by weight)
Cold isostatic pressing	• No energy consumption
Argon flow rate	• 50 ml/min (unless mentioned otherwise in literature)
Leg polishing	• 5 % height removed on either end from sintered samples

2.2.1.2. Use

In baseload coal-based power plant, it was assumed that waste heat is continuously emitted. In order to make assumptions about long-term TE performance and lifetime of chosen modules in these plants, a comparable application was considered: space shuttles, where TEs are used due to limited fuel supply and the constant need for energy. In such applications, TEs exhibit long lifetimes (~ 15-20 years) with negligible reduction in their conversion efficiency[34]. Similar results have also been observed for some of the chosen TE systems (not the exact modules), albeit for fewer hours of operation[54,130]. Hence, the baseload power plant was assumed to run continuously (i.e., 24 × 7) over 15 years with TE devices for this exploratory work, while accepting that real-life considerations necessitate their annual shut-down for maintenance. In other words, TE modules would operate over 131,400 hours (15 years × 365 days/year × 24 hours/day) in baseload power plants.

On the other hand, peak load natural gas (NG)-based power plant is considered in this work to meet only peak electricity demand. Hence, it was assumed that this plant operated for only 4 h (hours) continuously per day to address this function, based on the data available with the US Energy Information Administration[131]. Further, the lifetime of NG plants typically varies between 20 and 30 years[131–133]. Hence, it was assumed that the lifetime of NG plant was 25 years (or the average of this range). Thus, the total operating duration of TEs in peak load plants was 36,500 h (or 25 years × 365 days × 4 hours/day).

Finally, for automobiles, it was assumed that the lifetime of both generators (TEGs) was 100,000 miles – the typical distance assumed for any passenger vehicle with reference to warranty services offered by manufacturers/dealers. The automobile under consideration here was Chevrolet Suburban, for which these generators were evaluated[103,104]. In these studies, the authors have assumed that the generators are placed over different regions of the automobile exhaust pipe to recover waste heat that encompasses differing temperature regimes of exhaust waste heat: TEG-1 over 280-550°C, and TEG-2 over 100-550°C (SK-1 modules over 280-550°C, and BT-1 modules over 100-280°C), with cold side temperature being 100°C in either case. In terms of overall duration, the lifetime considered here translates to ~ 3,535 hours of automobile use.

Based on the above-described conditions, Table 2-9 shows the lifetime and associated reduction (or non-reduction) in conversion efficiency of TE devices with time for various applications. Also, given the exploratory nature of this work, it was assumed that only the fossil fuel involved in each application was replaced by the use of TE devices (for the sake of simplicity). In a more realistic scenario, the excess electricity produced could also replace the average U.S. grid-based electricity (2015-based figure, used in this study), which in turn would influence the environmental performance of TE devices. Nevertheless, this assumption about the nature of fuel replaced can help to evaluate the environmental outcome of TE devices with respect to the various fossil fuels they seek to replace in the present era. Also, it can be partially justified by the fact that since power producers are required to adjust their power supply in line with concerned demand, there is some justification for considering that the final electricity output could be reduced at the end of power plant itself, meaning that the TE device output replaces electricity produced by parent power plant (and not the remaining grid-based electricity production).

Table 2-9: Major assumptions used in LCA studies in this work

Use scenario	Assumptions		
	Lifetime	**Reduction in conversion efficiency over time**	**Fuel replaced**
Coal-based power plant	15 years[34,54,130] (24 × 7 use) or 131,400 h	Negligible or no reduction	Coal
NG-based power plant	25 years[131–133] (4 h/day) or 36,500 h	Based on TCRC value of module	Natural gas
Automobiles	100,000 miles or ~ 3,535 h	Based on TCRC of modules in TEGs	Gasoline

2.2.1.3. End-of-Life (EOL): Scenarios

At the end of their lives, components or infrastructure associated with each of the chosen applications are treated differently. Power plants are typically dismantled into individual components that are either recycled or disposed, unless the plant is salvaged and re-mediated, or is shuttered in as-is state without generating electricity[134]. A similar nature of process is also followed for automobiles, with its components segregated into two groups, one each for recycling and disposal[135]. Hence, both these aspects – disposal and recycling – were considered while envisioning EOL scenarios for TE devices in this work.

Traditionally, TE devices are disposed of at the end of their lives[96]. Hence, this was considered as the base EOL scenario: D-scenario (or disposal). However, it is possible to segregate individual TE device components and subject them to recycling or disposal (like for power plants and automobiles). Hence, the second EOL scenario (named P-scenario or practical) involved the recycling of practically possible components like heat exchanger and alumina plates, even as other components were disposed of. Open-loop recycling was considered for recycled components in this scenario due to the paucity of data on heat exchanger recycling[64] and its actual use for alumina plates via an existing commercial process[136]. Finally, in order to enhance sustainability by incorporating the vision of circular economy, the third EOL scenario – named CE-scenario (or circular economy) – envisaged the recovery and recycling of components and materials to the highest possible degree. In addition to the recycling assumptions used in P-scenario, the 6R-based material flow approach[101] was considered for recycling TEs in CE-scenario to conserve their scarce constituents and reduce harmful effects of their mining and processing. In terms of comparison, the three EOL scenarios represent the worst (D-scenario), mid (P-scenario) and best (CE-scenario) outcomes from the normative sense of end-of-life treatment in current world.

Table 2-10 summarizes the major assumptions related to the three EOL scenarios that were chosen to evaluate their ecological benefits and pitfalls for TEs, while more details about these EOL scenarios are provided in the sub-sections below. A key assumption behind these scenarios was that TE devices were rendered unattractive at the end of their lifetime and were not used for any secondary purpose. This aspect has been later considered separately in Chapter 6 on the principles for making this platform more sustainable and ecofriendly.

Table 2-10: End-of-life (EOL) scenarios considered

End-of-life scenario	**Assumptions**	**Aspects of 6R-based approach incorporated and other LCA-related considerations**
D-scenario (Disposal)	• Base EOL treatment/scenario • All TE device components are segregated[96] and disposed of at the end of their lifetime (in landfills).	None
P-scenario (Practical)	• Heat exchanger components are entirely recycled as they are made of metals. • Alumina plates are polished and recycled (recycling rate: 90 %) via commercially used process[136]; rest 10 % is disposed off	Recovery, remanufacture and reuse – only on practical basis Open-loop recycling

	• All other components – Same as D-scenario (due to small sizes and likely degradation in TE properties)	
CE-scenario (Circular Economy)	• Heat exchanger components and alumina plates – Same as P-scenario • TE legs – Cut by 0.5 mm on either end, followed by slow re-melting and annealing of remnant portions, and then gas atomization, for reuse as mixed elemental powders • All other components – Same as D- and P-scenarios	Recovery, remanufacture and reuse – to the maximum degree possible Closed-loop recycling for TEs Open-loop recycling for other recycled components
Travel distance involved for shifting modules to disposal/recycling entities = 100 miles		

A. D-scenario (Disposal)

Here, it was assumed that all the components were sent to a residual landfill facility at the end of lifetime of device. All calculations were based on the assumption that the landfill facility could handle up to 48,000 metric tons over its lifetime, and that after its dismantling (used in Ecoinvent database[137]), modular components were transported over 100 miles (~ 160.93 km).

B. P-scenario (Practical)

Assumptions were made in this scenario regarding open-loop recycling of heat exchanger components and alumina plates. Of these, alumina plates were considered to be recycled using an existing commercial process[136] at the rate of only 90 %, since these are typically connected to TE legs using soldering or thermal spraying techniques[138], so their removal is a must prior to the recycling of these plates. Hence, it was assumed that 10 % of these plates are shaved off and disposed (like in D-scenario), while the remaining share was recycled using a three-step process: (a) Polishing and hammer mill chopping of used alumina plates; (b) Melting of alumina along with bauxite for its recovery; and (c) Hammer mill chopping of recycled alumina for reuse. Metal tabs were assumed to be disposed of (i.e., D-scenario).

Further, heat exchanger components were assumed to be entirely recovered and recycled, while all other components were considered to be disposed of, as in D-scenario. Copper-based components were assumed to be converted to secondary copper, which may be used for the same or some other application.

C. CE-scenario (Circular Economy)

For CE-scenario, it was assumed that 90 wt. % of alumina plates and heat exchanger components (like in P-scenario), as well as a significant share of TE legs (both p- and n-type) were recovered, reprocessed and recycled. For the latter, 0.5 mm of TE legs was considered to be removed on either side, and the residual leg portion was re-melted and slowly annealed for reusing back in the same module, i.e., closed-loop recycling. This portion was removed on the logic that leg portions attached to metallic tabs may not be entirely pure and could get affected by diffusion from these tabs after long years of operation[34]. Hence, it was assumed that after dismantling from modules, TE legs were cut down by removing 0.5 mm on either side (Step 1), followed by melting (and slow cooling) and gas atomization of recovered portions (Step 2) for reuse as multi-elemental powders. Other major assumptions included considering both water and argon requirements in line with the considered equipment[139]. For the remaining components, EOL treatment was in line with that used for P-scenario.

2.2.1.4. Functional Unit

To determine the functional unit (FU), the nature of application and other factors were considered. For instance, since the original assumption was to use TE modules to harvest waste heat in both coal- and NG-based power plants, and each of these modules differ in their power output and waste heat input (Table 2-4), it was assumed that each module was used as a set. Further, it was assumed that the total waste heat input power harvested by each module set was 1000 W at any point of time, with the final electricity output determined by their respective instantaneous conversion efficiency. Assuming all modules to be operated as such sets, 1 kWh of electricity generation (over their lifetime) was chosen as the FU for LCA studies on both baseload and peak load power plants.

On the other hand, for automobiles, detailed analysis on conversion efficiency of TEGs is available in literature[104,140]. Since the final objective here is fuel saving or reduce fossil fuel consumption[141], net saving of 1 liter of gasoline was considered as the FU for this study. Table 2-11 shows the respective FU considered for the three applications.

Table 2-11: Functional unit for various LCA studies

<table>
<tr><th>Application</th><th>Functional unit</th></tr>
<tr><td>Coal-based power plant</td><td rowspan="2">1 kWh of electricity generated by each module set, assumed to convert 1000 W of waste heat input power into electricity</td></tr>
<tr><td>Natural gas-based power plant</td></tr>
<tr><td>Automobiles</td><td>1 liter of net fuel saving by each TEG</td></tr>
</table>

2.2.1.5. Termination Criterion

For all aspects of this work, a termination criterion of 1 % was used to determine the significance of different TE device components and life cycle stages on each impact category.

2.2.2. Inventory Development

2.2.2.1. Production

Using the aforementioned information on processing (Section 2.2.1.1), the *first-ever exhaustive inventory till date* was developed for production of TE devices (components, modules and generators). Several assumptions were made to develop this inventory, of which prominent ones are mentioned in Table 2-8. More information on these assumptions and their underlying reasons are provided in Sections 2 of Appendix-A and 2 of Appendix-C. Further, the calculated inventory for module-related components is given in Section 2 of Appendix-A (Tables A-2–A-29), while for other TEG components, it is given in Section 2 of Appendix-C (Tables C-1–C-4).

2.2.2.2. Use

For baseload coal-based power plant, assuming negligible reduction in conversion efficiency and continuous operation over 15 years, Table A-30 shows the total amount of electricity generated by each module over its lifetime, along with their corresponding reference flow. Additional details about the use stage are provided in Section 3 of Appendix-A. On the other hand, for NG-based power plants, the total amount of electricity generated was different as it involved a different lifetime and duration of usage, as well as individual TCRCs for each module. Table B-6 shows the total amount of electricity generated by each module in this case, along with the corresponding reference flow, while additional information is given in Section 3, Appendix-B.

For automobiles, TCRC of TEG-1 was chosen to be the same as that of SK-1 modules, while for TEG-2, respective number of SK-1 and BT-1 modules was used as weighting factor to determine its TCRC. Further, a detailed set of calculations had to be implemented to determine fuel saved by use of both these generators, keeping in mind their respective masses (Table 2-7) and calculated TCRC values. This detailed procedure is described in Section 3.2 of Appendix-C.

2.2.2.3. End-of-Life

Apart from the production stage, inventory was also developed in some detail for all EOL scenarios that have been described earlier, particularly the CE-scenario – a novel contribution of this work. While a basic description of involved steps in each scenario and major assumptions is provided in Section 2.2.1.3, more information and final inventory is given in Section 4 of Appendix-A (Tables A-31–A-46) for all TE module-related components, and in Section 2 of Appendix-C for generator-related components.

2.2.3. Impact Assessment & Interpretation

Using the exhaustive inventory developed for TE devices, their environmental impacts for all aforementioned applications were quantified using the hierarchist perspective of ReCiPe 2016 midpoint method[142] using Ecoinvent 3.5 database via Simapro 9.0 software. All modules were analyzed on eight impact categories: global warming

(GW), fossil resource scarcity (FRS), human toxicity – carcinogenic (HCT) and non-carcinogenic (HNT), ecotoxicity – terrestrial (TET), freshwater (FET) and marine (MET), and mineral resource scarcity (MRS). While FRS and GW were chosen as TEs are justified primarily on grounds of lowering the use of scarce fossil fuels and associated GHG emissions[141], other categories were considered due to scarcity and toxicity concerns of constituent elements in most TEs[56,57].

For each TE device, major impact contributors were identified for the production stage, and reasons behind their prominent contribution were determined using the exhaustive inventory. Subsequently, ecological impacts of all TE devices were studied across their entire life cycle for each considered application. In case of TE modules (used in power plants), the effect of optimal operational temperature range of these modules on ecological performance of this platform was analyzed. Conversely, for automobiles, the performance of both generators was compared for the chosen functional unit. Further, the benefits and pitfalls of all three EOL scenarios on environmental performance of TE devices was also evaluated.

CHAPTER THREE

ECOLOGICAL PROFILE OF THERMOELECTRICS FOR CONTINUOUS WASTE HEAT EMITTING APPLICATIONS

3. Results & Discussion

3.1. Impact Assessment: Results

3.1.1. Impacts: Production Stage

Table 3-1: Characterized impacts of TE modules (per one module)

Impacts	**Unit**	**BT-1**	**BT-2**	**SK-1**	**SK-2**	**HH**	**PT**	**SC**
GW	kgCO_2-eq	25.70	104.48	59.93	126.93	10.61	3.95	9.50
TET	kg 1,4-DCB eq	121.44	73.51	38.03	92.69	9.33	3.02	14.11
FET	kg 1,4-DCB eq	2.30	1.74	5.74	17.38	0.40	0.06	0.63
MET	kg 1,4-DCB eq	3.39	3.13	8.38	25.00	0.61	0.10	0.94
HCT	kg 1,4-DCB eq	1.15	3.08	2.75	6.84	0.39	0.12	0.98
HNT	kg 1,4-DCB eq	80.52	54.79	198.29	603.59	13.22	1.72	21.40
MRS	kg Cu-eq	0.31	0.18	0.17	0.57	0.10	0.02	1.06
FRS	kg oil-eq	6.85	27.01	15.53	32.85	2.74	1.02	2.54

The first objective is to analyze production-related impacts of TE modules by identifying prominent impact contributors and understanding reasons for their significant contribution. Table 3-1 shows characterized impacts of modules (per-module basis), while

Figure 3.1(a-g) shows the contribution of individual components to their impacts (scaled to 100 %) during production.

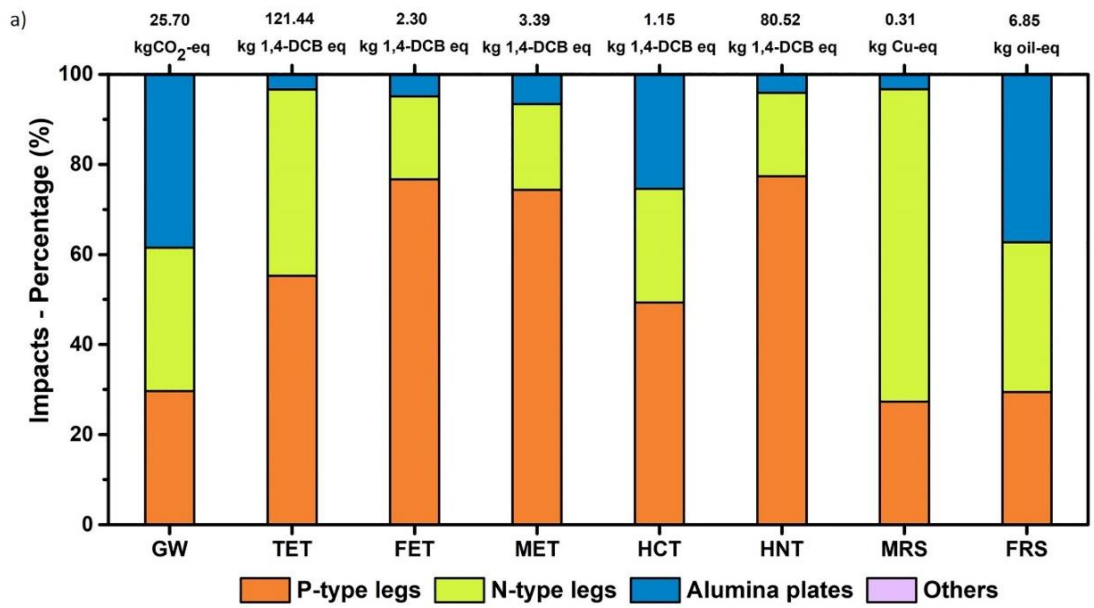

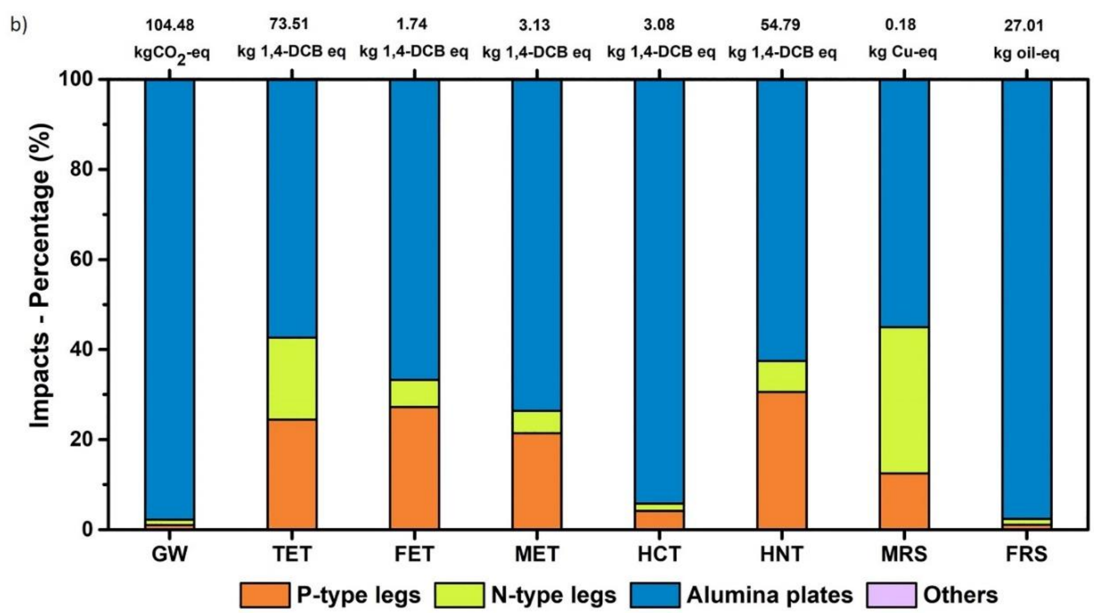

c)

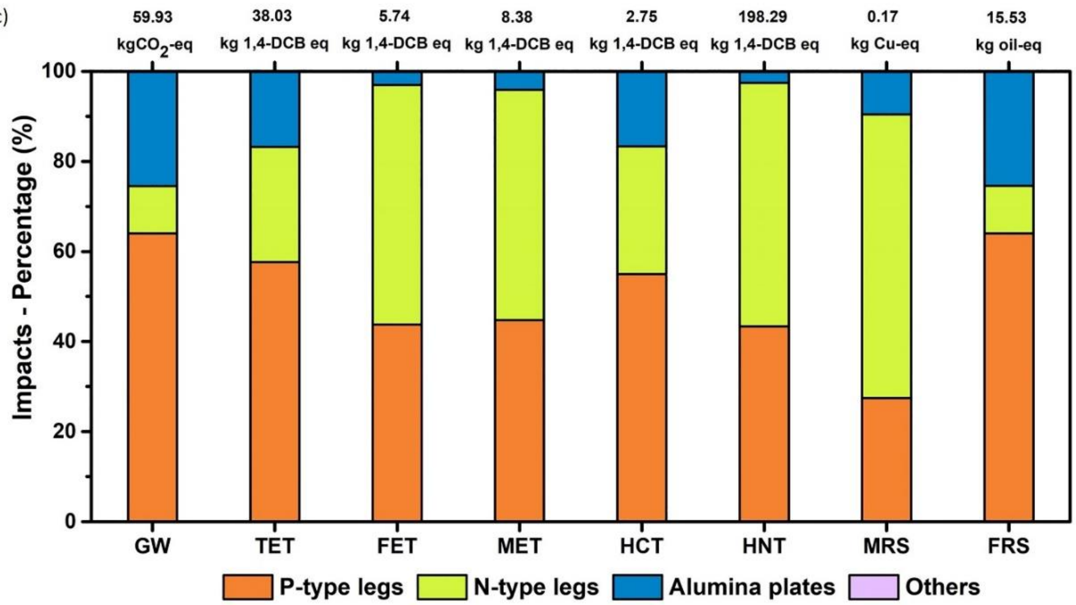

59.93
kgCO2-eq
38.03
kg 1,4-DCB eq
5.74
kg 1,4-DCB eq
8.38
kg 1,4-DCB eq
2.75
kg 1,4-DCB eq
198.29
kg 1,4-DCB eq
0.17
kg Cu-eq
15.53
kg oil-eq
Impacts - Percentage (%)
100
80
60
40
20
0
GW
TET
FET
MET
HCT
HNT
MRS
FRS
P-type legs
N-type legs
Alumina plates
Others

d)

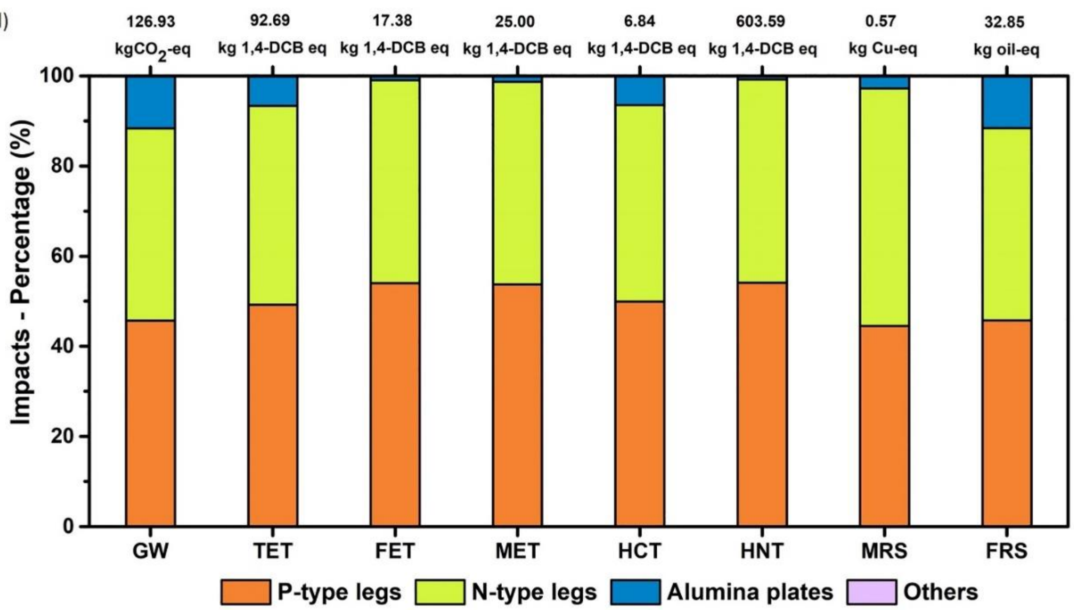

126.93
kgCO2-eq
92.69
kg 1,4-DCB eq
17.38
kg 1,4-DCB eq
25.00
kg 1,4-DCB eq
6.84
kg 1,4-DCB eq
603.59
kg 1,4-DCB eq
0.57
kg Cu-eq
32.85
kg oil-eq
Impacts - Percentage (%)
100
80
60
40
20
0
GW
TET
FET
MET
HCT
HNT
MRS
FRS
P-type legs
N-type legs
Alumina plates
Others

e)

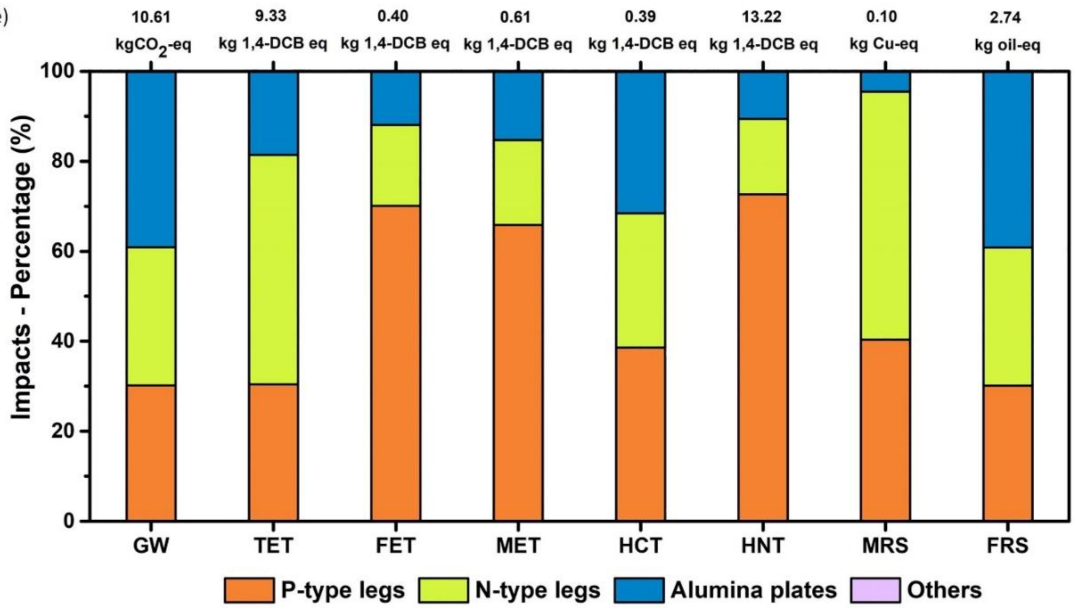
10.61
kgCO2-eq
9.33
kg 1,4-DCB eq
0.40
kg 1,4-DCB eq
0.61
kg 1,4-DCB eq
0.39
kg 1,4-DCB eq
13.22
kg 1,4-DCB eq
0.10
kg Cu-eq
2.74
kg oil-eq
Impacts - Percentage (%)
0
20
40
60
80
100
GW
TET
FET
MET
HCT
HNT
MRS
FRS
P-type legs
N-type legs
Alumina plates
Others

f)

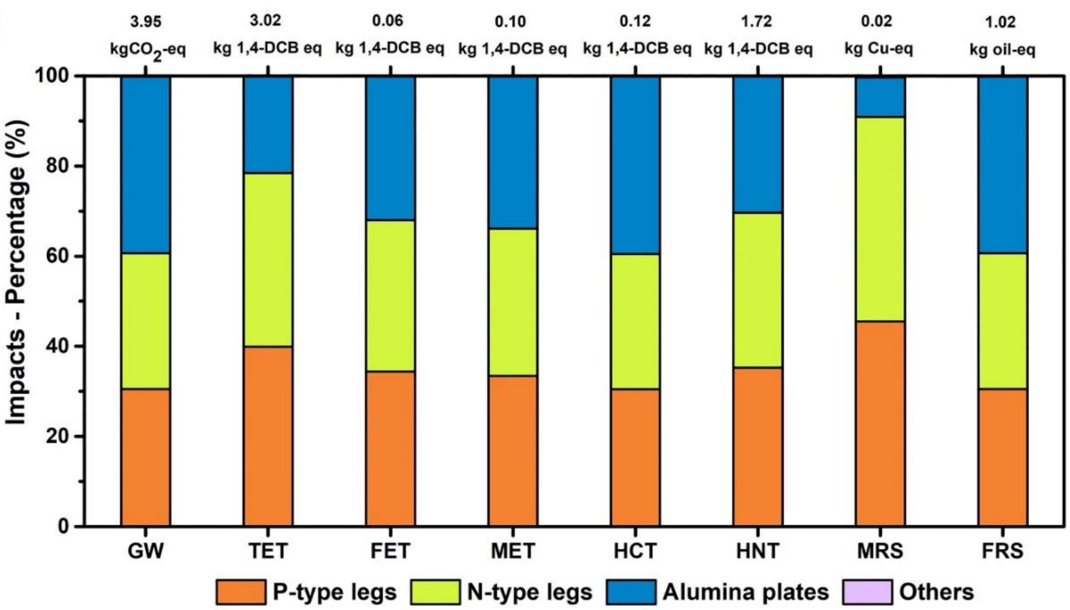
3.95
kgCO2-eq
3.02
kg 1,4-DCB eq
0.06
kg 1,4-DCB eq
0.10
kg 1,4-DCB eq
0.12
kg 1,4-DCB eq
1.72
kg 1,4-DCB eq
0.02
kg Cu-eq
1.02
kg oil-eq
Impacts - Percentage (%)
0
20
40
60
80
100
GW
TET
FET
MET
HCT
HNT
MRS
FRS
P-type legs
N-type legs
Alumina plates
Others

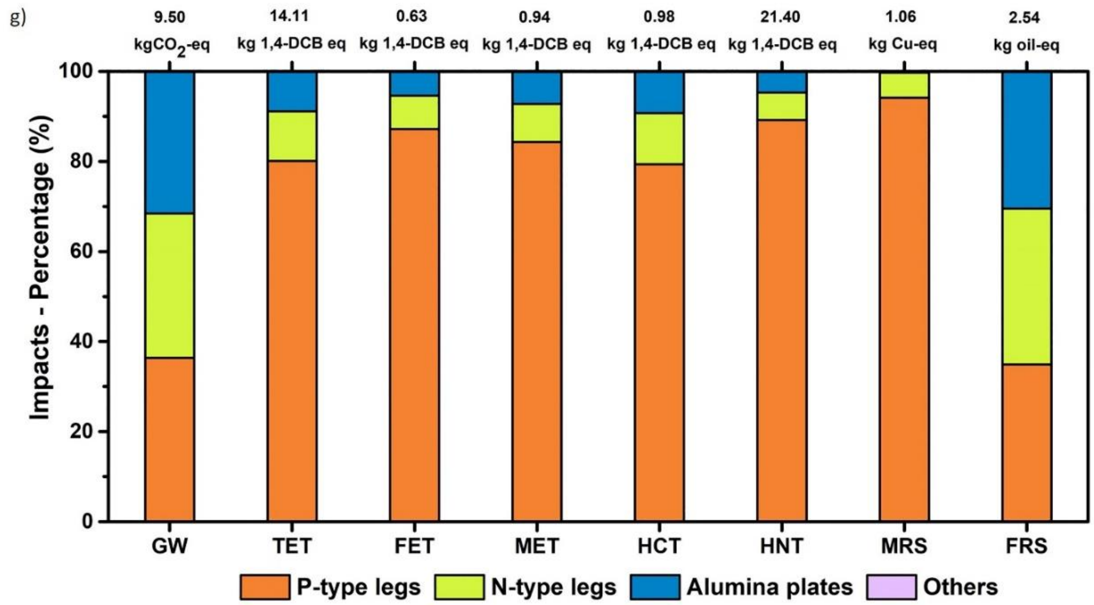

Figure 3.1: Environmental impacts of producing: (a) BT-1 module; (b) BT-2 module; (c) SK-1 module; (d) SK-2 module; (e) HH module; (f) PT module; and (g) SC module. Impacts are scaled to 100 % on respective units. Values at the top of each bar are characterized impacts.

3.1.1.1. BT-1 Module

For BT-1 (Figure 3.1(a)), p-type legs are observed to be the biggest contributor on five categories (TET, FET, MET, HCT and HNT), while n-type legs are seen to play a similar role on MRS category. On the remaining three impacts, both TE legs and alumina plates exhibit noteworthy contributions (≥ 20 % each).

Regarding toxicity-related categories, the prominence of TE legs is mainly because of the use of antimony (in p-type legs) and tellurium (in both legs) (Step 1, Tables Table A-2 and A-3), and their relationship with copper. Tellurium is produced from copper ores[143,144], while antimony is extracted and processed from stibnite ore via similar methodology as that used for copper[143]. Copper beneficiation leads to the emission of toxic sulfidic tailings that are stored in heaps/ponds, from where they seep into soil (TET) and water bodies (FET, MET), and also increase human-related toxicity levels (HCT and HNT)[143,145–148]. Also, since antimony has a greater role than tellurium, its use in p-type legs (~ 30 wt. %; Step 1, Table A-2) explains their higher contribution than n-type legs on these impacts.

On the other hand, scarcity of bismuth and tellurium has a predominant effect on MRS impact of TE legs, with bismuth being highly impactful of the two elements. As a result, n-type legs are more influential given their higher use of bismuth (~ 54 wt. %; Step 1,

Table A-3) over p-type counterparts (~ 13 wt. %; Step 1, Table A-2). Lastly, extensive amount of fossil-based electricity is used to process both TE legs and alumina plates, especially during the dicing of TE legs (Step 7, Tables A-2 and A-3) and sintering of alumina powders (Step 2, Table A-4). This consumes large amount of fossil fuels (FRS) and produces large emission of GHGs (GW) and toxic waste during coal mining (HCT).

3.1.1.2. BT-2 Module

Unlike BT-1, alumina plates are the most influential of all components for BT-2, with TE legs having a notable role (≥ 10 %) on only five impacts (TET, FET, MET, HNT and MRS) (Figure 3.1(b)).

Given the similarity in chemical composition of BT legs (Table 2-1) and processing of alumina plates for both BT modules (Tables A-4 and A-8), these observations are entirely explained by the same reasons as those described for individual components of

BT-1. However, the predominance of alumina plates for BT-2 is solely due to use of fewer processing steps (and thereby, associated energy requirement) for TE legs (Tables A-6 and A-7) than in BT-1 (Tables A-2 and A-3). In fact, this predominance extends to all impact categories, with coal-based electricity (CBE) also affecting water bodies through toxic waste emissions during coal mining (FET, MET) and increasing non-carcinogenic toxicity levels (HNT)[149–151]. Moreover, CBE generation also causes emission of heavy metals like mercury and chromium, which increases both soil/land-related (TET) and cancer-related human toxicity (HCT)[150,152–154].

Remarkably, on almost all categories, BT-2 has comparable or higher impact than BT-1 (Table 3-1). This is because: (a) Mass of BT-2 is nearly twice that of BT-1; and (b) Alumina plates have a much higher mass share in BT-2 (51.40 %) than BT-1 (38.70 %) (Table 2-3), which increases their overall role in harmful effects of this module.

3.1.1.3. SK-1 Module

Unlike BT-2, TE legs play the biggest role on all impacts for SK-1, with alumina plates consigned to notable roles (≥ 10 %) on only five categories (GW, FRS, TET, HCT and MRS) (Figure 3.1(c)). The predominance of TE legs is mainly due to heavy use of antimony (≥ 85 wt. % in both legs; see Step 1, Tables A-10 and A-11) and its resultant ecological impact (explained in Section 3.1.1.1).

Interestingly, although both TE legs have similar antimony content, p-type SK legs exhibit higher impacts on four categories (GW, FRS, TET and HCT), with n-type legs dominating on the other four impacts (FET, MET, HNT and MRS). The former supremacy of p-type legs is due to higher electricity usage for its processing, especially because of using energy-intensive steps like annealing and hot-pressing of p-type powders (Steps 6, 9 and 11, Table A-10), than for n-type legs (Table A-11). Such dominance seems remarkable, as p-type powders are annealed for shorter duration (10 days) than n-type powders (14 days). Nevertheless, it can be ascribed to use of quartz tubes for annealing p-type powders, which severely limits the amount of material that can be annealed in a single run of furnace. This raises the quantum of electricity needed to process the desired amount of powder, and thereby, its associated harmful effects (see Section 3.1.1.1), including toxic slag emitted while processing metal for building transmission infrastructure (TET).

Conversely, higher influence of n-type legs on remaining four impacts is linked to their larger share in mass of SK-1 (Table 2-3). This increases the amount of antimony used, and thereby, its toxicity-related impacts (FET, MET and HNT; see Section 3.1.1.1). On the remaining MRS impact, n-type legs are prominent due to the use of cobalt as constituent element (~ 85 % impact share). Cobalt ore is considered to be scarcer than that for antimony or most other TE constituent elements in Ecoinvent database[143,155], which explains its role. Lastly, electricity consumed to process individual components also accounts in substantial measure on toxicity-related impacts through coal mining-related toxic waste emissions (FET, MET, HCT and HNT).

3.1.1.4. SK-2 Module

Like for SK-1, TE legs predominantly account for all impacts of this module. However, there is one key difference: unlike SK-1, alumina plates are seen to be insignificant (< 10 %) on all impacts barring GW and FRS (Figure 3.1(d)). While the influential role of TE legs stems from similar reasons as those for SK-1, electricity contributes more to some of the toxicity-related impacts (such as TET and HCT). This is because more amount of electricity is required to process TE legs in SK-2, especially n-type legs (Table A-15), whose processing-related electricity usage is ~ 11 times that in SK-1 (Table A-11). This is mainly due to much higher electricity consumption (> 100 kWh/kg output) for annealing and hot pressing of n-type powders in SK-2 (Steps 3 and 7, Table A-15), while processing steps for its counterpart in SK-1 need ≤ 60 kWh/kg (Table A-11). Also, cobalt accounts predominantly for these legs' role on MRS impact for reasons described earlier (see Section 3.1.1.1).

Strikingly, characterized impacts of SK-2 module are 2-3 times that of SK-1 module on all categories (Table 3-1). This observation, as well as the minor role of alumina plates on most impacts, are explained mainly by three reasons. First, although the antimony content of p- and n-type legs is similar in both SK modules (~ 83-85 wt. %; Step 1 in Tables A-10, A-11, A-14 and A-15), TE legs have a higher mass share in SK-2 (~ 80 %) than SK-1 (~ 57 %) (Table 2-3). Second, the mass of SK-2 module is more than twice that of SK-1 (Table 2-3), which significantly enhances its impact on every category. Finally, more electricity is required to process TE legs in SK-2 module.

3.1.1.5. HH Module

Both p- and n-type legs are important on all categories for HH, as are alumina plates (≥ 10 % impact share) on all impacts except MRS (Figure 3.1(e)). P-type legs dominate on three toxicity categories (FET, MET and HNT), primarily through use of antimony (~ 30 wt. %; Step 1, Table A-18) as constituent element (see Section 3.1.1.1 for reasons). Alternatively, n-type legs are more influential on two other impacts (TET and MRS), largely due to use of nickel (~ 20 wt. %), tin (~ 40 wt. %) and hafnium (~ 30 wt. %) as constituent elements (Step 1, Table A-19). Of these, both nickel and hafnium contribute to TET through the respective emission of: (a) Sulfidic tailings during joint production of nickel and copper via ore beneficiation[143] (see Section 3.1.1.1); and (b) Harmful wastes during zirconium oxide production (on-route to hafnium processing) and coal mining prior to CBE generation for use in processing[143]. Conversely, tin and nickel are scarcer elements than other constituents, and are hence, more important for MRS impact of n-type legs, with cobalt and tin playing a similar role for p-type legs on this category. Lastly, apart from alumina powder sintering, large amount of electricity is consumed to process TE legs, especially during arc melting and hot pressing of powders for both TE legs (Steps 2 and 4, Tables A-18 and A-19). This explains the impact of different components on three categories (GW, FRS and HCT) (see Section 3.1.1.1).

3.1.1.6. PT Module

Barring MRS, both p- and n-type legs, as well as alumina plates, exhibit noteworthy contributions (≥ 20 %) on all impacts (Figure 3.1(f)). This is significantly different from other modules like SK-2 and can be attributed to the relatively higher mass share of alumina plates in this module (~ 41 %). On three categories (GW, FRS and HCT), such contributions are explained by the energy-intensive processing of individual components, particularly annealing and hot pressing of TE powders (Steps 3 and 5, Tables A-22 and A-23). Contrastingly, on toxicity-related impacts, impact contributions of TE legs stem from critical roles of tellurium (~ 38-39 wt. % in both legs; Step 1, Tables A-22 and A-23) and high processing-related electricity consumption. The underlying mechanisms through which tellurium and electricity affect environment have been provided earlier (see Sections 3.1.1.1 and 3.1.1.2). Further, the use of cobalt in diffusion barriers for both TE legs enhances their influence (~ 45.5 % impact share) on MRS category.

3.1.1.7. SC Module

Unlike the other modules, p-type legs are the predominant contributor (≥ 75 %) on six impacts (all except GW and FRS) (Figure 3.1(g)). Conversely, TE legs (p- and n-type) and alumina plates show significant, near-equal contributions on GW and FRS categories.

For GW and FRS impacts, the observations are explained by noteworthy mass share (~ 35 %) of alumina plates and high processing-related electricity use (reasons provided in Sections 3.1.1.1 and 3.1.1.2). Here, electricity is consumed during the sintering of alumina plates (Step 2, Table A-28), as well as in induction melting and SPS of TE powders (Steps 2 and 5, Tables A-26 and A-27).

On the remaining impacts, predominance of p-type legs is mainly due to its constituent elements. For instance, germanium is processed from zinc leaching residue generated during zinc smelting, and the associated toxic emissions generated in this process seep into soil/land and increase its toxicity (TET)[156,157] Similarly, molybdenum – a co-product of copper production[156] – also affects the environment (FET, MET and HNT) via toxic sulfidic tailings (as explained in Section 3.1.1.1). Additionally, manganese causes cancer-related toxicity via heavy metal emissions associated with its extraction and processing, especially through the slag emitted to process steel and copper for equipment used for manganese production[143]. Lastly, the scarcity of germanium ore leads to its predominant contribution on p-type legs' share of MRS impact. Remarkably, n-type legs have a modest role (< 15 %) on these impacts, partly due to the absence of these elements.

3.1.2. Impact: Life Cycle

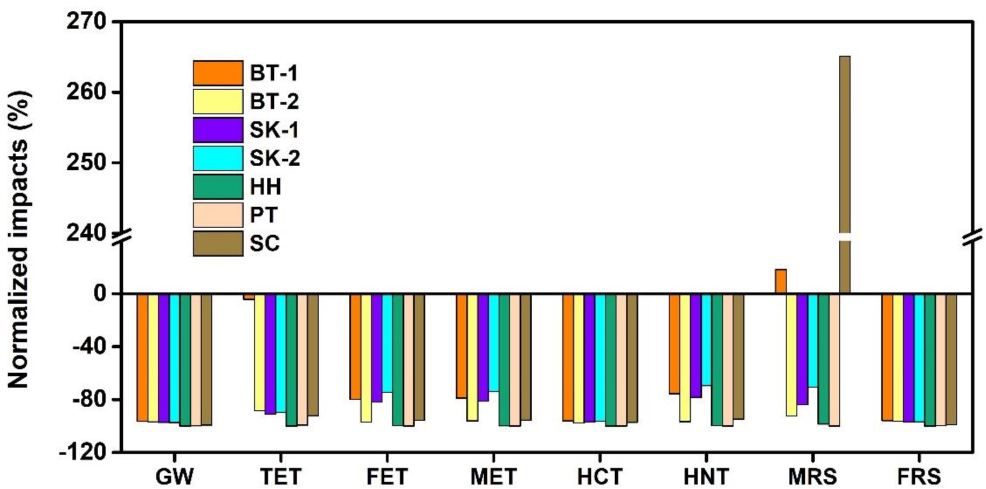

Figure 3.2: Life cycle impacts of TE modules, normalized by impacts of HH module

Apart from their production, this study also aims to understand the life cycle impacts of all modules upon use in baseload coal-based power plants as modular sets, while also understanding the effect of operational temperature range on ecological performance of modules. Hence, Figure 3.2 shows the normalized life cycle impacts of all modules for chosen functional unit for D-scenario (base EOL scenario), while Section 5 of Appendix-A presents the characterized impacts of all modules, segregated by contributions from individual life cycle stages. Here, any positive magnitude (impacts > 0 %) indicate harmful environmental effects, while negative magnitude (impacts < 0 %) are beneficial to ecology.

3.1.2.1. D-scenario (Disposal)

As can be seen (Figure 3.2), barring BT-1 and SC modules on MRS category, all modules show net positive effects on environment on all impacts. This is mainly due to the predominant beneficial effect of use stage of these modules, based on the assumption that only CBE (coal-based electricity) is replaced by their application. This in turn lowers the need for CBE generation from baseload plant, and thereby, its associated impacts. The avoided impacts include the non-emission of toxic wastes during coal mining and electricity generation, avoidance of using scarce coal as well as nickel and cobalt in steel equipment for electricity generation, and finally, non-emission of GHGs. This easily compensates for any harmful ecological effects caused by module production, typically by margins of 70-80 % on most impacts, and by 90-95 % on some impacts. Interestingly, the disposal stage has negligible influence on any impact for all modules, highlighting its irrelevance in shaping their ecological outcomes. Further, a comparison of these modules – or more appropriately, a comparison of their ecological performance in light of variation in their optimal operational temperature range – shows little difference in their overall positive effect on five categories. These are: (i) GW: 1.16-1.21 kg CO_2-eq; (ii) FET: 0.015-0.020 kg 1,4-DCB eq; (iii) MET: 0.021-0.028 kg 1,4-DCB eq; (iv) HCT: 0.047-0.049 kg 1,4-DCB eq; and (v) FRS: 0.262-0.274 kg oil-eq (Figure 3.2 and Tables A-47–A-53). This indicates that on most of the considered impacts, the nature of TE system (and their functional temperature range) has marginal effect on overall outcome of this platform.

In contrast, these modules show variation in performance on the three remnant categories (TET, MRS and HNT), all of which are related to the constituent elements used in TE legs. On TET, BT-1 shows the least positive benefit (0.010 kg 1,4-DCB eq), with other modules exhibiting a near-similar output (0.20-0.23 kg 1,4-DCB eq) (Figure 3.2 and Tables A-47–A-53). This divergence is due to toxic heavy metal emissions during the generation of CBE used to produce tellurium – a constituent element of TE legs for this module. On the other hand, for HNT, three modules show a lower range of positive benefits (BT-1, SK-1 and SK-2: 0.406-0.458 kg 1,4-DCB eq) than the other four modules (0.555-0.585 kg 1,4-DCB eq) (Figure 3.2 and Tables A-47–A-53). This is mainly due to the use of antimony as constituent element in TE legs of these modules, which accounts for higher negative effects of their production. Finally, on MRS category, two modules (BT-1 and SC) have negative environmental impacts (positive in magnitude) (Figure 3.2 and Tables A-47–A-53) as their production inflicts greater ecological harm than the positive benefits achieved by their electricity generation capabilities. Of these two modules, SC is more harmful due to the use of germanium and tin as constituents in p- and n-type legs respectively, for both elements are scarcer than all other constituents used in TE legs of chosen modules. Predictably, BT-2 does not show similar effects as BT-1 on these three categories due to the much lower mass share of TE legs for this module (Table 2-3).

Overall, HH and PT modules are observed to be most ecofriendly, which is expected given their better TE properties and high operational temperature range (Table 2-4). The converse logic also holds true for BT-1, which is seen to be the least ecofriendly by showing negative ecological effects on three categories (TET, HNT and MRS). Nevertheless, for the most part, it can be said that independent of the TE system chosen, beneficial effects can be obtained by use of TEs for continuous use-based applications where polluting fossil fuels like coal are used.

3.1.2.2. EOL Scenarios: A Comparison

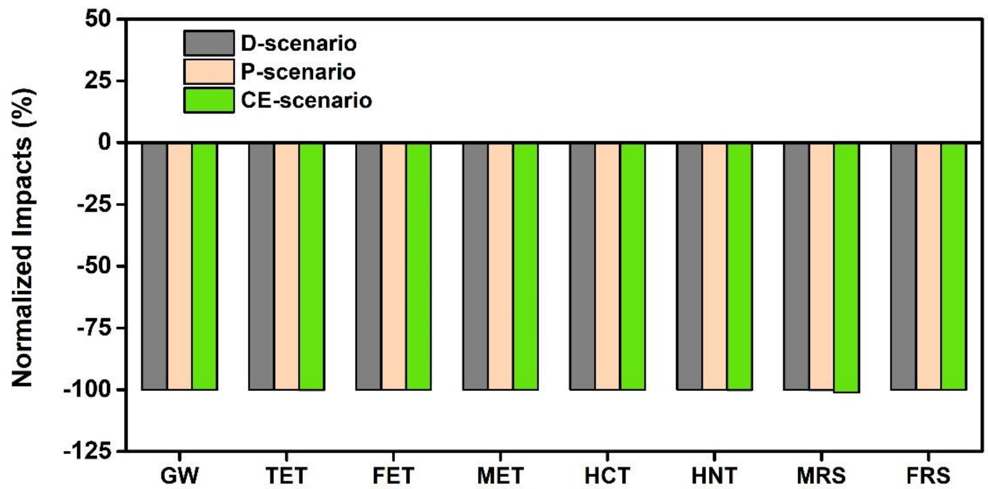

Figure 3.3: Life cycle environmental impacts of HH module under different EOL scenarios (normalized to impact under baseline D-scenario)

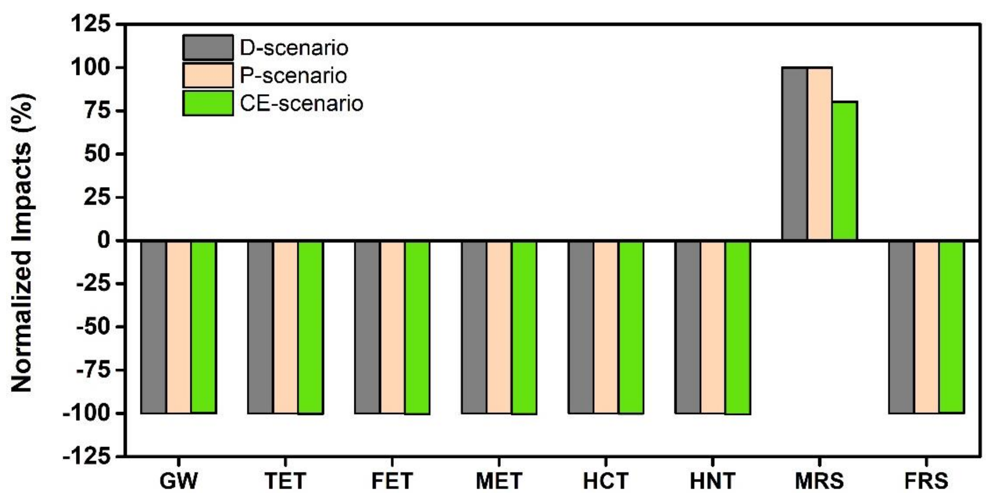

Figure 3.4: Life cycle environmental impacts of SC module under different EOL scenarios (normalized to impact under baseline D-scenario)

Figures 3.3 and 3.4 respectively compare the impacts of HH and SC modules respectively (as examples) for the three EOL scenarios, while Figures A.2–A.6 show the same for other five modules. Further, Tables A-54–A-60 present the characterized impacts of P-scenario, while Tables A-61–A-67 show the same for CE-scenario. As can be seen from all this data, P-scenario shows little change vis-à-vis D-scenario for all modules on each considered impact. This clearly demonstrates the negligible influence of alumina recycling in shaping ecological performance of chosen modules. A similar observation can also be made for CE-scenario on most impacts of these modules. However, the circular economy approach enables notable reduction (≥ 5 %) in certain cases, namely, TET (BT-1); FET, MET and HNT (SK-2); and MRS (BT-1, SK-2 and SC) (Figures A.2, A.5 and 33.3, and Tables A-47–A-67). All these variations are the outcome of recycling TE powders as this helps conserve scarce constituent elements and thereby, lowers associated impacts caused by their mining and processing. This is particularly true for toxicity-related impacts of antimony (SK-2) and tellurium (BT-1), as also for scarcity-related effects of cobalt (SK-2), bismuth (BT-1) and germanium and tin (SC). However, regardless of the considered EOL scenario, no variation is observed in relative order of ecofriendliness of modules.

3.2. Discussion

3.2.1. Module Production

Two factors clearly stand out in influencing production-related impacts of all modules: constituent elements used in TE legs, and high processing-related electricity consumption (Table 3-1 and Figure 3.1). Among these factors, the role of constituent elements, especially on toxicity-related impacts, is mainly due to the use of specific elements, such as antimony (BT and SK modules), tellurium (BT modules), cobalt (SK modules), and germanium, tin and manganese (all in SC module). Interestingly, some of these elements have been highlighted for their toxicity elsewhere[49,56,57,141], which raises valid concerns about the toxic nature of this platform. However, the results indicate that apart from these concerns related to elemental toxicity, life cycle toxicity of constituent elements – i.e., emission of toxic wastes during the mining and processing/refining of these elements – is an equally compelling issue that needs to be addressed.

Contrastingly, the large influence of processing-related electricity consumption stems mainly from the key role of specific processes and associated parameters – clearly an outcome of the detailed inventory developed in this work. Such processes include hot pressing and spark plasma sintering (SPS), induction or arc melting, and annealing of samples in quartz or silica tubes (like in SK-1). These processes consume large amounts of energy, either due to the energy-intensive nature of equipment used (like in hot pressing or SPS), large process times (like for sintering alumina powders, or annealing of TE legs in SK modules), or by limiting the amount of material for heating in a single furnace run (like by using quartz tubes for SK modules). Some of this energy consumption can be reduced by use of equipment that can process sintered samples of larger dimensions, but the dominance of this step suggests a strong need for more efforts on other aspects, like finding an alternative large-scale process to annealing of powders in quartz tubes.

3.2.2. Module: Life Cycle Performance

With regard to their life cycle performance, all modules are seen to be beneficial on the typical impacts on which their use is primarily justified – GW and FRS – irrespective of the TE material used (Figures 3.1–3.4, A.2–A.6 and Tables A-47–A-67). Further, since the life cycle GW impact of any product is reflective of energy consumed over its lifetime as most energy needs are met using fossil fuels, the positive GW benefit of all modules shows that TEs are a net energy-saving platform, independent of the material used.

On the other hand, a remarkable result is that despite the repeated concerns raised about toxicity of constituent elements for most TEs[49,56,57,141] the chosen modules are seen to benefit the environment on almost all toxicity-related impacts (barring TET for BT-1) (Figures 3.1–3.4 and A.2–A.6). Such divergence stems from the limited focus of researchers on elemental toxicity vis-à-vis the expanded focus of LCA methodology to accommodate life cycle toxicity (described in Section 3.2.1). Like for GW and FRS impacts, ecological effectiveness of all modules on toxicity-related impacts stems from the benefits achieved by avoiding coal-based electricity generation. Yet, such benefits are not always seen for the other prevailing concern with TE systems: scarcity of constituent elements, with two modules showing negative effect on MRS (BT-1 and SC).

Finally, among all the EOL scenarios considered in this work, both D- and P-scenarios are completely irrelevant in influencing the environmental performance of any module (Figures 3.1–3.4 and A.2–A.6). On the other hand, CE-scenario is seen to ameliorate impacts by a notable degree (≥ 10 %) on five categories across three modules: TET for BT-1; FET, MET and HNT for SK-2; and MRS for BT-1, SK-2 and SC, but has negligible effect in other cases. This implies that recycling of constituent elements may not always be a panacea for improving the ecological outcomes of TE materials or devices. Hence, the effectiveness of circular economy approach must be evaluated on a case-by-case basis, especially for other TEs that have not been analyzed in this work.

3.3. Life Cycle Impacts: Module vs Generator

A key assumption of this study is the exclusion of thermoelectric generator-specific components, especially heat exchanger, from the overall inventory. This can seem an issue, given that heat exchanger materials, particularly steel, have been observed to play an influential role on ecological impacts of TE generators elsewhere[98]. Nevertheless, the use stage is seen to significantly overpower the harm caused during production and EOL of modules on almost all impacts, independent of the EOL scenario considered (Figures 3.1–3.4 and A.2–A.6). Such wide difference – involving margins of ~ 70-75 % on most impacts – increases the likelihood of the larger outcome of net-ecofriendliness of thermoelectrics, even at the level of TE generators. For further validation though, the effects of heat exchanger must be carefully looked at – this has been done later in Chapter 5.

3.4. Ecofriendly Potential & Lessons for Stakeholders

The most noteworthy observation from this work is that barring in certain cases, the positive ecological benefits of use stage are observed to be significantly larger than the harmful effects of both production and EOL stages for chosen TE modules. This is remarkable given the paucity of information large-scale process parameters, which meant that parameters more suitable for lab/small-scale production were used for key energy-intensive processing steps, such as hot pressing and spark plasma sintering (Section 2, Appendix-A). In other words, the results of this study already account for a more energy-intensive module production. Since commercial production of TE modules is expected to have lower energy consumption than at lab/small-scale, it is highly probable for these results to also extend to real-life scenarios. Further, irrespective of their suggested operational temperature range (2-4), barring few exceptions, all of them exhibit positive benefits (Figures 3.1–3.4 and A.2–A.6). Together, these observations suggest that irrespective of the TE system employed, this platform is ecofriendly enough to be used to harvest waste heat in applications where coal is used as fuel and waste heat is constantly emitted, provided the desired temperature range is available for operation. Such applications can include both coal-based power plants, as well as industries like steel.

Apart from aforementioned results, the strong ecological credentials of TEs are further buttressed by a comparison of their performance with those of two widely used renewable energy technologies – wind-based and solar-based electricity (Table A-68). For instance, TE modules exhibit GHG emission reduction of ~ 1.16-1.21 kg CO_2-eq by replacing coal-based electricity in base EOL scenario (D-scenario). Strikingly, this is in line with GHG emission reduction achieved using both solar- (1.15 kg CO_2-eq) and wind-based electricity (1.2 kg CO_2-eq) as alternatives to coal-based electricity on per-kWh basis (same as functional unit chosen in this study) (values obtained from Simapro for US grid at plant)[137,142]. Similar results are observed for other categories as well barring two: TET and MRS (Table A-68). Of these, toxic emissions during production of highly pure silicon wafers for solar PV panels explains the high impact of solar-based electricity on TET (based on Simapro results)[142]. In contrast, both solar- and wind-based electricity require scarce elements – silicon for solar and nickel in steel for electricity generation equipment for wind (based on Simapro)[142]– which explains their respective impacts on MRS category. Admittedly, these results do not consider the absence of heat exchanger components, that could lower the beneficial effects of modules by reducing system conversion efficiency. Nonetheless, even if half of the estimated gains can be attained from these modules, it would amount to achieving ~ 50-60 % of benefits currently reaped from renewable energy. Moreover, these gains may well be achieved at a much lower cost compared to that of replacing fossil-based electricity with their renewable-based counterparts, whose erratic availability currently inhibits their use for meeting baseload power demand. In sum, all these results suggest the strong ecological relevance of TEs as an energy harvesting platform. Further, it also indicates a strong footing for thermoelectrics to join forces not only with existing renewable energy forms, but also with those likely to emerge in future (such as geothermal energy) towards ameliorating global environmental challenges[24].

CHAPTER FOUR

ECOLOGICAL PROFILE OF THERMOELECTRICS FOR PERIODIC WASTE HEAT EMITTING APPLICATIONS

4. Results and Discussion

4.1. Impact Assessment: Results

4.1.1. Impacts: Life Cycle

4.1.1.1. D-Scenario

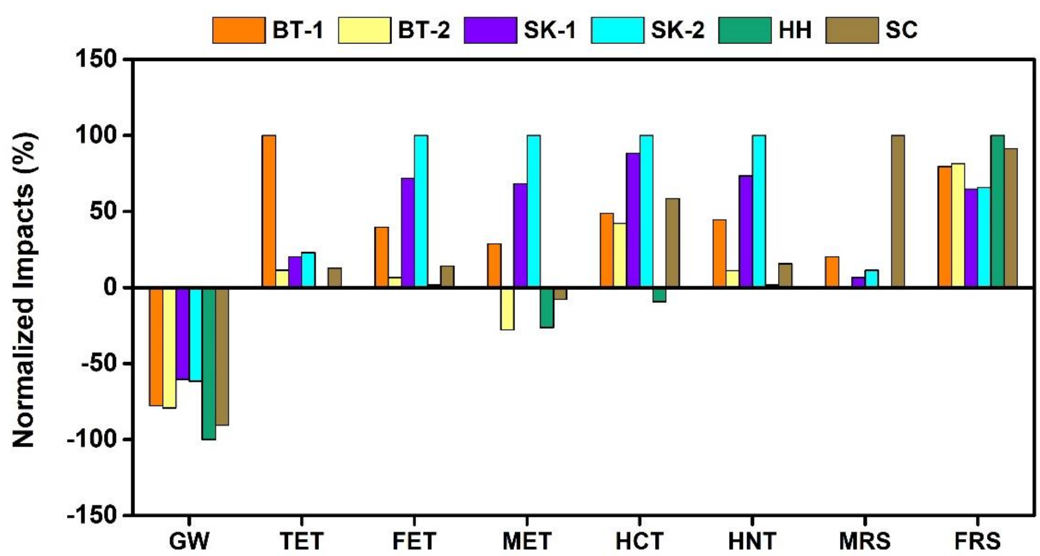

Figure 4.1: Life cycle impacts of various modules (D-scenario), normalized by the highest or lowest impact among these modules

Figure 4.1 shows the life cycle impacts of chosen modules, while Tables B-7–B-12 show their respective characterized impacts – all for the base EOL scenario (i.e., D-scenario). As can be seen, no TE module is observed to be ecologically beneficial on all impact categories, i.e., they do not show positive effects on all eight impacts.

Among the considered categories, all six modules are beneficial on GW and FRS impacts, with the benefits through their electricity generation overpowering the impacts caused during their production and EOL by a large degree (~ 59-97 %, depending on the module) (Figure 4.1 and Tables B-7–B-12). In terms of magnitude, these modules lower overall impact by 0.47-0.78 kg CO_2-eq (GW) and by 0.15-0.23 kg oil-eq (FRS). In contrast, no module exhibits positive benefits on all other categories, as their production stage is degrading enough for environment to overcome any ecological benefits accrued during the use stage. In particular, the gap between production (negative impact) and use stages (positive impact) for all six modules is vast on two categories: FET (~ 78-100 %, final impact: 0.001-0.044 kg 1,4-DCB eq) and HNT (~ 70-100 %, final impact: 0.021-1.528 kg 1,4-DCB eq). For the other four categories, barring HH (on TET, MET and HCT) and both BT-2 and SC modules (on MET alone), all modules exhibit negative performance, with a gap of ~ 50-100 % between their production and use stages. Also, the EOL stage (disposal) has negligible effect on any category (Figure 4.1 and Tables B-7–B-12). The reasons for production-related impacts of various modules is described in Chapter 3.

In the earlier work on coal-based power plants (Chapter 3)[158], the nature of modules chosen is seen to be inconsequential for life cycle impacts of this platform, as they replace a polluting form of electricity (coal-based). However, the nature of modules is seen to play an important role in this work, with HH showing the highest extent of beneficial effects. In contrast, different modules exhibit the worst performance on various categories, such as

SK on six impacts (all barring TET and MRS), BT-1 on TET and SC on MRS category (Figure 4.1 and Tables B-7–B-12).

4.1.1.2. EOL Scenario: A Comparison

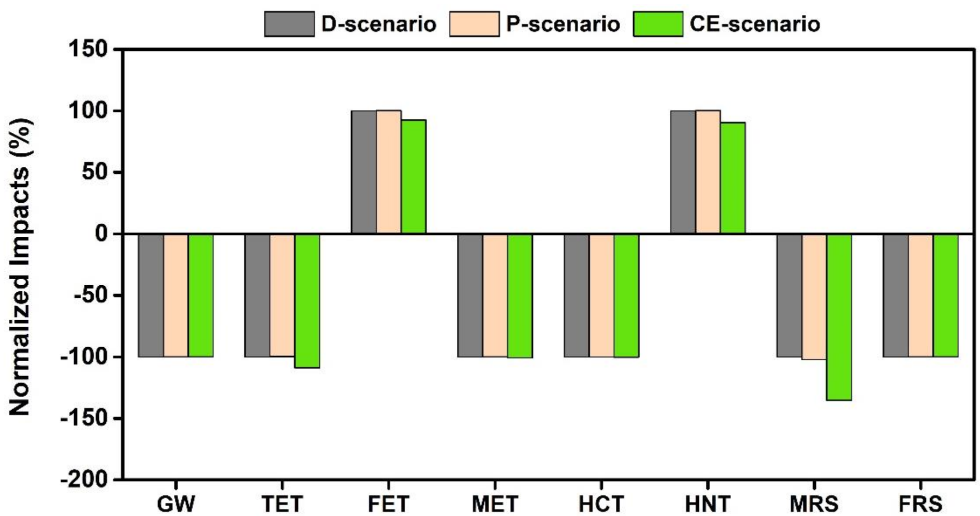

Figure 4.2: Comparison of life cycle impacts of HH module under various EOL scenarios (normalized by impact of D-scenario)

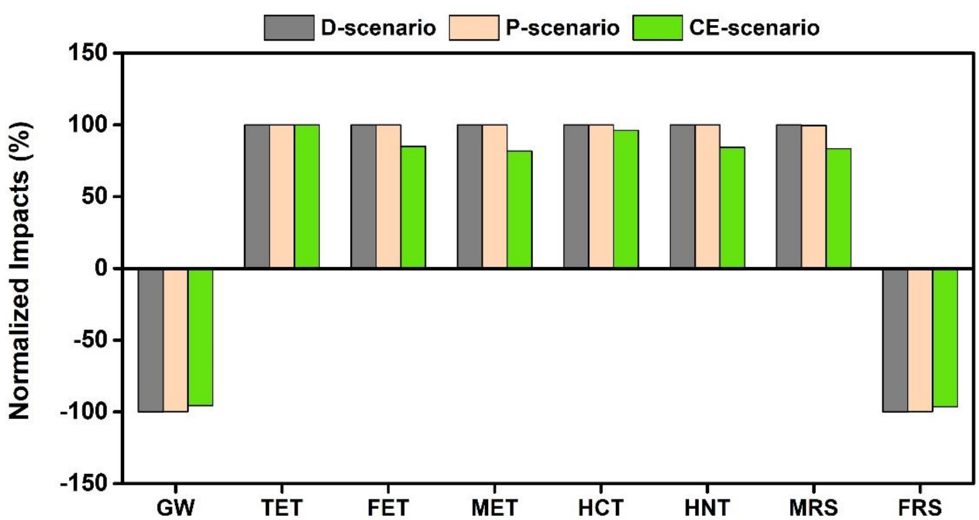

Figure 4.3: Comparison of life cycle impacts of SK-2 module under various EOL scenarios (normalized by impacts of D-scenario)

Figures 4.2 and 4.3 compare the respective life cycle impacts of HH and SK-2 modules (as examples) across all three EOL scenarios, while Figures B.1–B.4 show the same for the remaining four modules. Further, Tables B-13–B-24 show characterized impacts of all six modules under the two alternative EOL scenarios (P- and CE-scenario).

Like in case of their coal-based counterparts[158], negligible variation is seen in modular impacts with change in EOL treatment from D-scenario to P-scenario (recycling of alumina plates). In contrast, barring BT-1, circular economy approach (CE-scenario) enables significant reduction (≥ 5 %) for all modules on two categories (HNT and MRS) (Figures B.1–B.4, 4.2–4.3 and Tables B-13–B-24). Similar levels of impact reduction are also observed for: (a) Four modules on FET (SK-1, SK-2, HH and SC); (b) Three modules on MET (SK-1, SK-2 and SC); and (c) One module each on TET (BT-2) and HCT (SC) impacts (Figures B.1–B.4, 4.2–4.3 and Tables B-13–B-24). This indicates that unlike in earlier work, CE-scenario is somewhat more effective in improving ecological outcomes of TE devices for gas-based electricity, mainly with regard to toxicity- and scarcity-related categories.

4.2. Discussion

4.2.1. Module: Life Cycle Performance

The first interesting observation is that no TE module is seen to be ecologically beneficial on all categories (Figures B.1–B.4, 4.1–4.3 and Tables B-13–B-24). This is strikingly different from the results obtained for the very same modules in Chapter 3, where they exhibit positive ecological effects on almost all impacts. Such a stark contrast in performance stems mainly from two reasons.

The first reason is lower electricity generation (< 25 % of that for coal-based plants), which is an obvious outcome of two factors. One, TE modules are used for only 4 h/day or 36,500 hours overall – about one-third of that in Chapter 3, which is in line with the nature of both end-uses in terms of their operation and waste heat emission. Two, all modules exhibit reduction in their conversion efficiency with thermal cycling, with three modules (SK-1, SK-2 and SC) showing higher TCRCs (≥ 0.01 % per thermal cycle) (Table 2-5). This in turn is related to thermal stability of TE – an intrinsic property[53,54,159]. For instance, skutterudite (SK) systems have been reported to typically exhibit enhanced thermal degradation due to oxidation in ambient atmosphere at temperatures ≥ 400°C[160,161]. This is explained primarily by their use of antimony (Sb) as constituent element, since antimony is observed to segregate and oxidize in these systems and thus form an oxide layer on TE legs that causes deterioration in its contact with metallic tab to lower the modular conversion efficiency[54,160,161]. Hence, the highest TCRC values for SK modules among chosen systems (Table 2-5) can be explained by their oxidizing behavior.

The other key reason for stark difference in modular performance is the nature of electricity replaced by their use. While the previous work (Chapter 3) assumes replacement of coal-based electricity, this work considers the substitution of natural gas (NG)-based electricity. Literature shows that NG-based electricity is environmentally superior to its coal-based counterpart due to both the less-polluting nature of extraction and refining processes for primary fuel, as well as of subsequent electricity generation process[162,163].

This divergence is particularly acute for toxicity-related effects due to the large quantities of toxic elements (such as chromium and mercury) that are emitted during both coal mining and subsequent electricity generation[142,162]. Such lower impact of NG-based electricity reduces the scope for enhancing environmental benefits via use of modules, which explains their poor ecological outcomes, particularly on toxicity-related impacts (Figures B.1–B.4, 4.1–4.3 and Tables B-13–B-24).

The other notable result is that while no module shows good ecological output on all impacts, all modules perform creditably on GW and FRS categories by high margins, with their use dominating production-related impacts by ≥ 60 % (Figures B.1–B.4, Figures 4.1–4.3and Tables B-13–B-24). Thus, at least from the limited perspective of primary justifications that are proposed for use of TEs – fossil fuel conservation and reduction in greenhouse gas emissions[141] – this study suggests their effectiveness, independent of the TE material employed. This is in line with the earlier work as well[158].

4.2.2. Minimum Conditions for Optimal Performance

Regarding a comparison of modular performance, the previous work (Chapter 3) clarifies that such an exercise would not be prudent in light of differences in their optimal range of operational temperatures (Table 2-4). Nevertheless, to determine the minimum requirements that are required to make these modules ecologically effective on all categories, HH module was chosen as a test-case, given its best ecological output among all modules. Two hypothetical scenarios were considered for this module, one each having its conversion efficiency or TCRC kept as constant (the same as for original HH module) and the other parameter allowed to vary in a manner that could help in attaining positive outcomes on all categories, keeping everything else constant. Remarkably, calculations showed that even at extremely high and impossible levels of conversion efficiency (50 %), or even at TCRC = 0, this hypothetical HH module was incapable of accomplishing this aim (figure not shown). This was solely due to the extreme mismatch between negative effects of production and positive impacts of use for HH on FET category (~ 80 %) (Figures 4.1–4.3), which could not be lowered even with such drastic changes in its conversion efficiency or TCRC. Similar conclusions were obtained for other modules as well.

Subsequently, attempts were made to determine the minimal usage duration for all modules by considering an alternative hypothetical use scenario. Under this scenario, it was assumed that all modules would be recovered and used in as-is state over several peak-load NG power plants that operated under the same condition (4 h/day). An additional assumption was that each module would be used in this manner till its conversion efficiency reached 1 % of its original value due to thermal cycling. However, calculations showed that even under this hypothetical use case, no module exhibited positive impacts on all categories (not shown here), especially on FET and HNT impacts (where no module was seen to be ecofriendly). This was again, a major consequence of considering the substitution of NG-based electricity with that from these modules.

In sum, these findings suggest that even if: (a) Conversion efficiencies are dramatically improved; (b) TEs are used for longer duration over multiple plants of similar nature; and (c) Effect of thermal cycling on their conversion efficiencies are made negligible, existing TEs may still prove inadequate in overcoming negative effects of their production for periodic waste heat emitting applications. This implies that TE devices may be ecologically beneficial only for such applications where one or more of the following three possibilities are realistically achieved: (a) They are used for much longer duration per cycle; (b) They replace a more polluting form of energy source, such as coal; and/or (c) Their production-related impacts are lowered by a significant degree (by as much as ~ 70-80 %). Of these, the first two possibilities are entirely dictated by the nature of application, which shows that at least for peak-load NG-based power plants, this platform may not be ecologically suitable for large-scale application. In contrast, an exploration of the third possibility requires focusing on the complex interplay between optimal operational temperature range of modules (which also affects their conversion efficiency) and other factors that influence their life cycle performance, critical among which are three: (a) Mass of module; (b) Nature of constituent elements used in TE systems; and (c) Energy consumed till their production stage. To understand this in some detail, two systems are focused upon: HH (which shows the best performance among all modules if taken at face-value), and SK-2 (which ranks among the worst performers on same ground).

HH benefits from a number of advantages with regard to the aforementioned critical factors. First, it has the lowest mass among all modules (13.38 g/module) barring SC (Table 2-3). Further, even as its output power is the fourth-highest (15.5 W) among all modules, its conversion efficiency is the second-lowest (4.50 %) among all modules (Table 2-4). As a result, it requires the least number of individual modules (among all TE module sets) to convert 1000 W of waste heat into electricity (2.90) (Table 2-4). Also, HH shows the second-lowest amount of GW impact among all modules till the production stage on per-module basis (Table 3-1) – which is a strong indicator of energy consumption, given strong linkages between both aspects (GW and energy use). Thus, all these factors combine to lower the amount of constituent elements required for HH module set and thereby, its ecological impacts on all categories – lower use of constituents on toxicity- and scarcity-related categories, and lesser energy use on GW and FRS categories.

On the other hand, SK-2 module is seen to exhibit the largest production-related GW impact among all modules (on per-module basis) (Table 3-1), which indicates its high (fossil-based) energy requirement for processing[158]. This also accounts for its worst performance among all modules on FRS category. In addition, SK-2 also shows the poorest output on four toxicity-related impacts (FET, MET, HCT and HNT) (Figures B.1–B.4, 4.1–4.3 and Tables B-13–B-24). This is the outcome of its highest per-module mass among all systems (107.44 g/module; Table 2-3) and predominant use of antimony in its TE legs (Table 2-1). As described in Chapter 3, antimony is hazardous for environment on these categories via toxic sulfidic tailings emitted during extraction and processing[143,145–147,158]. However, on both TET and MRS, SK-2 performs better due to respective use of (toxic) tellurium in BT-1 module and scarce germanium in SC module[142,143,145–147,155,158].

This complex interplay between various factors encompassing production and use stages, implies the need for major advancements in developing novel TEs that: (a) Exhibit higher conversion efficiencies; (b) Use elements which are non-toxic by themselves and also help to avoid toxic waste emissions during their extraction and refining; and (c) Are produced using techniques that are efficient in their energy consumption. Any endeavor towards simultaneously addressing all these concerns will, however, be a highly onerous and challenging task to accomplish, as it would necessitate the involvement of multiple stakeholders, including researchers, potential end-users, TE module manufacturers, and even policymakers for commercialization of such systems.

CHAPTER FIVE

ECOLOGICAL PROFILE OF THERMOELECTRICS FOR AUTOMOTIVE APPLICATIONS (INTERMITTENT WASTE HEAT GENERATION)

5. Results & Discussion

5.1. Impact Assessment: Results

5.1.1. Impact Assessment: Production Stage

Like for TE modules, the first objective here is to understand the ecological impacts of considered TEGs during their production. In this regard, Figure 5.1(a-b) shows characterized impacts, with contributions from individual components, for both generators. A detailed analysis of these impacts is provided in the following sub-sections.

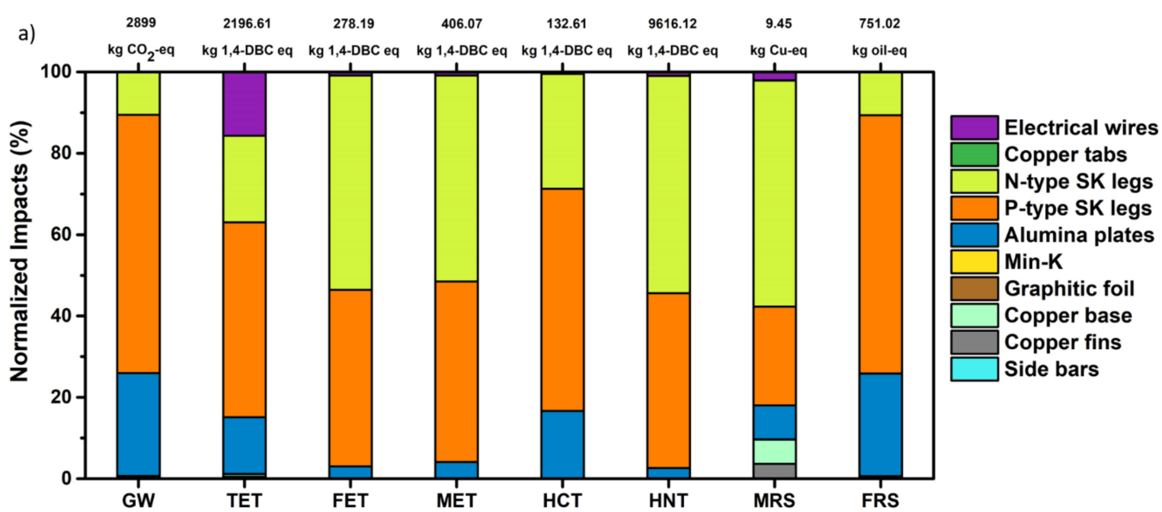

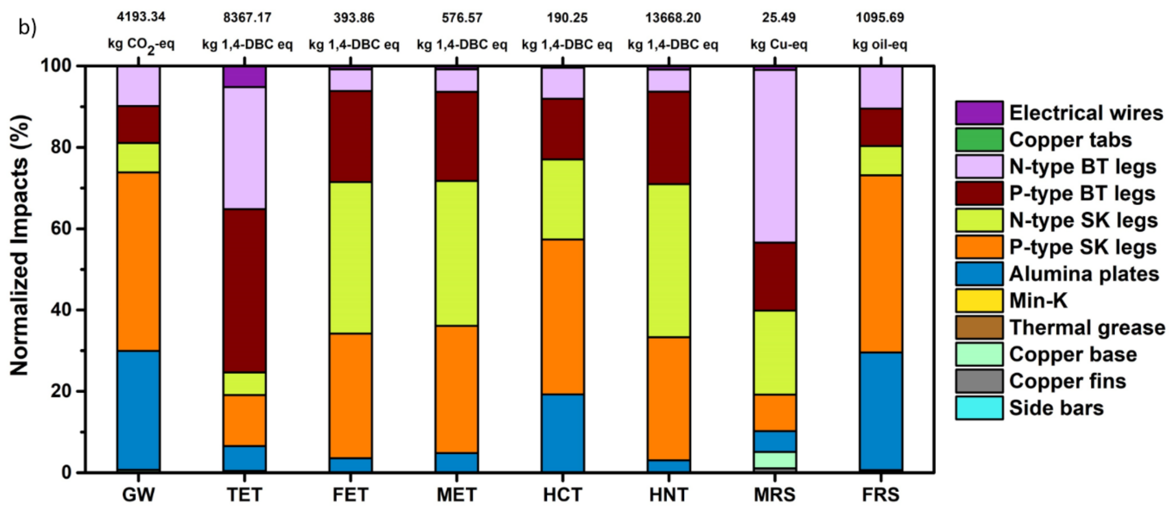

Figure 5.1: Environmental impacts, segregated by contributions from different components, for: (a) TEG-1 and (b) TEG-2

5.1.1.1. TEG-1

As can be seen (Figure 5.1(a)), TE module components, i.e., SK legs (both p- and n-type) and alumina plates – account for a predominant share (≥ 80 %) of impacts of TEG-1 on all categories. In fact, TE legs alone contribute ~ 70 % or more on all impacts. As explained in Chapter 3, this dominance is primarily due to two factors. First, both SK legs (p- and n-type) use extensive amount of antimony, whose mining and processing produce toxic sulfidic tailings to influence their performance on three categories (FET, MET and HNT)[143,145,146,148]. Second, large amounts of electricity are needed to process SK legs for p-type legs (annealing and hot pressing), n-type legs (induction melting and SPS) and alumina plates (sintering of alumina powders) (Tables A-10–A-12). Such large electricity use, fulfilled by the fossil-based US grid, increases greenhouse gas emissions (GW), reduces fossil fuel availability (FRS), and releases toxic waste during processes of fuel mining (particularly coal) and of metals for building related infrastructure (TET and

HCT)[149–154]. Apart from these factors, the relative scarcity of cobalt and antimony respectively explain the dominant effects of n- and p-type legs on MRS category[143,155,158], with cobalt playing the major role on this impact among both elements.

While modular components are influential on almost all categories, other components are seen to play notable roles on only two impacts. These are: (a) TET, with ~ 15 % contribution from electrical wires; and (b) MRS, with a combined contribution of ~ 12 % from electrical wires, copper fins and copper base (Figure 5.1(a)). Both these contributions stem from the use of copper in all these components. On TET, harmful emissions during copper extraction and processing play the dominant role[153]. Further, copper is also scarcer than a number of elements used across all TEG components, as borne out from its relatively higher scarcity-related coefficient in ReCiPe method[142]. This explains the significance of copper base and fins on MRS, as both components are fully made from copper and together constitute ~ 85 % of overall mass of the TEGs (Table 2-7).

5.1.1.2. TEG-2

Like for TEG-1, TE legs and alumina plates together account for the largest share of impacts of TEG-2 on all categories (Figure 5.1(b)). However, unlike TEG-1, this influence is far greater, with these components accounting for ≥ 94 % of all impacts of this generator. This is accompanied by the reduced relevance of other components, especially electrical wires, copper fins and base, on other categories such as TET and MRS (in contrast to TEG-1). Such observations are explained by the presence and resultant impact of BT legs, which account for ≥ 19 % impact of TEG-2 on all categories, including ≥ 60 % on both TET and MRS impacts.

The major reasons for high contribution of BT legs have been explained already in Chapter 3. Briefly, toxic sulfidic tailings produced during the extraction and processing of both antimony (used in p-type BT legs) and tellurium (used in both p- and n-type BT legs) accounts for substantial effect of these legs on all toxicity-related categories[143,145–148]. Furthermore, large amount of electricity is used to process alumina plates in BT-1 modules (Table A-4) which contributes in substantial measure towards their influence on all impacts barring MRS[149–154] In contrast, high scarcity of bismuth and tellurium ores, as reflected in their higher scarcity-related coefficients vis-à-vis antimony (or even copper)[155,164], account for the dominance of BT legs on MRS category.

5.1.2. *Impacts: Life Cycle*

Apart from their production, another important objective is to analyze the life cycle impacts of both the chosen TEGs – these are discussed in the following subsections, along with understanding the effect of end-of-life scenario.

5.1.2.1. D-Scenario (Disposal)

Figure 5.2 shows the normalized impacts of chosen generators, while Tables C-10 and C-11 show their characterized impacts for the base EOL scenario (D-scenario) as per the considered functional unit (1 liter of gasoline saving). As can be seen (Figure 5.2), both TEGs are found to be ecologically harmful on all impacts barring TEG-1 on TET category. While the use stage – involving gasoline savings – helps reduce impacts to a substantial extent (> 20 %) on three categories (GW, FRS and TET) for both TEGs, it provides negligible ecological benefits on other impacts. In fact, the production stage dominates over any benefits accrued during the use and/or EOL stages by ≥ 90 % on the remaining five categories, indicating the strongly negative ecological credentials of these generators. Also, irrespective of the generator considered, the disposal stage (EOL treatment) is observed to have a negligible effect on their performance.

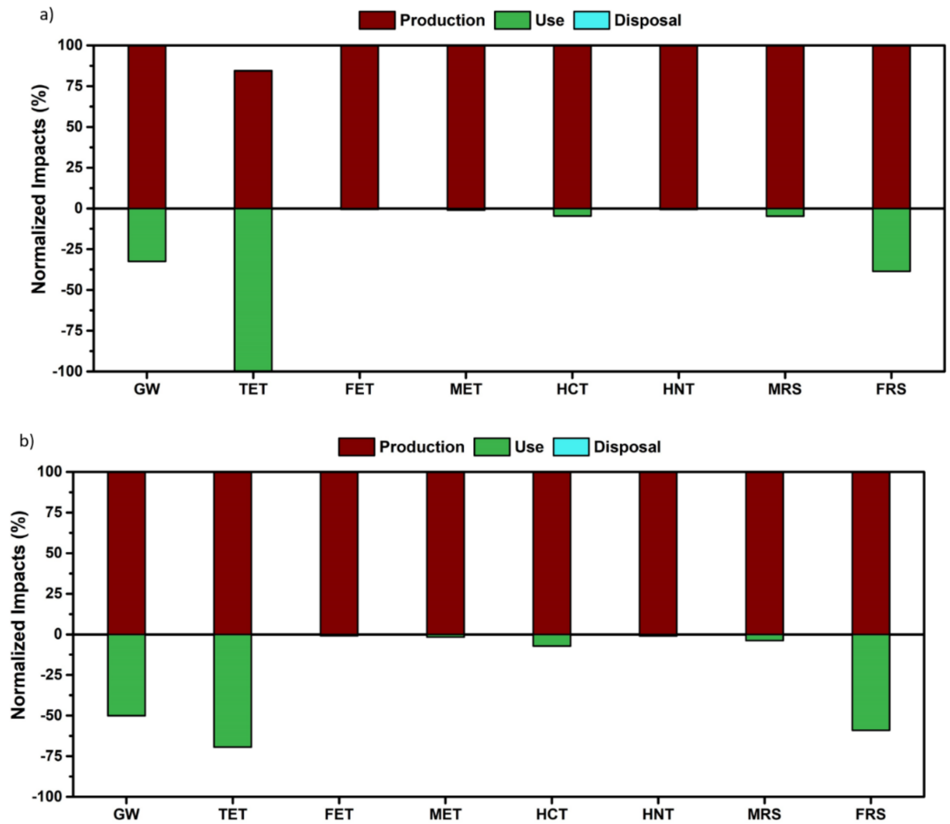

Figure 5.2: Life cycle impacts of: (a) TEG-1 and (b) TEG-2 (normalized to 100 %)

5.1.2.2. Other EOL Scenarios: A Comparison

Figure 5.3(a-b) shows a comparison of impacts of both TEGs under the considered EOL scenarios, while Tables C-12–C-15 show the characterized impacts of both TEGs (as per functional unit) for these scenarios.

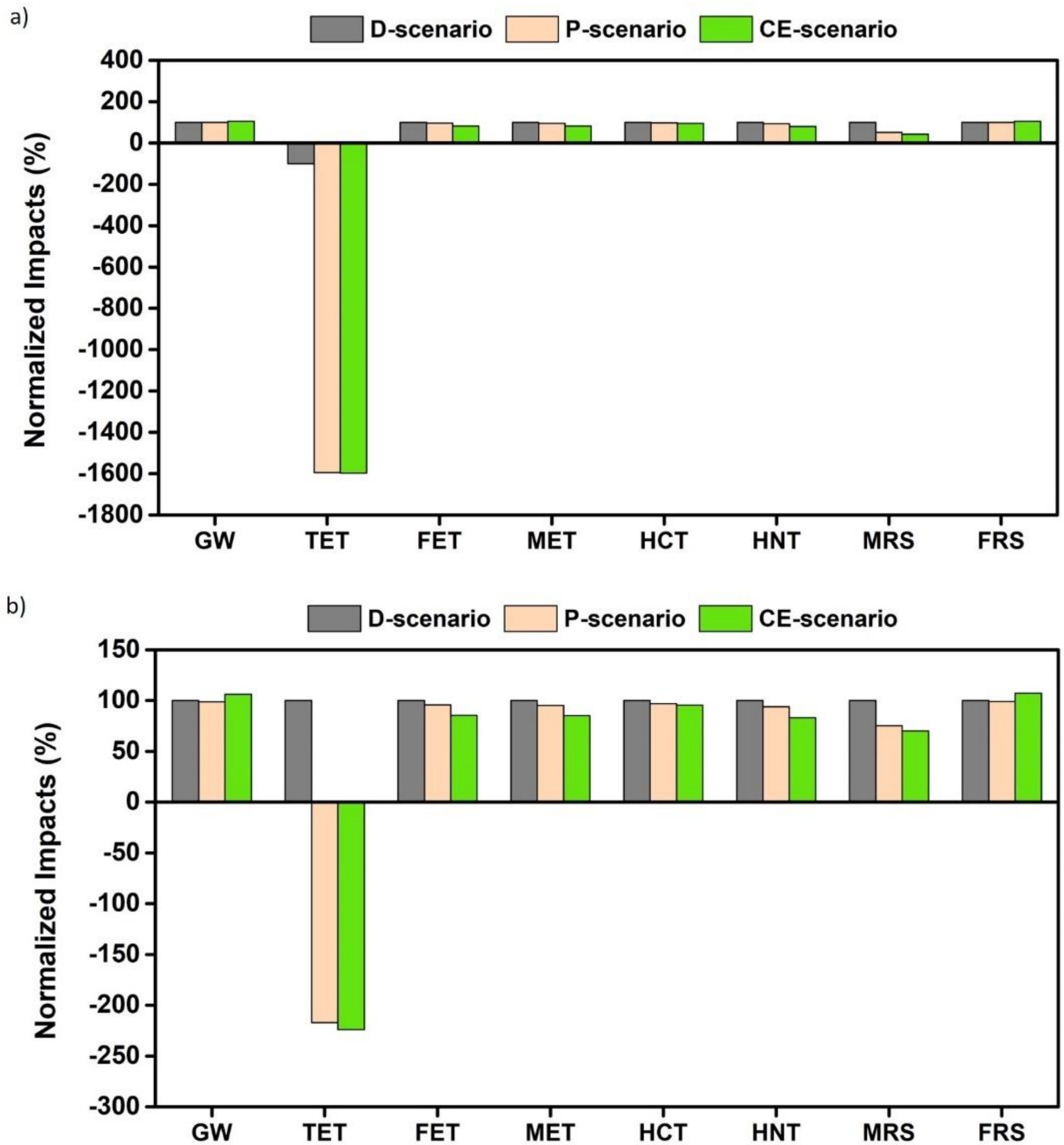

Figure 5.3: Comparison of life cycle environmental impacts of: (a) TEG-1 and (b) TEG-2 under various EOL scenarios

For P-scenario (practical), marginal reduction (< 10 %) is observed in absolute impacts on six categories (all except TET and MRS) for both TEGs when compared with

D-scenario (Figure 5.3). In contrast, a large decrease in impacts is observed on TET category (~ 1500 % for TEG-1; ~ 320 % for TEG-2), along with smaller-yet-significant decrease on MRS category (~ 50 % for TEG-1; ~ 25 % for TEG-2) in P-scenario vis-à-vis D-scenario (Figure 5.3). Such dramatic impact reduction on both categories is the outcome of recycling heat exchanger components, particularly copper base and fins, with negligible role of stainless-steel side bar recycling. This can be easily correlated with the aforementioned observation of both these copper-based components having notable impacts on TET and MRS categories on account of their parent metal (copper).

On the other hand, use of CE-scenario (circular economy) leads to a more diverse range of ecological performance. On GW and FRS impacts, both TEGs actually show a small increase (~ 4-8 %) over D-scenario (Figure 5.3). This is explained by the notable consumption of electricity (~ 10-12 kWh/kg of output powder) during cutting and subsequent re-melting of recovered TE legs (SK and BT) from concerned generators during their EOL treatment. Conversely, unlike in P-scenario, a substantial degree of impact reduction is observed for both TEGs on four toxicity-related impacts (all except TET) in CE-scenario (~ 5-20 %) vis-à-vis D-scenario (Figure 5.3). This can be ascribed to the partial avoidance of toxic sulfidic emissions associated with producing antimony (for SK legs and p-type BT legs) and tellurium (for BT legs) through recovery and recycling of these legs in CE-scenario. Finally, with regard to TET and MRS impacts, CE-scenario shows moderate decrease in MRS impact (~ 17 % for TEG-1; ~ 7 % for TEG-2) and negligible variation on TET category (< 3.50 % for both generators) over P-scenario (Figure 5.3and Tables C-12–C-15). Of these, the observation for MRS shows potential benefits of recycling scarce constituent elements like bismuth and tellurium (used in BT legs) or cobalt and antimony (used in SK legs)[142]. Contrastingly, the latter observation (on TET) indicates the limits of achieving ecological benefits by implementing the circular economy approach, given that copper recycling is already incorporated as a practical recycling step (P-scenario).

5.1.2.3. TEG-1 v/s TEG-2: A Comparison

Another important goal of this work is to compare the ecological performance of chosen TEGs, using the aforementioned functional unit (1 liter of net gasoline saving). Based on this functional unit, the reference flow for TEG-1 and TEG-2 were obtained as 3.38×10^{-3} and 1.51×10^{-3} units respectively. Figure 5.4 uses these reference flows to compare environmental impacts of both TEGs on chosen impact categories in D-scenario, while Figures C.1 and C.2 show the same comparison under P- and CE-scenarios respectively.

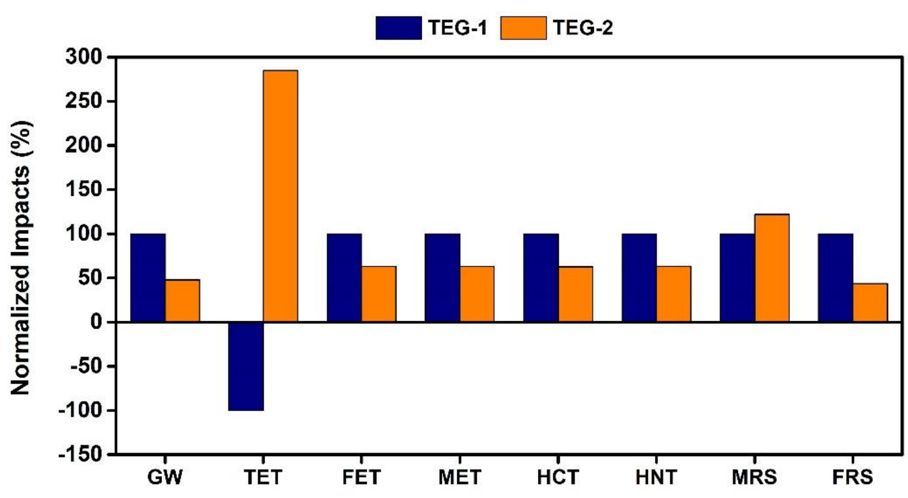

Figure 5.4: Comparison of life cycle impacts of TEG-1 and TEG-2, by normalizing impacts of TEG-1 as 100 %, for D-scenario

On D-scenario, TEG-2 shows better environmental performance than TEG-1 on six impact categories, including on four toxicity-related impacts (all barring TET, by ~ 35-40 %), as well as on GW and FRS impacts (by ~ 50-60 %) (Figure 5.4). In contrast, TEG-1 performs better than TEG-2 on the remaining two impacts (TET and MRS). This can be attributed to a combination of two factors. The first is higher conversion efficiency of TEG-2 (4.32 %) over TEG-1 (3.33 %)[103,104], which lowers the effective number of SK-1 modules needed in reference flow of TEG-2 to save 1 liter of gasoline (by replacing it with BT-1 modules). The second is the relative performance of SK-1 module over BT-1 on all eight categories, where SK-1 is seen to perform better on only two categories (TET and MRS), with BT-1 doing better on the remaining ones (Table 3-1). This in turn can be ascribed to two factors that are well-explained already in Chapter 3 and initial section of this chapter (Section 5.1.1): (a) Nature of constituent elements used; and (b) Electricity consumed during component processing. In simple terms, SK-1 modules are more hazardous on all impacts except TET and MRS due to: (a) Heavy use of antimony as constituent element in both p- and n-type SK legs (Tables A-10 and A-11), unlike in moderate amounts in p-type BT legs only (Tables A-2 and A-3); and (b) Much larger electricity consumption during TE leg processing for SK-1 modules (Tables A-10 and A-11) compared to BT-1 modules (Tables A-2 and A-3). Conversely, the better performance of SK-1 modules on TET and MRS impacts is related to: (a) Higher toxic contributions from tellurium mining and processing (TET); and (b) Higher scarcity of bismuth[164] and its substantial use in BT legs (Tables A-2 and A-3) vis-à-vis that of other constituent elements used in BT and SK legs (MRS). In fact, the latter two factors cause a dramatic shift in performance of both TEGs, with TEG-2 being worse than TEG-1 by ~ 400 % and ~ 21.50 % on TET and MRS respectively (Figure 5.4).

Like for D-scenario, the order of both generators in terms of their ecological performance remains the same in alternative EOL scenarios, with TEG-2 being better than TEG-1 on the same six categories and performing worse than it on TET and MRS impacts. However, an interesting outcome is seen for the difference in impacts of both generators under the three scenarios. On one hand, TEG-2 shows similar levels of performance vis-à-vis TEG-1 on six categories (all except TET and MRS) under all three EOL scenarios. However, this behavior is significantly altered for TET and MRS impacts. For TET, TEG-2 is more impactful than TEG-1 by ~ 60-62 % in P- and CE-scenarios (Figures C.1 and C.2), while exhibiting a complete reversal in D-scenario (Figure 5.4). This is due to the large beneficial effect of recycling copper fins in P-scenario, which causes a dramatic boost in ecological performance of TEG-2 compared to D-scenario. Yet, toxic sulfidic tailings produced during tellurium extraction and processing (for use in BT-1 modules) ensures that TEG-2 is not able to gain superiority over TEG-1 on TET impact. Conversely, the gap between performance of both TEGs increases from ~ 21.50 % in D-scenario (Figure 5.4) to ~ 81.50 % in P-scenario (Figure C.1) and ~ 103 % in CE-scenario (Figure C.2) – all in favor of TEG-1. This is the consequence of using large amount of scarce bismuth in BT legs[142,164], which lowers the scope for improving ecological performance of TEG-2 over TEG-1, even after use of circular economy approach, as a major chunk of it goes to waste.

5.2. Discussion

5.2.1. Production Stage

The first interesting observation from this work is the disproportionate mismatch between the mass of different TEG components (Table 2-7) and their contributions to environmental impacts of both TEGs (Figure 5.1). On one hand, despite their low share in mass (~ 6-7 %), TE legs account for the bulk majority of impacts (≥ 70 %) of both generators. In contrast, heat exchanger components are seen to have an insignificant effect on environmental performance of these TEGs, despite constituting ≥ 85 % of their respective masses. These stark differences can be ascribed to the same factors that have been previously discussed (nature of constituent elements used in various TEG components, and amount of electricity used in processing these components).

An excellent example of the first aforementioned factor is the difference in impact contributions of copper-based heat exchanger components (fins and base) and BT legs. Tellurium, used in BT legs, is obtained in low concentrations as a by-product of copper processing, after which it is processed further for subsequent use[143,165,166]. Hence, for the same quantity of tellurium and copper, a far greater amount of toxic sulfidic tailings would be emitted to produce tellurium than for copper. This explains the greater relevance of BT legs over copper-based components for environmental impacts of chosen TEGs.

Regarding the second factor, the role of energy-intensive processes for TE legs has already been discussed (Chapter 3 and Section 5.1.1). In complete contrast, stainless-steel and copper sheets – used to produce heat exchanger components – are manufactured on large scale using technologies that are highly optimized in terms of resource and energy consumption. As a result, these components have smaller or even negligible impacts on most categories. Thus, heat exchanger components can be expected to play a negligible role in influencing environmental impacts of TE devices, which suggests greater validity for LCA results obtained for TE modules earlier (Chapters 3 and 4).

Apart from the nature of constituent elements, another critical factor behind their contribution to ecological impacts of chosen generators is their respective quantities used in TE legs. To understand this aspect, Table C-16 shows the impacts of all constituent elements used in TE legs, as well as of copper, all on per-kg basis. As can be seen, these results are in line with aforementioned results on six impact categories (all barring GW and FRS). For instance, antimony dominates all other elements on four toxicity-related categories (all except TET) by a considerable margin, which explains its dominant role on these impacts for both TEGs. However, on GW and FRS impacts, rare-earth elements (lanthanum, ytterbium and didymium) are observed to show the highest effect among all elements – which is a strong deviation from results of this work. Yet, this is explained by the combination of low use of these rare-earth elements (in SK legs), as well as the highly energy-intensive nature of TE leg processing (especially for SK legs).

In sum, both the nature as well as amount of constituent elements used in TE legs, along with electricity consumed to produce them, are critical determinants of production-related environmental impacts of thermoelectrics.

5.2.2. Life Cycle Impacts

For life cycle impacts of chosen TEGs, two key results are obtained: one with reference to their environmental performance, and the other about effect of EOL scenarios.

5.2.2.1. Ecological Performance of TEGs

The first major result for both generators is their stark ineffectiveness in improving the environment on any of the chosen categories. This is notably different from the previous LCA work (Chapter 3), where all TE modules exhibit positive performance on the very same categories for coal-based power plants. Such deviation in environmental effects can be attributed to four reasons. First, both TEGs are used for 100,000 miles of travel, which translates to usage over ~ 3,535 h (based on times provided for various driving cycles in Table C-6). This is just a minor fraction (< 5 %) of total use duration of TE modules in coal-based power plants (131,400 h or 15 years of continuous usage, Table 2-9), which significantly lowers the amount of electricity produced in this study. Second, intermittent nature of waste heat generation in automobiles causes thermal cycling, further reducing the conversion efficiency of TEGs and thereby, their associated electricity output. Third, unlike in coal-based power plants, mass of generators (including that of heat exchanger components) affects their ability to save fossil fuels in automotive applications. Finally, the fossil fuel avoided – gasoline – has lower ecological impacts than coal, which substantially decreases the scope for comparative ecological benefits in this study over coal.

An important factor to keep here in mind is that poor ecological performance of TEGs as obtained here is in part the consequence of high production-related impacts, which are in part observed due to use of energy-intensive processes for TEGs, especially TE legs. Although such high energy consumption is partly the result of using parameters that are more suitable for small-scale production of these legs (mentioned in Chapters 2 and 3), the large difference between harmful impacts of production and beneficial effects of use stage indicates that it may not be bridged even after considering commercial-scale parameters.

Since both TEGs are observed to be ineffective on all categories, a number of hypothetical changes were considered to determine the necessary conditions under which these generators can become beneficial to environment. For this purpose, two parameters were separately varied – lifetime distance travelled, and thermal cycling reduction coefficient (TCRC) of modules – to determine the possibility of such conditions. For lifetime travel distance, its value was varied till the driving cycle at which the concerned generator showed no fuel saving when compared to the alternative hypothetical case of its non-use in Chevrolet Suburban (more details in Section 8.1 of Appendix-C). On the other hand, TCRC of modules was varied separately till positive environmental performance was achieved on all impacts (additional details given in Section 8.2 of Appendix-C).

A. Hypothetical Scenario I: Lifetime Travel Distance

Calculations showed that no further improvement in fuel savings could be achieved via use of TEG-1 for lifetime travel distance > 100,000 miles, as these savings vis-à-vis alternative scenario (non-use of TEGs) becomes zero at 90,000 miles of operation. In contrast, positive fuel savings were obtained for TEG-2 till ~ 266,000 miles – nearly thrice the lifetime distance of TEG-1 – with an estimated fuel saving of ~ 991 liters (of gasoline), more than 400 liters over original lifetime distance (100,000 miles). Upon inputting this fuel saving for TEG-2 and assuming CE-scenario as EOL scenario (the most ecofriendly among all EOL scenarios), the result obtained is shown in Figure C.3. As can be seen, barring TET, TEG-2 is observed to be bad for environment on all other categories.

Interestingly, while substantial impact reduction is seen on both GW and FRS impacts compared to original CE-scenario (~ 48 % and ~ 70 % respectively), little change is observed on toxicity-related impacts (barring TET) or on MRS category (< 5 % for all).

B. Hypothetical Scenario II: Thermal Cycling Reduction Coefficient (TCRC)

Since the objective of this scenario is to determine the minimum TCRC for obtaining positive environmental performance of TEGs on all impacts, the first step was to assume this value to be zero to determine if such performance could even be achieved in the first place. For zero TCRC, gasoline savings were obtained via calculations as ~ 860 liters for TEG-1 and ~ 1,100 liters for TEG-2. Such enhanced gasoline savings over the base scenario provide some benefits (Figure C.4), with both TEGs becoming ecologically beneficial on TET impact, and TEG-1 showing positive effects on FRS category as well. Nevertheless, neither of the two generators show ecological benefits on all categories.

From both the aforementioned hypothetical scenarios, it becomes clear that neither reduction in TCRC nor increase in lifetime travel distance are adequate enough in substantially enhancing ecological credentials of TEGs, despite enhancing their gasoline savings. On both counts, this is solely due to the less harmful effect of gasoline production and distribution on environment vis-à-vis that of CBE generation (Chapter 3).

5.2.2.2. Effect of EOL Scenarios

An important outcome of this work is the significant effect of alternative EOL scenarios (P- and CE-scenarios) over the base EOL scenario (D-scenario) (Figures 5.2–5.4 and Figures C.1–C.2). This is unlike in Chapters 3 and 4, where negligible difference is seen in impacts between the three EOL scenarios, and it is almost entirely due to contributions from copper-based heat exchanger components upon recycling. While it is true that even these alternative EOL scenarios cannot change the overall ecological credentials of this platform, such substantial benefits accrued from recycling copper-based TEG components shows the need for its implementation. Further, this learning can be easily applied to TEGs used in other kinds of applications, given that it is in this form that thermoelectrics are primarily deployed in various end-uses, such as in coal-based power plants, thereby enabling a further improvement of its ecological credentials.

CHAPTER SIX

GREEN PRINCIPLES FOR SUSTAINABLE THERMOELECTRICS

6. Principles for Sustainable Thermoelectrics (TEs)

6.1. Classification of Principles – Stage-wise

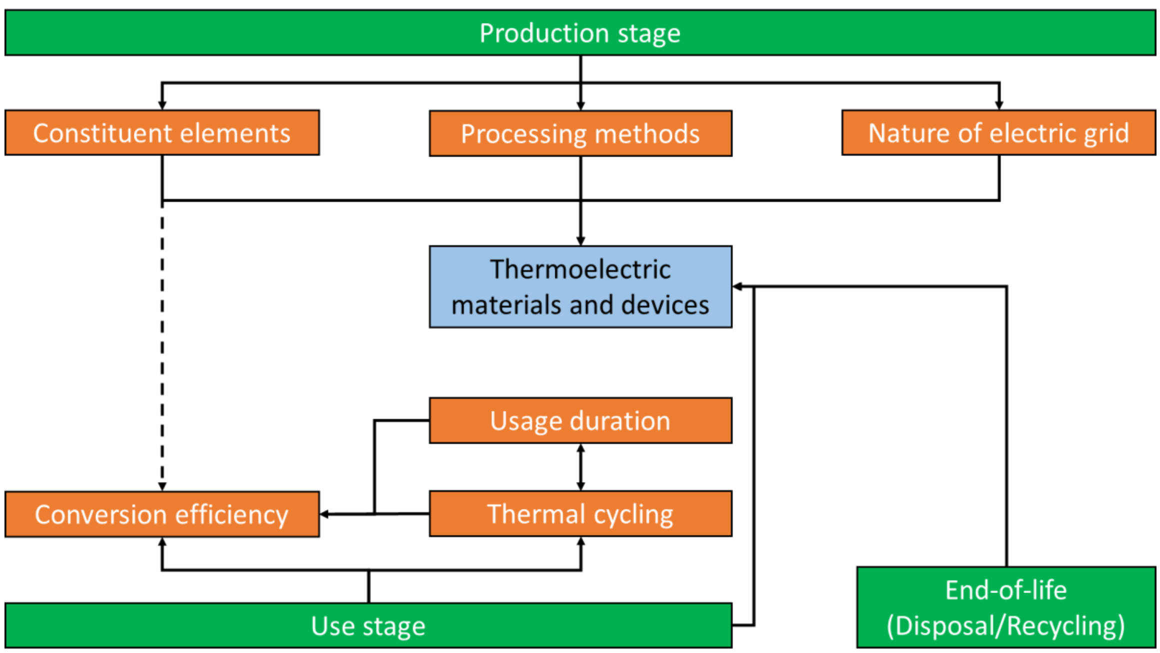

Figure 6.1: Parameters that influence ecological performance of thermoelectric materials and devices

As described in Chapter 2, the primary goal of this study is to use results from LCA of TE devices for various applications to develop principles for policymakers (in collaboration with other stakeholders) that can improve sustainability credentials of this platform. To achieve this aim, it is vital to focus on the typical life cycle of any TE device, which can be broadly classified into three main stages: (a) Factory gate (spanning the extraction of constituent elements and other raw materials, followed by the manufacture of device components and their final assembly); (b) Use and (c) End-of-life (EOL). For the use stage, the device can be potentially used in any application where waste heat is emitted, with such applications varying in their nature of waste heat generation (continuous or discontinuous) as well as in the nature of application itself (stationary or mobile). Figure 6.1 shows all the key parameters that determine and influence the principles described in this chapter, encompassing all the life cycle stages, based on the work in this dissertation as well as that in previous LCA studies and other literature on TEs[95–99].

6.2. Principles: List & Description

6.2.1. Principle #1: Minimize the Use of (and Exposure to) Toxic, Hazardous Elements in TE Materials

Toxicity of constituent elements used in TEs has emerged as a major concern over the last decade within the thermoelectric community[23,43,57,58]. It is also considered as among the key reasons behind their low attractiveness for large-scale applications due to the harmful effects of exposure of these elements on the health of laborers engaged in producing TE devices, while also hampering their recycling[52]. In particular, bismuth-telluride (BT) and lead-telluride (PT) – two TEs that dominate commercial production – are regularly pointed out in studies for their use of toxic constituents[43,45,49,167]. The elements that raise anxiety about these systems include: (a) Lead, which is highly poisonous[73,168–170] and is capable of causing serious and even irreversible neurological disorder in humans, because of which it is termed "*nerve poison*" and "*potent neurotoxin*" by the United Nations Environment Programme (UNEP)[171]; and (b) Chalcogenides (elements such as selenium and tellurium), which are fatal even at low concentrations ($\leq$ 0.2 mg/m^3)[52,169,170,172,173]. These apprehensions can also be extended to some alternative TEs that are otherwise proposed as non-toxic alternatives to BT and PT systems, such as sulfides[174,175] and selenides[174,176,177], due to the incorporation of some of these elements.

In order to resolve the problem of toxic constituent elements, several researchers have attempted to develop alternative TEs that involve their less/non-toxic counterparts. This has led to the arrival of numerous alternatives on the horizon, prominent among which include skutterudites (SK), oxides (OX), Half-Heusler alloys (HH), clathrates (CL), and silicides (SC)[14,22,23,30,48,49]. Yet, the unease about elemental toxicity can be extended to some of these systems as well because of two reasons. First, a number of these TEs also use chalcogenide elements in noteworthy amounts, such as CL[178,179] and SK[180]. In other words, these systems can be affected by the same concerns as those afflicting BT and PT systems. Second, many of these TEs use elements like antimony and germanium in considerably large amounts, such as SK and CL[49,181,182]. Both these elements are well known for their negative effects on human health when used in sizable proportion[52], which renders their large use as hazardous. Overall, these two reasons underline the challenges of simultaneous accomplishment of low elemental toxicity and good TE performance.

Yet, even as elemental toxicity causes disquiet, it is not the sole toxicity-related concern that affects this energy harvesting platform. As shown in Chapters 3-5 of this dissertation, an equally critical challenge posed by TEs is the life cycle toxicity of their constituent elements, i.e., toxicity-related environmental impacts caused by these elements from their extraction till their processing in the form desired for TE devices. The previous analyses demonstrate the predominant influence of constituent elements on life cycle toxicity impacts for both TE modules and generators, with other components exhibiting an insignificant role. In particular, two elements – antimony and tellurium – exert substantial negative toxicity effects for BT and SK modules[158,183,184] via toxic sulfidic tailings emitted during elemental processing, assuming similar extraction and refining processes as those used for copper[143,145–148]. These tailings also explain the dominant role of other elements that are used in the chosen modules, such as for molybdenum – a constituent of silicide (SC) module[156].

Figure 6.2 shows a comparison of the performance of different constituent elements used in the various TE modules analyzed in this work on their respective elemental and life cycle toxicities. Two interesting observations stand out from this figure. First, molybdenum is seen to be the most toxic element on life cycle basis, overshadowing the two major impact contributors on toxicity-related categories in this work - tellurium and antimony[158] – despite its significantly lower elemental toxicity vis-à-vis these two elements[172]. Conversely, the inherently toxic nature of lead[52,172] is in sharp contrast to its negligible contribution towards life cycle toxicity – an aspect also observed for PT modules[158]. Together, these two observations imply that elemental and life cycle toxicities are not always connected to each other and are thus independent challenges that must be resolved separately-yet-simultaneously to boost the ecological suitability of this platform.

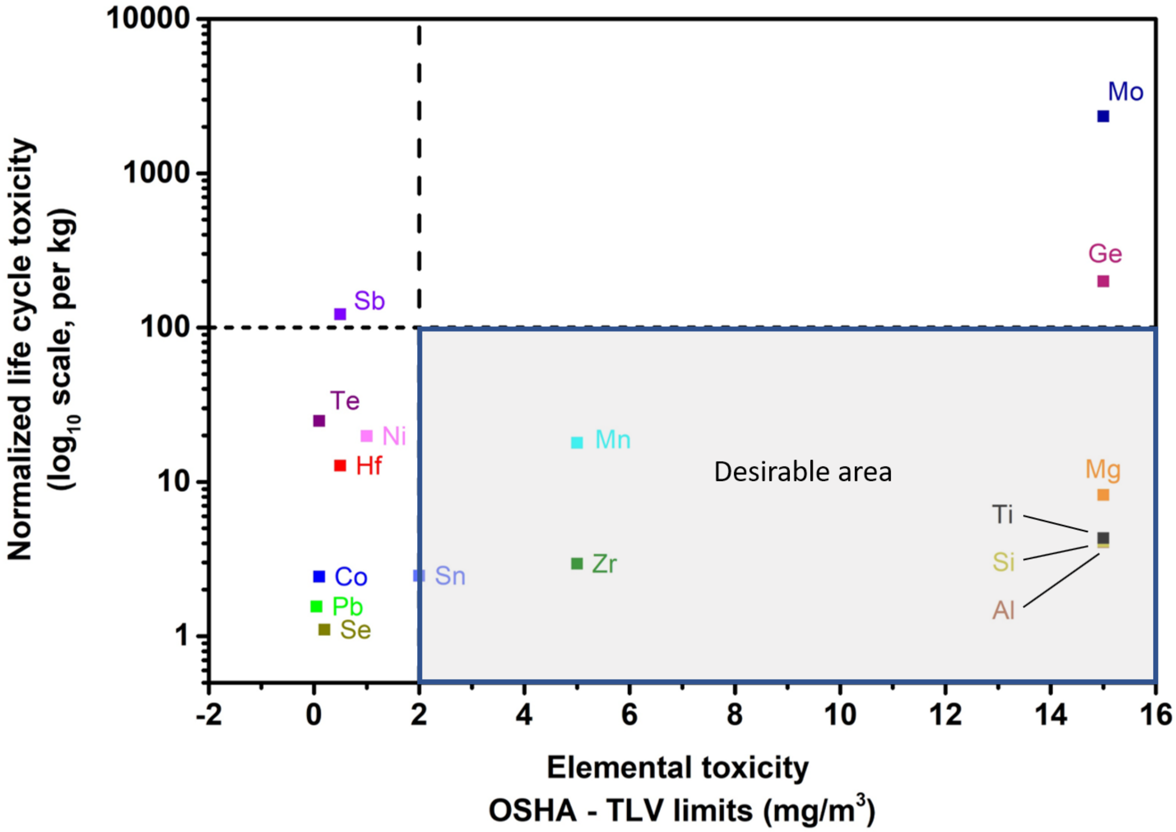

Figure 6.2: Elemental toxicity (as measured using threshold limit value or TLV limits of Occupational Safety and Health Administration or OSHA, U.S. government) v/s Normalized life cycle toxicity impact (on $\log_{10}$ scale)* of various constituent elements (on

---

* Threshold limit values (TLVs) "refer to airborne concentrations of chemical substances and represent conditions under which it is believed that nearly all workers may be repeatedly exposed, day after day, over a working lifetime, without adverse effects." [236] Hence, higher the TLV value for any element, lower is its toxicity (as workers can be exposed to higher concentration of this element), and vice-versa. TLVs are used to measure elemental toxicity commonly for workers, so it has been used. Since TLV values had not been measured by OSHA or Occupational Safety & Health Administration (under the U.S. government) for barium, bismuth, cerium, didymium, iron, lanthanum, sodium and ytterbium, these elements have not been shown in this graph. Regarding toxicity, five categories were used in Chapters 3-5 of this work: terrestrial ecotoxicity (TET), freshwater ecotoxicity (FET), marine ecotoxicity (MET), human carcinogenic toxicity (HCT), and

per-kg basis). The shaded area is the desirable area where elements exhibit lower toxicities, both at elemental and life cycle levels.

To determine the best elements from the perspective of addressing both toxicity measures, a minimal range of performance is proposed for both forms of toxicity. This range – marked in Figure 6.2 – requires that elemental toxicity must be higher than TLV value of 2 mg/m^3 (OSHA limit), while normalized life cycle toxicity value of the element must be lower than 100. Six elements are seen to meet these two criteria: magnesium (Mg), aluminum (Al), titanium (Ti), silicon (Si), manganese (Mn) and zirconium (Zr), apart from tin (Sn) that lies on the border of this region. In other words, it is modules that use these elements in larger quantities and avoid other elements – at least partially, if not entirely – that are preferable from the perspective of achieving lower toxicities at elemental and life cycle levels. Hence, any solutions that help attain this principle must be considered from the perspective of this figure. organic TEs are expected to involve less-toxic elements than their inorganic counterparts[44,185]. Further, the raw materials for such TEs would be organic in character, and are likely to be derived from crude oil reserves (via distillation), which is expected to have much lower life cycle toxicity effects than other fossil energy-related processes like coal-based electricity generation (Chapters 3 and 5). However, for organic TEs to be considered worthy from environmental perspective, it is vital that these are

---

human non-carcinogenic toxicity (HNT). Since literature does not indicate that these impacts can be added at the characterized level, they were normalized using the World 2010 as reference (state of the entire world in the year 2010) and then summed up to obtain the normalized life cycle toxicity level. For the graph, this sum is shown on $\log_{10}$ scale.

produced using methods or procedures that are enshrined in the philosophy of sustainability, such as the 12 principles of sustainable chemistry[70,102]. Further, the initial chemicals used for their synthesis and/or processing must also be ecofriendly, and these chemicals as well as the final TE must be easy to handle for both workers and final consumers without causing any significant negative impacts.

Conversely, for mid- and high-temperature applications, both Figure 6.2 and production-related impacts of TE modules (Figure 3.1: Environmental impacts of producing: (a) BT-1 module; (b) BT-2 module; (c) SK-1 module; (d) SK-2 module; (e) HH module; (f) PT module; and (g) SC module. Impacts are scaled to 100 % on respective units. Values at the top of each bar are characterized impacts.) indicate that at least one of the considered modules in this work – Half-Heusler (HH) – and another TE system (Mg_2Si or MS) hold some promise[14,45,186–189], given their use of aforementioned less-toxic elements (from both elemental and life cycle perspectives). Yet, adequate environmental analysis is essential to back these claims at the level of complete TE devices (i.e., as thermoelectric generators) for policymakers to ascertain the ecological suitability of available options for any application. Moreover, enhancement in potential number of such TE choices would require strong and dedicated efforts on the part of researchers towards discovering novel TEs that outperform existing ones on their toxic effects. Furthermore, it would necessitate coordination between policymakers, TE manufacturers and potential end-users to commercialize such sustainable TEs for enabling the real-life achievement of proposed environmental gains. Table 6-1 shows the desirable numerical values for parameters that are relevant for this first principle.

Table 6-1: Desirable numerical values for parameters associated with Principle #1

Type of toxicity	Desirable numerical value
Elemental toxicity	Threshold limit value (TLV) > 2 mg/m^3
Life cycle toxicity	Normalized value < 100
Both toxicity-related conditions must be met.	

6.2.2. *Principle #2: Minimize the Use of Scarce and Critical Elements in TE Materials*

Apart from toxicity, another key challenge posed by TE constituent elements is their scarcity or lack of abundance[23,52,57,58]. The severity of this issue can be gauged from the fact that it affects a wide range of TEs, be it the commonly-used BT and PT systems[52,176], or alternative TEs like SK, LAST/TAGS, Zintl phases (ZP) and SC[58]. Such scarcity remains a prime factor behind high prices of TE devices[49], whose prolongation is expected to lower possibilities for improving and sustaining their futuristic relevance.

Previous studies on TEs have traced the origins of this issue primarily to the use of four particular constituent elements. These are: (a) Bismuth (Bi, used in BT system); (b) Tellurium (Te, used in BT, PT, ZP and LAST/TAGS); (c) Antimony (Sb, employed in BT, ZP, SK and LAST/TAGS); and (d) Germanium (Ge, used primarily in CL and SC systems)[52,58,176]. Remarkably, the prominence of these elements is retained even upon shifting from their scarcity as an element to that on life cycle basis. As reported in earlier analysis (Chapters 3-5), two of these four elements – bismuth and germanium – dominate the respective life cycle scarcity impacts (MRS) of BT and SC modules. This is complemented by the noteworthy roles of tellurium (for BT module) and antimony (for BT and SK modules)[158,183]. Interestingly, apart from these four elements, another element exhibits an influential role: cobalt for both SK modules (Chapter 3). Nevertheless, these findings suggest a convergence between the elemental and life cycle notions of scarcity for TE constituent elements.

To further confirm the aforementioned convergence of both forms of scarcity, the two were plotted against each other for constituent elements used in the chosen modules. The results are shown in

Figure 6.3, where life cycle scarcity is depicted in the form of characterized MRS impact of various elements for 1 kg of their mass, while elemental scarcity is understood in terms of their respective reserves (obtained from USGS[190]). Notwithstanding some exceptions like selenium and tellurium that are scarcer on elemental basis but do not exhibit high MRS impact (in relative terms),

Figure 6.3 shows a near-convergence between both notions of scarcity. This suggests that the biggest contribution to life cycle scarcity of an element stems from its own scarcity, with the role of scarcity of other elements via their use in extraction and processing-related components and infrastructure being insignificant in the overall schema.

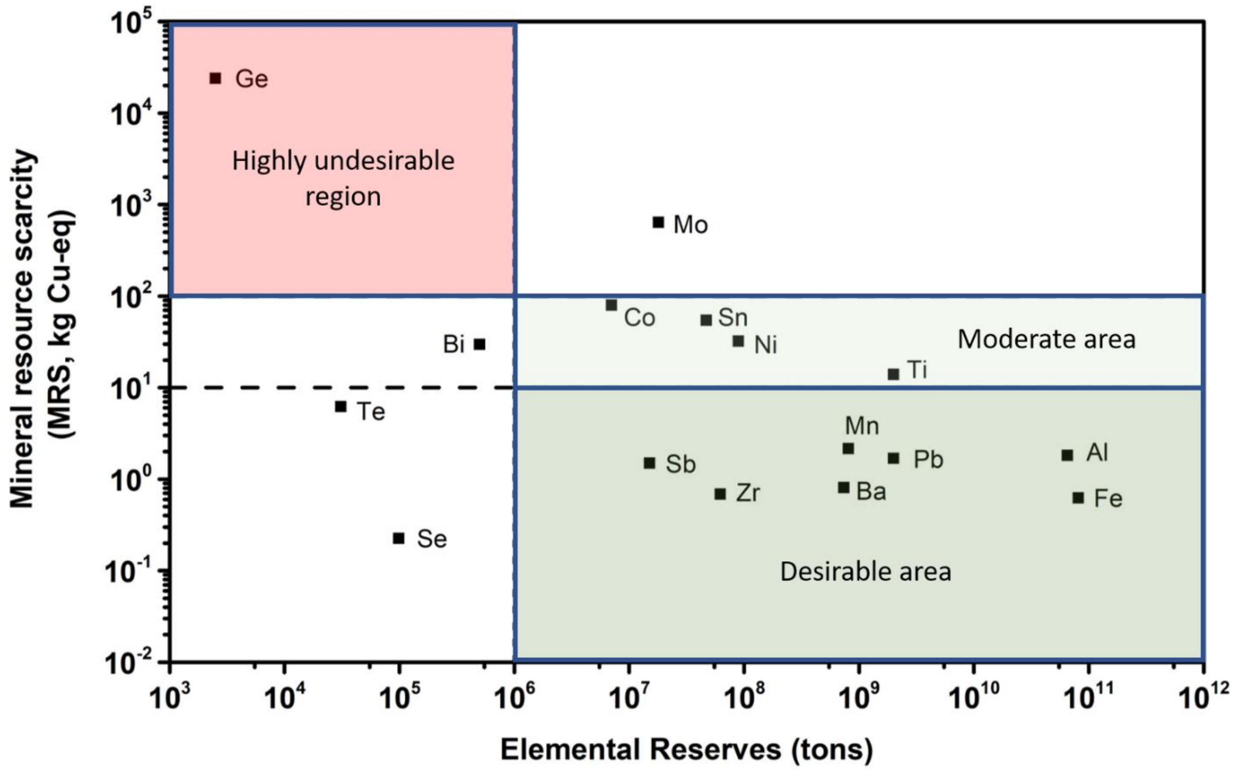

Figure 6.3: Comparison of life cycle scarcity (characterized MRS impact of elements, on per-kg basis) v/s elemental reserves (tons)[190] for constituent elements[2] (both x and y axes on $\log_{10}$ scales)

Based on the data for resource availability of elements and self-judgment, three regions have been marked in

Figure 6.3: desirable, moderate and completely undesirable (elements). As per this classification, 11 elements are seen to be either fully or moderately desirable, with the best

[2] Mineral resource scarcity (MRS) impact is considered for various constituent elements as an indicator of their life cycle scarcity, while elemental reserves is an indicator of their elemental scarcity. Elements for which elemental reserves were not available have been excluded from this analysis.

performance shown by iron and aluminum. The most interesting outcome here is for antimony – while it is seen to be in the desirable region (

Figure 6.3), its low elemental availability explains the aforementioned concerns about its large-scale use. Further, the use of cobalt – an element in the moderate zone in

Figure 6.3 – shows that its large-scale use must be approached cautiously, despite the divergence in its global reserves[52,58] vis-à-vis that predicted as per Ecoinvent database[143] using only low-concentration nickel ores (while ignoring high-concentration copper ones[191]).

Given the (near-)convergence between the two notions of scarcity, it would be prudent to focus solely on elemental scarcity, assuming that the other issue is automatically addressed. In this regard, numerous TEs have surfaced in recent decades[49] to ameliorate this dilemma, among which three stand out for potential promise: Half-Heusler (HH), oxides (OX) and organic (ORG) TEs[23,58,169]. For HH systems, this is because of two reasons: (a) These typically employ only one of the four aforementioned scarce elements – antimony, that too usually in much lower amounts (as dopants) than in say, SK modules[49,58] (also seen in Chapter 3); and (b) They involve considerable use of earth-abundant elements, such as hafnium, zirconium and titanium[52,58] (the latter two are shown in

Figure 6.3). On similar lines, a number of OX TEs also use relatively more abundant elements, such as sodium, zinc and titanium[52,58] (the last is shown in desirable region of

Figure 6.3). The likely better performance of OX TEs on this aspect is further buttressed by an estimation of life cycle scarcity impact of these three elements using ReCiPe 2016 midpoint method[142], which shows lower impacts for these elements than their scarce counterparts. Lastly, ORG TEs can help to address the quest for use of abundant constituents in low-temperature applications[43,44], particularly given the much lower scarcity-related impacts of crude oil refining process[184] over coal-based electricity[158] (Chapters 3 and 5). Yet, even as initial evidence seems promising, a thorough and comprehensive analysis is required for TE generators (full TE devices) based on these systems to assess the extent of benefits achievable via their use – an aspect that merits considerable attention in particular from policymakers.

Apart from scarcity, elemental availability also depends on various other factors that influence its supply – such as geopolitical, domestic and institutional ones, as well as those involving alternative uses of the concerned element[73,192,193]. These factors also apply to TE constituent elements, especially the second factor, as a number of such constituents are used for alternative clean energy technologies. For example, tellurium is an important constituent element of several TE systems (as described earlier), but it is equally critical for a major second-generation solar energy material – cadmium-telluride[194,195]. This pits the two technologies – thermoelectrics and solar energy – competitively against each other. In order to analyze the effect of this competition in influencing the supply of various elements, the US Department of Energy (U.S. DoE) has evaluated the criticality of elements based on two factors: supply risk, and importance to clean technologies[192]. Although this evaluation focuses only on 16 elements, it points to the criticality/nearcriticality of both tellurium (for above-mentioned reason) and rare-earth elements (used almost entirely in SK modules[49,103,104]) due to political risks that affect its supply from producing nations. Therefore, policymakers must carefully consider these factors while taking decisions on TEs involving the use of such elements, given their strong linkages to availability and final TE costs[49]. Further, since most commonly used TE elements have been neglected in the concerned US DoE study, a similar analysis of such elements is required to identify and detail other critical elements that must also be preferably avoided – thus acting as a guide for researchers engaged in developing alternative novel TEs. Table 6-2 shows the desired numerical values for parameters associated with the second principle.

Table 6-2: Desirable values for parameters associated with Principle #2

Scarcity-related parameter	**Desirable numerical range**
Elemental reserves	Reserves > 10^6 tons
Life cycle scarcity (MRS impact)	MRS < 10 kg Cu-eq

6.2.3. Principle #3: Use Cleaner Grids for Producing TE Materials/ Devices

Despite the vast spurt in renewable energy generation over the past decade, fossil fuels continue to meet the dominant share of global electricity demand[196]. This is due to several reasons, including the ease of meeting baseload demand via coal-based electricity[197], irregular availability of major renewable sources like wind and solar radiation[198], and financial unviability of battery storage (at present) for grid-based applications[199]. In addition to delaying the transition to a cleaner electric grid and lowering the resultant greenhouse gas (GHG) emissions[162], these factors also contribute towards increasing the harmful ecological effects of products that use such fossil-based electricity for one or more stages of their life cycle. This can be debilitating for the overall ecological output of products, services and technologies, and can even render them as damaging to planet in spite of certain ecological benefits over specific life cycle stages. Given the significance of this rationale, clean electricity use has been treated as a stand-alone sustainability principle in itself for other domains, such as green tribology[71] and grid-based batteries[72] that can strengthen the use of intermittent renewable energy technologies.

The aforementioned argument also holds for thermoelectrics (TEs), which are conventionally treated as ecofriendly since their usage conserves scarce fossil fuels and reduces associated GHG emissions[141]. Yet, as shown in Chapters 3-5, TE device production causes considerable harm to environment, in part due to the fossil-dominated nature of electricity used to process TE legs that negates the ecological benefits of their usage – either partially (Chapter 3)[158,183] or entirely (Chapters 4 and 5)[184]. Hence, given the environmental benefits conferred by clean electricity usage on other products and technologies, their use must be duly evaluated for TEs as well.

In this regard, an estimation exercise was undertaken by considering two hypothetical, alternative grid scenarios to determine the quantitative extent of ecological gains achievable by using cleaner electricity for TEG production. For this purpose, baseline scenario was used from Chapter 5[184], where the average U.S. 2015 electric grid mix is considered for processing TE legs and other components. For both hypothetical scenarios, a different electric grid mix was assumed to be used solely for TE legs and alumina plates, given their dominant contribution on this count to various impacts, with the remaining components assumed to be still processed using the U.S. 2015 electric grid. The two scenarios are: (a) Idaho 2015 grid scenario, where the Idaho grid, composed of ~ 85 % hydropower, ~ 8 % wind-based, and ~ 5.50 % natural gas-based electricity, is used[137]; and (b) Solar-wind grid – a hypothetical grid assumed to be composed of 50 % each of solar- and wind-based electricity. Together, these grid scenarios also helped to gauge the relative effect of three commonly used renewable energy technologies – solar, wind and hydropower – on the ecological impacts of TEs, and this analysis could be extended further to other products and services as well. For the sake of simplicity, it was assumed that in each of the baseline and two hypothetical scenarios, the generators were disposed of at the end of their life (i.e., D-scenario or disposal as EOL treatment). More details on these alternative grid scenarios are provided in Section 1 of Appendix-D, while detailed information on TEGs is given in Chapter 2 and Appendix-C.

Figures 6.4–6.5 (a-b) show a comparison of the life cycle environmental impacts of TEG-1 and TEG-2 for the baseline (U.S. 2015 electric grid) and both alternative grid scenarios, while Table D-3 provides the magnitude of characterized impacts. As is evident, both alternative scenarios cause a drastic reduction in fossil fuel use (FRS) and coupled GHG emissions (GW) for the two TEGs over the base scenario, with larger reductions observed for TEG-2. In fact, these reductions are so significant that they render both TEGs ecofriendly on these two categories – unlike in the base scenario. This underlines the large degree of ecological benefits that can be attained by use of clean electricity for processing TEs from the viewpoint of their conventional justifications.

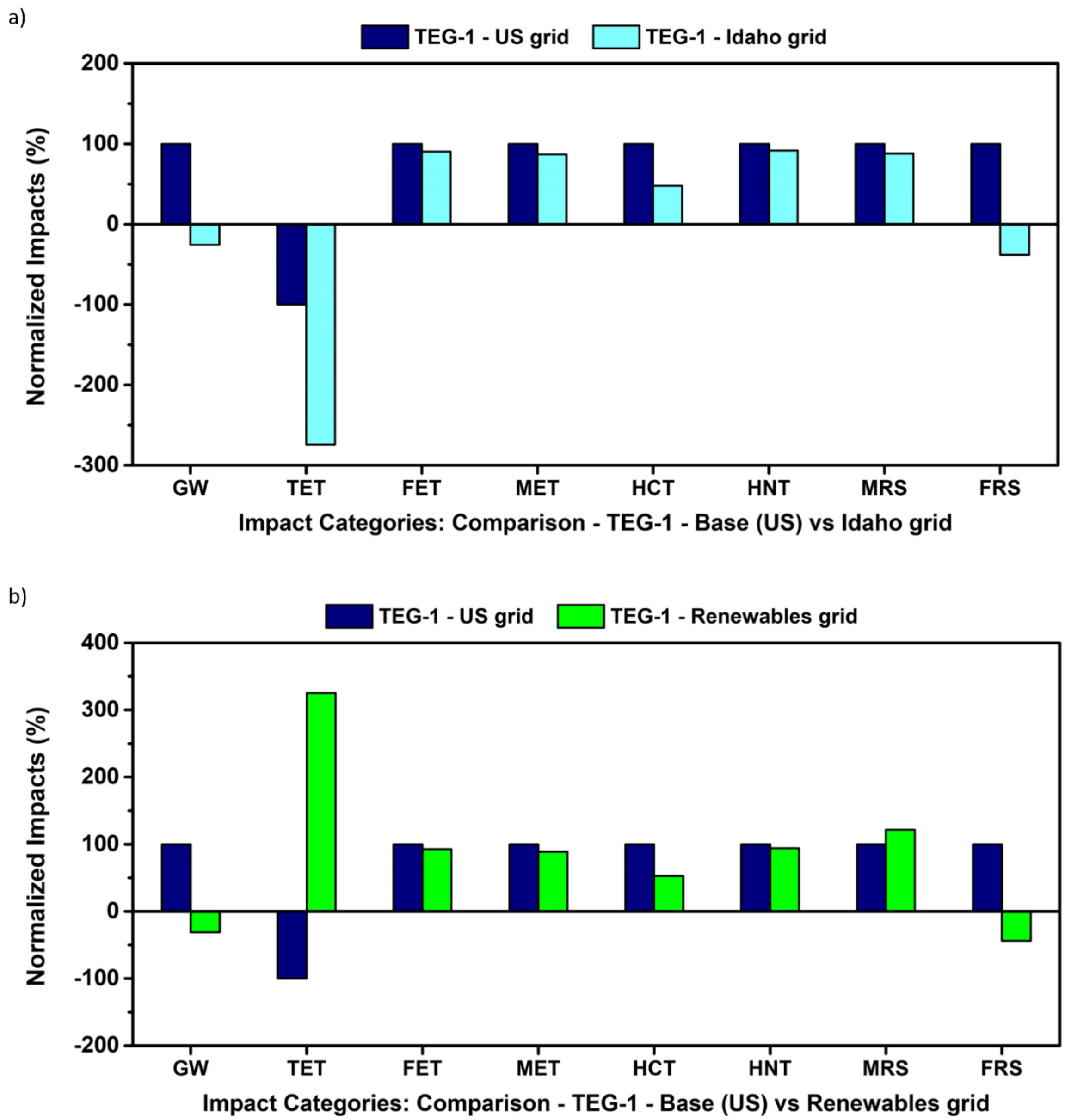

Figure 6.4: A comparison of life cycle environmental impacts of TEG-1 between the original scenario (average US 2015 electric grid) and: (a) Idaho grid; (b) Renewables grid for processing TE legs

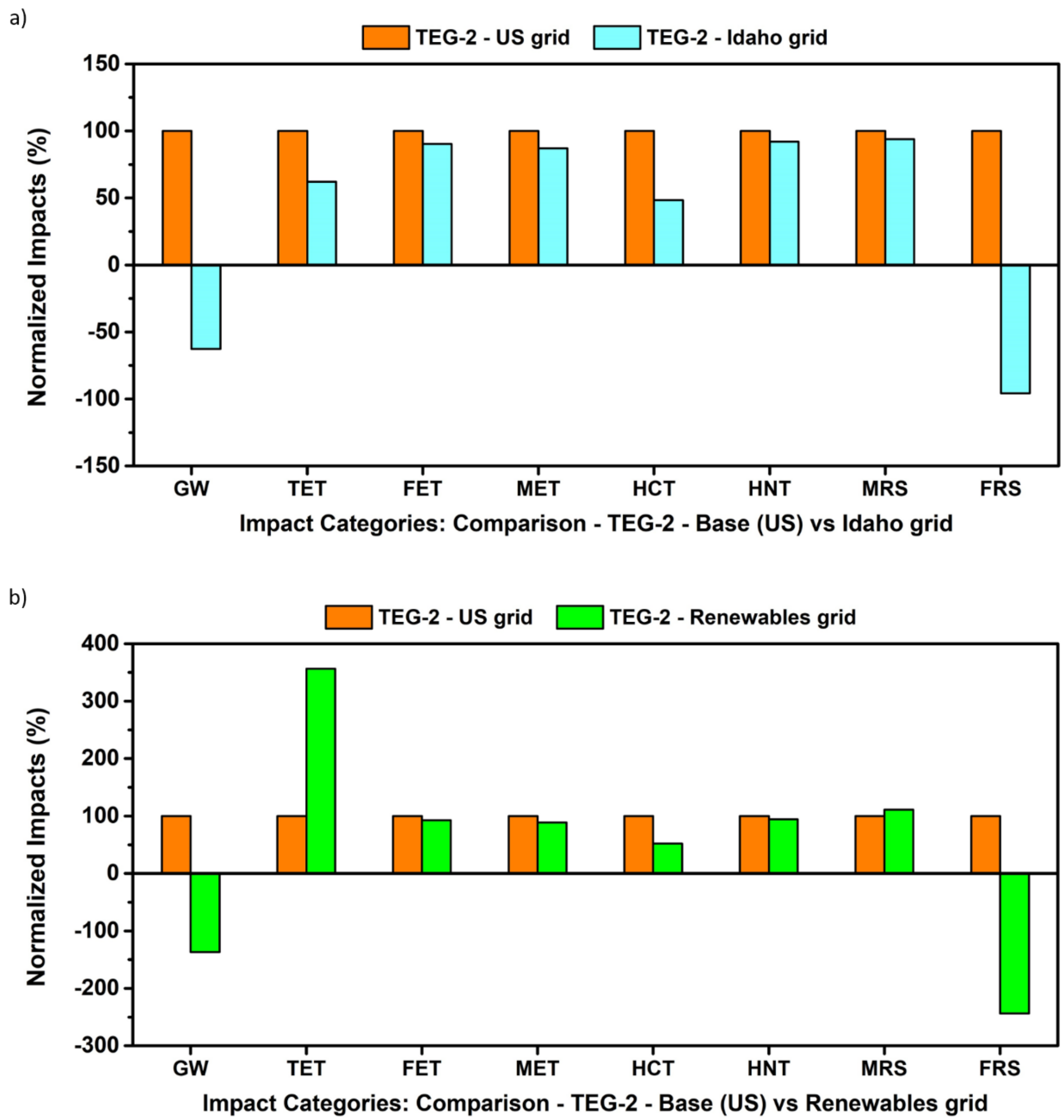

Figure 6.5: A comparison of life cycle environmental impacts of TEG-2 between the original scenario (average US 2015 electric grid) and: (a) Idaho grid; (b) Renewables grid for processing TE legs

Beyond GW and FRS impacts, a remarkable outcome to emerge from these alternative scenarios is their relative effect on the overall ecological performance of both

TEGs, including on the remaining six categories. On one hand, the solar-wind grid shows greater impact reduction than Idaho grid over the base scenario for both GW and FRS impacts, independent of the generator considered (Table D-3). This is mainly due to the large fossil fuel requirement and related GHG emissions for construction of large hydropower plants (Idaho grid), which easily outstrip fossil fuel use or GHG emissions involved in the construction of solar- and wind-based power plants (solar-wind grid)[137,142].

In contrast, the Idaho grid is seen to outperform solar-wind grid on remnant six categories for both TEGs. Strikingly, while the Idaho grid reduces impacts on all these categories for the two generators, the solar-wind grid achieves a similar outcome for only four of these impacts (all except TET and MRS). Of these, significant levels of decrease in impact are observed only on HCT (45-55 %) for both TEGs under these alternative scenarios vis-à-vis the baseline scenario (Table D-3) due to their replacement of CBE and its degrading effects via emission of carcinogenic substances like mercury[150,152,154]. On the other hand, much lower levels of reduction (5-15 %) are seen on the other three impacts for both TEGs (FET, MET and HNT) and on MRS for TEG-1. These observations are primarily due to the greater role of constituent elements used in TE legs (Te, Sb, Co and Bi) on these categories over that of electricity usage[184].

The most noticeable difference between the two alternative scenarios is however, observed for TET and MRS impacts of both TEGs. While the Idaho grid enables reduction on these impacts, including a substantial decrease in TET impact, the solar-wind grid is seen to be more damaging for ecology than even the base scenario (U.S. average 2015 grid). For TET, this divergence stems predominantly from the use of solar-based electricity through heavy use of copper in power generation equipment[153] and emission of toxic waste during silicon purification[142] (for subsequent use in solar panels). Conversely, the need for large amounts of copper, aluminum, nickel, silver and iron in electricity generation equipment for both solar- and wind-based electricity leads to their noteworthy contributions on MRS impact[142] for the solar-wind grid.

Overall, the results demonstrate the advantages of using cleaner forms of electricity in enhancing life cycle ecological output of TEs, especially regarding their traditional benefits of lower fossil fuel usage and GHG emissions[141]. These are broadly in sync with the principle as postulated on similar lines for batteries for both stationary[72] and mobile applications[73], given the ability of both energy technologies (TEs and batteries) to replace fossil-based energy. Yet, unlike these studies on batteries, this work also considers impacts beyond global warming. This enhanced scope helps to illustrate that cleaner grids may not always be ecologically suitable, as in case of the imagined solar-wind grid on TET and MRS categories. This points to the clear need for policymakers to focus on electric grid mix while advocating the use of TEs on large-scale, especially when TE manufacturers would focus on energy costs along with other factors in deciding on their final choice among the desirable location options for setting up their plants. A comprehensive analysis of grid mix in various regions must be accompanied by policies and mechanisms that incentivize the production of TEs and other energy technologies in regions served to a greater extent by cleaner forms of electricity. Such policies must not remain confined solely to tax breaks and subsidies, but should also explore the possibility of using non-monetary measures to discourage investment in regions where such electricity is not clean. Moreover, any such policy design or development must also account for recent improvements in efficiencies of renewable energy generation, and/or their raw material production, processing and refinement.

In terms of actual values, the extent of clean electricity in the grid mix option cannot be a single number, for it is related in turn to the kind of application for which the considered TE device is used for. For instance, TE modules perform quite well in coal-based power plants despite the use of fossil-heavy electricity for their processing (Chapter 3), but the gap is not addressed despite the use of renewables-based electricity for prominent components when considered for automobiles (Chapter 5, Figures 6.4–6.5). This divergence in their environmental performance is an outcome primarily borne out of the nature of fossil fuel replaced and the duration of usage for both applications. As a result, while it is perfectly fine to have a completely fossil-based electric grid for replacing coal-based energy with TEs in constant-use applications (Chapter 3), a 100 % renewables-based grid is inadequate in ensuring good ecological performance for the TE devices (modules and generators) used discontinuously for other applications (Chapters 4 and 5). Hence, the share of renewables in electric grid mix must be carefully evaluated for any TE device based on the nature of application it is sought to be used for. For obvious reasons, the preferred share value would be 100 % - i.e., an entirely renewables-based grid – to negate the use of fossil-based energy altogether. Nevertheless, such a shift must also consider the practical constraints associated with renewable energy technologies. Further, such a shift to cleaner electricity should prioritize the use of hydro-based electricity over other renewable energy technologies, given its greater ecofriendliness in relative terms (Figures

6.4–6.5). Table 6-3 shows the desirable share of renewables-based electricity needed to produce TE devices for different applications, based on the results obtained for this work.

Table 6-3: Cleaner grid-based electricity requirement for various applications (Principle #3)

Nature of fossil fuel replaced in application	**Duration of application and lifetime**	**Minimum desirable share (%) of renewables in electric grid mix used to produce TE devices**
Coal	Continuous use Long lifetimes	0 (i.e., renewables are not required at all)
	Continuous use Shorter lifetimes (e.g. < 3 years in this study)	100 (i.e., only renewables-based electricity must be used)
Natural gas	Continuous or discontinuous use Long/Short lifetimes	
Petroleum products		

6.2.4. *Principle #4: Minimize Production-Related Impacts Per Energy Service (Electricity Generated) via Use of Efficient Methods*

As described in the previous section, fossil-based electricity remains pivotal to production-related impacts of TE devices. Yet, it is not the lone factor behind these impacts, with the other major cause being the use of processing methods that consume vast amounts of both energy (electricity) and material for producing TE device components.

Regarding energy use, large amounts of electricity are used for TE leg processing, mainly due to the use of energy-intensive methods that consume > 75 kWh per kg of output material or powder (Tables A-2–A-29). These include methods for compaction-with-sintering (CWS), such as spark plasma sintering (SPS) and hot-pressing (HP), and annealing of powders in quartz tubes. For CWS techniques, this is the probable outcome of considering sample dimensions that are in line with small-scale production of TE samples, which were chosen due to paucity of alternative information (Chapters 2 and 3). The use of larger sample dimensions (height and/or diameter) can thus make CWS processes more energy-efficient. On the other hand, quartz tubes are used primarily to keep powders in vacuum during annealing (Table A-10). Yet, this restricts the amount of powder that can be heated in a single run of furnace, which increases the total quantity of electricity consumed for annealing. An alternative way to lower this energy intensity would be to use big containers where large amounts of powder can be heated in vacuum at temperatures ≥ 500°C. This would, however, be a challenging endeavor to realize due to the lack of a suitable industrial-scale equivalent of quartz tubes-based annealing process.

Apart from higher electricity consumption, another issue is the material-intensiveness of TE leg production, principally due to material losses associated with leg dicing process – as highlighted elsewhere[48,49]. Typically, TEs are produced as cylindrical samples through CWS techniques, after which they are polished and diced to final leg dimensions[48,49]. In Chapters 3-5, it was assumed that for leg dicing, only that portion of material was retained that corresponds to the square with the largest area on either of the circular ends (cross-section) of cylindrical samples, such that its diagonal was the diameter of this circle (a more detailed explanation is given in Section 2 of Appendix-A). Based on this definition, leg dicing efficiencies (LDEs) were calculated and obtained for various TE modules, varying from as low as ~ 10.50 % for BT-1 to as high as ~ 54 % for BT-2 module. This variation was the outcome of differences in dimensions of sintered cylindrical samples and final TE legs for each module. Thus, even assuming the best possible LDE, nearly half of the sintered powders would be lost under the definition of leg dicing used in this work. Further, the lost powders cannot be reused again, as they have been subjected to repeated thermal cycling, raising serious doubts about the repeatability of their TE properties for long-term purposes[53,200]. This significant amount of material wastage compounds the aforementioned twin effects of using large amount of fossil-based electricity and energy-intensive processing methods, thus negating ecological gains of this platform by a considerable degree.

To evaluate the quantitative extent of benefits that are forsaken due to lower LDEs, an alternative scenario was analyzed for both automotive TEGs evaluated in Chapter 5. This scenario envisaged higher LDEs over baseline scenario by adopting a different method of leg dicing. Under this method, dicing was undertaken by recovering material that corresponds to the maximum number of squares which can be formed on either of the circular ends of cylindrical sintered samples. Such a change in cutting methodology leads to drastic improvement in LDE of TE legs (BT: ~ 31.50 %; SK: ~ 52-53 %) over their original scenario (BT: ~ 10.50 %; SK: ~ 30-36 %), as shown in Section 4 of Appendix-D.

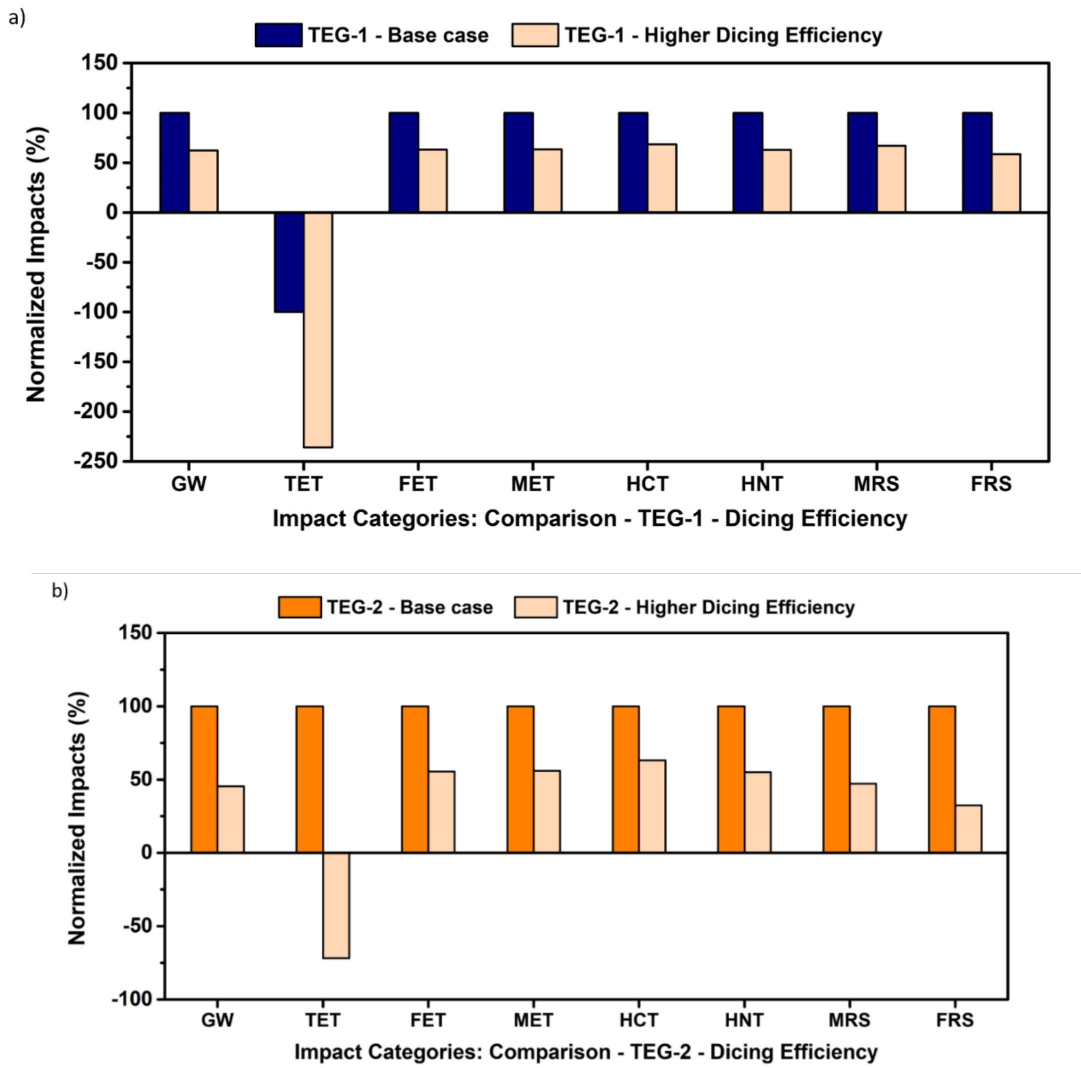

Figure 6.6: A comparison of environmental impacts under two scenarios – base scenario (original leg dicing efficiency) and alternative scenario (hypothetical increase in leg dicing efficiency) for TE legs in: (a) TEG-1 and (b) TEG-2

Figure 6.6(a-b) shows the effects of improving LDE for both TEGs, considering their disposal as the end-of-life (EOL) scenario, while Table D-4 provides the magnitude of characterized impacts for the two generators under base and improved LDE scenarios. As shown, enhancement in LDE causes substantial decrease in ecological impacts of both

TEGs on all categories. A greater extent of decline in impacts is observed for TEG-2 over TEG-1 due to additional material savings (or lower material usage) via improvement in LDE for BT legs. Among the various impacts, increase in LDE results in similar levels of impact reduction on four categories (FET, MET, HCT and HNT) for both generators (TEG-1: ~ 30-38 %; TEG-2: ~ 37-45 %). Conversely, higher LDE imparts substantially higher ecological effectiveness to TEG-2 (~ 53-68 %) over TEG-1 (~ 33-42 %) on three of the four remaining impacts (GW, FRS and MRS). Finally, in stark contrast to the above results, both generators reveal a dramatic fall in their TET impact, especially for TEG-2, which shows a complete reversal of its life cycle performance (from negative effects in base case to positive performance in higher LDE scenario). Nevertheless, TEG-2 also exhibits a much lower degree of reduction in impacts than TEG-1, unlike the aforementioned impacts (Table D-4). This can be ascribed to the vast gap in their respective TET impacts in the original scenario (Tables C-10 and C-11), which persists even after improvements in LDE for TE legs in the hypothetical scenario. The absence of a similar extent of gap on other impacts in base case explains the relative performance of both TEGs on other categories.

These results clearly justify the need to ensure higher efficiency of both energy and material usage for processing methods employed for TE legs. Given that leg dicing is unlikely to achieve higher efficiencies (> 85 %), it would be prudent to focus on their replacement with alternative techniques that perform better on both counts. Remarkably, this issue has gained prominence among TE researchers mainly during the previous decade, especially for using alternative processing methods[23,48,49]. The leading alternative in this path is selective laser sintering (SLS) – an additive manufacturing technique that is mainly deployed for 3D printing[201–203]. Interestingly, the use of SLS has been advocated mostly for its capability to decrease material wastage by helping avoid leg dicing processes altogether[201,202], even as its energy consumption has received relatively little attention. Rough calculations – described in Section 5 of Appendix-D – however, suggest that even at one-third efficiency of that in literature (15 kWh/kg, albeit for polymers and metals[204,205]), at the very least, SLS can halve the energy used in sintering processes. Still, more studies are required to determine the feasibility of obtaining direct TE legs via this technique for TE systems of the future, as well as to estimate and compare its ecological impacts with those of conventional manufacturing methods based on more accurate data. Apart from this aspect, policymakers must also focus on opportunities for developing other novel processing techniques that can further lower the energy and material consumption for TE leg processing and make these devices ecologically apt and commercially competitive for large-scale use.

A critical area to focus upon with reference to this principle, is the need to lower the large gap (ranging between 80 and 97 %) between production-related negative impacts and use-related positive effects of TE devices on toxicity- and scarcity-related impacts (Chapters 4 and 5). While reduction in sintering-related electricity consumption via use of techniques such as SLS can prove to be extremely useful in fulfilling this aim, it was not observed to be enough in ensuring positive ecological performance on all impacts for the devices considered in this work. Hence, there is a clear need for more alternative methods, both for sintering, and also for existing annealing processes that currently require quartz tubes, to help improve the ecological viability of this platform. Policymakers must work in collaboration with researchers and device manufacturers to develop such methods that can help address this aspect, through a combination of suitable tax policies, subsidies or financial incentives, and other non-monetary measures. Table 6-4 provides the extent of reduction that is required in production-related impacts to eliminate the gap between negative effects of production and positive benefits of use stage, based on the results obtained in previous chapters. While the non-required reduction in production-related impacts for coal-based power plants is applicable for future applications involving continuous waste heat emission and replacement of coal-based energy, the other results are applicable for all other kinds of applications.

Table 6-4: Extent of decline required in production-related impacts for eliminating their effects over and above use-related benefits (to evaluate effect of steps taken to implement Principle #4)

Application	**Extent (%) of reduction required in production-related impacts for eliminating their effect over and above use-related benefits**	**Categories on which reduction is required**
Baseload coal-based power plants	N.A.	N.A.
Peak load natural gas-based power plants	50 – 99.50	Toxicity- and scarcity-related categories (all barring GW and FRS)
Automobiles	30 – 99.50	All categories

6.2.5. *Principle #5: Maximize Conversion Efficiency Per Mass of TEs*

The central focus of researchers within the TE community is on increasing the heat-to-electricity conversion efficiency of this energy harvesting platform. This is exemplified by the numerous innovations and advancements in this field, such as the emergence of novel TEs, deployment of multiple topologies for TE devices, and certain choices for key determinant parameters (such as fill factor)[14,22–24,29,48,49,181]. While such confined focus ignores the negative ecological effects of their production and end-of-life (EOL) stages, conversion efficiency is still vital in shaping the functioning of these devices on some environmental impacts, such as global warming (GW) and fossil resource scarcity (FRS) (see in Chapters 3-5). Hence, attempts aimed at developing sustainable TEs (materials and devices) must concentrate on the interplay between the benefits of higher conversion efficiency in use stage, and the environmental effects of producing such TEs as well as of their end-of-life treatment.

Among the pertinent domains where such interplay is clearly observed is the mass of TE legs used in the final device. On one hand, the first four principles (Principles #1-4) together lead to the conclusion that this mass must be as low as possible in order to lower the detrimental ecological effects of device production. In fact, Chapters 3-5 highlight this to be extremely critical, as they show the disproportionate role of TE legs on ecological impacts of TE devices vis-à-vis their mass, with negligible contribution from other components barring ceramic plates. At the same time, lower use of TEs reduces the overall conversion efficiency of TE devices, since both the mass and nature of TE system influences the resultant device properties, including their output power. This conundrum between the two opposite effects, both of which are dependent on the mass of TEs employed, needs a viable resolution to boost the sustainability of this technology.

To tackle the aforementioned conundrum, two parameters are proposed for TE legs that merit deliberation and further consideration – namely, the ratios of: (a) Conversion efficiency-to-mass; and (b) Output power-to-mass, where the mass refers only to mass of TE legs. Both these ratios represent the amount of positive ecological outcomes by TE usage per unit of negative effects caused by their production and EOL treatment. This explains the rationale for maximizing these two ratios, while also enabling the avoidance of separate focus on individual impact categories. The reason for considering both the ratios instead of any one of them, is because while output power is more directly altered by the mass and number of TE legs, conversion efficiency is affected more by the nature of TE system used.

To validate the salience of proposed parameters, these ratios were calculated for the TE modules analyzed in this work, and the values are provided in Table 6-5. As can be seen, PT and HH modules exhibit the highest values for both conversion efficiency-to-mass (> 0.50 %/g) and output power-to-mass (> 2 W/g) ratios. On the contrary, SK-2 and BT-2 modules show the least values respectively for these ratios. Remarkably, the order of these two ratios for different modules is in line with their respective environmental output, with HH and PT modules exhibiting the best, and SK-2 and BT-2 showing the worst or near-worst performance for power plants (Chapters 3 and 4). While an exact comparison between different modules is not entirely appropriate given differences in their operational temperature ranges, this finding clearly shows the importance of both the proposed ratios, thus showcasing them as being pivotal in determining ecological effects of TEs.

Table 6-5: Ratios of conversion efficiency-to-mass and output power-to-mass of TE modules (mass here refers to mass of TE legs)

Module	**Total mass of TE legs (g)**	**Conversion efficiency (%)**	**Unit conversion efficiency (%/g)**	**Wattage (W)**	**Unit wattage (W/g)**
BT-1[105]	14.60	4.08	0.28	18	1.23
BT-2[106]	23.14	7.00	0.30	4.17	0.18
SK-1[103]	30.00	7.50	0.25	11.51	0.38
SK-2[107]	86.89	7.30	0.08	25.08	0.29
HH[108,109]	7.09	4.50	0.63	15.5	2.19
PT[110,111]	1.45	8.80	6.06	3.50	2.41
SC[106,112,113]	7.95	6.40	0.80	4.81	0.61

Apart from the TE material used, other parameters can also play a determinant role in shaping the output power and conversion efficiency of the concerned device. A prominent parameter in this context is the topology employed to construct TE devices. Conventionally, most commercial TE systems are developed based on the rectangular topology[48]. However, this constrains the ability to deploy this platform for other applications that demand other topologies, such as flexible systems in case of body-wearables[43,48]. Therefore, this aspect has gained greater attention in recent decades.

In order to understand the importance of topology for ecological benefits obtained by use of TEs, one of the studies used for automotive TEGs was considered[104], as it evaluates and compares TEGs that use only skutterudite (SK-1) modules in four different topologies. Table 6-6 shows the electrical output and output power-to-mass for each topology. A similar calculation could not be undertaken for the other proposed ratio (conversion efficiency-to-mass) due to lack of data on their respective system conversion efficiencies. As shown, the four topologies vary both in their output power-to-mass ratio (over a smaller range: 0.42-0.49 W/g) and final output power (over a much larger band of ~ 635 W for hexagonal and ~ 730 W for transverse configuration)[104]. This can be ascribed to the effects of topology on energy transfer from waste heat to heat exchanger components and later, to TE modules[104], which in turn influence the final TE conversion efficiency. Overall, this table shows the value of topology in determining ecological effectiveness of TE devices.

Table 6-6: Electrical output of TE generators for various topologies[104]

Topologies	**Mass of all modules**	**Output power (W)**	**Unit power (W/g)**
Hexagonal	1500.25	634.40	0.42
Longitudinal	1500.25	698.30	0.46
Cylindrical	1500.25	718.90	0.48
Transverse	1500.25	729.80	0.49
Type of module: SK-1; Number of modules = 50; Mass per module = 30.005 g			

In totality, these findings show that initiatives for developing newer TEs must be directed towards improving the proposed ratios and considering various topologies that can be applied to improve the environmental outcomes of this platform. Numerically, these findings signify the need to attain values of $\geq$ 0.50 %/g and $\geq$ 2 W/g for conversion efficiency-to-mass and output power-to-mass ratios respectively to achieve desirable environmental performance. Simultaneously, these ratios must complement existing factors of prime importance, such as the end-use application and its range of waste heat temperature, performance of various TEs (treated as potential options) in this temperature range, and also the mechanical and thermal stability of these options. Table 6-7 shows desirable numerical values for parameters associated with this principle.

Table 6-7: Desirable numerical values for parameters associated with Principle #5

Parameters for TE device	**Desirable values**
Conversion efficiency-to-mass	Greater than (>) 0.50%/g of TE legs used in device
Output power-to-mass	Greater than (>) 2 W/g of TE legs used in device

6.2.6. Principle #6: Minimize Efficiency Losses Over Time Due to Thermal Cycling

As described in Chapter 1, TEs are applicable for a diverse range of end-uses, particularly regarding the nature of their waste heat generation (continuous, periodic or intermittent)[158,183,184]. Among these, continuous waste heat emission has relatively lower or negligible effect on TE conversion efficiency (Chapter 3), while discontinuity leads to thermal cycling[19,116,183,184] (Chapters 4 and 5) that triggers a drop in their conversion efficiency and output power. Hence, thermal cycling depresses the extent of ecological benefits attainable via deployment of TEs, thereby affecting their overall life cycle sustainability (Chapters 4 and 5). This lays bare the importance of TCRC (thermal cycling reduction coefficient), and the rest of this section is devoted to this aspect.

TCRC values of modules analyzed in this dissertation (shown in Table 2-5) clearly indicate that both BT modules (BT-1 and BT-2) and HH exhibit the least TCRC values (≤ 0.005 % per cycle), while the two SK modules (SK-1 and SK-2) exhibit the highest TCRC values (0.022 % per cycle). This divergence is also reflected in their environmental output, with HH and SK modules showing the best and worst performance respectively. Such deviation in TCRC of different TEs stems largely from their other properties (i.e., beyond their TE performance) under the considered operational temperature conditions. For instance, as described in Chapter 4, SK systems are highly prone to oxidation and mechanical degradation in ambient/oxygen-rich atmosphere at elevated temperatures[160,161], which likely explains their higher TCRC value. Conversely, excellent mechanical and thermal stability of HH systems at higher temperatures (up to 1000 K)[208] is the probable reason behind their much lower TCRC values and higher ecological output.

Given the relevance of thermal cycling in influencing TE conversion efficiency, its effect has been studied for a number of TE systems, as highlighted in Appendix-B (Section 2). Yet, these studies are much less when compared to the number of initiatives directed towards developing novel TEs, including those with higher conversion efficiencies[14,22–24,29,48,49,181]. This makes it difficult to evaluate TEs from ecological perspective for a number of potential end-uses that involve thermal cycling, such as refrigeration[116], medical uses[215], and even the applications considered in this work. While new TEs with higher initial conversion efficiencies (vis-à-vis their mass) are definitely required, their TE properties must also be studied under repeated thermal cycling conditions that replicate actual operational setup to evaluate their large-scale suitability. To achieve this aim, multiple strategies should be developed to minimize the effect of thermal cycling on TE conversion efficiency – on the lines of strategies that have been designed to boost TE figure of merit[22,25]. Some initial strategies in this regard can focus on both developing novel, more-efficient TEs, as well as using barrier materials to lower the TCRC value to below 0.005 % per cycle – the higher limit of best-performing modules in this work. Hence, policymakers must focus on targeted action and collaboration with other stakeholders to achieve both these aspects (Principles #5 and #6) to ensure that TEs are ecologically preferable for applications involving thermal cycling for long-term duration. Table 6-8 shows the desired range for the lone parameter associated with this principle.

Table 6-8: Desirable numerical value of parameter critical to Principle #6

Parameter	Desirable numerical range
Thermal Cycling Reduction coefficient (TCRC)	Should be ≤ 0.005% per cycle

6.2.7. Principle #7: Maximize Benefits from Energy Generation Over Impacts Caused During Other Stages

As stated in the previous section, apart from TCRC, another crucial factor that influences the ecological output of TEs for chosen applications is their duration of use, both on per-cycle (i.e., duration of use per each cycle) and overall basis. Such lower usage in turn substantially diminishes the environmental benefits that can be achieved by harvesting energy using this platform, thus lowering its environmental effectiveness.

To validate the importance of this factor, TE modules were analyzed for applications involving periodic waste heat generation (Chapter 4). While retaining the same application as that considered in this analysis (natural gas-based power plant for peak demand), the focus here was solely on HH module as it outperformed all other modules.

Also, D-scenario (disposal) was assumed to be the EOL scenario. Based on these assumptions, initial calculations were made to estimate the minimum number of hours per cycle over which the HH module should be operated in order to exhibit ecological benefits on all impact categories. These calculations showed this number to be ~ 17.55 h, meaning that the gas-based power plant must function for a minimum period of 17 h 33 min every day over its entire lifetime (assumed as 25 years) for the HH module to be beneficial on all impacts (see Section 6 of Appendix-D). The necessity of using this module for such high length of time, both on per-cycle and overall duration, is primarily the outcome of much lower ecological impacts of natural gas-based electricity over its more polluting coal-based counterpart (Chapters 3 and 4). This forces the HH module to be used over a significantly longer duration to acquire enough leverage to compete with the harmful effects of its production on account of factors described in Chapter 3.

Apart from the afore-described calculation, another hypothetical scenario was considered that focused on using HH modules over a much longer lifetime than its initial value (25 years, the lifetime of a gas-based plant)[183]. For this scenario, the original TCRC as well as original per-cycle usage period (4 h) were retained, and it was instead imagined that the TE module was shifted after every 25-year period to a new NG-based plant, with the process repeated several times till the output wattage of module reached 1 % of its original value. Assuming zero emissions over this movement across power plants and the direct applicability of this module (as a set) in the new plant from old one without any modification, it was found that the HH module can be operated for a maximum of 251 years. In other words, assuming its use for one cycle per day, the HH module can be used over 10 gas-based power plants prior to reaching the end of its life. Yet, even after this long duration, this module did not become ecologically suitable on all impacts, and showed negative effects on one category (FET) (not shown here for paucity of space). Instead, it took an increase in per-cycle usage duration from 4 h to a minimum of ~ 6.52 h or 6 h 31 min per day for the HH module to show positive effects on all categories in this hypothetical scenario (impact results in Section 6 of Appendix-D).

From the aforementioned calculations, it becomes clear that a mere increase in overall usage duration is unlikely to be adequate in ensuring life cycle environmental sustainability of TEs. Instead, a three-pronged strategy is required to strengthen the ecological soundness of this platform. First, policymakers must identify the different sectors for which they seek to promote the application of TE devices. Second, they must engage with environmentalists and researchers to identify specific TE systems that exhibit ecological effectiveness for various end-uses, along with the minimum amount of time for which these systems must be operated for beneficial effects. At the same time, care must be taken to ensure that these TE systems show desirable performance on other aspects, such as high conversion efficiency (to mass) and long-term thermal and mechanical stability. Third, after determining the appropriate TEs for various sectors, policymakers must coordinate with concerned sectoral players (actual end-users) to encourage the use of this platform in their facilities for the desired length of time (both per-cycle and overall duration) for good ecological outcomes, provided it is practically achievable. Such encouragement should be intertwined with specific incentives – be it monetary (such as tax breaks) or non-monetary (like a framework to monitor the extent of use of TE devices) –

to boost the use of this technology. Also, sectors for which ecologically suitable TEs have not been identified must be separately categorized, and policymakers must work with researchers to develop novel TEs for such end-uses.

Since the application of this principle will be sector and device-specific, as explained above, the actual value for usage duration will differ on a case-to-case basis, and an absolute value cannot be necessarily provided, unlike for most other principles. Nevertheless, this should be extensively researched to identify potential sectors and materials for usage in these domains. For this study, the value of minimum lifetime for desirable environmental performance of all applications is provided in Table 6-9, based on which it can be concluded that this principle should be taken on case-to-case basis to determine the minimum operation and lifetime usage duration, keeping in mind the feasibility of doing so.

Table 6-9: Minimum lifetime required for desirable environmental performance of TE devices for considered applications (in earlier chapters)

Application	**TE devices**	**Minimum required lifetime for desirable environmental performance on all categories**
Baseload coal-based power plant	BT-1 module	~ 2.35 years (858 days)
	SK-1 module	~ 3.5 years (1278 days)
	SK-2 module	~ 5.5 years (2007 days)
	HH module	~ 1.55 years (566 days)
	PT module	~ 1.3 years (475 days)
	BT-2 module	

	SC module	Not possible, as positive performance not possible even upon extension in lifetime
Natural gas-based power plant	BT-1 module	Not possible, as positive performance not possible even upon extension in lifetime
	BT-2 module	
	SK-1 module	
	SK-2 module	
	HH module	
	SC module	
Automobiles	TEG-1	
	TEG-2	

6.2.8. Principle #8: Design for Secondary Usage and Circular Economy Approach as End-Of-Life (EOL) Scenario

Across the previous seven principles, focus has remained confined to two life cycle stages: production and primary use of TE devices. This ignores two other stages, namely, their (possible) secondary usage, and the treatment meted out to such devices at the end of their life (EOL). Both these stages have been reported to exert a substantial influence on environmental consequences and cost of other energy technologies, such as batteries[72,73], mainly via recovery of initial materials and avoidance of energy-intensive processing methods. Since both aspects are also crucial for TEs, their environmental effects must also be evaluated to determine their relevance.

For secondary use, its salience stems from two different aspects – the nature of primary use of TEs, and the fossil fuel replaced by their application. As shown earlier, TEs exhibit environmentally sound outcomes when they replace the more polluting coal-based electricity on continuous basis for longer duration (Chapter 3). In such cases, secondary use may not be essential for TE devices to ensure ecological suitability, as this has already been achieved in the primary use cycle. In stark contrast, they are harmful on some or all impacts when used to substitute the less-polluting natural gas (Chapter 4) or petroleum products (Chapter 5) by harvesting waste heat on discontinuous basis for shorter durations. In such primary end-use cases, secondary usage of TE devices can help to ameliorate their negative consequences, primarily by replacing a more polluting fossil fuel like coal and/or by application on constant basis for a considerable duration.

Regarding EOL treatment, its importance has already been highlighted in Chapters 3-5, which show weighty gains from the recycling of TE devices for applications where less-polluting fossil fuels are replaced (Chapters 4 and 5). This occurs due to two reasons. First, as described in previous chapters and reiterated in Section 6.2.2, a number of TE constituent elements are scarce, so their recycling helps to avoid probable challenges related to their unavailability and likely lowering of futuristic relevance. Second, TE devices also involve substantial use of metals for heat exchanger components, such as stainless steel and copper, that are potentially recyclable. Since the recycling of such metal-based components yields substantial ecological benefits (Chapter 5), it merits consideration in the overall framework to develop sustainable TEs.

In order to showcase the joint importance of both secondary (cascading) use and EOL stages, an alternative hypothetical scenario was envisaged for TEG-2 used in Chapter 5 for analysis. In the original situation, TEG-2 undergoes primary use over 100,000 miles of travel in Chevrolet Suburban, which corresponds to a total usage duration of ~ 3,535 h. Assuming its overall life to be 15 years of continuous use (Table 2-9), the left-over life of this generator is considered to be the difference between these two numbers, or 127,865 h (i.e., 131,400-3,535 h), or ~ 14.5 years. Given this extensive left-over lifetime, it is assumed that TEG-2 is used for this remaining period to harvest waste heat on continuous basis in a baseload coal-based power plant as its secondary usage application – since TE devices are seen to show the best performance for this among all chosen applications (Chapters 3-5). However, unlike in Chapter 3, here, the generator exhibits reduced conversion efficiency due to thermal cycling over its primary usage cycle. Furthermore, the circular economy approach (CE-scenario) is considered as the end-of-life (EOL) treatment to highlight its contribution in this hypothetical scenario.

Based on these assumptions, Figure 6.7 shows ecological impacts of TEG-2 under the original and hypothetical scenarios. As can be seen, the hypothetical scenario is observed to cause positive effects on all categories and easily outperforms the original scenario (which only uses circular economy approach but ignores any secondary usage). This shows the advantages as well as the need to implement both secondary/cascading use and material recovery and recycling to improve beneficial effects of this platform.

To enable real-life attainment of above-mentioned benefits, several steps are required to be undertaken, involving multiple stakeholders, as in case of other principles. The first and most immediate requirement is the creation of markets that ensure supply of TE devices from primary to secondary users and extend their life by delaying the time to EOL treatment. This would require advocacy on the part of researchers and policymakers for cascading of TE usage across end-uses where more polluting fossil fuels (such as coal) are used, and/or waste heat is emitted continuously. As described earlier, such market creation can be incentivized via subsidy provision and tax breaks, as well as via use of specific policies that mandate the secondary use of TE devices. However, these policies must also consider the nature of TE material being employed, since different TEs are optimal across divergent temperature ranges and can achieve varying degrees of ecological benefits in primary and secondary use cycles.

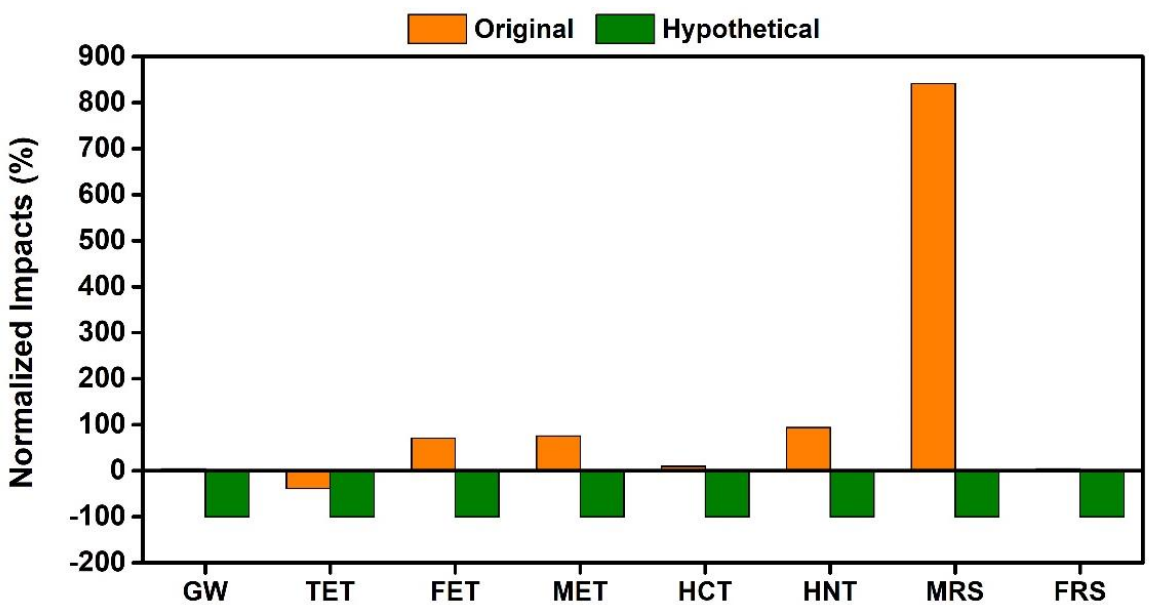

Figure 6.7: A comparison of life cycle environmental impacts of TEG-2 under original scenario (only primary use) and hypothetical scenario (involving cascading use), assuming circular economy as the end-of-life scenario

Apart from market creation, policymakers must also focus on the creation and sustained existence of relevant players in TE recycling market for efficient implementation of circular economy approach. For instance, recyclers must have strong tie-ups with primary and secondary users of TE devices – identified via analysis by policymakers – to recover them from numerous end-users, disassemble these devices, and recycle both metal-based components and TE legs (after appropriate reprocessing) for subsequent reuse. The advent of such players – a non-existent domain at present – requires dedicated efforts on the part of policymakers who must engage with businesses and entrepreneurs interested in this sector. A key feature of such efforts must be effective coordination and collaboration between them to ensure and enhance the economic viability of this new enterprise, as well as to scale-up all essential infrastructure to meet the recycling needs associated with large-scale application of TEs. In addition, policymakers must also concentrate on non-monetary regulations or measures, including exploring the possibility of restricting or even banning the landfilling of scarce or critical TE constituent elements. Such limits of landfilling are vital as they can help boost the environmental and economic benefits of material recovery, while also helping to evade any potential hazard caused by the dissociation of TEs in natural environment due to particular chemical reaction(s).

While landfilling of TE constituent elements must be discouraged, their recycling merits a thorough consideration of both their toxicity, as well as of the final TE material developed (both p- and n-type legs). Hence, appropriate safety and health standards must be developed and strictly enforced with regard to the handling of these materials by workers in TE industries. Lastly, it must be noted that even under the circular economy approach envisioned in Chapters 3-5, some amount of TE material is indeed disposed of. Hence, policies aimed at confining landfilling must also factor in these practical realities while imposing regulatory and other measures on TE manufacturers and other stakeholders. Simultaneously, this also opens new opportunities for TE researchers to develop alternative reprocessing technologies that can enable greater degree of recovery for constituent elements used in TE legs – an aspect that should be given top priority within the community.

Finally, since this principle focuses on considering two approaches (cascading use and circular economy), which are strict values, and since secondary usage has nothing specific beyond the requirement for use in applications involving continuous waste heat emission and replacing coal energy for longer lifetime, no numerical values are proposed per se in terms of making this platform more sustainable. However, as an additional summary, Table 6-10 shows the numerical values for the various principles described.

Table 6-10: Numerical values and other features for various principles

Principle	**Parameters/Situations**	**Desirable numerical values**
Principle #1: Minimize the Use of (and Exposure to) Toxic, Hazardous Elements in TE Materials	Elemental toxicity	TLV $\geq$ 2 mg/m^3
	Life cycle toxicity	Normalized value $\leq$ 100
Principle #2: Minimize the Use of Scarce and Critical Elements in TE Materials	Elemental reserves	Reserves $\geq 10^6$ tons
	Life cycle scarcity	MRS (Characterized impact) $\leq$ 10 kg Cu-eq
Principle #3: Use Cleaner Grids for	Applications involving coal-based energy and continuous	Not required

Producing TE Materials/ Devices	waste heat emission for longer lifetimes	
	All other applications	100 % renewables-based grid
Principle #4: Minimize Production-Related Impacts Per Energy Service (Electricity Generated) via Use of Efficient Methods	Gap between production-related negative impacts and use-related benefits for various applications	Baseload coal-based power plants: Not required Other applications: 50-100 %
Principle #5: Maximize Conversion Efficiency Per Mass of TEs	Conversion efficiency-to-mass	≥ 0.50%/g of TE legs (in device)
	Output power-to-mass	≥ 2 W/g of TE legs (in device)
Principle #6: Minimize Efficiency Losses Over Time Due to Thermal Cycling	Thermal cycling reduction coefficient	≤ 0.005% per cycle
Principle #7: Maximize Benefits from Energy Generation Over Impacts Caused During Other Stages	Usage duration will be application-specific	
Principle #8: Design for Secondary Usage and Circular Economy Approach as End-Of-Life (EOL) Scenario	Type of secondary application preferred: Replacing coal-based energy No value applicable	

6.3. Discussion: Convergence & Trade-offs

The first key aspect to note is that prior to applying the postulated principles, one should keep in mind the relationship between the concerned principle and the nature of application for which thermoelectrics (TEs) are sought to be used. For instance, the dominance of metal-based heat exchanger components in mass of TEG is coupled with their insignificant negative ecological contributions (Chapter 5), so higher mass of TE devices may not necessarily prove to be a stumbling block for stationary applications. However, it would be decisive in its influence on fuel savings and associated reduction in impacts for mobile applications, i.e., both passenger and freight vehicles. This signifies a heightened relevance of Principle #5 (enhancing conversion efficiency-to-mass and output power-to-mass ratios) for mobile purposes over their static counterparts. On similar lines, since all stationary applications need not constantly emit waste heat, principles aimed at lowering reduction in conversion efficiency via thermal cycling or usage duration (Principles #6 and #7) are critical only for discontinuous waste heat emission. In contrast, certain other principles, such as focus on cleaner electric grid (Principle #3) and reducing material use intensity (Principle #4) are relevant irrespective of the final application, so they should always be followed. Policymakers must thus, take note of these relationships while formulating their policies or taking other steps to engage or encourage other stakeholders for achieving the desired outcomes in line with making this platform more sustainable and ecofriendly.

Second, it is important to realize that the proposed principles provide a framework that enables policymakers to interact with other concerned stakeholders for identifying possibilities of their simultaneous implementation via dedicated actions to achieve the larger goal. This would, however, require extensive amount of collaboration and coordination among and within these stakeholders, particularly researchers in TE domain, TE module manufacturers, end-users of TE devices, and environmentalists (apart from policymakers). For instance, policymakers would have to engage with researchers within the TE domain on developing novel TEs that simultaneously: (a) Exhibit high conversion efficiencies per mass (Principle #5); (b) Use less-toxic and earth-abundant elements (Principles #1 and #2); and (c) Are processed using novel techniques that are frugal in their material and energy usage (Principle #4). Yet, this lone step requires a thorough analysis on determining toxicity and scarcity of elements commonly used or proposed to be used in TE systems, both on elemental and life cycle basis, as well as assessing ecological credentials of newly developed processing techniques. This in turn would necessitate collaboration and coordination between policymakers, TE researchers and environmentalists. The development of such processing techniques would also require joint efforts on the part of policymakers with TE module manufacturers and researchers interested in developing such techniques. This would need to be accompanied with the testing of TE devices for various end-uses, which would again merit joint efforts from policymakers with concerned end-users, and also on identifying the appropriate TE device choices for specific applications. All these steps, culminating in the final adoption of commercially produced TE devices by concerned end-users, would require the use of various policies (monetary and non-monetary), mandates and other measures to promote sustainability in this domain.

Third, even as collaborative/coordinated initiatives should be promoted, it is equally critical to recognize the trade-offs that exist between the different proposed principles, as well as to consider all the principles together while focusing on developing sustainable TEs. A good example in this context is the trade-off between the need to enhance TE conversion efficiency versus the use of often toxic and scarce elements to obtain these efficiencies. On one hand, tellurium and antimony are extremely vital in achieving high conversion efficiency of TEs (ZT > 0.8) like BT and SK respectively[49,58]. Yet, as mentioned earlier, both these elements present concerns regarding toxicity and scarcity on either or both of elemental and life cycle basis. Conversely, TEs that use less-toxic (only on elemental basis) and relatively more abundant elements, such as HH and OX, exhibit relatively lesser ZT values on average (up to 0.8)[58], barring some exceptions[49]. Another set of inconsistencies that can emerge from the postulated principles is regarding the financial viability of this platform. For instance, even as OX systems may be less-toxic despite their low ZT, they could also exhibit significantly higher costs[49,58], which may make these infeasible for large-scale use in most applications barring, say, in flexible body-wearables. This makes it critical for policymakers and other stakeholders to realize these inconsistencies between the different principles. An adequate measure would thus be to conduct thorough environmental analysis, while taking into account the specificities and key aspects of the concerned application for all proposed TE devices, and using the underlying results to arrive at the final choices.

Overall, the desired efforts needed to develop sustainable TEs must focus on the fullest possibility of both coordination and collaboration among various stakeholders, as well as on ameliorating the trade-offs between the proposed principles to the maximum possible degree, in order to ensure success of initiatives directed towards developing sustainable TEs.

CHAPTER SEVEN

SUMMARY AND FUTURE WORK

7. Conclusions

7.1. LCA of TEs

In this dissertation, ecological profile of thermoelectric devices was explored for a number of applications that spanned a diverse range in their nature of waste heat generation and mobility. Commercially produced or near-commercial TE modules were chosen, and their ecological performance was assessed on multiple categories encompassing global warming, fossil resource use, toxicity and scarcity. Detailed inventory was developed for all TE device components, particularly for TE modules that were chosen in the three LCA exercises, while three representative example applications were considered: (a) Baseload coal-based power plant that generate waste heat continuously; (b) Peak load natural gas-based power plant that produce waste heat periodically; and (c) Automobiles that produce waste heat intermittently. While TE modules were evaluated for both types of power plants, two TE generators were considered for use in automobiles.

7.1.1. Production Stage

Across all LCA studies, results show that till their production, TE devices harm the environment by use of elements that are toxic and scarce over their life cycle, as well as through large consumption of electricity for their processing, especially for TE legs. The work on automobiles shows that barring on some categories, heat exchanger components are almost entirely irrelevant in influencing production-related impacts of TE devices. This further lends credibility to the analysis of only TE modules in the first two LCA studies (Chapters 3 and 4).

7.1.2. Life Cycle (Use & EOL)

A vast diversity is seen in results of TE devices for the considered applications. On one hand, for coal-based power plants, all TE modules exhibit vast degree of positive benefits on chosen impact categories, with the use stage easily surpassing negative effects of production and EOL by ~ 70-75 % on most impacts. In fact, these benefits are sizeable enough when compared with the ecofriendly potential of established renewable energy technologies like solar and wind energy.

In contrast, for natural gas-based power plants that operate for only a few hours per day, no TE module is seen to be ecologically beneficial on all impacts, especially on FET and HNT. This is seen to be outcome of both lower harmful effects of natural gas-based electricity over their coal-based counterparts, as well as lower amount of electricity generation by TEs. This work also shows a complex interplay between factors associated with production (mass and nature of elements used, and electricity consumed to process them) and those involved with use (conversion efficiency and output power) of modules).

Finally, for automobiles, none of the two TEGs show positive benefits on impacts barring one exception. This suggests the limitations of existing approach on solely focusing on enhancing conversion efficiency and increasing fuel savings, while not recognizing the importance of lowering production-related impacts via specific initiatives.

With regard to EOL scenarios, the three example applications witness divergent results. On one hand, none of the EOL scenarios has a decisive effect in overturning the ecological performance of TE modules on any of the impact categories for both coal- and gas-based power plants. Conversely, the use of heat exchanger-based components, especially those made from copper, has a decisive effect in influencing environmental outcomes of TEGs on some impacts. This clearly shows the tangible ecological benefits that can be accrued by recovery and recycling of metal-based components in TE devices.

7.2. Principles of Sustainable TEs and Implications for Stakeholders

Based on the aforementioned LCA studies on TE devices in this dissertation and elsewhere, eight key principles were postulated for developing sustainable thermoelectrics that span the entire life cycle of this platform. For the production stage, the need to use less-toxic (from both elemental and life cycle perspectives) and more earth-abundant elements in TEs was stressed on. In addition, the importance of producing TE devices in locations served by cleaner grids and using techniques that were less intensive in their energy and material usage was also highlighted. All these steps are especially important in light of high impacts of production stage that negatively affect the performance of TEs for two of three example applications in this dissertation.

For use stage, two parameters were introduced that needed to be maximized for achieving higher benefits during use stage per impact during production: conversion efficiency-to-mass and output power-to-mass (where mass referred to mass of TE legs). This was complemented by the need to maintain these ratios over longer life of TE devise with minimal thermal cycling, with the latter two factors posited as additional principles of consideration for making TEs eco-friendlier. Finally, for the end-of-life stage, the importance of incorporating the circular economy vision in life cycle of TE devices, particularly for their metallic components and TE legs, was also shown in terms of their ability to strengthen ecological validity of this technology. For all principles, significance was demonstrated through reference to concerned literature and use of specific scenarios that highlight their ability to shape the environmental performance of TE devices.

Apart from the development of principles, focus was also laid on the need for effective coordination and collaboration between various stakeholders for undertaking efforts in line with the postulated principles to develop novel, sustainable TEs. Simultaneously, the significance of analyzing trade-offs that accompany these principles was also buttressed for consideration by TE researchers and other stakeholders. Together, it is these joint efforts that can help propel TEs in the domain of commercially viable ecofriendly technologies that can join forces with other renewable energy forms to enhance the potential of this platform.

7.3. Future Work

Admittedly, this work explored the ecological profile of thermoelectrics for different applications using numerous assumptions, especially regarding TE modules used in power plants (coal- and gas-based). However, there is a clear need to use this work as the basis for a deeper study on environmental performance of thermoelectric devices that understands them in a relatively more comprehensive sense. For instance, heat exchanger components – typically used in any TE device (generator) – were excluded for genuine reasons in this dissertation for both power plant-related analyses, but this should definitely be addressed in any future work, especially for natural gas-based power plants. This is important particularly because while heat exchanger components reduce the overall system conversion efficiency, they also offer possibilities for ameliorating impacts via recovery and recycling, as shown in Chapter 5. In fact, these components could even make some of the existing TEs ecologically beneficial for gas-based power plants (peak load) and other such periodic waste heat emitting applications, as well as for continuous waste heat emitting end-uses where less-polluting fossil fuels are used.

Apart from the consideration of heat exchanger components, another key feature that is required in future LCA studies is a more critical emphasis on multiple other aspects that combine to provide a clear analysis of long-term environmental performance of this platform. Such analysis must focus on several aspects. First, it is critical to evaluate the practical manner in which TE devices can be used in any application, and therefore, such analysis must typically accompany the evaluation of TE performance of such devices for the concerned application. This can ensure that other critical aspects, such as the effects of TE devices on thermodynamics of waste heat flow, or those of chemical composition of waste heat gas on TE conversion efficiencies, are already factored in the final system conversion efficiency exhibited by these devices. Such joint evaluation – of both TE and environmental performance – of these devices must be further extended to long-term usage, particularly for large-scale commercial applications, such as industries, power plants, and automobiles, to assess their overall prospects. Moreover, this evaluation must also factor in the effects of discontinuity in waste heat emission – like that considered in this work. A detailed, exhaustive exercise of the kind described here can enable a thorough comparison of various TE materials that can be potentially used for the considered application, provided they can be used across the same operational temperature range – essential for greater validity of LCA study. Lastly, such a detailed exercise can be combined with long-term cost analysis of TEs to provide a comprehensive overview of their thermodynamic, environmental and economic feasibility. Overall, this entire gamut of efforts across multiple end-uses can help policymakers in identifying potential TEs that can be used for different kinds of applications, while also helping them and other stakeholders to focus on ways through which these materials can be made commercially viable for desired end-uses.

A key focus of efforts on evaluating long-term performance of TEs must be to vary the functional unit and determine its effect on environmental performance of TE devices. For instance, instead of focusing on per-unit of fuel saving or energy generation, it would be more prudent to look at how TEs that harvest the same amount of energy over the same duration (say, 1000 W of heat energy over 15 years) perform and compare against each other. Here, both the amount of energy as well as duration of use can be varied to estimate their respective and combined effects on life-cycle ecological outcomes of this platform.

Apart from novel TEs, it is important to develop techniques that are frugal in their material and energy use, as highlighted in Principle #4 (Chapter 6). Thorough research is needed on this aspect, both in terms of development and commercialization of such techniques through in-house research and essential coordination with module manufacturers. Environmental analysis of such techniques must also be undertaken at the same time as their development to determine if these should be further promoted or not.

It must be understood that while circular economy approach has been proposed in this work, it still remains a novel aspect for thermoelectric domain given the lack of suitable techniques for recycling TE legs. The method suggested in this dissertation is an adaptation of the traditional pyrometallurgical approach where the desired part is melted and then slowly cooled to get back the material in its near-original state. However, this must actually be tested and studied in detail for different TEs prior to its advocation for even commercialization. Other approaches for recovery and recycling of TE materials must also be developed, tested and evaluated for both their recycling and ecological performance, prior to further development for commercial advancement.

APPENDIX-A

SUPPORTING INFORMATION FOR CHAPTER 3

A. Ecological Profile of Thermoelectrics for Continuous Waste Heat Emitting Applications

1. Introduction

For the cradle-to-grave life cycle assessment (LCA) of thermoelectric (TE) modules, this Appendix provides detailed inventory analysis and results on characterized impacts for chosen modules. It was assumed that after procuring the desired inputs, all TE modules were manufactured in the US, using the average 2015 U.S. electric grid mix for processing their individual components (due to paucity of more recent data).

2. Modules: Inventory for Production

The respective steps for processing individual components of TE modules, especially TE legs, has been provided in Chapter 2. Based on literature, for TE legs, a number of common steps are used to process powders and produce these legs, such as melting, annealing, ball milling, and sintering (either hot-pressing or spark plasma sintering). Table A-1 shows the equipment and common process parameters used for such equipment, along with supporting literature. For equipment, the primary consideration was ensuring the possibility of large-scale production of TE modules that would be commensurate with their commercialization or near-commercial state. This is especially true in case of annealing, spark plasma sintering (SPS) and hot-pressing equipment, particularly through the use of multi-cavity dies for hot pressing to make multiple sintered samples together. On the other hand, since there was complete lack of information on typical parameters used for a number of these processes, the maximal values of these parameters for at least small-scale production of module components, especially TE legs, were considered. This explains, for instance, the use of 2-inch diameter and 0.5-inch height as maximum values for samples sintered using either of hot-pressing or SPS.

Using these parameters and the various steps used, a detailed inventory for each of these components was calculated and is provided below. Each calculation was undertaken assuming 1,000 kg of major material as the output for concerned process (barring in some cases). Electricity consumption was calculated while keeping in mind the wattage of chosen equipment, time of usage as pointed out in concerned literature, and the volume of packing assumed for various processes, such as annealing.

Table A-1: Equipment & common process parameters used

Processes	**Equipment used**	**Common process parameters that were used or assumed (unless specified otherwise in literature)**
Ball milling	Pulverisette 5/4 Planetary Mill[216]	• Ball-to-powder ratio = 10:1 (by weight) • Maximum volume usage per vial: 95 % • Mode of milling: Wet milling • Volume of wet milling fluid used: 40 % of total vial volume • Typical fluid used: Ethanol, unless specified otherwise • Material loss per run: 5 %
Annealing or Sintering	11-RO-4812036-20A or 11-SC-369624-25A, depending on the temperature[217]	• Quartz/Silica tubes: 6 mm inner diameter, 10 mm outer diameter, length is 95 % of length of furnace • Alternative ways of placing samples: Ceramic boats • Dimensions of boats specific to nature of system considered and other sample dimensions required

		• Mass loss per run: 5 % (when no quartz tubes are used)
Spark plasma sintering	H-HP D 10[218]	• Sample diameter: 2 inches max. • Sample height: 0.5-inch max.
Hot pressing	QIH 15L[219]	
Cold isostatic pressing	N.A.	• No energy consumed
Induction melting	IT-KTV-65/100/1650[220]	• Parameters assumed from equipment details
Arc melting	Arc 200 Cold Crucible Arc Melting Furnace and Casting Module[221]	• Parameters assumed from equipment details
Powder mixing	N.A.	• No energy consumed – assumed to be done manually
TE leg polishing	NANO 1200T Manual polisher[222]	• Used with a polisher recirculating filter system for water • Desired flow rate of water = 0.8 gallons/min • Additional equipment: 8/10 inch single-wheel, bench top grinder/polisher • Number of samples polished in a single run of polishing: 3

The methodology that was used to estimate leg dicing efficiency (LDE) in this work can be understood by taking an example, for which p-type legs for SK-1 module are considered. Dimensions for these legs are 4 mm × 4 mm × 4 mm[103] (Table 2-2), while the cylindrical sintered samples from which these legs are made were considered to have initial dimensions of diameter of 2 inch or 50.8 mm, and height of 0.5 inch or 12.75 mm. However, prior to leg dicing, polishing of these sintered samples was considered to be conducted, during which it was assumed that 5 % of height was shaved off on either side, meaning that the sample had a new height of 11.43 mm after polishing step.

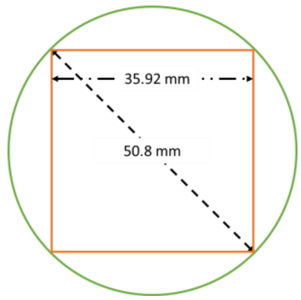

Figure A.1: Diameter of (circular end of) cylindrical sample and maximum length of square that can be removed

Now, at either end of this sintered sample, the diameter of the circular end is 50.8 mm. First, the maximum length of square that can be formed on this circle was calculated, meaning that the diagonal of this square is the diameter of this circle (i.e., 50.8 mm) in this scenario (Figure A.1). Through calculations, this value was obtained as 35.92 mm. This mode of cutting was considered as it was expected to yield the maximum amount of material for the same setting of cutting (i.e., no need to handle dicing equipment separately for each length and width of cutting across different runs for the cylinder). Hence, the square that can be easily cut using dicing equipment at either of the circular ends of sintered and polished samples, would be this square, with the length of cutting through the sample being the height of this cylinder (i.e., 11.43 mm). Next, the total number of cuts that needed to be made along the length, width and height of this sample (cylinder) was calculated to determine the final number of TE legs that can be obtained from 1 cylinder. Also, this kept in mind the thickness of dicing blade, which is considered to be 0.35 mm[223]. These values – total number of cuts, and total number of TE legs, are shown in the following equations.

$$Number\ of\ cuts\ along\ length = \frac{Length\ of\ square}{Length\ of\ TE\ leg + Sample\ blade\ thickness}$$

$$= integer\left(\frac{35.92\ mm}{(4 + 0.35)\ mm}\right) = 8$$

$$Number\ of\ cuts\ along\ width = \frac{Width\ of\ square}{Width\ of\ TE\ leg + Sample\ blade\ thickness}$$

$$= integer\left(\frac{35.92\ mm}{(4 + 0.35)\ mm}\right) = 8$$

$$Number\ of\ cuts\ along\ height = \frac{Height\ of\ square}{Height\ of\ TE\ leg + Sample\ blade\ thickness}$$

$$= integer\left(\frac{11.43\ mm}{(4 + 0.35)\ mm}\right) = 2$$

$$Total\ no.of\ legs\ per\ 1\ cylinder\ sample$$
$$= No.of\ cuts\ along\ (length \times width \times height) = 8 \times 8 \times 2 = 128$$

Subsequently, this total no. of legs was multiplied by the mass of 1 leg, which is the product of volume of leg and density of material, to obtain the total mass of legs produced from one-cylinder sample.

$$Total\ mass\ of\ all\ legs\ per\ 1\ cylinder\ sample$$
$$= No.of\ legs\ per\ cylinder\ sample\ \times Mass\ of\ 1\ leg, or$$
$$\Rightarrow Total\ mass\ of\ all\ legs\ per\ 1\ cylinder\ sample$$
$$= 128\ \times (4\ mm)^3 \times Density\ of\ material$$

Dicing efficiency is the ratio of mass obtained as legs to the initial mass of cylinder.

$$Dicing\ efficiency = \frac{Total\ mass\ of\ all\ legs\ per\ 1\ cylinder\ sample}{Total\ mass\ of\ initial\ cylinder}, or$$

$$\Rightarrow Dicing\ efficiency = \frac{128\ \times (4\ mm)^3 \times Density\ of\ material}{\pi \times (25\ mm)^2 \times 11.43\ mm \times Density\ of\ material}, or$$

$$\Rightarrow Dicing\ efficiency = 35.36\ \%$$

2.1. BT-1 Module

Tables A-2 and A-3 show the respective inventory for producing p- and n-type legs for BT-1 module, while Tables A-4 and A-5 respectively provide the inventory details for alumina plates and copper tabs used in this module.

Table A-2: Inventory for producing p-type leg (BT-1 module)

Step 1: Powder Mixing			
Type of Parameter	**Parameter**	**Value**	**Unit**
Output Material	$Bi_{0.4}Sb_{1.6}Te_3$ powders	1000.00	kg
Input Materials	Bismuth (Bi)	126.42	kg
	Antimony (Sb)	294.64	kg
	Tellurium (Te)	578.94	kg
Step 2: Annealing (@ 850°C, 1.5 h)			
Type of Parameter	**Parameter**	**Value**	**Unit**
Output Material	$Bi_{0.4}Sb_{1.6}Te_3$ - Annealed	1000.00	kg
Input Material	$Bi_{0.4}Sb_{1.6}Te_3$ powders	1052.63	kg
Input Energy	Electricity	16666.82	kWh
Output Waste: Solid	$Bi_2Te_{2.4}Se_{0.6}$ powders II (Landfill)	52.63	kg
Step 3: Ball Milling			
Type of Parameter	**Parameter**	**Value**	**Unit**
Output Material	$Bi_{0.4}Sb_{1.6}Te_3$ powders II	1000.00	kg
Input Materials	$Bi_{0.4}Sb_{1.6}Te_3$ - Annealed	1052.63	kg
	Ethanol	281.76	kg
Input Energy	Electricity	109.37	kWh
Output Waste: Liquid	Ethanol	281.76	kg
Output Waste: Solid	$Bi_{0.4}Sb_{1.6}Te_3$ powders II (Landfill)	52.63	kg
Step 4: Cold Isostatic Pressing (@ 800 MPa) (No electricity consumption assumed)			
Type of Parameter	**Parameter**	**Value**	**Unit**
Output Material	$Bi_{0.4}Sb_{1.6}Te_3$ - CIP Sample	1000.00	kg

Input Material	$Bi_{0.4}Sb_{1.6}Te_3$ powders II	1052.63	kg
Output Waste: Solid	$Bi_{0.4}Sb_{1.6}Te_3$ powders II	52.63	kg
Step 5: Annealing (@ 400°C, 10 h)			
Type of Parameter	**Parameter**	**Value**	**Unit**
Output Material	$Bi_{0.4}Sb_{1.6}Te_3$ - Ingot	1000.00	kg
Input Materials	$Bi_{0.4}Sb_{1.6}Te_3$ - CIP Sample	1000.00	kg
	Argon	1.53	kg
	Electricity	45625.76	kWh
Output Waste: Air	Argon	1.53	kg
Step 6: Ingot Polishing			
Type of Parameter	**Parameter**	**Value**	**Unit**
Output Material	$Bi_{0.4}Sb_{1.6}Te_3$ - Polished Ingot	1000.00	kg
Input Materials	$Bi_{0.4}Sb_{1.6}Te_3$ - Ingot	1111.11	kg
	Water	38401.68	kg
Input Energy	Electricity	5504.24	kWh
Output Waste: Solid	$Bi_{0.4}Sb_{1.6}Te_3$ - Landfill	111.11	kg
Output Waste: Liquid	Waste water	38512.79	kg
Step 7: Leg Dicing			
Type of Parameter	**Parameter**	**Value**	**Unit**
Output Material	$Bi_{0.4}Sb_{1.6}Te_3$ - Legs	1000.00	kg
Input Materials	$Bi_{0.4}Sb_{1.6}Te_3$ - Polished Ingot	9542.59	kg
	Borax	1090.81	kg
	Sodium nitrate	1090.81	kg
	Water	291305.43	kg
Input Energy	Electricity	359122.35	kWh
Output Waste: Liquid	Waste water	293487.06	kg
Output Waste: Solid	$Bi_{0.4}Sb_{1.6}Te_3$ (Landfill)	8542.59	kg

Table A-3: Inventory for producing n-type leg (BT-1 module)

Step 1: Powder Mixing			
Type of Parameter	**Parameter**	**Value**	**Unit**
Output Material	$Bi_2Te_{2.4}Se_{0.6}$ powders	1000.00	kg
Input Materials	Bismuth (Bi)	541.70	kg
	Tellurium (Te)	396.90	kg
	Selenium (Se)	61.40	kg
Step 2: Annealing (@ 850°C, 1.5 h)			
Type of Parameter	**Parameter**	**Value**	**Unit**
Output Material	$Bi_2Te_{2.4}Se_{0.6}$ - Annealed	1000.00	kg
Input Material	$Bi_2Te_{2.4}Se_{0.6}$ powders	1052.63	kg
Input Energy	Electricity	15063.28	kWh
Output Waste: Solid	$Bi_2Te_{2.4}Se_{0.6}$ powders II (Landfill)	52.63	kg
Step 3: Ball Milling			
Type of Parameter	**Parameter**	**Value**	**Unit**
Output Material	$Bi_2Te_{2.4}Se_{0.6}$ powders II	1000.00	kg
Input Materials	$Bi_2Te_{2.4}Se_{0.6}$ - Annealed	1052.63	kg
	Ethanol	273.24	kg
Input Energy	Electricity	106.06	kWh
Output Waste: Liquid	Ethanol	273.24	kg
Output Waste: Solid	$Bi_2Te_{2.4}Se_{0.6}$ powders II (Landfill)	52.63	kg
Step 4: Cold Isostatic Pressing (@800 MPa) (No electricity consumption assumed)			
Type of Parameter	**Parameter**	**Value**	**Unit**
Output Material	$Bi_2Te_{2.4}Se_{0.6}$ - CIP Sample	1000.00	kg
Input Material	$Bi_2Te_{2.4}Se_{0.6}$ powders II	1052.63	kg
Output Waste: Solid	$Bi_2Te_{2.4}Se_{0.6}$ powders II	52.63	kg
Step 5: Annealing (@ 400°C, 10 h)			
Type of Parameter	**Parameter**	**Value**	**Unit**

Output Material	$Bi_2Te_{2.4}Se_{0.6}$ - Ingot	1000.00	kg
Input Materials	$Bi_2Te_{2.4}Se_{0.6}$ - CIP Sample	1000.00	kg
	Argon	1.38	kg
	Electricity	41236.04	kWh
Output Waste: Air	Argon	1.38	kg
Step 6: Ingot Polishing			
Type of Parameter	**Parameter**	**Value**	**Unit**
Output Material	$Bi_2Te_{2.4}Se_{0.6}$ - Polished Ingot	1000.00	kg
Input Materials	$Bi_2Te_{2.4}Se_{0.6}$ - Ingot	1111.11	kg
	Water	34707.00	kg
Input Energy	Electricity	4974.67	kWh
Output Waste: Liquid	Waste water	34818.12	kg
Step 7: Leg Dicing			
Type of Parameter	**Parameter**	**Value**	**Unit**
Output Material	$Bi_2Te_{2.4}Se_{0.6}$ - Legs	1000.00	kg
Input Materials	$Bi_2Te_{2.4}Se_{0.6}$ - Polished Ingot	9542.59	kg
	Borax	985.87	kg
	Sodium nitrate	985.87	kg
	Water	263278.57	liters
Input Energy	Electricity	324570.74	kWh
Output Waste: Liquid	Waste water	265250.30	kg
Output Waste: Solid	$Bi_2Te_{2.4}Se_{0.6}$ (Landfill)	8542.59	kg

Table A-4: Inventory for producing alumina plates (BT-1 module)

Step 1: Ball Milling			
Type of Parameter	**Parameter**	**Value**	**Unit**
Output Material	Alumina - Ball milled powder	1000.00	kg
Input Materials	Alumina	1052.63	kg

	Ethanol	349.30	kg
Input Energy	Electricity	19523.70	kWh
Output Waste: Liquid	Ethanol	349.30	kg
Output Waste: Solid	Alumina powder	52.63	kg
Step 2: Sintering (@ 1500°C, 1 h, 3°C/min) (Assuming zero energy consumption for cold isostatic pressing)			
Type of Parameter	**Parameter**	**Value**	**Unit**
Output Material	Alumina plate - Sintered	1000.00	kg
Input Materials	Alumina - Ball milled powder	1052.63	kg
Input Energy	Electricity	6397787.35	kWh
Output Waste: Solid	Alumina powder	52.63	kg
Step 3: Polishing			
Type of Parameter	**Parameter**	**Value**	**Unit**
Output Material	Alumina plate - Final	1000.00	kg
Input Materials	Alumina plate - Sintered	1111.11	kg
	Water	7131.29	kg
Input Energy	Electricity	1467.86	kWh
Output Waste: Solid	Alumina plate	111.11	kg

Table A-5: Inventory for producing copper tabs (BT-1 module)

Type of Parameter	**Parameter**	**Value**	**Unit**
Output Material	Copper tabs	1000.00	kg
Input Materials	Copper sheet	1000.32	kg
Input Energy	Electricity	69416.35	kWh
Output Waste: Solid	Copper	0.32	kg

2.2. BT-2 Module

Tables A-6, A-7, A-8 and A-9 give the inventory details for p-type legs, n-type legs, alumina plates and copper tabs used in BT-2 module respectively.

Table A-6: Inventory for producing p-type leg (BT-2 module)

Step 1: Powder Mixing			
Type of Parameter	**Parameter**	**Value**	**Unit**
Output Material	$Bi_{0.4}Sb_{1.6}Te_3$ powders	1000.00	kg
Input Materials	Bismuth (Bi)	126.42	kg
	Antimony (Sb)	294.64	kg
	Tellurium (Te)	578.94	kg
Step 2: Hot pressing (@ 700 kg/cm^2, 15 min, 770 K)			
Type of Parameter	**Parameter**	**Value**	**Unit**
Output Material	$Bi_{0.4}Sb_{1.6}Te_3$ - Hot ingot I	1000.00	kg
Input Materials	$Bi_{0.4}Sb_{1.6}Te_3$ powders	1052.63	kg
	Argon	69.18	kg
Input Energy	Electricity	29213.25	kWh
Output Emissions: Air	Argon	69.18	kg
Output Emissions: Solid	$Bi_{0.4}Sb_{1.6}Te_3$ powders (Landfill)	52.63	kg
Step 3: Ingot Polishing			
Type of Parameter	**Parameter**	**Value**	**Unit**
Output Material	$Bi_{0.4}Sb_{1.6}Te_3$ - Polished Ingot	1000.00	kg
Input Materials	$Bi_{0.4}Sb_{1.6}Te_3$ - Hot ingot II	1111.11	kg
	Water	135.72	kg
Input Energy	Electricity	19.45	kWh
Output Waste: Liquid	Waste water	246.83	kg
Step 4: Leg Dicing			
Output Material	$Bi_{0.4}Sb_{1.6}Te_3$ - Legs	1000.00	kg
Input Materials	$Bi_{0.4}Sb_{1.6}Te_3$ - Polished Ingot	1741.49	kg
	Borax	12.18	kg
	Sodium nitrate	12.18	kg
	Water	3251.89	kg

Input Energy	Electricity	4008.95	kWh
Output Waste: Liquid	Waste water	3276.25	kg
Output Waste: Solid	$Bi_{0.4}Sb_{1.6}Te_3$ (Landfill)	741.49	kg

Table A-7: Inventory for producing n-type leg (BT-2 module)

Step 1: Powder Mixing			
Type of Parameter	**Parameter**	**Value**	**Unit**
Output Material	$Bi_2Te_{2.4}Se_{0.6}$ powders	1000.00	kg
Input Materials	Bismuth (Bi)	541.70	kg
	Tellurium (Te)	396.90	kg
	Selenium (Se)	61.40	kg
Step 2: Hot pressing (@ 700 kg/cm^2, 15 min, 770 K)			
Type of Parameter	**Parameter**	**Value**	**Unit**
Output Material	$Bi_2Te_{2.4}Se_{0.6}$ - Hot ingot I	1000.00	kg
Input Materials	$Bi_2Te_{2.4}Se_{0.6}$ powders	1052.63	kg
	Argon	62.52	kg
Input Energy	Electricity	26402.60	kWh
Output Emissions: Air	Argon	62.52	kg
Output Emissions: Solid	$Bi_2Te_{2.4}Se_{0.6}$ powders (Landfill)	52.63	kg
Step 3: Ingot Polishing			
Type of Parameter	**Parameter**	**Value**	**Unit**
Output Material	$Bi_2Te_{2.4}Se_{0.6}$ - Polished Ingot	1000.00	kg
Input Materials	$Bi_2Te_{2.4}Se_{0.6}$ - Hot ingot II	1111.11	kg
	Water	122.66	kg
Input Energy	Electricity	17.58	kWh
Output Waste: Liquid	Waste water	233.78	kg
Step 4: Leg Dicing			
Type of Parameter	**Parameter**	**Value**	**Unit**

Output Material	$Bi_2Te_{2.4}Se_{0.6}$ - Legs	1000.00	kg
Input Materials	$Bi_2Te_{2.4}Se_{0.6}$ - Polished Ingot	1833.62	kg
	Borax	10.99	kg
	Sodium nitrate	10.99	kg
	Water	2934.64	liters
Input Energy	Electricity	3617.84	kWh
Output Waste: Liquid	Waste water	2956.62	kg
Output Waste: Solid	$Bi_2Te_{2.4}Se_{0.6}$ (Landfill)	833.62	kg

Table A-8: Inventory for producing alumina plates (BT-2 module)

Step 1: Ball Milling			
Type of Parameter	**Parameter**	**Value**	**Unit**
Output Material	Alumina - Ball milled powder	1000.00	kg
Input Materials	Alumina	1052.63	kg
	Ethanol	349.30	kg
Input Energy	Electricity	19523.70	kWh
Output Waste: Liquid	Ethanol	349.30	kg
Output Waste: Solid	Alumina powder	52.63	kg
Step 2: Sintering (@ 1500°C, 1 h, 3°C/min) (Assuming zero energy consumption for cold isostatic pressing)			
Type of Parameter	**Parameter**	**Value**	**Unit**
Output Material	Alumina plate - Sintered	1000.00	kg
Input Materials	Alumina - Ball milled powder	1052.63	kg
Input Energy	Electricity	868030.18	kWh
Output Waste: Solid	Alumina powder	52.63	kg
Step 3: Polishing			
Type of Parameter	**Parameter**	**Value**	**Unit**
Output Material	Alumina plate - Final	1000.00	kg
Input Materials	Alumina plate - Sintered	1111.11	kg

	Water	4054.49	kg
Input Energy	Electricity	834.55	kWh
Output Waste: Solid	Alumina plate	4165.60	kg

Table A-9: Inventory for producing copper tabs (BT-2 module)

Type of Parameter	**Parameter**	**Value**	**Unit**
Output Material	Copper tabs	1000.00	kg
Input Materials	Copper sheet	1000.54	kg
Input Energy	Electricity	288057.16	kWh
Output Waste: Solid	Copper	0.54	kg

2.3. SK-1 Module

Tables A-10, A-11, A-12 and A-13 give the respective inventory details for p- and n-type legs, alumina plates and copper tabs of SK-1 module.

Table A-10: Inventory for producing p-type leg (SK-1 module)

Step 1: Powder Mixing			
Type of Parameter	**Parameter**	**Value**	**Unit**
Output Material	$Fe_{3.45}Ni_{0.6}Sb_{12}$	1000.00	kg
Input Materials	Iron (Fe)	114.07	kg
	Nickel (Ni)	20.85	kg
	Antimony (Sb)	865.08	kg
Step 2: Melting (Quartz Tube, @ 950°C)			
Type of Parameter	**Parameter**	**Value**	**Unit**
Output Material	Molten $Fe_{3.45}Ni_{0.6}Sb_{12}$	1000.00	kg
Input Material	$Fe_{3.45}Ni_{0.6}Sb_{12}$	1000.00	kg
Input Energy	Electricity	12380.18	kWh
Step 3: Quenching to Room Temperature (Assumed to consume no energy – Sample is just kept out to cool)			

Step 4: Addition of didymium to make $DD_{0.76}Fe_{3.45}Ni_{0.6}Sb_{12}$			
Type of Parameter	**Parameter**	**Value**	**Unit**
Output Material	$DD_{0.76}Fe_{3.45}Ni_{0.6}Sb_{12}$	1000.00	kg
Input Materials	Didymium (DD)	60.89	kg
	Molten $Fe_{3.45}Ni_{0.6}Sb_{12}$	939.11	kg
Step 5: Vacuum-sealing in Quartz Tube (Negligible energy consumption – Assumed)			
Step 6: Heating (@ 600°C, 3 days; @ 720°C, 2 days)			
Type of Parameter	**Parameter**	**Value**	**Unit**
Output Material	$DD_{0.76}Fe_{3.45}Ni_{0.6}Sb_{12}$ - Heated Set I	1000.00	kg
Input Material	$DD_{0.76}Fe_{3.45}Ni_{0.6}Sb_{12}$	1000.00	kg
Input Energy	Electricity	425961.80	kWh
Step 7: Sample Melting (@ 950°C)			
Type of Parameter	**Parameter**	**Value**	**Unit**
Output Material	$DD_{0.76}Fe_{3.45}Ni_{0.6}Sb_{12}$ - Melting	1000.00	kg
Input Material	$DD_{0.76}Fe_{3.45}Ni_{0.6}Sb_{12}$ - Heated Set I	1000.00	kg
Input Energy	Electricity	9633.47	kWh
Step 8: Air Quenching (Assumed to have zero energy consumption)			
Step 9: Annealing (@ 600°C for 5 days)			
Type of Parameter	**Parameter**	**Value**	**Unit**
Output Material	$DD_{0.76}Fe_{3.45}Ni_{0.6}Sb_{12}$ - Annealed Set	1000.00	kg
Input Material	$DD_{0.76}Fe_{3.45}Ni_{0.6}Sb_{12}$ - Melting	1000.00	kg
Input Energy	Electricity	424569.01	kWh
Step 10: Ball Milling			
Type of Parameter	**Parameter**	**Value**	**Unit**
Output Material	$DD_{0.76}Fe_{3.45}Ni_{0.6}Sb_{12}$ - Powders	1000.00	kg
Input Materials	$DD_{0.76}Fe_{3.45}Ni_{0.6}Sb_{12}$ - Annealed Set	1052.63	kg
	Cyclohexane	177.41	kg

Input Energy	Electricity	836.94	kWh
Output Emissions: Liquid	Cyclohexane	177.41	kg
Output Emissions: Solid	$DD_{0.76}Fe_{3.45}Ni_{0.6}Sb_{12}$ - Powders	52.63	kg
Step 11: Hot Pressing (@ 600°C, 50 MPa, Ar atm)			
Type of Parameter	**Parameter**	**Value**	**Unit**
Output Material	$DD_{0.76}Fe_{3.45}Ni_{0.6}Sb_{12}$ - Ingot	1000.00	kg
Input Materials	$DD_{0.76}Fe_{3.45}Ni_{0.6}Sb_{12}$ - Powders	1052.63	kg
	Argon	295.49	kg
Input Energy	Electricity	131352.53	kWh
Output Emissions: Air	Argon	295.49	kg
Output Emissions: Solid	$DD_{0.76}Fe_{3.45}Ni_{0.6}Sb_{12}$ - Powders	52.63	kg
Step 12: Ingot Polishing			
Type of Parameter	**Parameter**	**Value**	**Unit**
Output Material	$DD_{0.76}Fe_{3.45}Ni_{0.6}Sb_{12}$ - Polished Ingot	1000.00	kg
Input Materials	$DD_{0.76}Fe_{3.45}Ni_{0.6}Sb_{12}$ - Ingot	1111.11	kg
	Water	1005.30	kg
Input Energy	Electricity	206.92	kWh
Output Waste: Liquid	Waste water	1116.41	kg
Step 13: Leg Dicing			
Type of Parameter	**Parameter**	**Value**	**Unit**
Output Material	$DD_{0.76}Fe_{3.45}Ni_{0.6}Sb_{12}$ - Legs	1000.00	kg
Input Materials	$DD_{0.76}Fe_{3.45}Ni_{0.6}Sb_{12}$ - Polished Ingot	2827.96	kg
	Borax	18.29	kg
	Sodium nitrate	18.29	kg
	Water	4883.11	liters
Input Energy	Electricity	6019.92	kWh
Output Waste: Liquid	Waste water	4919.68	kg

Output Waste: Solid	$DD_{0.76}Fe_{3.45}Ni_{0.6}Sb_{12}$ (Landfill)	1827.96	kg

Table A-11: Inventory for producing n-type leg (SK-1 module)

Step 1: Powder Mixing			
Type of Parameter	**Parameter**	**Value**	**Unit**
Output Material	$Ba_{0.08}La_{0.05}Yb_{0.04}Co_4Sb_{12}$ powders	1000.00	kg
Input Material	Barium (Ba)	6.38	kg
	Lanthanum (La)	4.03	kg
	Ytterbium (Yb)	4.02	kg
	Cobalt (Co)	136.92	kg
	Antimony (Sb)	848.65	kg
Step 2: Induction Melting			
Type of Parameter	**Parameter**	**Value**	**Unit**
Output Material	$Ba_{0.08}La_{0.05}Yb_{0.04}Co_4Sb_{12}$ melt	1000.00	kg
Input Materials	$Ba_{0.08}La_{0.05}Yb_{0.04}Co_4Sb_{12}$ powders	1000.00	kg
	Argon	0.96	kg
Input Energy	Electricity	23323.80	kWh
Output Waste: Air	Argon	0.96	kg
Step 3: Quenching to Room Temperature (Assumed to consume no energy – Sample is just kept out to cool)			
Step 4: Annealing (@ 750°C, 1 week)			
Type of Parameter	**Parameter**	**Value**	**Unit**
Output Material	$Ba_{0.08}La_{0.05}Yb_{0.04}Co_4Sb_{12}$ - Annealed I	1000.00	kg
Input Material	$Ba_{0.08}La_{0.05}Yb_{0.04}Co_4Sb_{12}$ melt	1052.63	kg
Input Energy	Electricity	7046.83	kWh
Output Waste: Solid	$Ba_{0.08}La_{0.05}Yb_{0.04}Co_4Sb_{12}$ powders (Landfill)	52.63	kg
Step 5: Ball Milling			

Type of Parameter	Parameter	Value	Unit
Output Material	$Ba_{0.08}La_{0.05}Yb_{0.04}Co_4Sb_{12}$ - Powders I	1000.00	kg
Input Materials	$Ba_{0.08}La_{0.05}Yb_{0.04}Co_4Sb_{12}$ - Annealed I	1052.63	kg
	Ethanol	468.29	kg
Input Energy	Electricity	545.30	kWh
Output Waste: Liquid	Ethanol	468.29	kg
Output Waste: Solid	$Ba_{0.08}La_{0.05}Yb_{0.04}Co_4Sb_{12}$ - Powders I	52.63	kg
Step 6: Cold Isostatic Pressing (Assumption – No energy consumed)			
Type of Parameter	**Parameter**	**Value**	**Unit**
Output Material	$Ba_{0.08}La_{0.05}Yb_{0.04}Co_4Sb_{12}$ - CIP Sample	1000.00	kg
Input Material	$Ba_{0.08}La_{0.05}Yb_{0.04}Co_4Sb_{12}$ - Powders I	1052.63	kg
Output Waste: Solid	$Ba_{0.08}La_{0.05}Yb_{0.04}Co_4Sb_{12}$ - Powders I	52.63	kg
Step 7: Annealing (@ 750°C, 1 week)			
Type of Parameter	**Parameter**	**Value**	**Unit**
Output Material	$Ba_{0.08}La_{0.05}Yb_{0.04}Co_4Sb_{12}$ - Annealed II	1000.00	kg
Input Material	$Ba_{0.08}La_{0.05}Yb_{0.04}Co_4Sb_{12}$ - CIP Sample	1000.00	kg
Input Energy	Electricity	7520.53	kWh
Step 8: Ball Milling			
Type of Parameter	**Parameter**	**Value**	**Unit**
Output Material	$Ba_{0.08}La_{0.05}Yb_{0.04}Co_4Sb_{12}$ - Powders II	1000.00	kg
Input Materials	$Ba_{0.08}La_{0.05}Yb_{0.04}Co_4Sb_{12}$ - Annealed II	1052.63	kg
	Ethanol	400.44	kg

Input Energy	Electricity	509.09	kWh
Output Waste: Liquid	Ethanol	400.44	kg
Output Waste: Solid	$Ba_{0.08}La_{0.05}Yb_{0.04}Co_4Sb_{12}$ - Powders II	52.63	kg
Step 9: Spark Plasma Sintering (SPS, @ 650°C, 50 MPa)			
Type of Parameter	**Parameter**	**Value**	**Unit**
Output Material	$Ba_{0.08}La_{0.05}Yb_{0.04}Co_4Sb_{12}$ - SPS Ingot	1000.00	kg
Input Materials	$Ba_{0.08}La_{0.05}Yb_{0.04}Co_4Sb_{12}$ - Powders II	1052.63	kg
	Argon	9.13	kg
Input Energy	Electricity	59737.18	kWh
Output Waste: Air	Argon	9.13	kg
Output Waste: Solid	$Ba_{0.08}La_{0.05}Yb_{0.04}Co_4Sb_{12}$ - Powders II	52.63	kg
Step 10: Ingot Polishing			
Type of Parameter	**Parameter**	**Value**	**Unit**
Output Material	$Ba_{0.08}La_{0.05}Yb_{0.04}Co_4Sb_{12}$ - Polished Ingot	1000.00	kg
Input Materials	$Ba_{0.08}La_{0.05}Yb_{0.04}Co_4Sb_{12}$ - SPS Ingot	1111.11	kg
	Water	1109.35	kg
Input Energy	Electricity	228.34	kWh
Output Waste: Liquid	Waste water	1220.46	kg
Step 11: Leg Dicing			
Type of Parameter	**Parameter**	**Value**	**Unit**
Output Material	$Ba_{0.08}La_{0.05}Yb_{0.04}Co_4Sb_{12}$ - Legs	1000.00	kg
Input Materials	$Ba_{0.08}La_{0.05}Yb_{0.04}Co_4Sb_{12}$ - Polished Ingot	3297.71	kg
	Borax	21.35	kg

	Sodium nitrate	21.35	kg
	Water	5701.75	kg
Input Energy	Electricity	7029.13	kWh
Output Waste: Liquid	Waste water	5744.45	kg
Output Waste: Solid	$Ba_{0.08}La_{0.05}Yb_{0.04}Co_4Sb_{12}$ (Landfill)	2297.71	kg

Table A-12: Inventory for producing alumina plates (SK-1 module)

Step 1: Ball Milling			
Type of Parameter	**Parameter**	**Value**	**Unit**
Output Material	Alumina - Ball milled powder	1000.00	kg
Input Materials	Alumina	1052.63	kg
	Ethanol	349.30	kg
Input Energy	Electricity	19523.70	kWh
Output Waste: Liquid	Ethanol	349.30	kg
Output Waste: Solid	Alumina powder	52.63	kg
Step 2: Sintering (@ 1500°C, 1 h, 3°C/min) (assuming zero energy consumption for cold isostatic pressing)			
Type of Parameter	**Parameter**	**Value**	**Unit**
Output Material	Alumina plate - Sintered	1000.00	kg
Input Materials	Alumina - Ball milled powder	1052.63	kg
Input Energy	Electricity	919316.71	kWh
Output Waste: Solid	Alumina powder	52.63	kg
Step 3: Polishing			
Type of Parameter	**Parameter**	**Value**	**Unit**
Output Material	Alumina plate - Final	1000.00	kg
Input Materials	Alumina plate - Sintered	1111.11	kg
	Water	4450.20	kg
Input Energy	Electricity	916.00	kWh
Output Waste: Solid	Alumina plate	4561.31	kg

Table A-13: Inventory for producing copper tabs (SK-1 module)

Type of Parameter	Parameter	Value	Unit
Output Material	Copper tabs	1000.00	kg
Input Materials	Copper sheet	1001.74	kg
Input Energy	Electricity	9768.48	kWh
Output Waste: Solid	Copper	1.74	kg

2.4. SK-2 Module

Tables A-14, A-15, A-16 and A-17 give the respective inventory details for p- and n-type legs, alumina plates and copper tabs of SK-2 module.

Table A-14: Inventory for producing p-type leg (SK-2 module)

Step 1: Powder Mixing			
Type of Parameter	**Parameter**	**Value**	**Unit**
Output Material	$Ce_yFe_xCo_{4-x}Sb_{12}$ powders	1000.00	kg
Input Materials	Cerium (Ce)	22.66	kg
	Iron (Fe)	49.03	kg
	Cobalt (Co)	84.41	kg
	Antimony (Sb)	843.90	kg
Step 2: Annealing (Quartz tube sealed under pressure, @ 1100°C, 30 h, 5 K/min)			
Type of Parameter	**Parameter**	**Value**	**Unit**
Output Material	$Ce_yFe_xCo_{4-x}Sb_{12}$ - Annealed Set I	1000.00	kg
Input Material	$Ce_yFe_xCo_{4-x}Sb_{12}$ powders	1000.00	kg
Input Energy	Electricity	153768.37	kWh
Step 3: Quenching in Water Bath (Assumed to have zero energy consumption)			
Step 4: Ball Milling			
Type of Parameter	**Parameter**	**Value**	**Unit**
Output Material	$Ce_yFe_xCo_{4-x}Sb_{12}$ - Powders Set I	1000.00	kg
Input Materials	$Ce_yFe_xCo_{4-x}Sb_{12}$ - Annealed Set I	1052.63	kg

	Ethanol	466.35	kg
Input Energy	Electricity	543.04	kWh
Output Waste: Liquid	Ethanol	466.35	kg
Output Waste: Solid	$Ce_yFe_xCo_{4-x}Sb_{12}$ - Powders Set I (Landfill)	52.63	kg
Step 5: Cold Isostatic Pressing (Assumed to consume zero energy)			
Type of Parameter	**Parameter**	**Value**	**Unit**
Output Material	$Ce_yFe_xCo_{4-x}Sb_{12}$ - CIP	1000.00	kg
Input Material	$Ce_yFe_xCo_{4-x}Sb_{12}$ - Powders Set I	1052.63	kg
Output Waste: Solid	$Ce_yFe_xCo_{4-x}Sb_{12}$ - Powders Set I (Landfill)	52.63	kg
Step 6: Annealing (Silica Tubes, @ 700°C, 7 days)			
Type of Parameter	**Parameter**	**Value**	**Unit**
Output Material	$Ce_yFe_xCo_{4-x}Sb_{12}$ - Annealed Set II	1000.00	kg
Input Material	$Ce_yFe_xCo_{4-x}Sb_{12}$ - CIP	1000.00	kg
Input Energy	Electricity	149088.75	kWh
Step 7: Ball Milling			
Type of Parameter	**Parameter**	**Value**	**Unit**
Output Material	$Ce_yFe_xCo_{4-x}Sb_{12}$ - Powders Set II	1000.00	kg
Input Materials	$Ce_yFe_xCo_{4-x}Sb_{12}$ - Annealed Set II	1052.63	kg
	Ethanol	466.35	kg
Input Energy	Electricity	543.04	kWh
Output Waste: Liquid	Ethanol	466.35	kg
Output Waste: Solid	$Ce_yFe_xCo_{4-x}Sb_{12}$ - Powders Set II (Landfill)	52.63	kg
Step 8: Washing with Acids (No electricity assumed to be consumed)			
Type of Parameter	**Parameter**	**Value**	**Unit**
Output Material	$Ce_yFe_xCo_{4-x}Sb_{12}$ - Washed Set	1000.00	kg

Input Materials	$Ce_yFe_xCo_{4-x}Sb_{12}$ - Powders Set II	1111.11	kg
	Hydrochloric acid (HCl)	173.43	kg
	Nitric acid (HNO_3)	221.93	kg
Output Waste: Liquid	Waste water	395.36	kg
Output Waste: Solid	$Ce_yFe_xCo_{4-x}Sb_{12}$ - Washed Set (Landfill)	111.11	kg
Step 9: Plasma Activated Sintering (SPS, @ 600°C, 15 min)			
Type of Parameter	**Parameter**	**Value**	**Unit**
Output Material	$Ce_yFe_xCo_{4-x}Sb_{12}$ - Ingot	1000.00	kg
Input Material	$Ce_yFe_xCo_{4-x}Sb_{12}$ - Washed Set	1052.63	kg
	Argon	11.62	kg
Input Energy	Electricity	75986.03	kWh
Output Waste: Air	Argon	11.62	kg
Output Waste: Solid	$Ce_yFe_xCo_{4-x}Sb_{12}$ - Washed Set (Landfill)	52.63	kg
Step 10: Ingot Polishing			
Type of Parameter	**Parameter**	**Value**	**Unit**
Output Material	$Ce_yFe_xCo_{4-x}Sb_{12}$ - Polished Ingot	1000.00	kg
Input Materials	$Ce_yFe_xCo_{4-x}Sb_{12}$ - Ingot	1111.11	kg
	Water	1082.93	kg
Input Energy	Electricity	222.90	kWh
Output Waste: Liquid	Waste water	1194.05	kg
Step 11: Leg Dicing			
Type of Parameter	**Parameter**	**Value**	**Unit**
Output Material	$Ce_yFe_xCo_{4-x}Sb_{12}$ - Legs	1000.00	kg
Input Materials	$Ce_yFe_xCo_{4-x}Sb_{12}$ - Polished Ingot	3064.18	kg
	Borax	14.45	kg
	Sodium nitrate	14.45	kg

	Water	3857.74	kg
Input Energy	Electricity	4755.83	kWh
Output Waste: Liquid	Waste water	3886.63	kg
Output Waste: Solid	$Ce_yFe_xCo_{4-x}Sb_{12}$ (Landfill)	2064.18	kg

Table A-15: Inventory for producing n-type leg (SK-2 module)

Step 1: Powder Mixing			
Type of Parameter	**Parameter**	**Value**	**Unit**
Output Material	$Yb_{0.3}Co_4Sb_{12}$ - Powders	1000.00	kg
Input Materials	Ytterbium (Yb)	29.68	kg
	Cobalt (Co)	134.80	kg
	Antimony (Sb)	835.52	kg
Step 2: Melting (@ 1100°C, 12 h, graphite crucible in quartz tube)			
Type of Parameter	**Parameter**	**Value**	**Unit**
Output Material	$Yb_{0.3}Co_4Sb_{12}$ - Molten Set	1000.00	kg
Input Material	$Yb_{0.3}Co_4Sb_{12}$ - Powders	1000.00	kg
Input Energy	Electricity	23439.54	kWh
Step 3: Quenching in Saltwater (Assumed to consume zero energy)			
Step 4: Annealing (@ 660°C, 7 days, quartz tube + graphite crucible)			
Type of Parameter	**Parameter**	**Value**	**Unit**
Output Material	$Yb_{0.3}Co_4Sb_{12}$ - Annealed Set	1000.00	kg
Input Material	$Yb_{0.3}Co_4Sb_{12}$ - Molten Set	1000.00	kg
Input Energy	Electricity	238679.56	kWh
Step 5: Ball Milling			
Type of Parameter	**Parameter**	**Value**	**Unit**
Output Material	$Yb_{0.3}Co_4Sb_{12}$ - Milled Powders	1000.00	kg
Input Materials	$Yb_{0.3}Co_4Sb_{12}$ - Annealed Set	1052.63	kg
	Ethanol	280.49	kg

Input Energy	Electricity	326.61	kWh
Output Waste: Liquid	Ethanol	280.49	kg
Output Waste: Solid	$Yb_{0.3}Co_4Sb_{12}$ - Milled Powders (Landfill)	52.63	kg
Step 6: Sieving (Assumed to consume no energy)			
Step 7: Hot pressing (@ 30 mm graphite dies; 620-640 °C, 55-60 MPa)			
Type of Parameter	**Parameter**	**Value**	**Unit**
Output Material	$Yb_{0.3}Co_4Sb_{12}$ - Ingot	1000.00	kg
Input Materials	$Yb_{0.3}Co_4Sb_{12}$ - Milled Powders	1052.63	kg
	Argon	333.01	kg
Input Energy	Electricity	140628.30	kWh
Output Waste: Air	Argon	333.01	kg
Output Waste: Solid	$Yb_{0.3}Co_4Sb_{12}$ - Milled Powders	52.63	kg
Step 8: Ingot Polishing			
Type of Parameter	**Parameter**	**Value**	**Unit**
Output Material	$Yb_{0.3}Co_4Sb_{12}$ - Polished Ingot	1000.00	kg
Input Materials	$Yb_{0.3}Co_4Sb_{12}$ - Ingot	1111.11	kg
	Water	1055.98	kg
Input Energy	Electricity	217.36	kWh
Output Waste: Liquid	Waste water	1167.09	kg
Step 9: Leg Dicing			
Type of Parameter	**Parameter**	**Value**	**Unit**
Output Material	$Yb_{0.3}Co_4Sb_{12}$ - Legs	1000.00	kg
Input Materials	$Yb_{0.3}Co_4Sb_{12}$ - Polished Ingot	3432.10	kg
	Borax	15.99	kg
	Sodium nitrate	15.99	kg
	Water	4270.09	liters
Input Energy	Electricity	5264.19	kWh

Output Waste: Liquid	Waste water	4302.07	kg
Output Waste: Solid	$Yb_{0.3}Co_4Sb_{12}$ (Landfill)	2432.10	kg

Table A-16: Inventory for producing alumina plates (SK-2 module)

Step 1: Ball Milling			
Type of Parameter	**Parameter**	**Value**	**Unit**
Output Material	Alumina - Ball milled powder	1000.00	kg
Input Materials	Alumina	1052.63	kg
	Ethanol	349.30	kg
Input Energy	Electricity	19523.70	kWh
Output Waste: Liquid	Ethanol	349.30	kg
Output Waste: Solid	Alumina powder	52.63	kg
Step 2: Sintering (@ 1500°C, 1 h, 3°C/min) (Assuming zero energy consumption for cold isostatic pressing)			
Type of Parameter	**Parameter**	**Value**	**Unit**
Output Material	Alumina plate - Sintered	1000.00	kg
Input Materials	Alumina - Ball milled powder	1052.63	kg
Input Energy	Electricity	3606086.71	kWh
Output Waste: Solid	Alumina powder	52.63	kg
Step 3: Polishing			
Type of Parameter	**Parameter**	**Value**	**Unit**
Output Material	Alumina plate - Final	1000.00	kg
Input Materials	Alumina plate - Sintered	1111.11	kg
	Water	4593.74	kg
Input Energy	Electricity	945.55	kWh
Output Waste: Solid	Alumina plate	111.11	kg

Table A-17: Inventory for producing copper tabs (SK-2 module)

Type of Parameter	**Parameter**	**Value**	**Unit**

Output Material	Copper tabs	1000.00	kg
Input Materials	Copper sheet	1005.31	kg
Input Energy	Electricity	29581.60	kWh
Output Waste: Solid	Copper	5.31	kg

2.5. HH Module

Tables A-18, A-19, A-20 and A-21 give the respective inventory details for p-type legs, n-type legs, alumina plates and copper tabs of HH module.

Table A-18: Inventory for producing p-type leg (HH module)

Step 1: Powder Mixing			
Type of Parameter	**Parameter**	**Value**	**Unit**
Output Material	$Hf_{0.5}Zr_{0.5}CoSb_{0.8}Sn_{0.2}$ - Powder	1000.00	kg
Input Materials	Hafnium (Hf)	283.37	kg
	Zirconium (Zr)	144.83	kg
	Cobalt (Co)	187.13	kg
	Antimony (Sb)	309.29	kg
	Tin (Sn)	75.39	kg
Step 2: Arc Melting of Elements			
Type of Parameter	**Parameter**	**Value**	**Unit**
Output Material	$Hf_{0.5}Zr_{0.5}CoSb_{0.8}Sn_{0.2}$ - Arc Melting Set	1000.00	kg
Input Materials	$Hf_{0.5}Zr_{0.5}CoSb_{0.8}Sn_{0.2}$ - Powder	1000.00	kg
	Water (recycled)	1218.00	liters
	Argon	15.52	kg
Input Energy	Electricity	58000.00	kWh
Output Waste: Air	Argon	15.52	kg
Output Waste: Liquid	Water	1218.00	kg
Step 3: Ball Milling (@ 20 h)			

Type of Parameter	Parameter	Value	Unit
Output Material	$Hf_{0.5}Zr_{0.5}CoSb_{0.8}Sn_{0.2}$ - Powders	1000.00	kg
Input Materials	$Hf_{0.5}Zr_{0.5}CoSb_{0.8}Sn_{0.2}$ - Arc Melting Set	1052.63	kg
	Ethanol	258.74	kg
Input Energy	Electricity	12051.40	kWh
Output Waste: Liquid	Ethanol	258.74	kg
Output Waste: Solid	$Hf_{0.5}Zr_{0.5}CoSb_{0.8}Sn_{0.2}$ - Powders (Landfill)	52.63	kg
Step 4: Hot Pressing (@ 1000-1050°C)			
Type of Parameter	**Parameter**	**Value**	**Unit**
Output Material	$Hf_{0.5}Zr_{0.5}CoSb_{0.8}Sn_{0.2}$ - Ingot	1000.00	kg
Input Materials	$Hf_{0.5}Zr_{0.5}CoSb_{0.8}Sn_{0.2}$ - Powders	1052.63	kg
	Argon	298.35	kg
Input Energy	Electricity	125994.06	kWh
Output Waste: Air	Argon	298.35	kg
Output Waste: Solid	$Hf_{0.5}Zr_{0.5}CoSb_{0.8}Sn_{0.2}$ - Powders (Landfill)	52.63	kg
Step 5: Ingot Polishing			
Type of Parameter	**Parameter**	**Value**	**Unit**
Output Material	$Hf_{0.8}Ti_{0.2}CoSb_{0.8}Sn_{0.2}$ - Polished Ingot	1000.00	kg
Input Materials	$Hf_{0.8}Ti_{0.2}CoSb_{0.8}Sn_{0.2}$ - Ingot	1111.11	kg
	Water	792.77	kg
Input Energy	Electricity	163.18	kWh
Output Waste: Liquid	Waste water	903.88	kg
Step 6: Leg Dicing			
Type of Parameter	**Parameter**	**Value**	**Unit**
Output Material	$Hf_{0.8}Ti_{0.2}CoSb_{0.8}Sn_{0.2}$ - Legs	1000.00	kg

Input Materials	$Hf_{0.8}Ti_{0.2}CoSb_{0.8}Sn_{0.2}$ - Polished Ingot	3491.31	kg
	Borax	34.28	kg
	Sodium nitrate	34.28	kg
	Water	9154.54	kg
Input Energy	Electricity	11285.75	kWh
Output Waste: Liquid	Waste water	9223.10	kg
Output Waste: Solid	$Hf_{0.8}Ti_{0.2}CoSb_{0.8}Sn_{0.2}$ (Landfill)	2491.31	kg

Table A-19: Inventory for producing n-type leg (HH module)

Step 1: Powder mixing			
Type of Parameter	**Parameter**	**Value**	**Unit**
Output Material	$Hf_{0.5}Ti_{0.25}Zr_{0.25}NiSn_{0.99}Sb_{0.01}$ - Powder	1000.00	kg
Input Materials	Hafnium (Hf)	296.05	kg
	Titanium (Ti)	39.70	kg
	Zirconium (Zr)	75.65	kg
	Nickel (Ni)	194.70	kg
	Tin (Sn)	389.86	kg
	Antimony (Sb)	4.04	kg
Step 2: Arc Melting of Elements			
Type of Parameter	**Parameter**	**Value**	**Unit**
Output Material	$Hf_{0.5}Ti_{0.25}Zr_{0.25}NiSn_{0.99}Sb_{0.01}$ - Arc Melting Set	1000.00	kg
Input Materials	$Hf_{0.5}Ti_{0.25}Zr_{0.25}NiSn_{0.99}Sb_{0.01}$ - Powder	1000.00	kg
	Water (recycled)	1218.00	liters
	Argon	15.52	kg
Input Energy	Electricity	58000.00	kWh
Output Waste: Air	Argon	15.52	kg

Output Waste: Liquid	Water	1218.00	kg
Step 3: Ball Milling (@ 20 h)			
Type of Parameter	**Parameter**	**Value**	**Unit**
Output Material	$Hf_{0.5}Ti_{0.25}Zr_{0.25}NiSn_{0.99}Sb_{0.01}$ - Powders	1000.00	kg
Input Materials	$Hf_{0.5}Ti_{0.25}Zr_{0.25}NiSn_{0.99}Sb_{0.01}$ - Arc Melting Set	1052.63	kg
	Ethanol	260.26	kg
Input Energy	Electricity	12122.52	kWh
Output Waste: Liquid	Ethanol	260.26	kg
Output Waste: Solid	$Hf_{0.5}Ti_{0.25}Zr_{0.25}NiSn_{0.99}Sb_{0.01}$ - Powders (Landfill)	52.63	kg
Step 4: Hot pressing (@ 1000-1050°C)			
Type of Parameter	**Parameter**	**Value**	**Unit**
Output Material	$Hf_{0.5}Ti_{0.25}Zr_{0.25}NiSn_{0.99}Sb_{0.01}$ - Ingot	1000.00	kg
Input Materials	$Hf_{0.5}Ti_{0.25}Zr_{0.25}NiSn_{0.99}Sb_{0.01}$ - Powders	1052.63	kg
	Argon	305.31	kg
Input Energy	Electricity	128930.66	kWh
Output Waste: Air	Argon	305.31	kg
Output Waste: Solid	$Hf_{0.5}Ti_{0.25}Zr_{0.25}NiSn_{0.99}Sb_{0.01}$ - Powders (Landfill)	52.63	kg
Step 5: Ingot Polishing			
Type of Parameter	**Parameter**	**Value**	**Unit**
Output Material	$Hf_{0.5}Ti_{0.25}Zr_{0.25}NiSn_{0.99}Sb_{0.01}$ - Polished Ingot	1000.00	kg
Input Materials	$Hf_{0.5}Ti_{0.25}Zr_{0.25}NiSn_{0.99}Sb_{0.01}$ - Ingot	1111.11	kg
	Water	811.25	kg

Input Energy	Electricity	166.98	kWh
Output Waste: Liquid	Waste water	922.36	kg
Step 6: Leg Dicing			
Type of Parameter	**Parameter**	**Value**	**Unit**
Output Material	$Hf_{0.5}Ti_{0.25}Zr_{0.25}NiSn_{0.99}Sb_{0.01}$ - Legs	1000.00	kg
Input Materials	$Hf_{0.5}Ti_{0.25}Zr_{0.25}NiSn_{0.99}Sb_{0.01}$ - Polished Ingot	3491.31	kg
	Borax	35.08	kg
	Sodium nitrate	35.08	kg
	Water	9367.91	kg
Input Energy	Electricity	11548.80	kWh
Output Waste: Liquid	Waste water	9438.07	kg
Output Waste: Solid	$Hf_{0.5}Ti_{0.25}Zr_{0.25}NiSn_{0.99}Sb_{0.01}$ (Landfill)	2491.31	kg

Table A-20: Inventory for producing alumina plates (HH module)

Step 1: Ball Milling			
Type of Parameter	**Parameter**	**Value**	**Unit**
Output Material	Alumina - Ball milled powder	1000.00	kg
Input Materials	Alumina	1052.63	kg
	Ethanol	349.30	kg
Input Energy	Electricity	19523.70	kWh
Output Waste: Liquid	Ethanol	349.30	kg
Output Waste: Solid	Alumina powder	52.63	kg
Step 2: Sintering (@ 1500°C, 1 h, 3°C/min) (Assuming zero energy consumption for cold isostatic pressing)			
Type of Parameter	**Parameter**	**Value**	**Unit**
Output Material	Alumina plate - Sintered	1000.00	kg
Input Materials	Alumina - Ball milled powder	1052.63	kg

Input Energy	Electricity	913348.27	kWh
Output Waste: Solid	Alumina powder	52.63	kg
Step 3: Polishing			
Type of Parameter	**Parameter**	**Value**	**Unit**
Output Material	Alumina plate - Final	1000.00	kg
Input Materials	Alumina plate - Sintered	1111.11	kg
	Water	16353.65	kg
Input Energy	Electricity	3366.13	kWh
Output Waste: Solid	Alumina plate	16464.76	kg

Table A-21: Inventory for producing copper tabs (HH module)

Type of Parameter	**Parameter**	**Value**	**Unit**
Output Material	Copper tabs	1000.00	kg
Input Materials	Copper sheet	1002.49	kg
Input Energy	Electricity	24808.88	kWh
Output Waste: Solid	Copper	2.49	kg

2.6. PT Module

Tables A-22, A-23, A-24 and A-25 give the respective inventory details for p- and n-type legs, alumina plates and copper tabs of PT module. For copper patterns, the same inventory was used as that for copper tabs, while the polyethylene film was approximated to be the same as that of polyethylene (for simplicity).

Table A-22: Inventory for producing p-type leg (PT module)

Step 1: Powder Mixing			
Type of Parameter	**Parameter**	**Value**	**Unit**
Output Material	PbTe-2 % MgTe, doped with 4 % Na	1000.00	kg
Input Materials	Lead (Pb)	606.60	kg
	Tellurium (Te)	389.10	kg

	Magnesium (Mg)	1.50	kg
	Sodium (Na)	2.80	kg
Step 2: Glove Box Mixing & Powder Filling in Quartz Tube			
Type of Parameter	**Parameter**	**Value**	**Unit**
Output Material	PbTe-2 % MgTe, doped with 4 % Na - Sealed	1000.00	kg
Input Materials	PbTe-2 % MgTe, doped with 4 % Na	1000.00	kg
	Nitrogen	34.97	kg
Step 3: Annealing (@ 1050°C, ~ 70 K/h)			
Type of Parameter	**Parameter**	**Value**	**Unit**
Output Material	PbTe-2% MgTe, doped with 4 % Na - Annealed Set I	1000.00	kg
Input Material	PbTe-2% MgTe, doped with 4 % Na - Sealed	1000.00	kg
Input Energy	Electricity	335126.64	kWh
Step 4: Diffusion Barrier - Preparation			
Type of Parameter	**Parameter**	**Value**	**Unit**
Output Material	$Co_{0.8}Fe_{0.2}$	1000.00	kg
Input Materials	Cobalt (Co)	808.47	kg
	Iron (Fe)	191.53	kg
Step 5: Hot Pressing (@ 500°C, 1 h, 30 MPa)			
Type of Parameter	**Parameter**	**Value**	**Unit**
Output Material	P-type leg - Hot pressed ingot	1000.00	kg
Input Materials	PbTe-2 % MgTe, doped with 4 % Na - Annealed Set I	626.03	kg
	$Co_{0.8}Fe_{0.2}$	426.61	kg
	Argon	1272.76	kg

Input Energy	Electricity	537486.41	kWh
Output Waste: Air	Argon	1272.76	kg
Output Wastes: Solid	PbTe-2 % MgTe, doped with 4 % Na - Powders (Landfill)	31.30	kg
	$Co_{0.8}Fe_{0.2}$ - Powders (Landfill)	21.33	kg
Step 6: Ingot Polishing			
Type of Parameter	**Parameter**	**Value**	**Unit**
Output Material	P-type leg - Polished ingot	1000.00	kg
Input Materials	P-type leg - Hot pressed ingot	1116.34	kg
	Water	221.13	kg
Input Energy	Electricity	31.69	kWh
Output Waste: Liquid	Waste water	337.46	kg
Step 7: Leg Dicing			
Type of Parameter	**Parameter**	**Value**	**Unit**
Output Material	P-type leg - Legs	1000.00	kg
Input Materials	P-type leg - Polished ingot	2625.33	kg
	Borax	35.19	kg
	Sodium nitrate	35.19	kg
	Water	9398.17	kg
Input Energy	Electricity	11586.10	kWh
Output Waste: Liquid	Waste water	9468.56	kg
Output Waste: Solid	P-type leg (Landfill)	1625.33	kg

Table A-23: Inventory for producing n-type leg (PT module)

Step 1: Powder Mixing			
Type of Parameter	**Parameter**	**Value**	**Unit**
Output Material	PbTe, doped with 0.2 % PbI_2	1000.00	kg
Input Materials	Lead (Pb)	617.63	kg
	Tellurium (Te)	379.61	kg

	Lead iodide (PbI_2)	2.75	kg
Step 2: Glove Box Mixing & Powder Filling in Quartz Tube			
Type of Parameter	**Parameter**	**Value**	**Unit**
Output Material	PbTe, doped with 0.2 % PbI_2 - Sealed	1000.00	kg
Input Materials	PbTe, doped with 0.2 % PbI_2	1000.00	kg
	Nitrogen	36.13	kg
Step 3: Annealing (@ 1050°C, ~ 70 K/h)			
Type of Parameter	**Parameter**	**Value**	**Unit**
Output Material	PbTe, doped with 0.2 % PbI_2 - Annealed Set	1000.00	kg
Input Material	PbTe, doped with 0.2 % PbI_2 - Sealed	1000.00	kg
Input Energy	Electricity	346268.96	kWh
Step 4: Diffusion Barrier - Preparation			
Type of Parameter	**Parameter**	**Value**	**Unit**
Output Material	$Co_{0.8}Fe_{0.2}$	1000.00	kg
Input Materials	Cobalt (Co)	808.47	kg
	Iron (Fe)	191.53	kg
Step 5: Hot Pressing (@ 500°C, 1 h, 30 MPa)			
Type of Parameter	**Parameter**	**Value**	**Unit**
Output Material	N-type leg - Hot pressed ingot	1000.00	kg
Input Materials	PbTe, doped with 0.2 % PbI_2 - Annealed Set	617.70	kg
	$Co_{0.8}Fe_{0.2}$	434.93	kg
	Argon	1272.76	kg
Input Energy	Electricity	537486.41	kWh
Output Waste: Air	Argon	1272.76	kg
Output Wastes: Solid	PbTe, doped with 0.2 % PbI_2 - Powders (Landfill)	30.89	kg

	$Co_{0.8}Fe_{0.2}$ - Powders (Landfill)	21.75	kg
Step 6: Ingot Polishing			
Type of Parameter	**Parameter**	**Value**	**Unit**
Output Material	N-type leg - Polished ingot	1000.00	kg
Input Materials	N-type leg - Hot pressed ingot	1118.88	kg
	Water	564.88	kg
Input Energy	Electricity	84.34	kWh
Output Waste: Liquid	Waste water	683.76	kg
Step 7: Leg Dicing			
Type of Parameter	**Parameter**	**Value**	**Unit**
Output Material	N-type leg - Legs	1000.00	kg
Input Materials	N-type leg - Polished ingot	2634.86	kg
	Borax	35.19	kg
	Sodium nitrate	35.19	kg
	Water	9638.21	liters
Input Energy	Electricity	11882.02	kWh
Output Waste: Liquid	Waste water	9708.60	kg
Output Waste: Solid	N-type leg (Landfill)	1634.86	kg

Table A-24: Inventory for producing alumina plates (PT module)

Step 1: Ball Milling			
Type of Parameter	**Parameter**	**Value**	**Unit**
Output Material	Alumina - Ball milled powder	1000.00	kg
Input Materials	Alumina	1052.63	kg
	Ethanol	349.30	kg
Input Energy	Electricity	19523.70	kWh
Output Waste: Liquid	Ethanol	349.30	kg
Output Waste: Solid	Alumina powder	52.63	kg

Step 2: Sintering (@ 1500°C, 1 h, 3°C/min) (Assuming zero energy consumption for cold isostatic pressing)			
Type of Parameter	**Parameter**	**Value**	**Unit**
Output Material	Alumina plate - Sintered	1000.00	kg
Input Materials	Alumina - Ball milled powder	1052.63	kg
Input Energy	Electricity	883844.78	kWh
Output Waste: Solid	Alumina powder	52.63	kg
Step 3: Polishing			
Type of Parameter	**Parameter**	**Value**	**Unit**
Output Material	Alumina plate - Final	1000.00	kg
Input Materials	Alumina plate - Sintered	1111.11	kg
	Water	42534.64	kg
Input Energy	Electricity	8755.05	kWh
Output Waste: Solid	Alumina plate	42645.75	kg

Table A-25: Inventory for producing copper tabs (PT module)

Material	Parameter	Quantity	Unit
Output Material	Copper tabs	1000.00	kg
Input Materials	Copper sheet	1012.59	kg
Input Energy	Electricity	4729.17	kWh
Output Waste: Solid	Copper	12.59	kg

2.7. SC Module

Tables A-26, A-27, A-28 and A-29 give the respective inventory details for p-type legs, n-type legs, alumina plates and aluminum tabs of SC module.

Table A-26: Inventory for producing p-type leg (SC module)

Step 1: Powder Mixing			
Type of Parameter	**Parameter**	**Value**	**Unit**

Output Material	$(Mn_{0.98}Mo_{0.02})(Si_{0.9865}Al_{0.0035}Ge_{0.01})_{1.74}$	1000.00	kg
Input Materials	Manganese (Mn)	510.83	kg
	Molybdenum (Mo)	18.21	kg
	Silicon (Si)	457.41	kg
	Aluminum (Al)	1.56	kg
	Germanium (Ge)	11.99	kg
Step 2: Induction Furnace Melting			
Type of Parameter	**Parameter**	**Value**	**Unit**
Output Material	$(Mn_{0.98}Mo_{0.02})(Si_{0.9865}Al_{0.0035}Ge_{0.01})_{1.74}$ Melt	1000.00	kg
Input Materials	$(Mn_{0.98}Mo_{0.02})(Si_{0.9865}Al_{0.0035}Ge_{0.01})_{1.74}$	1000.00	kg
	Argon	1.13	kg
Input Energy	Electricity	27532.73	kWh
Output Waste: Air	Argon	1.13	kg
Step 3: Jaw Crushing			
Type of Parameter	**Parameter**	**Value**	**Unit**
Output Material	$(Mn_{0.98}Mo_{0.02})(Si_{0.9865}Al_{0.0035}Ge_{0.01})_{1.74}$ - Jaw crushed powder	1000.00	kg
Input Material	$(Mn_{0.98}Mo_{0.02})(Si_{0.9865}Al_{0.0035}Ge_{0.01})_{1.74}$ Melt	1052.63	kg
Input Energy	Electricity	31.62	kWh
Output Waste: Solid	$(Mn_{0.98}Mo_{0.02})(Si_{0.9865}Al_{0.0035}Ge_{0.01})_{1.74}$ - Powder (Landfill)	52.63	kg
Step 4: Ball Milling			
Type of Parameter	**Parameter**	**Value**	**Unit**
Output Material	$(Mn_{0.98}Mo_{0.02})(Si_{0.9865}Al_{0.0035}Ge_{0.01})_{1.74}$ - Powder	1000.00	kg

Input Materials	$(Mn_{0.98}Mo_{0.02})(Si_{0.9865}Al_{0.0035}Ge_{0.01})_{1.74}$ - Jaw crushed powder	1052.63	kg
	Ethanol	307.41	kg
Input Energy	Electricity	357.96	kWh
Output Waste: Liquid	Ethanol	307.41	kg
Output Waste: Solid	$(Mn_{0.98}Mo_{0.02})(Si_{0.9865}Al_{0.0035}Ge_{0.01})_{1.74}$ - Powder (Landfill)	52.63	kg
Step 5: Plasma Activated Sintering (SPS)			
Type of Parameter	**Parameter**	**Value**	**Unit**
Output Material	$(Mn_{0.98}Mo_{0.02})(Si_{0.9865}Al_{0.0035}Ge_{0.01})_{1.74}$ - SPS Ingot	1000.00	kg
Input Materials	$(Mn_{0.98}Mo_{0.02})(Si_{0.9865}Al_{0.0035}Ge_{0.01})_{1.74}$ - Powder	1052.63	kg
	Argon	13.36	kg
Input Energy	Electricity	87379.10	kWh
Output Waste: Air	Argon	13.36	kg
Output Waste: Solid	$(Mn_{0.98}Mo_{0.02})(Si_{0.9865}Al_{0.0035}Ge_{0.01})_{1.74}$ - Powder (Landfill)	52.63	kg
Step 6: Ingot Polishing			
Type of Parameter	**Parameter**	**Value**	**Unit**
Output Material	$(Mn_{0.98}Mo_{0.02})(Si_{0.9865}Al_{0.0035}Ge_{0.01})_{1.74}$ - Polished Ingot	1000.00	kg
Input Materials	$(Mn_{0.98}Mo_{0.02})(Si_{0.9865}Al_{0.0035}Ge_{0.01})_{1.74}$ - SPS Ingot	1111.11	kg
	Water	304.65	kg
Input Energy	Electricity	318.55	kWh
Output Waste: Liquid	Waste water	415.76	kg
Step 7: Leg Dicing			
Type of Parameter	**Parameter**	**Value**	**Unit**

Output Material	$(Mn_{0.98}Mo_{0.02})(Si_{0.9865}Al_{0.0035}Ge_{0.01})_{1.74}$ - Legs	1000.00	kg
Input Materials	$(Mn_{0.98}Mo_{0.02})(Si_{0.9865}Al_{0.0035}Ge_{0.01})_{1.74}$ - Polished Ingot	4203.27	kg
	Borax	28.32	kg
	Sodium nitrate	28.32	kg
	Water	7562.60	kg
Input Energy	Electricity	9323.20	kWh
Output Waste: Liquid	Waste water	7619.24	kg
Output Waste: Solid	$(Mn_{0.98}Mo_{0.02})(Si_{0.9865}Al_{0.0035}Ge_{0.01})_{1.74}$ (Landfill)	3203.27	kg

Table A-27: Inventory for producing n-type leg (SC module)

Step 1: Powder Mixing			
Type of Parameter	**Parameter**	**Value**	**Unit**
Output Material	$Mg_2Si_{0.4}Sn_{0.6}$	1000.00	kg
Input Materials	Magnesium (Mg)	370.87	kg
	Silicon (Si)	85.71	kg
	Tin (Sn)	543.42	kg
Step 2: Induction Furnace Melting			
Type of Parameter	**Parameter**	**Value**	**Unit**
Output Material	$Mg_2Si_{0.4}Sn_{0.6}$ - Melt	1000.00	kg
Input Materials	$Mg_2Si_{0.4}Sn_{0.6}$	1000.00	kg
	Argon	1.99	kg
Input Energy	Electricity	48227.86	kWh
Output Waste: Air	Argon	1.99	kg
Step 3: Jaw Crushing			
Type of Parameter	**Parameter**	**Value**	**Unit**
Output Material	$Mg_2Si_{0.4}Sn_{0.6}$ - Jaw crushed powder	1000.00	kg

Input Material	$Mg_2Si_{0.4}Sn_{0.6}$ - Melt	1052.63	kg
Input Energy	Electricity	31.62	kWh
Output Waste: Solid	$Mg_2Si_{0.4}Sn_{0.6}$ - Jaw crushed powder (Landfill)	52.63	kg
Step 4: Ball Milling			
Type of Parameter	**Parameter**	**Value**	**Unit**
Output Material	$Mg_2Si_{0.4}Sn_{0.6}$ - Powder	1000.00	kg
Input Materials	$Mg_2Si_{0.4}Sn_{0.6}$ - Jaw crushed powder	1052.63	kg
	Ethanol	393.23	kg
Input Energy	Electricity	457.90	kWh
Output Waste: Liquid	Ethanol	393.23	kg
Output Waste: Solid	$Mg_2Si_{0.4}Sn_{0.6}$ - Powder (Landfill)	52.63	kg
Step 5: Plasma Activated Sintering (SPS)			
Type of Parameter	**Parameter**	**Value**	**Unit**
Output Material	$Mg_2Si_{0.4}Sn_{0.6}$ - SPS Ingot	1000.00	kg
Input Materials	$Mg_2Si_{0.4}Sn_{0.6}$ - Powder	1052.63	kg
	Argon	23.40	kg
Input Energy	Electricity	153058.08	kWh
Output Waste: Air	Argon	23.40	kg
Output Waste: Solid	$Mg_2Si_{0.4}Sn_{0.6}$ - Powder (Landfill)	52.63	kg
Step 6: Annealing			
Type of Parameter	**Parameter**	**Value**	**Unit**
Output Material	$Mg_2Si_{0.4}Sn_{0.6}$ - Ingot	1000.00	kg
Input Material	$Mg_2Si_{0.4}Sn_{0.6}$ - SPS Ingot	1000.00	kg
Input Energy	Electricity	694.60	kWh
Step 7: Ingot Polishing			
Type of Parameter	**Parameter**	**Value**	**Unit**
Output Material	$Mg_2Si_{0.4}Sn_{0.6}$ - Polished Ingot	1000.00	kg

Input Materials	$Mg_2Si_{0.4}Sn_{0.6}$ - Ingot	1111.11	kg
	Water	533.65	kg
Input Energy	Electricity	558.00	kWh
Output Waste: Liquid	Waste water	644.76	kg
Step 8: Leg Dicing			
Type of Parameter	**Parameter**	**Value**	**Unit**
Output Material	$Mg_2Si_{0.4}Sn_{0.6}$ - Legs	1000.00	kg
Input Materials	$Mg_2Si_{0.4}Sn_{0.6}$ - Polished Ingot	4203.27	kg
	Borax	49.60	kg
	Sodium nitrate	49.60	kg
	Water	13247.07	liters
Input Energy	Electricity	16331.03	kWh
Output Waste: Liquid	Waste water	13346.28	kg
Output Waste: Solid	$Mg_2Si_{0.4}Sn_{0.6}$ - Landfill	3203.27	kg

Table A-28: Inventory for producing alumina plates (SC module)

Step 1: Ball Milling			
Type of Parameter	**Parameter**	**Value**	**Unit**
Output Material	Alumina - Ball milled powder	1000.00	kg
Input Materials	Alumina	1052.63	kg
	Ethanol	349.30	kg
Input Energy	Electricity	19523.70	kWh
Output Waste: Liquid	Ethanol	349.30	kg
Output Waste: Solid	Alumina powder	52.63	kg
Step 2: Sintering (@ 1500°C, 1 h, 3°C/min) (Assuming zero energy consumption for cold isostatic pressing)			
Type of Parameter	**Parameter**	**Value**	**Unit**
Output Material	Alumina plate - Sintered	1000.00	kg
Input Materials	Alumina - Ball milled powder	1052.63	kg

Input Energy	Electricity	837154.93	kWh
Output Waste: Solid	Alumina powder	52.63	kg
Step 3: Polishing			
Type of Parameter	**Parameter**	**Value**	**Unit**
Output Material	Alumina plate - Final	1000.00	kg
Input Materials	Alumina plate - Sintered	1111.11	kg
	Water	20795.57	kg
Input Energy	Electricity	4280.42	kWh
Output Waste: Solid	Alumina plate	20906.68	kg

Table A-29: Inventory for producing aluminum tabs (SC module)

Type of Parameter	**Parameter**	**Value**	**Unit**
Output Material	Aluminum tabs	1000.00	kg
Input Materials	Aluminum sheet	1002.16	kg
Input Energy	Electricity	34400.27	kWh
Output Waste: Solid	Aluminum	2.16	kg

3. Modules: Electricity Generation (Use Stage)

Based on the number of modules used for each chosen module system (Table 2-4) and assumptions made in Chapter 2, Table A-30 shows: (a) Amount of electricity generated by each module system over its lifetime (15 years of continuous operation); and (b) Reference flow for the considered functional unit (1 kWh of electricity generated). All these calculations assumed that 1000 W of input waste heat power was available for conversion to electricity and that the modules were operated at their optimal range of hot and cold side temperatures for obtaining the best-possible output.

Table A-30: Amount of electricity generated and reference flow for every module

Module system	**η (%)**	**Output Electricity (kWh)**	**Reference flow (p)**
BT-1	4.08	5361.12	1.87×10^{-4}

BT-2	7.00	9198.00	1.09×10^{-4}
SK-1	7.50	9855.00	1.01×10^{-4}
SK-2	7.30	9592.20	1.04×10^{-4}
HH	4.50	5913.00	1.69×10^{-4}
PT	8.80	11563.20	8.65×10^{-5}
SC	6.40	8409.60	1.19×10^{-4}

4. *Modules: EOL Scenarios*

Three end-of-life (EOL) scenarios were considered in this study, all of which have been described in Chapter 2. For each of these EOL scenarios, the assumption was that prior to their occurrence, individual modules were dismantled into their respective components and these were separately subjected to the corresponding EOL scenario. All related inventory details, as well as a discussion of the 6R-based approach that was used in this work, have been provided in the following subsections.

4.1. 6R-Based Approach

The 6R-based approach for material flow[101] focuses on reducing the amount of raw material required to produce the desired product. In practical terms, this approach involves practice of six key steps (summary reproduced below):

- Reduce: Use of resources, energy and materials prior to and during manufacturing, as well as emissions and wastes during use.
- Reuse: Either the product entirely, or its components after its first lifetime for subsequent life cycles
- Recycle: Convert wastes into new, useful materials or even products
- Recover: Collect, disassemble, sort and clean products at end of their lifetime for subsequent reuse
- Redesign: Convert recycled/recovered products or materials into new, next-generation products

- Remanufacture: Re-process used products, either to restore to original state (closed loop recycling) or for reuse in a new application (open loop recycling)

4.2. Disposal Scenario (D-Scenario)

Table A-31 shows the inventory for disposal of individual components of TE modules.

Table A-31: Inventory for the disposal of individual components

Type of Parameter	**Parameter**	**Value**	**Unit**
Output Material	Powders (for disposal)	1000.00	kg
Input Material	Component	1000.00	kg
Infrastructure	Residual material landfill facility	2.08×10^{-6}	p
Transportation required	Lorry (16-32 tons, EURO4)	160.93	ton-km

4.3. Practical Scenario (P-Scenario)

Inventory for disposal-related aspect of these legs was the same as that used for D-scenario, while that for recycling of alumina plates is provided in A-32.

Table A-32: Inventory for the recycling of alumina plates

Type of Parameter	**Parameter**	**Value**	**Unit**
Output Material	Aluminum oxide	2000.00	kg
Input Materials	Bauxite	2881.00	kg
	Sodium hydroxide (Caustic soda)	78.96	kg
	Quicklime	40.30	kg
	Alumina Powders	1052.63	kg
	Sea water	565.00	kg
	Surface water	2571.00	kg
Input Energy	Electricity	26361.71	kWh
Waste for recovery	Bauxite residue	2.30	kg
	Other	5.60	kg
Waste for disposal	Red mud (dry)	1354.00	kg

	Waste (non-hazardous)	8.50	kg
	Waste (hazardous)	9.28	kg
Transportation required	Transport involved	3261.24	ton-km
Output Emissions: Air	Particulates	0.56	kg
	SO_2	2.40	kg
	NO_2	0.68	kg
	Mercury (+II, heavy metals to air)	0.0002	kg
	Water vapor (inorganic emissions to air)	1200.00	kg
Output Emissions: Water	Suspended solids	0.02	kg
	Oil and grease	0.77	kg
	Mercury (+II, heavy metals to fresh water)	7×10^{-8}	kg
	Water (treated waste water release to surface water)	1360.00	kg

4.4. Circular Economy Scenario (CE-Scenario)

With regard to alumina plates, P-scenario was used as discussed in previous section, (Table A-32), while metallic tabs were considered to be disposed of under D-scenario (Table A-31). For TE legs, their recycling was considered as per the scenario mentioned in Chapter 2.

4.4.1. BT-1 Module

Tables A-33 and A-34 provide the respective inventory details for recovery, reprocessing and reuse of p- and n-type legs of BT-1 module.

Table A-33: Inventory details for recycling of p-type legs (BT-1 module)

Type of Parameter	Parameter	Value	Unit
Output Material	P-type TE Leg - Powder - Recycled (Step 1)	1000.00	kg

Input Materials	P-type TE Leg - Original	2216.07	kg
	Argon (Step 2)	55490.71	kg
	Water	48554.37	kg
Input Energy	Electricity (Step 1)	1492.01	kWh
	Electricity (Step 2)	11560.56	kWh
Output Waste: Air	Argon	55490.71	kg
Output Waste: Water	Waste water	48554.37	kg
Output Waste: Solid	P-type material (Landfill after treatment)	1216.07	kg
Transport Distance	Distance involved	100.00	miles
		552.35	ton-km

Table A-34: Inventory details for recycling of n-type legs (BT-1 module)

Type of Parameter	**Parameter**	**Value**	**Unit**
Output Material	N-type TE Leg Material - Recycled (Step 1)	1000.00	kg
Input Materials	N-type TE Leg - Original	2216.07	kg
	Argon (Step 2)	50556.98	kg
	Water	44237.36	kg
Input Energy	Electricity (Step 1)	1348.46	kWh
	Electricity (Step 2)	10532.70	kWh
Output Waste: Air	Argon	50556.98	kg
Output Waste: Water	Waste water	44237.36	kg
Output Waste: Solid	N-type material (Landfill after treatment)	1216.07	kg
Transport Distance	Distance involved	100.00	miles
		552.35	ton-km

4.4.2. *BT-2 Module*

Tables A-35 and A-36 provide the respective inventory details for recovery, reprocessing and reuse of p- and n-type legs of BT-2 module.

Table A-35: Inventory details for recycling of p-type legs (BT-2 module)

Type of Parameter	Parameter	Value	Unit
Output Material	P-type TE Leg - Powder - Recycled (Step 1)	1000.00	kg
Input Materials	P-type TE Leg - Original	2216.07	kg
	Argon (Step 2)	55490.71	kg
	Water	48554.37	kg
Input Energy	Electricity (Step 1)	1176.93	kWh
	Electricity (Step 2)	11560.56	kWh
Output Waste: Air	Argon	55490.71	kg
Output Waste: Water	Waste water	48554.37	kg
Output Waste: Solid	P-type material (Landfill after treatment)	1216.07	kg
Transport Distance	Distance involved	100.00	miles
		552.35	ton-km

Table A-36: Inventory details for recycling of n-type legs (BT-2 module)

Type of Parameter	Parameter	Value	Unit
Output Material	N-type TE Leg Material - Recycled (Step 1)	1000.00	kg
Input Materials	N-type TE Leg - Original	2216.07	kg
	Argon (Step 2)	50556.98	kg
	Water	44237.36	kg
Input Energy	Electricity (Step 1)	1063.69	kWh
	Electricity (Step 2)	10532.70	kWh

Output Waste: Air	Argon	50556.98	kg
Output Waste: Water	Waste water	44237.36	kg
Output Waste: Solid	N-type material (Landfill after treatment)	1216.07	kg
Transport Distance	Distance involved	100.00	miles
		552.35	ton-km

4.4.3. *SK-1 Module*

Tables A-37 and A-38 provide the respective inventory details for recovery, reprocessing and reuse of p- and n-type legs of SK-1 module.

Table A-37: Inventory details for recycling of p-type legs (SK-1 module)

Type of Parameter	**Parameter**	**Value**	**Unit**
Output Material	P-type TE Leg - Powder - Recycled (Step 1)	1000.00	kg
Input Materials	P-type TE Leg - Original	1477.38	kg
	Argon (Step 2)	52326.34	kg
	Water	45785.55	kg
Input Energy	Electricity (Step 1)	926.00	kWh
	Electricity (Step 2)	10901.32	kWh
Output Waste: Air	Argon	52326.34	kg
Output Waste: Water	Waste water	45785.55	kg
Output Waste: Solid	P-type material (Landfill after treatment)	477.38	kg
Transport Distance	Distance involved	100.00	miles
		314.59	ton-km

Table A-38: Inventory details for recycling of n-type legs (SK-1 module)

Type of Parameter	Parameter	Value	Unit
Output Material	N-type TE Leg Material - Recycled (Step 1)	1000.00	kg
Input Materials	N-type TE Leg - Original	1477.38	kg
	Argon (Step 2)	51614.73	kg
	Water	45162.89	kg
Input Energy	Electricity (Step 1)	912.31	kWh
	Electricity (Step 2)	10753.07	kWh
Output Waste: Air	Argon	51614.73	kg
Output Waste: Water	Waste water	45162.89	kg
Output Waste: Solid	N-type material (Landfill after treatment)	477.38	kg
Transport Distance	Distance involved	100.00	miles
		314.59	ton-km

4.4.4. *SK-2 Module*

Tables A-39 and A-40 provide the respective inventory details for recovery, reprocessing and reuse of p- and n-type legs of SK-2 module.

Table A-39: Inventory details for recycling of p-type legs (SK-2 module)

Type of Parameter	Parameter	Value	Unit
Output Material	P-type TE Leg - Powder - Recycled (Step 1)	1000.00	kg
Input Materials	P-type TE Leg - Original	1278.50	kg
	Argon (Step 2)	50486.06	kg
	Water	44175.30	kg
Input Energy	Electricity (Step 1)	328.83	kWh
	Electricity (Step 2)	10517.93	kWh

Output Waste: Air	Argon	50486.06	kg
Output Waste: Water	Waste water	44175.30	kg
Output Waste: Solid	P-type material (Landfill after treatment)	278.50	kg
Transport Distance	Distance involved	100.00	miles
		250.57	ton-km

Table A-40: Inventory details for recycling of n-type legs (SK-2 module)

Type of Parameter	**Parameter**	**Value**	**Unit**
Output Material	N-type TE Leg Material - Recycled (Step 1)	1000.00	kg
Input Materials	N-type TE Leg - Original	1278.50	kg
	Argon (Step 2)	54752.20	kg
	Water	47908.17	kg
Input Energy	Electricity (Step 1)	359.15	kWh
	Electricity (Step 2)	11406.71	kWh
Output Waste: Air	Argon	54752.20	kg
Output Waste: Water	Waste water	47908.17	kg
Output Waste: Solid	N-type material (Landfill after treatment)	278.50	kg
Transport Distance	Distance involved	100.00	miles
		250.57	ton-km

4.4.5. *HH Module*

Tables A-41 and A-42 provide the respective inventory details for recovery, reprocessing and reuse of p- and n-type legs of HH module.

Table A-41: Inventory details for recycling of p-type legs (HH module)

Type of Parameter	Parameter	Value	Unit
Output Material	P-type TE Leg - Powder - Recycled (Step 1)	1000.00	kg
Input Materials	P-type TE Leg - Original	2216.07	kg
	Argon (Step 2)	42154.46	kg
	Water	36885.15	kg
Input Energy	Electricity (Step 1)	2596.42	kWh
	Electricity (Step 2)	8782.18	kWh
Output Waste: Air	Argon	42154.46	kg
Output Waste: Water	Waste water	36885.15	kg
Output Waste: Solid	P-type material (Landfill after treatment)	1216.07	kg
Transport Distance	Distance involved	100.00	miles
		552.35	ton-km

Table A-42: Inventory details for recycling of n-type legs (HH module)

Type of Parameter	Parameter	Value	Unit
Output Material	N-type TE Leg Material - Recycled (Step 1)	1000.00	kg
Input Materials	N-type TE Leg - Original	2216.07	kg
	Argon (Step 2)	43038.83	kg
	Water	37658.98	kg
Input Energy	Electricity (Step 1)	2656.94	kWh
	Electricity (Step 2)	8966.42	kWh
Output Waste: Air	Argon	43038.83	kg
Output Waste: Water	Waste water	37658.98	kg
Output Waste: Solid	N-type material (Landfill after treatment)	1216.07	kg

Transport Distance	Distance involved	100.00	miles
		552.35	ton-km

4.4.6. *PT Module*

Tables A-43 and A-44 provide the respective inventory details for recovery, reprocessing and reuse of p- and n-type legs of PT module.

Table A-43: Inventory details for recycling of p-type legs (PT module)

Type of Parameter	**Parameter**	**Value**	**Unit**
Output Material	P-type TE Leg - Powder - Recycled (Step 1)	1000.00	kg
Input Materials	P-type TE Leg - Original	1749.78	kg
	Argon (Step 2)	47507.93	kg
	Water	41569.44	kg
Input Energy	Electricity (Step 1)	11110.30	kWh
	Electricity (Step 2)	9897.49	kWh
Output Waste: Air	Argon	47507.93	kg
Output Waste: Water	Waste water	41569.44	kg
Output Waste: Solid	P-type material (Landfill after treatment)	749.78	kg
Transport Distance	Distance involved	100.00	miles
		402.26	ton-km

Table A-44: Inventory details for recycling of n-type legs (PT module)

Type of Parameter	**Parameter**	**Value**	**Unit**
Output Material	N-type TE Leg Material - Recycled (Step 1)	1000.00	kg
Input Materials	N-type TE Leg - Original	1762.93	kg
	Argon (Step 2)	48947.49	kg

	Water	42829.05	kg
Input Energy	Electricity (Step 1)	11479.69	kWh
	Electricity (Step 2)	10197.39	kWh
Output Waste: Air	Argon	48947.49	kg
Output Waste: Water	Waste water	42829.05	kg
Output Waste: Solid	N-type material (Landfill after treatment)	762.93	kg
Transport Distance	Distance involved	100.00	miles
		406.50	ton-km

4.4.7. *SC Module*

Tables A-45 and A-46 provide the respective inventory details for recovery, reprocessing and reuse of p- and n-type legs of SC module.

Table A-45: Inventory details for recycling of p-type legs (SC module)

Type of Parameter	**Parameter**	**Value**	**Unit**
Output Material	P-type TE Leg - Powder - Recycled (Step 1)	1000.00	kg
Input Materials	P-type TE Leg - Original	1300.73	kg
	Argon (Step 2)	70343.42	kg
	Water	61550.50	kg
Input Energy	Electricity (Step 1)	2698.33	kWh
	Electricity (Step 2)	14654.88	kWh
Output Waste: Air	Argon	70343.42	kg
Output Waste: Water	Waste water	61550.50	kg
Output Waste: Solid	P-type material (Landfill after treatment)	300.73	kg
Transport Distance	Distance involved	100.00	miles

		257.73	ton-km

Table A-46: Inventory details for recycling of n-type legs (SC module)

Type of Parameter	Parameter	Value	Unit
Output Material	N-type TE Leg Material - Recycled (Step 1)	1000.00	kg
Input Materials	N-type TE Leg - Original	1300.73	kg
	Argon (Step 2)	120052.59	kg
	Water	105046.02	kg
Input Energy	Electricity (Step 1)	4726.55	kWh
	Electricity (Step 2)	25010.96	kWh
Output Waste: Air	Argon	120052.59	kg
Output Waste: Water	Waste water	105046.02	kg
Output Waste: Solid	N-type material (Landfill after treatment)	300.73	kg
Transport Distance	Distance involved	100.00	miles
		257.73	ton-km

5. *Modules: Life cycle Environmental Impacts (D-scenario)*

Tables A-47–A-53 show the characterized impacts of all TE modules (per module set) that utilize 1000 W of input heat power for conversion to electricity, for the D-scenario, segregated by contributions of different life cycle stages.

Table A-47: Characterized impacts of BT-1 module for D-scenario

Impact category	Unit	Production	Use	EOL	Total
GW	kg CO_2 eq	0.05	-1.21	1.93×10^{-6}	-1.16
TET	kg 1,4-DCB	0.22	-0.23	4.67×10^{-6}	-0.01

FET	kg 1,4-DCB	4.20×10^{-3}	-2.04×10^{-2}	2.13×10^{-8}	-1.62×10^{-2}
MET	kg 1,4-DCB	0.01	-0.03	3.45×10^{-8}	-0.02
HCT	kg 1,4-DCB	2.10×10^{-3}	-4.95×10^{-2}	6.14×10^{-8}	-4.74×10^{-2}
HNT	kg 1,4-DCB	0.15	-0.59	7.62×10^{-7}	-0.44
MRS	kg Cu eq	5.69×10^{-4}	-4.88×10^{-4}	5.22×10^{-9}	8.14×10^{-5}
FRS	kg oil eq	1.25×10^{-2}	-2.75×10^{-1}	7.78×10^{-7}	-2.62×10^{-1}

Table A-48: Characterized impacts of BT-2 module for D-scenario

Impact category	**Unit**	**Production**	**Use**	**EOL**	**Total**
GW	kg CO_2 eq	0.04	-1.21	8.69×10^{-7}	-1.17
TET	kg 1,4-DCB	0.03	-0.23	2.10×10^{-6}	-0.20
FET	kg 1,4-DCB	7.34×10^{-4}	-2.04×10^{-2}	9.56×10^{-9}	-1.97×10^{-2}
MET	kg 1,4-DCB	1.32×10^{-3}	-0.03	1.55×10^{-8}	-0.03
HCT	kg 1,4-DCB	1.30×10^{-3}	-4.95×10^{-2}	2.76×10^{-8}	-4.82×10^{-2}
HNT	kg 1,4-DCB	0.02	-0.59	3.42×10^{-7}	-0.57
MRS	kg Cu eq	7.60×10^{-5}	-4.88×10^{-4}	2.35×10^{-9}	-4.12×10^{-4}
FRS	kg oil eq	1.14×10^{-2}	-2.75×10^{-1}	3.50×10^{-7}	-2.63×10^{-1}

Table A-49: Characterized impacts of SK-1 module for D-scenario

Impact category	**Unit**	**Production**	**Use**	**EOL**	**Total**
GW	kg CO_2 eq	0.04	-1.21	1.50×10^{-6}	-1.17
TET	kg 1,4-DCB	0.03	-0.23	3.62×10^{-6}	-0.21
FET	kg 1,4-DCB	3.80×10^{-3}	-2.04×10^{-2}	1.65×10^{-8}	-1.66×10^{-2}
MET	kg 1,4-DCB	0.01	-0.03	2.68×10^{-8}	-0.02
HCT	kg 1,4-DCB	1.82×10^{-3}	-4.95×10^{-2}	4.76×10^{-8}	-4.77×10^{-2}
HNT	kg 1,4-DCB	0.13	-0.59	5.90×10^{-7}	-0.46
MRS	kg Cu eq	1.15×10^{-4}	-4.88×10^{-4}	4.05×10^{-9}	-3.73×10^{-4}

FRS	kg oil eq	1.03×10^{-2}	-2.75×10^{-1}	6.03×10^{-7}	-2.65×10^{-1}

Table A-50: Characterized impacts of SK-2 module for D-scenario

Impact category	**Unit**	**Production**	**Use**	**EOL**	**Total**
GW	kg CO_2 eq	0.04	-1.21	1.40×10^{-6}	-1.17
TET	kg 1,4-DCB	0.03	-0.23	3.38×10^{-6}	-0.20
FET	kg 1,4-DCB	5.28×10^{-3}	-2.04×10^{-2}	1.54×10^{-8}	-1.51×10^{-2}
MET	kg 1,4-DCB	0.01	-0.03	2.50×10^{-8}	-0.02
HCT	kg 1,4-DCB	2.08×10^{-3}	-4.95×10^{-2}	4.45×10^{-8}	-4.74×10^{-2}
HNT	kg 1,4-DCB	0.18	-0.59	5.51×10^{-7}	-0.41
MRS	kg Cu eq	1.74×10^{-4}	-4.88×10^{-4}	3.78×10^{-9}	-3.15×10^{-4}
FRS	kg oil eq	9.97×10^{-3}	-2.75×10^{-1}	5.63×10^{-7}	-2.65×10^{-1}

Table A-51: Characterized impacts of HH module for D-scenario

Impact category	**Unit**	**Production**	**Use**	**EOL**	**Total**
GW	kg CO_2 eq	0.01	-1.21	2.82×10^{-7}	-1.21
TET	kg 1,4-DCB	4.58×10^{-3}	-0.23	6.81×10^{-7}	-0.23
FET	kg 1,4-DCB	1.96×10^{-4}	-2.04×10^{-2}	3.10×10^{-9}	-2.02×10^{-2}
MET	kg 1,4-DCB	3.01×10^{-4}	-0.03	5.03×10^{-9}	-0.03
HCT	kg 1,4-DCB	1.94×10^{-4}	-4.95×10^{-2}	8.96×10^{-9}	-4.93×10^{-2}
HNT	kg 1,4-DCB	0.01	-0.59	1.11×10^{-7}	-0.58
MRS	kg Cu eq	4.89×10^{-5}	-4.88×10^{-4}	7.61×10^{-10}	-4.39×10^{-4}
FRS	kg oil eq	1.34×10^{-3}	-2.75×10^{-1}	1.13×10^{-7}	-2.74×10^{-1}

Table A-52: Characterized impacts of PT module for D-scenario

Impact category	**Unit**	**Production**	**Use**	**EOL**	**Total**

GW	kg CO_2 eq	0.01	-1.21	4.88×10^{-7}	-1.20
TET	kg 1,4-DCB	0.01	-0.23	1.18×10^{-6}	-0.22
FET	kg 1,4-DCB	1.21×10^{-4}	-2.04×10^{-2}	5.37×10^{-9}	-2.03×10^{-2}
MET	kg 1,4-DCB	2.26×10^{-4}	-0.03	8.72×10^{-9}	-0.03
HCT	kg 1,4-DCB	2.57×10^{-4}	-4.95×10^{-2}	1.55×10^{-8}	-4.92×10^{-2}
HNT	kg 1,4-DCB	3.74×10^{-3}	-0.59	1.92×10^{-7}	-0.59
MRS	kg Cu eq	4.20×10^{-5}	-4.88×10^{-4}	1.32×10^{-9}	-4.46×10^{-4}
FRS	kg oil eq	2.22×10^{-3}	-2.75×10^{-1}	1.96×10^{-7}	-2.73×10^{-1}

Table A-53: Characterized impacts of SC module for D-scenario

Impact category	**Unit**	**Production**	**Use**	**EOL**	**Total**
GW	kg CO_2 eq	0.02	-1.21	8.42×10^{-7}	-1.20
TET	kg 1,4-DCB	0.02	-0.23	2.03×10^{-6}	-0.21
FET	kg 1,4-DCB	1.00×10^{-3}	-2.04×10^{-2}	9.26×10^{-9}	-1.94×10^{-2}
MET	kg 1,4-DCB	1.49×10^{-3}	-0.03	1.50×10^{-8}	-0.03
HCT	kg 1,4-DCB	1.54×10^{-3}	-4.95×10^{-2}	2.68×10^{-8}	-4.79×10^{-2}
HNT	kg 1,4-DCB	0.03	-0.59	3.32×10^{-7}	-0.56
MRS	kg Cu eq	1.67×10^{-3}	-4.88×10^{-4}	2.27×10^{-9}	1.18×10^{-3}
FRS	kg oil eq	4.01×10^{-3}	-2.75×10^{-1}	3.39×10^{-7}	-2.71×10^{-1}

6. EOL Scenarios: A Comparison

Figures A.2–A.6 compare the ecological performance of all modules barring HH and SC under the three EOL scenarios, while Tables A-54–A-60 and A-61–A-67 show the characterized impacts of the modules under P- and CE-scenario respectively.

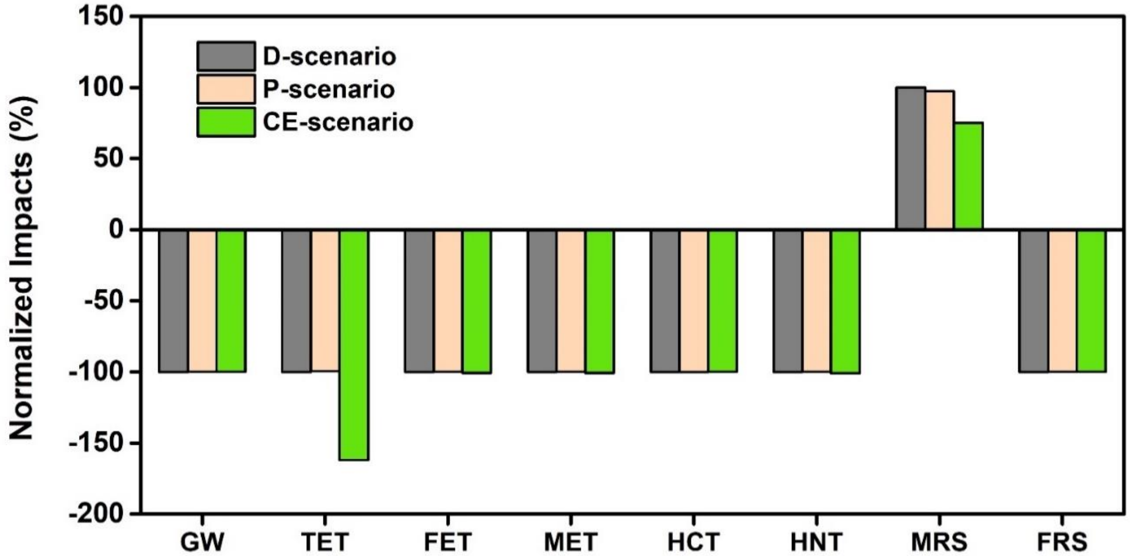

Figure A.2: Life cycle environmental impacts of BT-1 module under different EOL scenarios (normalized to impact under baseline D-scenario)

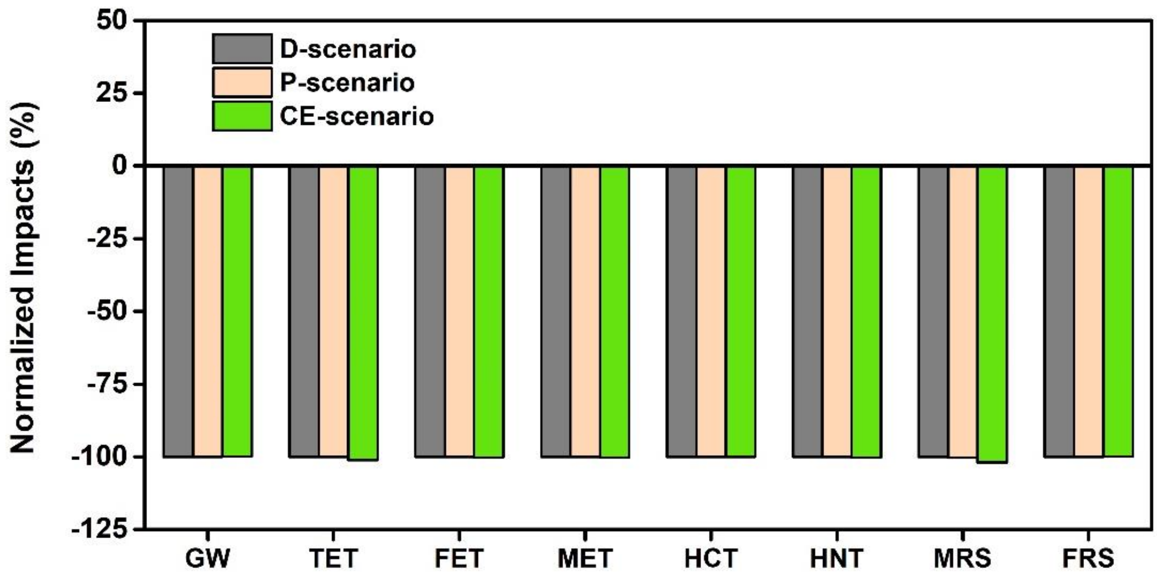

Figure A.3: Life cycle environmental impacts of BT-2 module under different EOL scenarios (normalized to impact under baseline D-scenario)

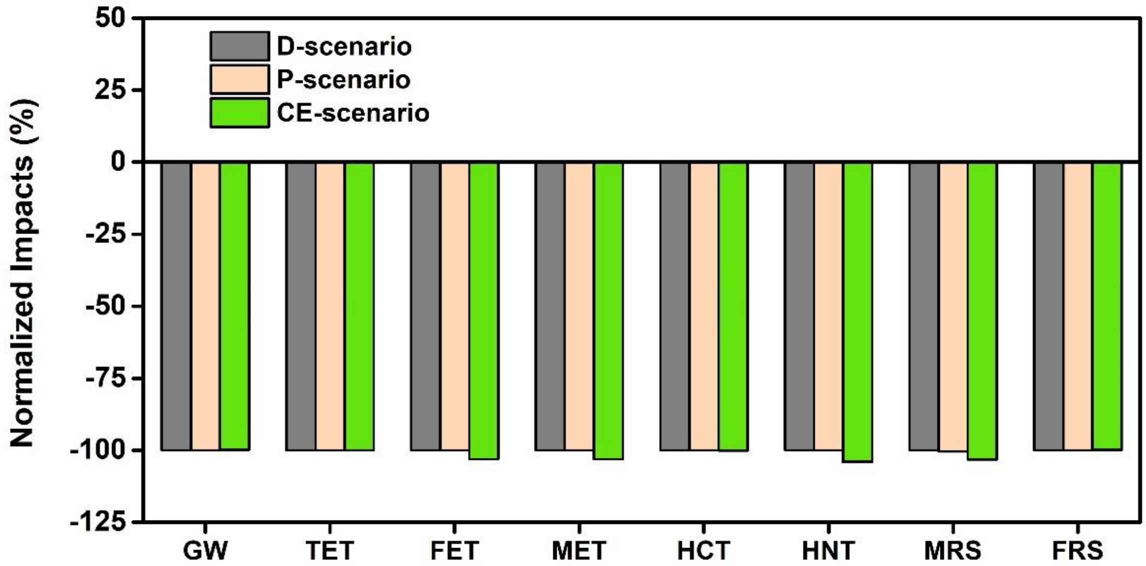

Figure A.4: Life cycle environmental impacts of SK-1 module under different EOL scenarios (normalized to impact under baseline D-scenario)

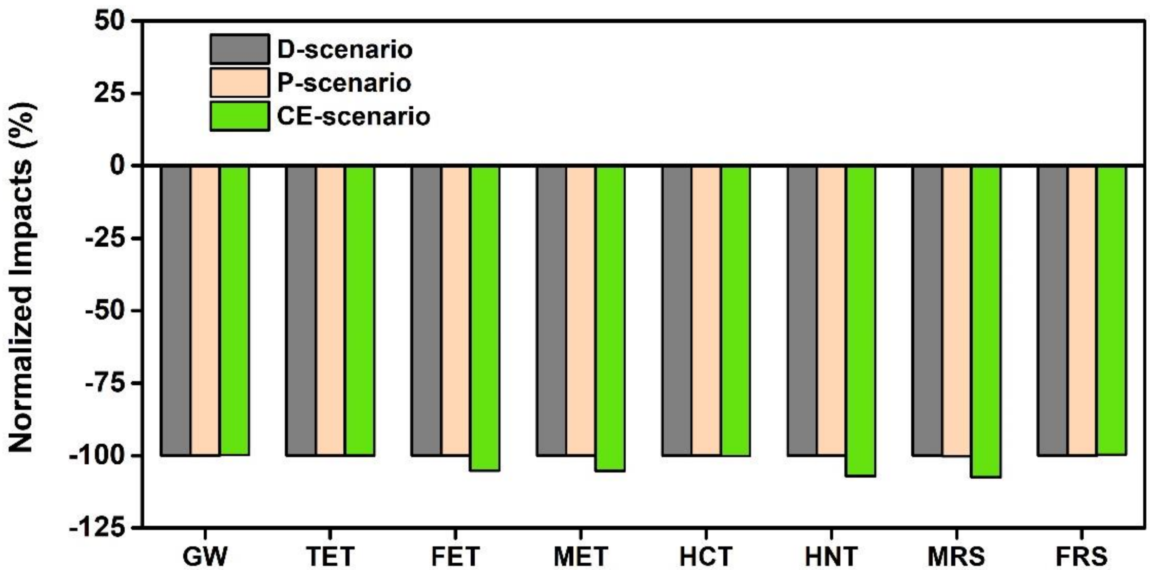

Figure A.5: Life cycle environmental impacts of SK-2 module under different EOL scenarios (normalized to impact under baseline D-scenario)

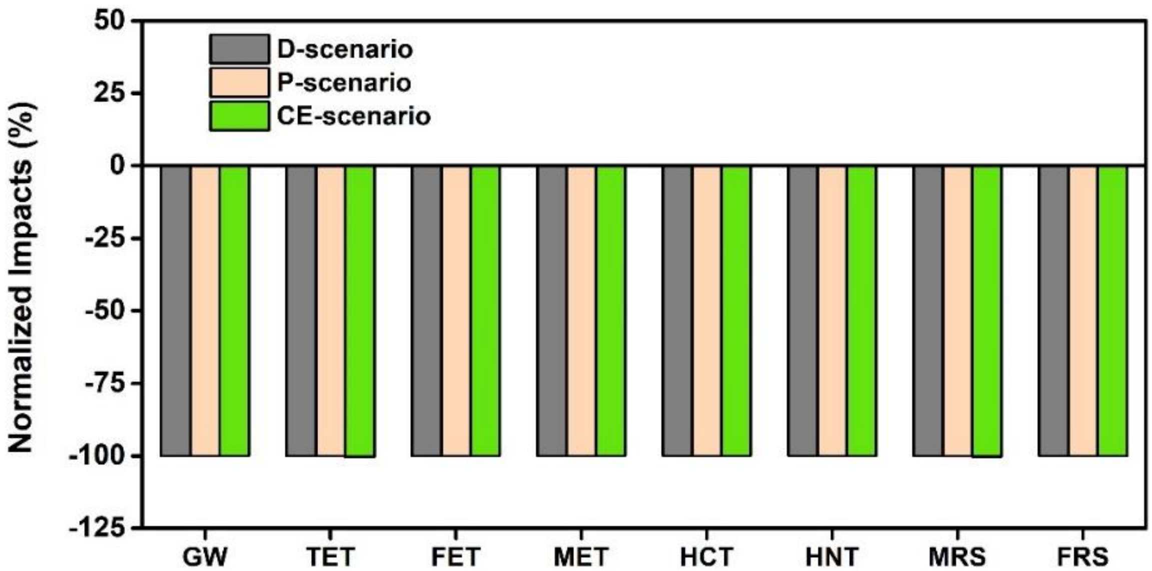

Figure A.6: Life cycle environmental impacts of PT module under different EOL scenarios (normalized to impact under baseline D-scenario)

6.1. P-Scenario

Table A-54: Characterized impacts of BT-1 module for P-scenario

Impact category	Unit	Production	Use	EOL	Total
GW	kg CO_2 eq	0.05	-1.21	2.40×10^{-4}	-1.16
TET	kg 1,4-DCB	0.22	-0.23	4.70×10^{-5}	-0.01
FET	kg 1,4-DCB	4.20×10^{-3}	-2.04×10^{-2}	1.83×10^{-6}	-1.62×10^{-2}
MET	kg 1,4-DCB	0.01	-0.03	4.44×10^{-6}	-0.02
HCT	kg 1,4-DCB	2.10×10^{-3}	-4.95×10^{-2}	-2.91×10^{-7}	-4.74×10^{-2}
HNT	kg 1,4-DCB	0.15	-0.59	6.87×10^{-5}	-0.44
MRS	kg Cu eq	5.69×10^{-4}	-4.88×10^{-4}	-2.06×10^{-6}	7.93×10^{-5}
FRS	kg oil eq	1.25×10^{-2}	-2.75×10^{-1}	6.44×10^{-5}	-2.62×10^{-1}

Table A-55: Characterized impacts of BT-2 module for P-scenario

Impact category	Unit	Production	Use	EOL	Total
GW	kg CO_2 eq	0.04	-1.21	1.43×10^{-4}	-1.17
TET	kg 1,4-DCB	0.03	-0.23	2.74×10^{-5}	-0.20
FET	kg 1,4-DCB	7.34×10^{-4}	-2.04×10^{-2}	1.09×10^{-6}	-1.97×10^{-2}
MET	kg 1,4-DCB	1.32×10^{-3}	-0.03	2.65×10^{-6}	-0.03
HCT	kg 1,4-DCB	1.30×10^{-3}	-4.95×10^{-2}	-1.83×10^{-7}	-4.82×10^{-2}
HNT	kg 1,4-DCB	0.02	-0.59	4.09×10^{-5}	-0.57
MRS	kg Cu eq	7.60×10^{-5}	-4.88×10^{-4}	-1.23×10^{-6}	-4.13×10^{-4}
FRS	kg oil eq	1.14×10^{-2}	-2.75×10^{-1}	3.84×10^{-5}	-2.63×10^{-1}

Table A-56: Characterized impacts of SK-1 module for P-scenario

Impact category	Unit	Production	Use	EOL	Total
GW	kg CO_2 eq	0.04	-1.21	1.86×10^{-4}	-1.17
TET	kg 1,4-DCB	0.03	-0.23	3.64×10^{-5}	-0.21
FET	kg 1,4-DCB	3.80×10^{-3}	-2.04×10^{-2}	1.42×10^{-6}	-1.66×10^{-2}
MET	kg 1,4-DCB	0.01	-0.03	3.44×10^{-6}	-0.02
HCT	kg 1,4-DCB	1.82×10^{-3}	-4.95×10^{-2}	-2.25×10^{-7}	-4.77×10^{-2}
HNT	kg 1,4-DCB	0.13	-0.59	5.32×10^{-5}	-0.46
MRS	kg Cu eq	1.15×10^{-4}	-4.88×10^{-4}	-1.60×10^{-6}	-3.75×10^{-4}
FRS	kg oil eq	1.03×10^{-2}	-2.75×10^{-1}	4.99×10^{-5}	-2.65×10^{-1}

Table A-57: Characterized impacts of SK-2 module for P-scenario

Impact category	Unit	Production	Use	EOL	Total
GW	kg CO_2 eq	0.04	-1.21	8.35×10^{-5}	-1.17
TET	kg 1,4-DCB	0.03	-0.23	1.80×10^{-5}	-0.20

FET	kg 1,4-DCB	5.28×10^{-3}	-2.04×10^{-2}	6.39×10^{-7}	-1.51×10^{-2}
MET	kg 1,4-DCB	0.01	-0.03	1.54×10^{-6}	-0.02
HCT	kg 1,4-DCB	2.08×10^{-3}	-4.95×10^{-2}	-7.67×10^{-8}	-4.74×10^{-2}
HNT	kg 1,4-DCB	0.18	-0.59	2.39×10^{-5}	-0.41
MRS	kg Cu eq	1.74×10^{-4}	-4.88×10^{-4}	-7.08×10^{-7}	-3.15×10^{-4}
FRS	kg oil eq	9.97×10^{-3}	-2.75×10^{-1}	2.25×10^{-5}	-2.65×10^{-1}

Table A-58: Characterized impacts of HH module for P-scenario

Impact category	Unit	Production	Use	EOL	Total
GW	kg CO_2 eq	0.01	-1.21	3.76×10^{-5}	-1.21
TET	kg 1,4-DCB	4.58×10^{-3}	-0.23	7.31×10^{-6}	-0.23
FET	kg 1,4-DCB	1.96×10^{-4}	-2.04×10^{-2}	2.86×10^{-7}	-2.02×10^{-2}
MET	kg 1,4-DCB	3.01×10^{-4}	-0.03	6.94×10^{-7}	-0.03
HCT	kg 1,4-DCB	1.94×10^{-4}	-4.95×10^{-2}	-4.61×10^{-8}	-4.93×10^{-2}
HNT	kg 1,4-DCB	0.01	-0.59	1.07×10^{-5}	-0.58
MRS	kg Cu eq	4.89×10^{-5}	-4.88×10^{-4}	-3.22×10^{-7}	-4.40×10^{-4}
FRS	kg oil eq	1.34×10^{-3}	-2.75×10^{-1}	1.01×10^{-5}	-2.74×10^{-1}

Table A-59: Characterized impacts of PT module for P-scenario

Impact category	Unit	Production	Use	EOL	Total
GW	kg CO_2 eq	0.01	-1.21	6.40×10^{-5}	-1.20
TET	kg 1,4-DCB	0.01	-0.23	1.25×10^{-6}	-0.22
FET	kg 1,4-DCB	1.21×10^{-4}	-2.04×10^{-2}	4.88×10^{-7}	-2.03×10^{-2}
MET	kg 1,4-DCB	2.26×10^{-4}	-0.03	1.18×10^{-6}	-0.03
HCT	kg 1,4-DCB	2.57×10^{-4}	-4.95×10^{-2}	-7.83×10^{-8}	-4.92×10^{-2}
HNT	kg 1,4-DCB	3.74×10^{-3}	-0.59	1.83×10^{-5}	-0.59
MRS	kg Cu eq	4.20×10^{-5}	-4.88×10^{-4}	-5.49×10^{-7}	-4.47×10^{-4}

FRS	kg oil eq	2.22×10^{-3}	-2.75×10^{-1}	1.72×10^{-5}	-2.73×10^{-1}

Table A-60: Characterized impacts of SC module for P-scenario

Impact category	Unit	Production	Use	EOL	Total
GW	kg CO_2 eq	0.02	-1.21	9.53×10^{-5}	-1.20
TET	kg 1,4-DCB	0.02	-0.23	1.88×10^{-5}	-0.21
FET	kg 1,4-DCB	1.00×10^{-3}	-2.04×10^{-2}	7.27×10^{-7}	-1.94×10^{-2}
MET	kg 1,4-DCB	1.49×10^{-3}	-0.03	1.76×10^{-6}	-0.03
HCT	kg 1,4-DCB	1.54×10^{-3}	-4.95×10^{-2}	-1.13×10^{-7}	-4.79×10^{-2}
HNT	kg 1,4-DCB	0.03	-0.59	2.72×10^{-5}	-0.56
MRS	kg Cu eq	1.67×10^{-3}	-4.88×10^{-4}	-8.16×10^{-7}	1.18×10^{-3}
FRS	kg oil eq	4.01×10^{-3}	-2.75×10^{-1}	2.56×10^{-5}	-2.71×10^{-1}

6.2. CE-Scenario

Table A-61: Characterized impacts of BT-1 module for CE-scenario

Impact category	Unit	Production	Use	EOL	Total
GW	kg CO_2 eq	0.05	-1.21	1.71×10^{-3}	-1.16
TET	kg 1,4-DCB	0.22	-0.23	-6.07×10^{-3}	-0.01
FET	kg 1,4-DCB	4.20×10^{-3}	-2.04×10^{-2}	-9.67×10^{-5}	-1.63×10^{-2}
MET	kg 1,4-DCB	0.01	-0.03	-1.37×10^{-4}	-0.02
HCT	kg 1,4-DCB	2.10×10^{-3}	-4.95×10^{-2}	3.26×10^{-5}	-4.73×10^{-2}
HNT	kg 1,4-DCB	0.15	-0.59	-3.93×10^{-3}	-0.45
MRS	kg Cu eq	5.69×10^{-4}	-4.88×10^{-4}	-2.03×10^{-5}	6.11×10^{-5}
FRS	kg oil eq	1.25×10^{-2}	-2.75×10^{-1}	4.22×10^{-4}	-2.62×10^{-1}

Table A-62: Characterized impacts of BT-2 module for CE-scenario

Impact category	Unit	Production	Use	EOL	Total
GW	kg CO_2 eq	0.04	-1.21	6.82×10^{-4}	-1.17
TET	kg 1,4-DCB	0.03	-0.23	-2.22×10^{-3}	-0.20
FET	kg 1,4-DCB	7.34×10^{-4}	-2.04×10^{-2}	-3.51×10^{-5}	-1.97×10^{-2}
MET	kg 1,4-DCB	1.32×10^{-3}	-0.03	-4.91×10^{-5}	-0.03
HCT	kg 1,4-DCB	1.30×10^{-3}	-4.95×10^{-2}	1.19×10^{-5}	-4.82×10^{-2}
HNT	kg 1,4-DCB	0.02	-0.59	-1.43×10^{-3}	-0.57
MRS	kg Cu eq	7.60×10^{-5}	-4.88×10^{-4}	-7.92×10^{-6}	-4.20×10^{-4}
FRS	kg oil eq	1.14×10^{-2}	-2.75×10^{-1}	1.69×10^{-4}	-2.63×10^{-1}

Table A-63: Characterized impacts of SK-1 module for CE-scenario

Impact category	Unit	Production	Use	EOL	Total
GW	kg CO_2 eq	0.04	-1.21	1.72×10^{-3}	-1.17
TET	kg 1,4-DCB	0.03	-0.23	-9.08×10^{-5}	-0.21
FET	kg 1,4-DCB	3.80×10^{-3}	-2.04×10^{-2}	-5.10×10^{-4}	-1.71×10^{-2}
MET	kg 1,4-DCB	0.01	-0.03	-7.11×10^{-4}	-0.02
HCT	kg 1,4-DCB	1.82×10^{-3}	-4.95×10^{-2}	-4.88×10^{-5}	-4.77×10^{-2}
HNT	kg 1,4-DCB	0.13	-0.59	-1.85×10^{-2}	-0.48
MRS	kg Cu eq	1.15×10^{-4}	-4.88×10^{-4}	-1.20×10^{-5}	-3.85×10^{-4}
FRS	kg oil eq	1.03×10^{-2}	-2.75×10^{-1}	4.31×10^{-4}	-2.64×10^{-1}

Table A-64: Characterized impacts of SK-2 module for CE-scenario

Impact category	Unit	Production	Use	EOL	Total
GW	kg CO_2 eq	0.04	-1.21	2.56×10^{-3}	-1.17
TET	kg 1,4-DCB	0.03	-0.23	-1.43×10^{-5}	-0.20

FET	kg 1,4-DCB	5.28×10^{-3}	-2.04×10^{-2}	-7.91×10^{-4}	-1.59×10^{-2}
MET	kg 1,4-DCB	0.01	-0.03	-1.10×10^{-3}	-0.02
HCT	kg 1,4-DCB	2.08×10^{-3}	-4.95×10^{-2}	-7.14×10^{-5}	-4.75×10^{-2}
HNT	kg 1,4-DCB	0.18	-0.59	-0.03	-0.43
MRS	kg Cu eq	1.74×10^{-4}	-4.88×10^{-4}	-2.35×10^{-5}	-3.38×10^{-4}
FRS	kg oil eq	9.97×10^{-3}	-2.75×10^{-1}	6.45×10^{-4}	-2.64×10^{-1}

Table A-65: Characterized impacts of HH module for CE-scenario

Impact category	**Unit**	**Production**	**Use**	**EOL**	**Total**
GW	kg CO_2 eq	0.01	-1.21	1.02×10^{-4}	-1.21
TET	kg 1,4-DCB	4.58×10^{-3}	-0.23	-1.52×10^{-4}	-0.23
FET	kg 1,4-DCB	1.96×10^{-4}	-2.04×10^{-2}	-1.14×10^{-5}	-2.02×10^{-2}
MET	kg 1,4-DCB	3.01×10^{-4}	-0.03	-1.58×10^{-5}	-0.03
HCT	kg 1,4-DCB	1.94×10^{-4}	-4.95×10^{-2}	-7.75×10^{-7}	-4.93×10^{-2}
HNT	kg 1,4-DCB	0.01	-0.59	4.35×10^{-4}	-0.58
MRS	kg Cu eq	4.89×10^{-5}	-4.88×10^{-4}	-4.90×10^{-6}	-4.44×10^{-4}
FRS	kg oil eq	1.34×10^{-3}	-2.75×10^{-1}	2.62×10^{-5}	-2.74×10^{-1}

Table A-66: Characterized impacts of PT module for CE-scenario

Impact category	**Unit**	**Production**	**Use**	**EOL**	**Total**
GW	kg CO_2 eq	0.01	-1.21	2.95×10^{-4}	-1.20
TET	kg 1,4-DCB	0.01	-0.23	-6.82×10^{-4}	-0.22
FET	kg 1,4-DCB	1.21×10^{-4}	-2.04×10^{-2}	-1.02×10^{-6}	-2.03×10^{-2}
MET	kg 1,4-DCB	2.26×10^{-4}	-0.03	-1.27×10^{-6}	-0.03
HCT	kg 1,4-DCB	2.57×10^{-4}	-4.95×10^{-2}	7.10×10^{-6}	-4.92×10^{-2}
HNT	kg 1,4-DCB	3.74×10^{-3}	-0.59	-1.07×10^{-4}	-0.59
MRS	kg Cu eq	4.20×10^{-5}	-4.88×10^{-4}	-1.13×10^{-6}	-4.47×10^{-4}

FRS	kg oil eq	2.22×10^{-3}	-2.75×10^{-1}	7.51×10^{-5}	-2.73×10^{-1}

Table A-67: Characterized impacts of SC module for CE-scenario

Impact category	Unit	Production	Use	EOL	Total
GW	kg CO_2 eq	0.02	-1.21	1.98×10^{-3}	-1.19
TET	kg 1,4-DCB	0.02	-0.23	-6.28×10^{-4}	-0.21
FET	kg 1,4-DCB	1.00×10^{-3}	-2.04×10^{-2}	-7.02×10^{-5}	-1.95×10^{-2}
MET	kg 1,4-DCB	1.49×10^{-3}	-0.03	-1.00×10^{-4}	-0.03
HCT	kg 1,4-DCB	1.54×10^{-3}	-4.95×10^{-2}	-7.81×10^{-5}	-4.80×10^{-2}
HNT	kg 1,4-DCB	0.03	-0.59	-3.02×10^{-3}	-0.56
MRS	kg Cu eq	1.67×10^{-3}	-4.88×10^{-4}	-2.33×10^{-4}	9.49×10^{-4}
FRS	kg oil eq	4.01×10^{-3}	-2.75×10^{-1}	4.83×10^{-4}	-2.70×10^{-1}

7. Thermoelectrics vs Renewables

In order to estimate the ecofriendly potential of thermoelectrics vis-à-vis existing renewable energy technologies, ecological performance of chosen TE modules in this study is compared with that of two established renewable energy forms: solar- and wind-based electricity. Table A-68 shows the performance of the seven modules (under base EOL scenario) as well as these two renewable energy technologies, all of which replace coal-based electricity, for the sake of common comparison. To enable like-for-like comparison, all sources of energy used are considered on per-kWh basis, with solar or wind-based electricity replacing 1 kWh of their coal-based counterpart at the plant-level. Also, all solar- and wind-based figures are based on the US grid, as this study assumes the production of thermoelectrics inside the United States.

Table A-68: Life cycle performance of thermoelectrics vs renewables

Impact category	BT-1	BT-2	SK-1	SK-2	HH	PT	SC	SBE	WBE

GW	-1.16	-1.17	-1.17	-1.17	-1.21	-1.20	-1.20	-1.15	-1.20
TET	-0.01	-0.20	-0.21	-0.20	-0.23	-0.22	-0.21	1.13	-0.10
FET	-0.02	-0.02	-0.02	-0.02	-0.02	-0.02	-0.02	-0.02	-0.02
MET	-0.02	-0.03	-0.02	-0.02	-0.03	-0.03	-0.03	-0.02	-0.03
HCT	-0.05	-0.05	-0.05	-0.05	-0.05	-0.05	-0.05	-0.04	-0.05
HNT	-0.44	-0.57	-0.46	-0.41	-0.58	-0.59	-0.56	-0.43	-0.56
MRS (values in $\times 10^{-4}$)	0.82	-4.12	-3.73	-3.15	-4.39	-4.46	1.18	5.72	8.21
FRS	-0.26	-0.26	-0.26	-0.27	-0.27	-0.27	-0.27	-0.26	-0.27
SBE: Solar-based electricity; WBE: Wind-based electricity									

APPENDIX-B

SUPPORTING INFORMATION FOR CHAPTER 4

B. Ecological Profile of Thermoelectrics for Periodic Waste Heat Emitting Applications

1. Introduction

For cradle-to-grave life cycle assessment (LCA) of thermoelectric (TE) modules used in a periodically waste heat generating application, this Appendix provides details on chosen modules and results on their characterized impacts. Information on inventory of the chosen modules is available in previous study (Chapter 3)[158].

2. Modules: Thermal Cycling

Since the application considered in this study (Chapter 4) involves thermal cycling that in turn reduces conversion efficiency of TE modules (explained in Chapter 2), data regarding such reduction in conversion efficiency with each thermal cycle – referred to as thermal cycling reduction coefficient (TCRC) – is important while evaluating the ecological credentials of this platform. However, as mentioned in Chapter 4, no TCRC data is available in literature for one of the aforementioned seven modules (PT), while for the other six modules, such data is not directly available. Instead, multiple studies report TCRC data for the four TE material systems that constitute these six modules, but under differing operational conditions. Hence, for each of these four systems, specific choices had to be made with regard to considering their TCRC for this study. These choices were primarily made based on the temperature range of operation considered in literature vis-à-vis that suitable for the given module of consideration. However, when appropriate, other factors were also considered. The following sub-sections highlight the final TCRC values chosen in this study, based on the values arrived at in literature.

2.1. TCRC: BT System

Five studies – two based on the same module – have been undertaken on evaluating trends for either or both of conversion efficiency and output power of BT modules over multiple thermal cycles[19,53,116,206,209]. Of these, four provide data on variation in either of thermoelectric figure of merit (ZT), conversion efficiency or output power of concerned BT module, while the fifth study[206] provides an equation for change in normalized conversion efficiency and output power with number of thermal cycles. Table B-1 provides the data on hot and cold side temperatures, as well as the TCRC for first four papers, while Table B-2 provides information on this equation and TCRC for the final fifth study.

Table B-1: Details regarding TCRC of BT systems in literature

Parameters	**Park et. al (2012)**[116]	**Hatzikraniotis et. al (2010)**[53]	**Barako et. al (2012, 2013)**[19,209]
Maximum hot side temperature (T_H, °C)	160	200	146
Minimum hot side temperature (T_H, °C)	30	30	-20
Cold side temperature (T_C, °C)	20	24	23
Time of cycling (mins) - per cycle	3	30	1
Number of cycles	6000	6000	-
Number of effective cycles for reduction	4000	6000	
Initial ZT	-	0.74	0.624
Final ZT	-	0.63	0.58, 0.0197
Initial Z	-	0.00247	-
Final Z	-	0.00211	-
Reduction in power (%)	11.00	14.00	-

Reduction in power (%) per cycle	0.0029	0.0025	-

Table B-2: Details regarding TCRC of BT modules in literature

Parameters	**Wang et. al (2019)**[206]
Equation for efficiency - Normalized	$\eta = 1 - (1.40 \times 10^{-6} \times \exp(2.93 \times \log_{10} N_{cycle})$
Equation for power - Normalized	$P_{output} = 1 - (7.24 \times 10^{-5} \times \exp(2.08 \times \log_{10} N_{cycle})$
Reduction in power (%) per cycle – based on equation (9125 cycles)	0.0035

Since TCRC was unavailable for the combination of two studies[19,209], this study was ignored. Further, of the remaining three studies, only two provide data on operational temperature range[53,116], both of which are not in sync with that used for the two BT modules considered in this work. Hence, the remaining study was chosen[206], in part as it showed the highest TCRC (i.e., the worst-case scenario among all five studies) for this module (0.0035 % per cycle; Table B-2).

2.2. TCRC: SK System

In contrast to BT modules, only two studies seek to evaluate the performance of SK modules/materials under thermal cycling[54,210]. Table B-3 provides data on operational temperature ranges and TCRC values computed using these studies. Since the temperature ranges of operation for first paper[54] were more in line with that optimal for the two SK modules considered here (Table B-3), and since this system shows a higher TCRC (i.e., taking into account the worst-case scenario) than the other study[210], it was considered for this LCA work (i.e., TCRC = 0.2216 % per cycle).

Table B-3: Details regarding TCRC of SK modules in literature

Parameters	Ochi et. al (2014)[54]	Biswas et. al (2012)[210]
Maximum hot side temperature (T_H, °C)	600	400
Minimum hot side temperature (T_H, °C)	200	50
Cold side temperature (T_C, °C)	40	30
Time of cycling (mins) - per cycle	120	45
Number of cycles	450	200
Number of effective cycles for reduction	450	200
Initial ZT	-	0.9
Final ZT	-	0.85
Initial efficiency (%)	-	7.45
Final efficiency (%)	-	7.16
Initial power (W)	29.5	7.45
Final power (W)	26.7	7.16
Reduction in power or power density (%)	9.49	3.94
Reduction in power (%) per cycle	0.0222	0.0201

2.3. TCRC: HH System

Four studies have sought to estimate the effect of thermal cycling on conversion efficiency of HH modules/materials/systems[159,211–213]. Table B-4 provides details on TCRC of HH material or system in these four studies. Of these, the first paper results in an extremely high TCRC (~ 0.033 % per cycle)[211], which is unlike the other three studies (TCRC: ~ 0.004-0.005 % per cycle)[159,212,213]. Hence, the first paper was ignored[211], while among the other studies, the fourth study was chosen as it shows the worst TCRC (0.005 % per cycle)[159] among the latter three studies.

Table B-4: Details regarding TCRC of HH modules in literature

Parameters	Jacques et. al (2018)[211]	Rausch et. al (2015)[212]	Joshi et. al (2014)[213]	Bartholomé et. al (2014)[159]
Maximum hot side temperature (T_H, °C)	600	700	600	-
Minimum hot side temperature (T_H, °C)	100	100	100	-
Cold side temperature (T_C, °C)	30	30	100	-
Time of cycling (mins) - per cycle	115	130	1	-
Number of cycles	110	500	1000	200
Number of effective cycles for reduction	110	500	1000	200
Initial power (W)	8.5	-	-	-
Final power (W)	8.2	-	-	-
Reduction in power or power density (%)	3.53	2.00	4.00	1.00
Reduction in power (%) per cycle	0.0327	0.0040	0.0041	0.0050

2.4. TCRC: SC System

Two studies have sought to analyze TE performance under thermal cycling for SC modules/materials. Table B-5 provides details on TCRC for this system under these two studies. Of these, the second paper was chosen, as its operational temperature range is in line with that for the SC module considered in this study.

Table B-5: Details regarding TCRC of SC modules in literature

Parameters	**Skomedal et. al (2016)**[214]	**Tarantik et. al (2015)**[207]
Maximum hot side temperature (T_H, °C)	450	550
Minimum hot side temperature (T_H, °C)	150	350
Cold side temperature (T_C, °C)	25	20
Time of cycling (mins) - per cycle	55	45
Number of cycles	160	100
Number of effective cycles for reduction	160	100
Initial power (W)	0.11	0.71
Final power (W)	0.07	0.7
Reduction in power or power density (%)	36.36	1.41
Reduction in power (%) per cycle	0.2821	0.0142

Thus, based on aforementioned choices, the final TCRC chosen for each module is provided in Table 2-5 and used for subsequent calculation.

3. Modules: Electricity Generation and Final Conversion Efficiency

Based on the TCRCs considered for chosen modules, total amount of electricity generated by each module set (by harvesting 1000 W of waste heat) in NG-based plant was calculated (Table B-6). For the sake of comparison, the amount of electricity produced by each of these module sets (from Chapter 3) is also provided.

Table B-6: Amount of electricity generated (in kWh) by each TE module set

Modules	**NG-based plant (Chapter 4)**	**Coal-based plant (Chapter 3)**
BT-1	1275.14	5361.12
BT-2	2187.74	9198.00
SK-1	1174.66	9855.00
SK-2	1143.33	9592.20
HH	1317.48	5913.00

SC	1310.22	8409.60

4. Modules: Life Cycle Environmental Impacts

4.1. D-Scenario

Tables B-7–B-12 show the characterized impacts of all TE modules (per module set) based on functional unit, segregated by contributions from individual life cycle stages.

Table B-7: Life cycle impacts of BT-1 module (D-scenario)

Impact category	Unit	Production	Use	EOL	Total
GW	kg CO_2 eq	0.20	-0.81	8.13×10^{-6}	-0.61
TET	kg 1,4-DCB	0.93	-0.03	1.96×10^{-5}	0.90
FET	kg 1,4-DCB	0.02	-2.01×10^{-4}	8.94×10^{-8}	0.02
MET	kg 1,4-DCB	0.03	-0.01	1.45×10^{-7}	0.01
HCT	kg 1,4-DCB	0.01	-2.11×10^{-3}	2.58×10^{-7}	0.01
HNT	kg 1,4-DCB	0.62	-0.01	3.20×10^{-6}	0.61
MRS	kg Cu eq	2.39×10^{-3}	-2.82×10^{-4}	2.20×10^{-8}	2.11×10^{-3}
FRS	kg oil eq	0.05	-0.23	3.27×10^{-6}	-0.18

Table B-8: Life cycle impacts of BT-2 module (D-scenario)

Impact category	Unit	Production	Use	EOL	Total
GW	kg CO_2 eq	0.19	-0.81	3.65×10^{-6}	-0.62
TET	kg 1,4-DCB	0.13	-0.03	8.82×10^{-6}	0.10
FET	kg 1,4-DCB	3.09×10^{-3}	-2.01×10^{-4}	4.02×10^{-8}	2.89×10^{-3}
MET	kg 1,4-DCB	0.01	-0.01	6.52×10^{-8}	-0.01
HCT	kg 1,4-DCB	5.48×10^{-3}	-2.11×10^{-3}	1.16×10^{-7}	3.37×10^{-3}
HNT	kg 1,4-DCB	0.10	-0.01	1.44×10^{-6}	0.09
MRS	kg Cu eq	3.20×10^{-4}	-2.82×10^{-4}	9.87×10^{-9}	3.80×10^{-5}
FRS	kg oil eq	0.05	-0.23	1.47×10^{-6}	-0.18

Table B-9: Life cycle impacts of SK-1 module (D-scenario)

Impact category	Unit	Production	Use	EOL	Total
GW	kg CO_2 eq	0.33	-0.81	1.26×10^{-5}	-0.47
TET	kg 1,4-DCB	0.21	-0.03	3.03×10^{-5}	0.18
FET	kg 1,4-DCB	0.03	-2.01×10^{-4}	1.38×10^{-7}	0.03
MET	kg 1,4-DCB	0.05	-0.01	2.24×10^{-7}	0.03
HCT	kg 1,4-DCB	0.02	-2.11×10^{-3}	3.99×10^{-7}	0.01
HNT	kg 1,4-DCB	1.10	-0.01	4.95×10^{-6}	1.09
MRS	kg Cu eq	9.64×10^{-4}	-2.82×10^{-4}	3.39×10^{-8}	6.28×10^{-4}
FRS	kg oil eq	0.09	-0.23	5.06×10^{-6}	-0.15

Table B-10: Life cycle impacts of SK-2 module (D-scenario)

Impact category	Unit	Production	Use	EOL	Total
GW	kg CO_2 eq	0.32	-0.81	1.17×10^{-5}	-0.48
TET	kg 1,4-DCB	0.24	-0.03	2.83×10^{-5}	0.21
FET	kg 1,4-DCB	0.04	-2.01×10^{-4}	1.29×10^{-7}	0.04
MET	kg 1,4-DCB	0.06	-0.01	2.10×10^{-7}	0.05
HCT	kg 1,4-DCB	0.02	-2.11×10^{-3}	3.73×10^{-7}	0.02
HNT	kg 1,4-DCB	1.54	-0.01	4.62×10^{-6}	1.53
MRS	kg Cu eq	1.46×10^{-3}	-2.82×10^{-4}	3.17×10^{-8}	1.18×10^{-3}
FRS	kg oil eq	0.08	-0.23	4.72×10^{-6}	-0.15

Table B-11: Life cycle impacts of HH module (D-scenario)

Impact category	Unit	Production	Use	EOL	Total
GW	kg CO_2 eq	0.02	-0.81	1.27×10^{-6}	-0.78
TET	kg 1,4-DCB	0.02	-0.03	3.06×10^{-6}	-0.01
FET	kg 1,4-DCB	8.80×10^{-4}	-2.01×10^{-4}	1.39×10^{-8}	6.79×10^{-4}

MET	kg 1,4-DCB	1.35×10^{-3}	-0.01	2.26×10^{-8}	-0.01
HCT	kg 1,4-DCB	8.70×10^{-4}	-2.11×10^{-3}	4.02×10^{-8}	-1.24×10^{-3}
HNT	kg 1,4-DCB	0.03	-0.01	4.99×10^{-7}	0.02
MRS	kg Cu eq	2.19×10^{-4}	-2.82×10^{-4}	3.42×10^{-9}	-6.24×10^{-5}
FRS	kg oil eq	0.01	-0.23	5.09×10^{-7}	-0.23

Table B-12: Life cycle impacts of SC module (D-scenario)

Impact category	**Unit**	**Production**	**Use**	**EOL**	**Total**
GW	kg CO_2 eq	0.10	-0.81	5.41×10^{-6}	-0.71
TET	kg 1,4-DCB	0.14	-0.03	1.30×10^{-5}	0.11
FET	kg 1,4-DCB	0.01	-2.01×10^{-4}	5.94×10^{-8}	0.01
MET	kg 1,4-DCB	0.01	-0.01	9.65×10^{-8}	-3.40×10^{-3}
HCT	kg 1,4-DCB	0.01	-2.11×10^{-3}	1.72×10^{-7}	0.01
HNT	kg 1,4-DCB	0.22	-0.01	2.13×10^{-6}	0.21
MRS	kg Cu eq	0.01	-2.82×10^{-4}	1.46×10^{-8}	0.01
FRS	kg oil eq	0.03	-0.23	2.17×10^{-6}	-0.21

4.2. Life Cycle Impacts: Comparison of EOL Scenarios

For various EOL scenarios, Figures B.1–B.4 compare life cycle impacts of modules (barring HH and SK-2), while Tables B-13–B-24 show characterized impacts.

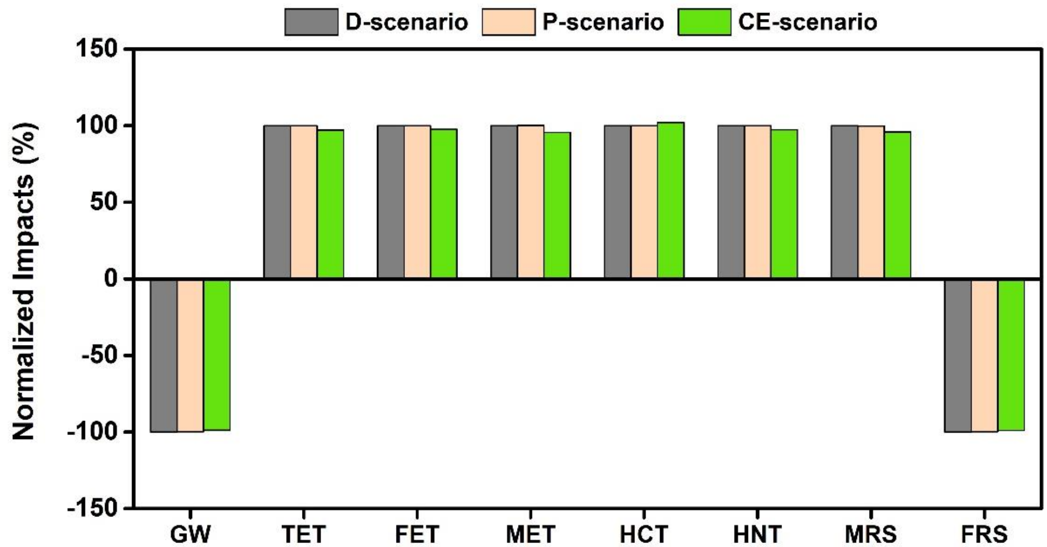

Figure B.1: Comparison of life cycle impacts of BT-1 module under various EOL scenarios (normalized by impact of D-scenario)

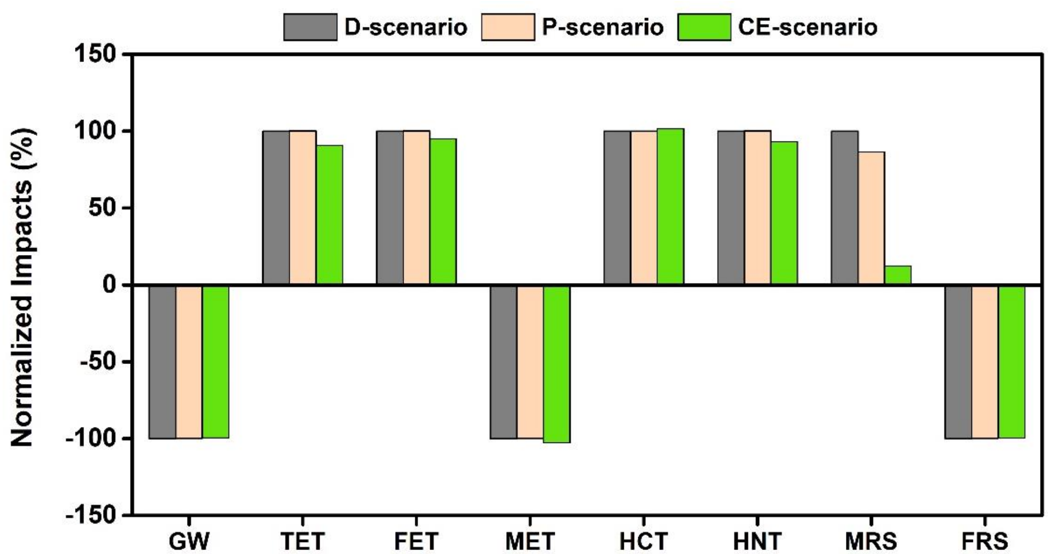

Figure B.2: Comparison of life cycle impacts of BT-2 module under various EOL scenarios (normalized by impacts of D-scenario)

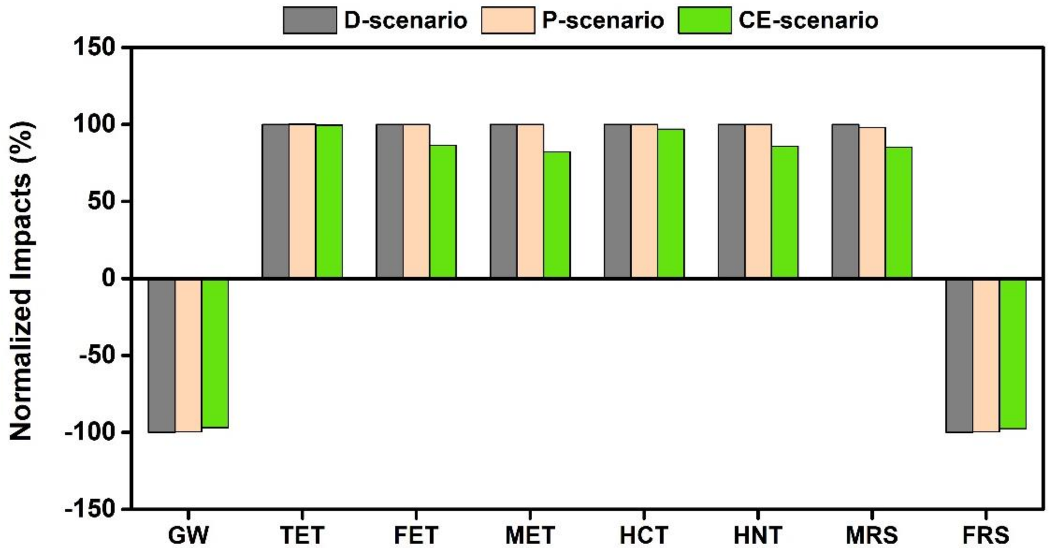

Figure B.3: Comparison of life cycle impacts of SK-1 module under various EOL scenarios (normalized by impacts of D-scenario)

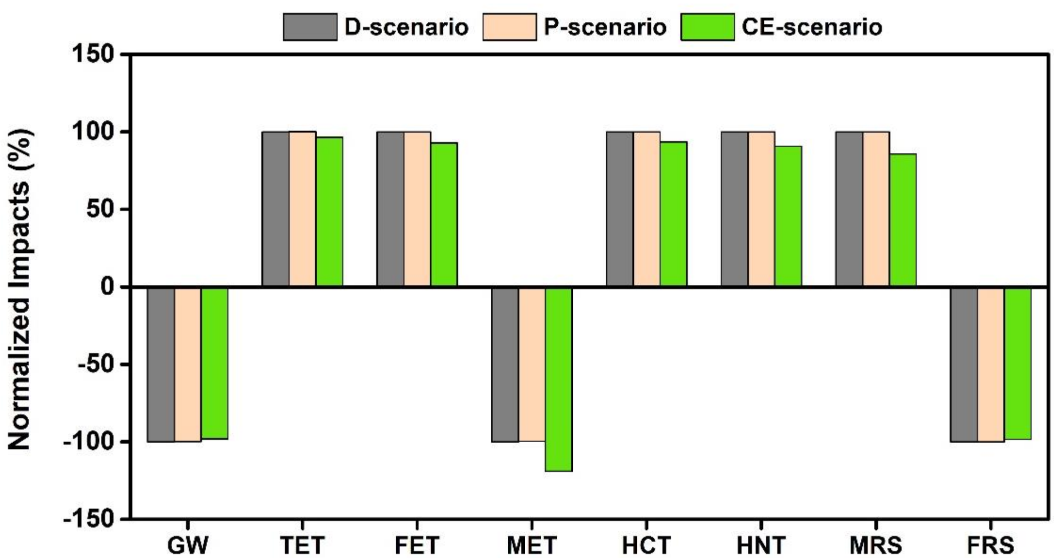

Figure B.4: Comparison of life cycle impacts of SC module under various EOL scenarios (normalized by impacts of D-scenario)

Table B-13: Life cycle impacts of BT-1 module (P-scenario)

Impact category	Unit	Production	Use	EOL	Total
GW	kg CO_2 eq	0.20	-0.81	1.01×10^{-3}	-0.61
TET	kg 1,4-DCB	0.93	-0.03	1.98×10^{-4}	0.90

FET	kg 1,4-DCB	0.02	-2.01×10^{-4}	7.70×10^{-6}	0.02
MET	kg 1,4-DCB	0.03	-0.01	1.87×10^{-5}	0.01
HCT	kg 1,4-DCB	0.01	-2.11×10^{-3}	-1.22×10^{-6}	0.01
HNT	kg 1,4-DCB	0.62	-0.01	2.89×10^{-4}	0.61
MRS	kg Cu eq	2.39×10^{-3}	-2.82×10^{-4}	-8.67×10^{-6}	2.10×10^{-3}
FRS	kg oil eq	0.05	-0.23	2.71×10^{-4}	-0.18

Table B-14: Life cycle impacts of BT-2 module (P-scenario)

Impact category	Unit	Production	Use	EOL	Total
GW	kg CO_2 eq	0.19	-0.81	6.03×10^{-4}	-0.62
TET	kg 1,4-DCB	0.13	-0.03	1.15×10^{-4}	0.10
FET	kg 1,4-DCB	3.09×10^{-3}	-2.01×10^{-4}	4.59×10^{-6}	2.89×10^{-3}
MET	kg 1,4-DCB	0.01	-0.01	1.11×10^{-5}	-0.01
HCT	kg 1,4-DCB	0.01	-2.11×10^{-3}	-7.68×10^{-7}	3.37×10^{-3}
HNT	kg 1,4-DCB	0.10	-0.01	1.72×10^{-4}	0.09
MRS	kg Cu eq	3.20×10^{-4}	-2.82×10^{-4}	-5.18×10^{-6}	3.28×10^{-5}
FRS	kg oil eq	0.05	-0.23	1.61×10^{-4}	-0.18

Table B-15: Life cycle impacts of SK-1 module (P-scenario)

Impact category	Unit	Production	Use	EOL	Total
GW	kg CO_2 eq	0.33	-0.81	1.56×10^{-3}	-0.47
TET	kg 1,4-DCB	0.21	-0.03	3.06×10^{-4}	0.18
FET	kg 1,4-DCB	0.03	-2.01×10^{-4}	1.19×10^{-5}	0.03
MET	kg 1,4-DCB	0.05	-0.01	2.88×10^{-5}	0.03
HCT	kg 1,4-DCB	0.02	-2.11×10^{-3}	-1.89×10^{-6}	0.01
HNT	kg 1,4-DCB	1.10	-0.01	4.46×10^{-4}	1.09
MRS	kg Cu eq	9.64×10^{-4}	-2.82×10^{-4}	-1.34×10^{-5}	6.69×10^{-4}
FRS	kg oil eq	0.09	-0.23	4.19×10^{-4}	-0.15

Table B-16: Life cycle impacts of SK-2 module (P-scenario)

Impact category	Unit	Production	Use	EOL	Total
GW	kg CO_2 eq	0.32	-0.81	7.00×10^{-4}	-0.48
TET	kg 1,4-DCB	0.24	-0.03	1.51×10^{-4}	0.21
FET	kg 1,4-DCB	0.04	-2.01×10^{-4}	5.36×10^{-6}	0.04
MET	kg 1,4-DCB	0.06	-0.01	1.29×10^{-5}	0.05
HCT	kg 1,4-DCB	0.02	-2.11×10^{-3}	-6.44×10^{-7}	0.02
HNT	kg 1,4-DCB	1.54	-0.01	2.01×10^{-4}	1.53
MRS	kg Cu eq	1.46×10^{-3}	-2.82×10^{-4}	-5.93×10^{-6}	1.17×10^{-3}
FRS	kg oil eq	0.08	-0.23	1.89×10^{-4}	-0.15

Table B-17: Life cycle impacts of HH module (P-scenario)

Impact category	Unit	Production	Use	EOL	Total
GW	kg CO_2 eq	0.02	-0.81	1.69×10^{-4}	-0.78
TET	kg 1,4-DCB	0.02	-0.03	3.28×10^{-5}	-0.01
FET	kg 1,4-DCB	8.80×10^{-4}	-2.01×10^{-4}	1.29×10^{-6}	6.80×10^{-4}
MET	kg 1,4-DCB	1.35×10^{-3}	-0.01	3.11×10^{-6}	-0.01
HCT	kg 1,4-DCB	8.70×10^{-4}	-2.11×10^{-3}	-2.07×10^{-7}	-1.24×10^{-3}
HNT	kg 1,4-DCB	0.03	-0.01	4.82×10^{-5}	0.02
MRS	kg Cu eq	2.19×10^{-4}	-2.82×10^{-4}	-1.45×10^{-6}	-6.38×10^{-5}
FRS	kg oil eq	0.01	-0.23	4.52×10^{-5}	-0.23

Table B-18: Life cycle impacts of SC module (P-scenario)

Impact category	Unit	Production	Use	EOL	Total
GW	kg CO_2 eq	0.10	-0.81	6.12×10^{-4}	-0.71
TET	kg 1,4-DCB	0.14	-0.03	1.2×10^{-4}	0.11
FET	kg 1,4-DCB	0.01	-2.01×10^{-4}	4.67×10^{-6}	0.01

MET	kg 1,4-DCB	0.01	-0.01	1.13×10^{-5}	-3.39×10^{-3}
HCT	kg 1,4-DCB	0.01	-2.11×10^{-3}	-7.24×10^{-7}	0.01
HNT	kg 1,4-DCB	0.22	-0.01	1.75×10^{-4}	0.21
MRS	kg Cu eq	0.01	-2.82×10^{-4}	-5.24×10^{-6}	0.01
FRS	kg oil eq	0.03	-0.23	1.64×10^{-4}	-0.21

Table B-19: Life cycle impacts of BT-1 module (CE-scenario)

Impact category	**Unit**	**Production**	**Use**	**EOL**	**Total**
GW	kg CO_2 eq	0.20	-0.81	0.01	-0.60
TET	kg 1,4-DCB	0.93	-0.03	-0.03	0.88
FET	kg 1,4-DCB	0.02	-2.01×10^{-4}	-4.07×10^{-4}	0.02
MET	kg 1,4-DCB	0.03	-0.01	-5.74×10^{-4}	0.01
HCT	kg 1,4-DCB	0.01	-2.11×10^{-3}	1.37×10^{-4}	0.01
HNT	kg 1,4-DCB	0.62	-0.01	-0.02	0.59
MRS	kg Cu eq	2.39×10^{-3}	-2.82×10^{-4}	-8.52×10^{-5}	2.03×10^{-3}
FRS	kg oil eq	0.05	-0.23	1.77×10^{-3}	-0.18

Table B-20: Life cycle impacts of BT-2 module (CE-scenario)

Impact category	**Unit**	**Production**	**Use**	**EOL**	**Total**
GW	kg CO_2 eq	0.19	-0.81	0.00	-0.62
TET	kg 1,4-DCB	0.13	-0.03	-0.01	0.09
FET	kg 1,4-DCB	3.09×10^{-3}	-2.01×10^{-4}	-1.48×10^{-4}	2.74×10^{-3}
MET	kg 1,4-DCB	0.01	-0.01	-2.07×10^{-4}	-0.01
HCT	kg 1,4-DCB	0.01	-2.11×10^{-3}	4.99×10^{-5}	3.42×10^{-3}
HNT	kg 1,4-DCB	0.10	-0.01	-0.01	0.08
MRS	kg Cu eq	3.20×10^{-4}	-2.82×10^{-4}	-3.33×10^{-5}	4.71×10^{-6}
FRS	kg oil eq	0.05	-0.23	7.12×10^{-4}	-0.18

Table B-21: Life cycle impacts of SK-1 module (CE-scenario)

Impact category	Unit	Production	Use	EOL	Total
GW	kg CO_2 eq	0.33	-0.81	0.01	-0.46
TET	kg 1,4-DCB	0.21	-0.03	0.00	0.18
FET	kg 1,4-DCB	0.03	-2.01×10^{-4}	-4.28×10^{-3}	0.03
MET	kg 1,4-DCB	0.05	-0.01	-0.01	0.03
HCT	kg 1,4-DCB	0.02	-2.11×10^{-3}	-4.09×10^{-4}	0.01
HNT	kg 1,4-DCB	1.10	-0.01	-0.15	0.94
MRS	kg Cu eq	9.64×10^{-4}	-2.82×10^{-4}	-1.00×10^{-4}	5.82×10^{-4}
FRS	kg oil eq	0.09	-0.23	0.00	-0.14

Table B-22: Life cycle impacts of SK-2 module (CE-scenario)

Impact category	Unit	Production	Use	EOL	Total
GW	kg CO_2 eq	0.32	-0.81	0.02	-0.46
TET	kg 1,4-DCB	0.24	-0.03	-1.20×10^{-4}	0.21
FET	kg 1,4-DCB	0.04	-2.01×10^{-4}	-0.01	0.04
MET	kg 1,4-DCB	0.06	-0.01	-0.01	0.04
HCT	kg 1,4-DCB	0.02	-2.11×10^{-3}	-5.99×10^{-4}	0.01
HNT	kg 1,4-DCB	1.54	-0.01	-0.24	1.29
MRS	kg Cu eq	1.46×10^{-3}	-2.82×10^{-4}	-1.97×10^{-4}	9.78×10^{-4}
FRS	kg oil eq	0.08	-0.23	0.01	-0.14

Table B-23: Life cycle impacts of HH module (CE-scenario)

Impact category	Unit	Production	Use	EOL	Total
GW	kg CO_2 eq	0.02	-0.81	4.59×10^{-4}	-0.78
TET	kg 1,4-DCB	0.02	-0.03	-6.84×10^{-4}	-0.01
FET	kg 1,4-DCB	8.80×10^{-4}	-2.01×10^{-4}	-5.10×10^{-5}	6.28×10^{-4}

MET	kg 1,4-DCB	1.35×10^{-3}	-0.01	-7.07×10^{-5}	-0.01
HCT	kg 1,4-DCB	8.70×10^{-4}	-2.11×10^{-3}	-3.48×10^{-6}	-1.24×10^{-3}
HNT	kg 1,4-DCB	0.03	-0.01	-1.95×10^{-3}	0.02
MRS	kg Cu eq	2.19×10^{-4}	-2.82×10^{-4}	-2.20×10^{-5}	-8.44×10^{-5}
FRS	kg oil eq	0.01	-0.23	1.18×10^{-4}	-0.23

Table B-24: Life cycle impacts of SC module (CE-scenario)

Impact category	Unit	Production	Use	EOL	Total
GW	kg CO_2 eq	0.10	-0.81	1.27×10^{-2}	-0.70
TET	kg 1,4-DCB	0.14	-0.03	-4.03×10^{-3}	0.11
FET	kg 1,4-DCB	0.01	-2.01×10^{-4}	-4.50×10^{-4}	0.01
MET	kg 1,4-DCB	0.01	-0.01	-6.42×10^{-4}	-4.04×10^{-3}
HCT	kg 1,4-DCB	0.01	-2.11×10^{-3}	-5.01×10^{-4}	0.01
HNT	kg 1,4-DCB	0.22	-0.01	-1.94×10^{-2}	0.19
MRS	kg Cu eq	1.07×10^{-2}	-2.82×10^{-4}	-1.50×10^{-3}	0.01
FRS	kg oil eq	0.03	-0.23	3.10×10^{-3}	-0.20

APPENDIX-C

SUPPORTING INFORMATION FOR CHAPTER 5

C. Ecological Profile of Thermoelectrics for Automotive Applications (Intermittent Waste Heat Generation)

1. Introduction

For cradle-to-grave LCA of TEGs, this Appendix provides detailed inventory for heat exchanger and other components that are used in addition to modules in chosen generators. It was assumed that after procuring the desired inputs, both generators were manufactured in the US, using the average 2015 U.S. electric grid mix for processing various individual components (due to unavailability of more recent data).

2. TEG – Heat Exchanger Components

2.1. Heat Exchangers

Tables C-1, C-2 and C-3 respectively provide the inventory for copper TEG base, copper fins, and SS side bars for both TEGs for both SK-1 and BT-1 modules.

Table C-1: Inventory of copper base

For TEG-1 (Only skutterudite modules)				
Type of Parameter	**Material**	**Value**	**Unit**	**Remark**
Process output	Copper base	1000	kg	
Process inputs	Copper sheet	1047.23	kg	Based on the loss of ~ 4.5 % of material during cutting, as obtained through calculations

	Electricity	11.41	kWh	Used to cut copper sheet to sizes required to produce copper fins
Emission output: Solid waste	Copper sheet (Hazardous waste, landfill)	47.23	kg	
For TEG-2 (Skutterudite + Bismuth Telluride modules)				
Type of Parameter	**Material**	**Value**	**Unit**	**Remark**
Process output	Copper base	1000	kg	
Process inputs	Copper sheet	1131.18	kg	Based on the loss of ~ 11.5 % of material during cutting, as obtained through calculations.
	Electricity	10.35	kWh	Used to cut the copper sheet to sizes required to produce copper fins
Emission output: Solid waste	Copper sheet (Hazardous waste, landfill)	131.18	kg	

Table C-2: Inventory of copper fins

For TEG-1 (Only skutterudite modules)				
Type of Parameter	**Material**	**Value**	**Unit**	**Remark**
Process output	Copper fins	1000	kg	
Process inputs	Copper sheet	1105.39	kg	Based on the loss of ~ 10 % of material during cutting, as obtained through calculations

	Electricity	8.42	kWh	Used to cut copper sheet to sizes required to produce copper fins
Emission output: Solid waste	Copper (Hazardous waste, landfill)	105.39	kg	
For TEG-2 (Skutterudite + Bismuth Telluride modules)				
Type of Parameter	**Material**	**Value**	**Unit**	**Remark**
Process output	Copper fins	1000	kg	
Process inputs	Copper sheet	1153.06	kg	Based on the loss of ~ 13 % of material during cutting, as obtained through calculations
	Electricity	17.89	kWh	Used to cut copper sheet to sizes required to produce copper fins
Emission output: Solid waste	Copper (Hazardous waste, landfill)	153.06	kg	

Table C-3: Inventory of side bars

Type of Parameter	Material	Value	Unit
Process output	SS Side Bars	1000	kg
Process input	Cold-rolled SS plate	1000	kg

2.2. Min-K (Thermal Insulation)

Table C-4 shows the inventory for Min-K.

Table C-4: Inventory of Min-K (as obtained from company source[128,129])

Type of Parameter	Material	Value	Unit
Process output	Min-K	1000	kg
Process inputs	Silica (SiO_2)	815.57	kg
	Alumina (Al_2O_3)	4.46	kg
	Titanium dioxide (TiO_2)	114.18	kg
	Iron oxide (Fe_2O_3)	2.72	kg
	Calcium oxide (CaO)	51.22	kg
	Magnesium oxide (MgO)	9.79	kg
	Sodium oxide (Na_2O)	1.52	kg
	Potassium oxide (K_2O)	0.54	kg
	Water (H_2O)	5043.78	kg
Emission output: Air	Water (H_2O)	5043.78	kg

3. Use Stage: Electricity Generation and Fuel Savings

3.1. Thermal Cycling Reduction Coefficient (TCRC)

Since use of TEs in automobiles involve thermal cycling that reduces conversion efficiency of TE modules, data regarding such reduction in conversion efficiency with each thermal cycle – referred to as *thermal cycling reduction coefficient* (TCRC) – is important while evaluating the ecological credentials of this platform. This TCRC data was directly taken from that calculated for SK and BT modules in previous Appendix (Table 2-5).

3.2. ***Gasoline Savings: Calculation Procedure and Actual Savings***

Typically, prior to estimating gasoline savings, it is important to calculate the fuel consumed without the use of thermoelectric generator. Hence, this step was first undertaken, and then estimated the fuel saved by using it, as well as the excess fuel consumed due to its mass. The difference between the two was the net amount of fuel saved by the generator. However, this entire process was conducted using a complicated procedure that is described in the following sub-sections, step-by-step.

3.2.1. Step 1

In order to determine the amount of fuel consumed without a thermoelectric, it is necessary to have an idea of the distance travelled as well as the fuel economy of the vehicle. Prior to 2008, fuel economy (FE) values for automobiles were calculated by considering only two kinds of driving – city and highway[224]. For both kinds of driving, FE was first estimated using UDDS (urban dynamometer driving schedule) and HWFET (highway fuel economy test cycle) cycles respectively[224,225], after which it was combined to obtain the final FE (in the ratio of 55 % for city driving and 45 % for highway driving) – this method is termed the 2-cycle fuel economy. However, after 2008, this calculation was modified by considering five kinds of driving cycles, which go beyond city and highway driving cycles[226]. Further, another change to evaluating fuel economy for urban driving since 2008 has been the replacement of UDDS procedure with FTP (federal test procedure) (FTP-72)[224]. Subsequently, FE values for the five cycles (under 5-cycle FE method) are then used to estimate city and highway driving FE values, which in turn are used to obtain the final FE value of a vehicle (with same ratio of 55 % for city driving and 45 % for highway driving) – this is termed the 5-cycle fuel economy (FE). Since the formulas for obtaining these city and highway driving fuel economies are highly complicated in 5-cycle method[227], the correlation between the old 2-cycle FE method and the new 5-cycle method was used, based on Equations 1 and 2 given below[228]. This automatically converts the idea of city and urban FE values (provided using 5-cycle method at present) into the same values using the 2-cycle method (i.e., based on FTP and HWFET cycles respectively). The 5-cycle FE values for city and highway driving cycles for Chevrolet Suburban are available in public domain[229] as 15 mpg and 22 mpg respectively. These were used to obtain the city and highway driving FE values for 2-cycle method respectively, using the equations given below.

$$FE_{city,5-cycle} = \frac{1}{0.004091 + \frac{1.1601}{FE_{FTP}}} \quad \ldots\ldots (1)$$

$$FE_{highway,5-cycle} = \frac{1}{0.003191 + \frac{1.2945}{FE_{HWFET}}} \quad \ldots\ldots(2)$$

3.2.2. *Step 2*

In this step, the amount of energy (E) needed for driving the vehicle under both FTP and HWFET cycles was estimated using Equation 3, where the three individual terms (that were summed up) referred to three components: inertial (mass-dependent), aerodynamic (dependent on countering aerodynamic drag of vehicle), and rolling (to counter rolling resistance faced by vehicle). It turns out that the integral parts of each of these terms are vehicle-independent (i.e., they are the same, irrespective of the vehicle considered), so it is a constant value. Hence, Equation 3 can be converted into Equation 4.

$$E = \int_0^{cycle} P.dt$$

$$= m\int_0^{cycle} V\frac{dV}{dt}dt + \frac{C_d A\rho}{2}\int_0^{cycle} V^3 dt + f_r mg\int_0^{cycle} V dt \quad \ldots\ldots(3)$$

$$E = m\beta_1 + \frac{C_d A\rho}{2}\beta_2 + f_r mg\beta_3 \quad \ldots\ldots(4)$$

Based on the raw data provided for both FTP and HWFET cycles (velocity against time) in EPA database[224], values of β_1, β_2 and β_3 were calculated (by integrating the parameters) – these are provided in Table C-5.

Table C-5: Values of vehicle-independent coefficients for Equation 4 (above)

Cycle	$\boldsymbol{\beta_1}$	$\boldsymbol{\beta_2}$	$\boldsymbol{\beta_3}$
FTP	3,026	4,549,910	17,770
HWFET	1,165	8,539,652	16,507

Further, values of total load (m = mass of vehicle + test load of 136 kg, representing weight of 2 average persons) and frontal area of vehicle (85 % of length multiplied by width of vehicle) for Chevrolet Suburban (A)[229] were obtained/calculated, and rough values were used for aerodynamic drag coefficient (C_d= 0.36) (assumed to be same as that given in[230]), density of air (ρ = 1.225 kg/m^3)[231], rolling resistance (f_r = 0.008)[232] and acceleration due to gravity (g = 9.81 m/s^2) to calculate the total energy (E) needed to drive the vehicle per cycle (FTP or HWFET). This total energy was calculated separately for both FTP and HWFET cycles – all of which assumed the non-usage of TEGs.

3.2.3. *Step 3*

Having obtained the fuel economy values for FTP and HWFET cycles in Step 1 itself, tank capacity of Chevrolet Suburban[229] was used to estimate the total distance that the vehicle can travel on either of these cycles alone in a single fuel tank. Using this, two parameters were estimated: (a) Total number of driving cycles (of either kind, 2-cycle method) that the vehicle can cover in 1 entire fuel tank; and (b) Total driving energy that is available over 1 fuel tank (product of total gasoline used and energy content of gasoline). Further, the total energy needed for driving per cycle (obtained as E in Step 2) was multiplied with the total number of driving cycles, for both city and highway driving, to obtain the total energy needed for driving in a single fuel tank. The ratio of these two quantities – total driving energy needed to total driving energy provided by gasoline – is the tank-to-wheel (TTW) efficiency of car, without the use of TEGs. In addition, the aforementioned information was used to estimate the amount of fuel (gasoline) consumed per cycle (for each kind of driving cycle), as well as the energy content of this fuel.

3.2.4. *Step 4*

A thermoelectric generator can only meet those needs of a car that are met using electricity (i.e., only for electronics). Since these needs are currently met by alternator in any automobile, first, the total amount of energy consumed by the alternator over 1 cycle of each kind (FTP or HWFET) was calculated by multiplying three values – current used by alternator, voltage of alternator, and time for which the alternator is used (i.e., duration of any driving cycle). More information on these values is provided in Table C-6.

Table C-6: Information on alternator energy consumption

Parameters & Unit	Value
Current (A)	150[229]
Voltage (V)	14[233]
Time (t, seconds)[224]	Driving cycle: City (1,874), Highway (765)

Finally, fuel energy consumed over both city and driving cycles over the lifetime of the vehicle (100,000 miles) was summed up and obtained as 21,624.90 liters of fuel.

3.2.5. *Step 5*

Any TEG, upon use, adds to the mass of the vehicle. Hence, the incremental energy needed to drive this additional mass was calculated using Equation 4 (above). Obviously, since aerodynamic drag does not change with addition of mass, the second term becomes zero, while the other terms were non-zero (as the mass of vehicle is affected). Upon adding this incremental energy to the total energy needed to drive per cycle, total energy needed to drive Chevrolet Suburban after fitting the TEG onto it was obtained.

3.2.6. *Step 6*

While the conversion efficiency of both TEGs from chosen studies[104,140] corresponds to FTP cycle (i.e., city driving conditions), no information is available on the same under highway driving conditions. However, it is well known that the conversion efficiency of any device is typically dependent on temperature difference between its hot and cold ends. Assuming the cold side temperature to be constant, it can be said that the hot side temperature is likely to increase during highway driving due to higher speeds vis-à-vis city driving, as also the rate of exhaust gas flow. Thus, there is enough reason to believe that the efficiency of both generators will be higher during highway driving than their value during city driving. However, since there is no information on how much this efficiency increase can be, the same conversion efficiency was assumed for these TEGs under both driving conditions (i.e., highway driving efficiency = city driving efficiency). However, these are merely original values, and thermal cycling occurs after each thermal cycle. Hence, it was assumed for sake of simplicity that each driving cycle (FTP or HWFET) corresponds to 1 thermal cycle, and an overall equal distribution of both driving cycles was considered over the lifetime of vehicle. For each driving cycle, conversion efficiency of the generator was calculated by taking into consideration the TCRC values mentioned (Table 2-5).

Using these figures, the amount of energy generated by each TEG was calculated, assuming that ~ 60 % of fuel energy was lost as exhaust waste heat[234]. It is the TCRC-affected conversion efficiency figure for each driving cycle (i.e., each thermal cycle) that was used to obtain the total energy generated by the generator. This value was compared with the energy consumed by the alternator for both FTP and HWFET cycles. In both types of driving, it was found that the energy produced by both TEGs was lower than that consumed by the alternator, so that it replaced only a part of energy consumed by the alternator, and this part of energy was then considered to be additionally available for driving. Another assumption made in this aspect was that of the total energy produced by TEGs, only 90 % was considered as going to alternator, with 10 % assumed to be lost.

3.2.7. *Step 7*

Now, the total energy available for driving was calculated as the sum of two terms: (a) One, the product of TTW (tank-to-wheel) efficiency and fuel energy provided for Chevrolet Suburban without use of any TEG; and (b) Additional energy generated by the TEG (i.e., wattage of generator, multiplied by total driving time) for every driving cycle (FTP or HWFET). This total energy available for driving was then divided by fuel energy provided by the vehicle overall, to estimate the new TTW efficiency of vehicle with use of TEGs. Using this new TTW efficiency (η_{t2w}), fuel economy (FE, 2-cycle method) was estimated for FET and HWFET cycles using Equation 5, where E_{drive} is the energy needed for driving per cycle, $\rho_{gasoline}$ is energy density of gasoline, and l_{cycle} is the length of driving cycle, all considering the use of TEGs.

$$FE = \eta_{t2w} \frac{\rho_{gasoline}}{E_{drive}} l_{cycle} \quad \ldots\ldots (5)$$

Based on this formula, fuel economy was obtained under the 2-cycle method. This was later inputted into Equations 1 or 2 (as the case may be) to obtain the city and highway driving FE values for 5-cycle method. Finally, total distance travelled by Chevrolet Suburban on either kinds of driving was divided with these FE values to estimate the total fuel consumed under each driving cycle. All these calculations were undertaken separately for each driving (thermal) cycle, and then the fuel consumed across all driving cycles was summed up to obtain overall fuel consumption. Table C-7 shows the overall fuel consumption upon use of either of the two generators and the obtained fuel savings.

Table C-7: Fuel consumption and savings upon use of TEGs

Parameters	TEG-1	TEG-2
Fuel consumed without use of TEGs (liters)	21,624.90	21,624.90
Fuel consumed with use of TEGs (liters)	21,328.92	20,963.95
Fuel saved with use of TEGs (liters)	295.98	660.95

4. *End-of-Life (EOL) Scenarios*

Three end-of-life (EOL) scenarios were considered in this study (same as in previous chapters) and inventory for these scenarios is provided in following sub-sections.

4.1. Disposal Scenario (D-Scenario)

Inventory for D-scenario is the same as given in Table A-31.

4.2. Practical Scenario (P-Scenario)

Inventory is produced in Tables C-8 (for copper-based components) and C-9 (for stainless-steel side bars) for recycling of heat exchanger components in P-scenario. Copper-based components were assumed to be converted to secondary copper, which may be used for the same or some other application.

Table C-8: Inventory for the recycling of copper-based heat exchanger components (base and fins)

Type of Parameter	Parameter	Value	Unit

Output Material	Copper, secondary	1000	kg
Input Materials	Copper base/fins	1000	kg
	Occupation, arable land, unspecified use, US	0.92	m^2a
	Water, river, US	5.07	m^3
	Oil, crude	76.41	kg
	Coal, bituminous, 24.8 MJ per kg	201.15	kg
	Chemicals inorganic, at plant/GLO US-EI U	0.0889	kg
	Chemicals organic, at plant/GLO US-EI U	18.29	kg
	Sulfuric acid (98 % H_2SO_4), at plant/RER Mass	0.0073	ton
Input Energy	Electricity, medium voltage, at grid, 2015/US US-EI U	286.62	kWh
Output Emissions: Air	Carbon dioxide	331.49	kg
	Particulates	39.32	g
	Sulfur dioxide	400.38	g
	Nitrogen oxides	946.84	g
	Arsenic	4.04	g
	Lead	0.22	g
	Copper	0.39	g
	Nickel	0.00848	g
	Sulfuric acid	0.21	g
Output Emissions: Water	Phosphorus	0.0154	g
	Copper	0.19	g
	Lead	0.0165	g
	Nickel	0.24	g
	Ammonia	0.2	g
	Arsenic	0.00651	g
Final Waste flows	Hazardous waste, unspecified treatment	4.66	kg

Waste to treatment	Disposal, municipal solid waste, 0 % water, to sanitary landfill	1.06	kg

Table C-9: Inventory for recycling of stainless-steel side bars

Type of Parameter	Material	Quantity required	Unit
Output Material	Side re-bar	1000	kg
Input Materials	Steel side bars	1000	kg
Input Energy	Electricity (for sorting)	0	kWh
	Electricity (for shredding)	50	kWh
	Electricity - Primary Energy (For melting, refining)	1.8	GJ
	Electricity (For rebar formation)	175	kWh
Transportation required	Transport involved (Assumed)	100	miles
		160.934	km
		160.934	ton-km

4.3. Circular Economy Scenario (CE-Scenario)

Inventory for recycling TE legs is provided in Tables A-33–A-46.

5. Modules: Life cycle Environmental Impacts

5.1. *D-Scenario*

Tables C-10 and C-11 show the respective characterized impacts of both TEGs, segregated by contributions of different life cycle stages, for the D-scenario.

Table C-10: Characterized impacts of TEG-1 for D-scenario

Impact category	Unit	Production	Use	Disposal	Total
GW	kg CO_2 eq	9.79	-3.18	3.53×10^{-3}	6.62
TET	kg 1,4-DCB	7.42	-8.79	8.53×10^{-3}	-1.36

FET	kg 1,4-DCB	0.94	-4.91×10^{-3}	3.88×10^{-5}	0.94
MET	kg 1,4-DCB	1.37	-0.01	6.30×10^{-5}	1.36
HCT	kg 1,4-DCB	0.45	-0.02	1.12×10^{-4}	0.43
HNT	kg 1,4-DCB	32.49	-0.21	1.39×10^{-3}	32.28
MRS	kg Cu eq	0.03	-1.49×10^{-3}	9.54×10^{-6}	0.03
FRS	kg oil eq	2.54	-0.98	1.42×10^{-3}	1.56

Table C-11: Characterized impacts of TEG-2 for D-scenario

Impact category	Unit	Production	Use	Disposal	Total
GW	kg CO_2 eq	6.34	-3.18	2.14×10^{-3}	3.17
TET	kg 1,4-DCB	12.66	-8.79	5.18×10^{-3}	3.87
FET	kg 1,4-DCB	0.60	-4.91×10^{-3}	2.36×10^{-5}	0.59
MET	kg 1,4-DCB	0.87	-0.01	3.83×10^{-5}	0.86
HCT	kg 1,4-DCB	0.29	-0.02	6.81×10^{-5}	0.27
HNT	kg 1,4-DCB	20.68	-0.21	8.45×10^{-4}	20.47
MRS	kg Cu eq	0.04	-1.49×10^{-3}	5.79×10^{-6}	0.04
FRS	kg oil eq	1.66	-0.98	8.62×10^{-4}	0.68

5.2. P-Scenario

Tables C-12 and C-13 show the respective characterized impacts of both TEGs, segregated by contributions of different life cycle stages, for the P-scenario.

Table C-12: Characterized impacts of TEG-1 for P-scenario

Impact category	Unit	Production	Use	Practical	Total
GW	kg CO_2 eq	9.79	-3.18	-0.06	6.56
TET	kg 1,4-DCB	7.42	-8.79	-20.32	-21.69
FET	kg 1,4-DCB	0.94	-4.91×10^{-3}	-0.04	0.89
MET	kg 1,4-DCB	1.37	-0.01	-0.07	1.29
HCT	kg 1,4-DCB	0.45	-0.02	-0.01	0.41

HNT	kg 1,4-DCB	32.49	-0.21	-2.03	30.25
MRS	kg Cu eq	0.03	-1.49×10^{-3}	-0.02	0.02
FRS	kg oil eq	2.54	-0.98	-0.01	1.55

Table C-13: Characterized impacts of TEG-2 for P-scenario

Impact category	**Unit**	**Production**	**Use**	**Disposal**	**Total**
GW	kg CO_2 eq	6.34	-3.18	-0.03	3.13
TET	kg 1,4-DCB	12.66	-8.79	-12.28	-8.41
FET	kg 1,4-DCB	0.60	-4.91 × 10-3	-0.03	0.57
MET	kg 1,4-DCB	0.87	-0.01	-0.04	0.82
HCT	kg 1,4-DCB	0.29	-0.02	-0.01	0.26
HNT	kg 1,4-DCB	20.68	-0.21	-1.23	19.25
MRS	kg Cu eq	0.04	-1.49 × 10-3	-0.01	0.03
FRS	kg oil eq	1.66	-0.98	-0.01	0.67

5.3. CE-Scenario

Tables C-14 and C-15 show the respective characterized impacts of both TEGs, segregated by contributions of different life cycle stages, for the CE-scenario.

Table C-14: Characterized impacts of TEG-1 for CE-scenario

Impact category	**Unit**	**Production**	**Use**	**Disposal**	**Total**
GW	kg CO_2 eq	9.79	-3.18	0.32	6.93
TET	kg 1,4-DCB	7.42	-8.79	-20.35	-21.72
FET	kg 1,4-DCB	0.94	-4.91×10^{-3}	-0.17	0.77
MET	kg 1,4-DCB	1.37	-0.01	-0.24	1.11
HCT	kg 1,4-DCB	0.45	-0.02	-0.03	0.40
HNT	kg 1,4-DCB	32.49	-0.21	-6.57	25.72
MRS	kg Cu eq	0.03	-1.49×10^{-3}	-0.02	0.01
FRS	kg oil eq	2.54	-0.98	0.08	1.64

Table C-15: Characterized impacts of TEG-2 for CE-scenario

Impact category	Unit	Production	Use	Disposal	Total
GW	kg CO_2 eq	6.34	-3.18	0.20	3.36
TET	kg 1,4-DCB	12.66	-8.79	-12.55	-8.68
FET	kg 1,4-DCB	0.60	-4.91×10^{-3}	-0.09	0.51
MET	kg 1,4-DCB	0.87	-0.01	-0.13	0.73
HCT	kg 1,4-DCB	0.29	-0.02	-0.01	0.25
HNT	kg 1,4-DCB	20.68	-0.21	-3.42	17.05
MRS	kg Cu eq	0.04	-1.49×10^{-3}	-0.01	0.03
FRS	kg oil eq	1.66	-0.98	0.05	0.73

6. EOL Scenarios: A Comparison

Figures C.1 and C.2 respectively show the life cycle environmental impacts of chosen generators for various EOL scenarios. In all cases, a negative magnitude of impact represents positive effect on environment, and vice-versa.

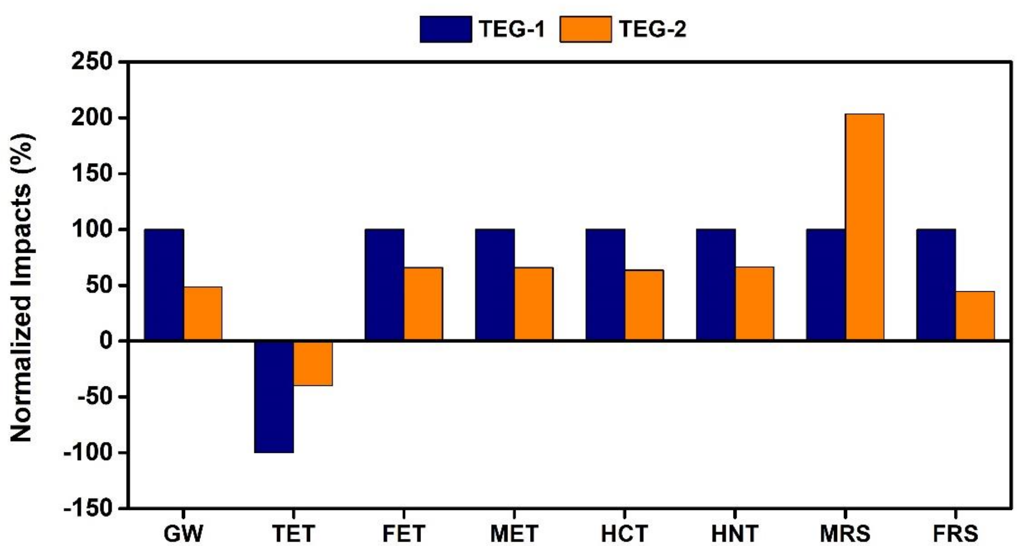

Figure C.1: Comparison of life cycle impacts of TEG-1 and TEG-2 for chosen functional unit (1 liter of gasoline saving) – P-scenario

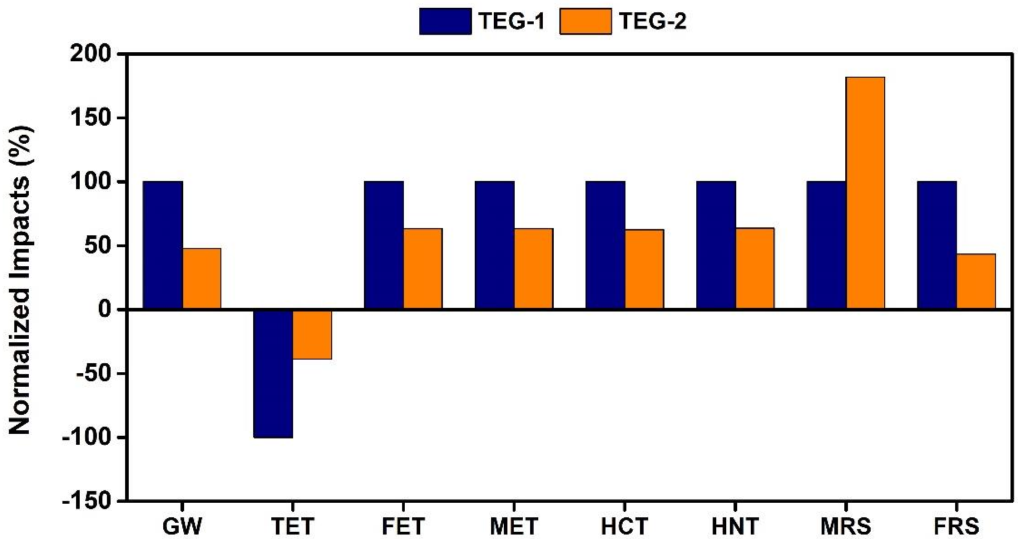

Figure C.2: Comparison of life cycle impacts of TEG-1 and TEG-2 for chosen functional unit (1 liter of gasoline saving) – CE-scenario

7. Environmental impacts – Elemental basis

Table C-16 shows environmental impacts of producing 1 kg of various elements used in TE legs of both generators, as well as of copper (used in copper base and fins).

Table C-16: Environmental impacts of producing 1 kg of various elements used in TE legs of both TEGs, as well as of copper

Impact category	**Unit**	**Ba**	**Bi**	**Co**	**Cu**	**DD**	**Fe**
GW	kg CO_2 eq	17.43	33.90	28.99	8.54	118.91	22.15
TET	kg 1,4-DCB	20.96	19.08	62.74	2065.16	283.00	23.44
FET	kg 1,4-DCB	0.73	0.26	0.79	14.82	3.85	0.44
MET	kg 1,4-DCB	1.09	0.38	1.15	21.49	5.89	0.67
HCT	kg 1,4-DCB	0.78	0.53	1.08	3.60	4.15	2.85
HNT	kg 1,4-DCB	35.97	8.45	32.10	547.65	127.20	10.40
MRS	kg Cu eq	0.10	3.56	9.60	1.18	0.34	0.07
FRS	kg oil eq	4.20	11.39	7.42	2.64	44.04	5.69

Impact category	Unit	La	Ni	Se	Sb	Te	Yb
GW	kg CO_2 eq	55.23	14.67	14.52	24.94	23.05	118.24
TET	kg 1,4-DCB	155.55	849.29	23.98	115.16	1240.67	404.31
FET	kg 1,4-DCB	2.04	7.51	0.36	49.27	9.16	3.55
MET	kg 1,4-DCB	3.06	10.82	0.53	68.66	13.28	5.22
HCT	kg 1,4-DCB	2.01	2.01	0.56	10.58	2.83	4.34
HNT	kg 1,4-DCB	67.88	254.37	10.12	1732.45	333.84	112.81
MRS	kg Cu eq	0.18	3.87	0.03	0.18	0.75	0.36
FRS	kg oil eq	21.88	3.57	4.29	6.22	6.30	37.37

8. *Environmental Impacts – Alternative Scenarios*

Figure C.3 shows the comparison of life cycle impacts of TEG-2 under base case and longer lifetime travel distance (assuming that the generator is better over its non-use, as discussed in Chapter 5), while Figure C.4(a-b) compares the life cycle impacts of both generators under with and without use of TCRC in fuel savings.

8.1. *Hypothetical Alternative Scenario – Lifetime Travel Distance*

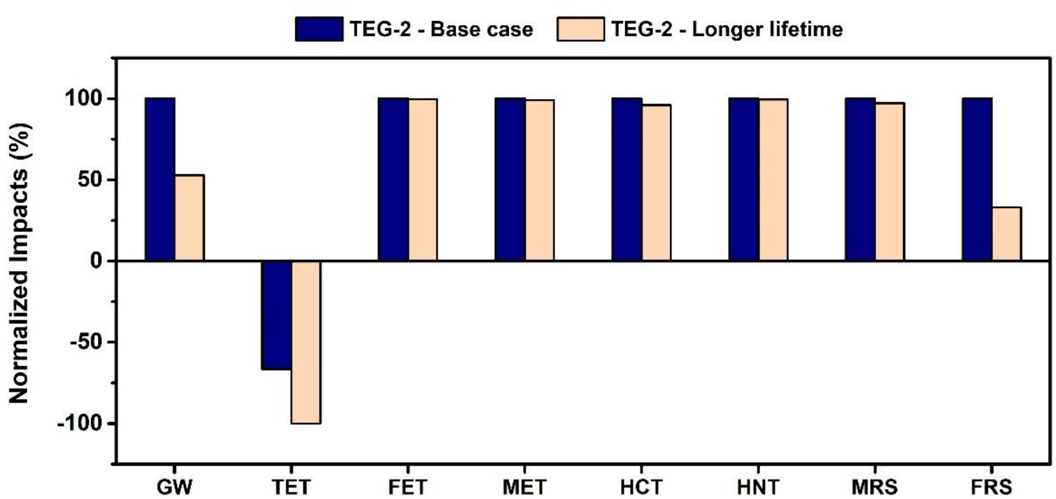

Figure C.3: Life cycle environmental impacts of TEG-2 in two scenarios: (a) Base case and (b) Longer lifetime travel distance

8.2. Hypothetical Alternative Scenario – No TCRC

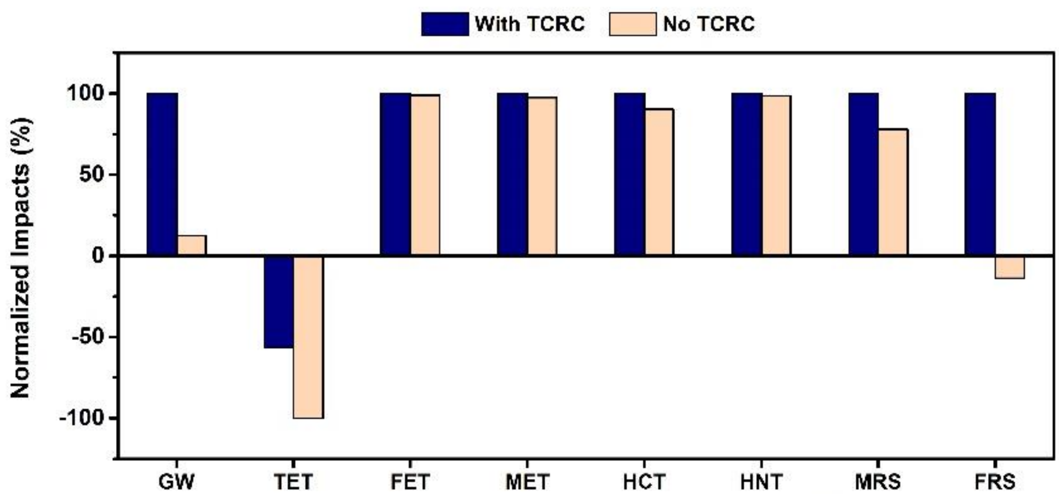

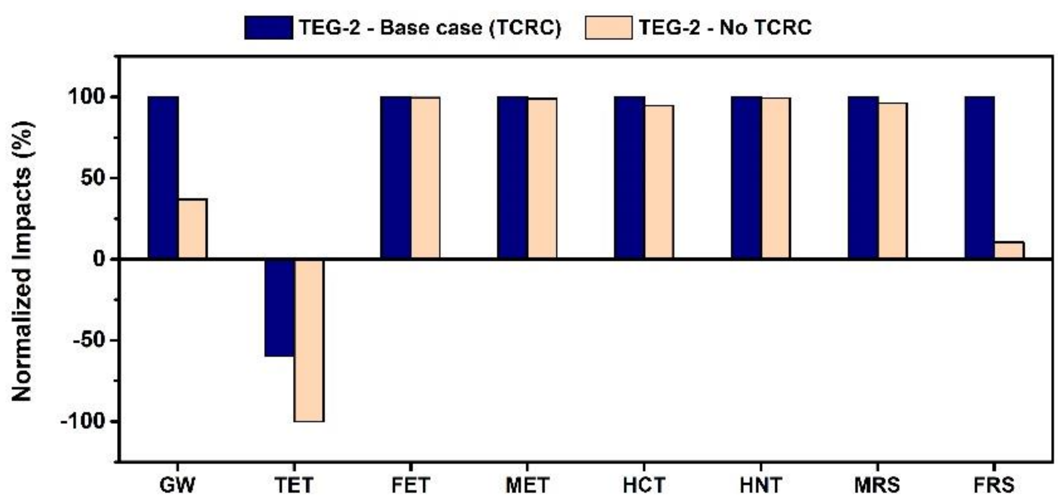

Figure C.4: Life cycle environmental impacts of both generators under base case and without any TCRC distance for: (a) TEG-1 (top) and (b) TEG-2 (bottom)

APPENDIX-D

SUPPORTING INFORMATION FOR CHAPTER 6

D. Green Principles for Sustainable Thermoelectrics

1. Nature of Electric Grid

1.1. U.S. Average 2015 Electric Grid

In all original scenarios in Chapters 3-5, the average U.S. 2015 electric grid mix was assumed to be used for processing TE legs and other TE device components. This grid was used due to paucity of more recent data in Ecoinvent database[137]. The source-wise composition of this grid is provided in Table D-1.

Table D-1: Grid composition of average U.S. 2015 electric grid mix

Source of electricity	Share (%) in production
Coal	33.74 %
Natural gas	33.21 %
Nuclear	19.83 %
Hydropower	6.24 %
Wind	4.75 %
Oil	0.71 %
Solar PV	0.66 %
Geothermal	0.42 %
Industrial gas	0.16 %
Petroleum coke	0.16 %
Wood	0.11 %

1.2. Idaho Mix

Table D-2: Grid composition of Idaho 2015 electric grid mix[137]

Source of electricity	Share (%) in production
Hydropower	84.71 %
Wind	8.26 %
Natural gas	5.47 %
Biogas	1.17 %
Geothermal	0.39 %

1.3. Solar-Wind grid

For the hypothetical solar-wind electric grid, a mix of 50 % contribution from solar photovoltaic (solar PV) and the remnant 50 % from wind-based electricity was assumed.

2. Environmental impacts under alternative/hypothetical scenarios

Table D-3 presents the environmental impacts of TEG-1 and TEG-2 for the original and two alternative hypothetical scenarios – Idaho grid and solar-wind grid.

Table D-3: Characterized life cycle impacts of TEGs under various grid scenarios (D-scenario or disposal as EOL treatment)

Impact category	Unit	TEG-1			TEG-2		
		Base case	Idaho grid	S-W grid	Base case	Idaho grid	S-W grid
GW	kg CO_2 eq	1959	-504	-610	2093	-1312	-1458
TET	kg 1,4-DCB	-403	-1103	1309	2561	1592	4927
FET	kg 1,4-DCB	276.75	249.49	256.15	390.63	352.95	362.16
MET	kg 1,4-DCB	401.83	348.91	356.63	567.10	493.93	504.60
HCT	kg 1,4-DCB	126.47	60.59	66.58	176.51	85.43	93.71
HNT	kg 1,4-DCB	9556	8764	9000	13533	12439	12764
MRS	kg Cu eq	9.01	7.92	10.95	24.51	23.00	27.19

FRS	kg oil eq	461.75	-174.70	-202.22	449.36	-430.56	-468.61
S-W grid: Solar-wind grid (50 % solar- and 50 % wind-based electricity)							

3. *Methodology for calculating leg dicing efficiency (LDE)*

3.1. Original Scenario

The original method of calculating LDE is provided in Section 2 of Appendix-A.

3.2. Efficient Leg Dicing Scenario

In the efficient leg dicing scenario, the only difference that occurs is that the dicing equipment position was assumed to be repeatedly modified to ensure that the maximum number of small squares – encapsulating the dimensions of TE legs – could be formed at each circular end of the cylindrical sintered-and-polished sample, with the height cutting continued along with the height of sample dimension. As a result, based on an external source[235], it was calculated that a maximum number of 96 squares could be obtained on either of the circular ends. However, the number of cuts or TE legs that could be obtained along the height dimension remained the same as in original leg dicing scenario (i.e., 2). Hence, the total number of samples that could be formed is 96 multiplied by 2, or 192. Hence, dicing efficiency was calculated from the following equations and obtained below.

$$Dicing\ efficiency = \frac{Total\ mass\ of\ all\ legs\ per\ 1\ cylinder\ sample}{Total\ mass\ of\ initial\ cylinder}$$

$$= \frac{192 \times (4\ mm)^3 \times Density\ of\ material}{\pi \times (25\ mm)^2 \times 11.43\ mm \times Density\ of\ material}$$

$$\Rightarrow Dicing\ efficiency = 53.04\ \%$$

Thus, an increase in leg dicing efficiency was observed in this scenario.

4. Leg Dicing Efficiency Scenarios: Environmental Impacts

Table D-4 presents the environmental impacts of TEG-1 and TEG-2 for the original and hypothetical scenarios of leg dicing efficiency.

Table D-4: Characterized life cycle impacts of TEGs under LDE scenarios (D-scenario or disposal as EOL treatment)

Impact category	**Unit**	**TEG-1**		**TEG-2**	
		Original scenario	**Higher Dicing Efficiency**	**Original scenario**	**Higher Dicing Efficiency**
GW	kg CO_2 eq	1959.05	1220.08	2093.42	949.46
TET	kg 1,4-DCB	-402.58	-949.81	2560.68	-1840.06
FET	kg 1,4-DCB	276.75	174.47	390.63	216.85
MET	kg 1,4-DCB	401.83	254.75	567.10	317.20
HCT	kg 1,4-DCB	126.47	86.53	176.51	111.40
HNT	kg 1,4-DCB	9555.54	6002.31	13532.55	7448.12
MRS	kg Cu eq	9.01	6.03	24.51	11.59
FRS	kg oil eq	461.75	269.94	449.36	145.69

5. Selective Laser Sintering – Electricity Consumption

Based on available literature[204,205], the unit electricity consumption (i.e., electricity consumed to process 1 kg of final part or output) is 15 kWh/kg. Assuming that this process is only 33.33 % efficient (one-third efficient) for producing TE legs from cylinder samples, the unit electricity consumed would be 15 kWh divided by 33.33 %, i.e. 45 kWh/kg.

6. Environmental Impacts of HH module

For the HH module, minimum usage duration was estimated such that it showed ecofriendliness on all considered impacts. For this, two cases were considered – one of increasing usage duration per cycle, while keeping its lifetime constant, while the other case focused on increasing overall lifetime while keeping per-cycle usage duration constant. In either case, the application was gas-based power plant (taken from Chapter 4), and the modules were assumed to be disposed of at the end of their lifetime (D-scenario as EOL treatment). Table D-5 shows the impacts of all three scenarios – the original scenario in Chapter 3[183], and of these two new cases.

Table D-5: Characterized life cycle impacts of HH modules under various scenarios (D-scenario or disposal as EOL treatment)

Impact category	**Unit**	**HH module: Original scenario**	**Case I: Higher per-cycle usage duration (17 h 33 min)**	**Case II: Longer lifetime (6 h 31 min)**
GW	kg CO_2 eq	-1030.85	-4627.21	-4627.17
TET	kg 1,4-DCB	-10.23	-136.67	-136.67
FET	kg 1,4-DCB	0.89	-2.00×10^{-3}	-1.99×10^{-3}
MET	kg 1,4-DCB	-15.27	-73.04	-73.04
HCT	kg 1,4-DCB	-1.63	-11.05	-11.05
HNT	kg 1,4-DCB	27.08	-11.21	-11.21
MRS	kg Cu eq	-0.08	-1.34	-1.34
FRS	kg oil eq	-298.48	-1336.49	-1336.48

REFERENCES

1. Calder, K. E. Japan’s Energy Angst: Asia’s Changing Energy Prospects and the View from Tokyo. *Strateg. Anal.* **32**, 123–129 (2008).
2. Sreenivas, A. & Iyer, R. K. *A comprehensive, multi-dimensional energy index for India*. (Prayas Energy Group, 2014).
3. Cohen, G., Joutz, F. & Loungani, P. Measuring energy security: Trends in the diversification of oil and natural gas supplies. *Energy Policy* **39**, 4860–4869 (2011).
4. Hosseini, S. E. & Wahid, M. A. Hydrogen production from renewable and sustainable energy resources: Promising green energy carrier for clean development. *Renew. Sustain. Energy Rev.* **57**, 850–866 (2016).
5. Pereira, E. G., Da Silva, J. N., De Oliveira, J. L. & MacHado, C. S. Sustainable energy: A review of gasification technologies. *Renew. Sustain. Energy Rev.* **16**, 4753–4762 (2012).
6. Baños, R. *et al.* Optimization methods applied to renewable and sustainable energy: A review. *Renew. Sustain. Energy Rev.* **15**, 1753–1766 (2011).
7. Vine, E. Breaking down the silos: The integration of energy efficiency, renewable energy, demand response and climate change. *Energy Effic.* **1**, 49–63 (2008).
8. Masson-Delmotte, V. *et al. Global Warming of 1.5°C. An IPCC Special Report on the impacts of global warming of 1.5°C above pre-industrial levels and related global greenhouse gas emission pathways, in the context of strengthening the global response to the threat of climate change,*. (2018).

9. Yilmaz, S. & Selim, H. A review on the methods for biomass to energy conversion systems design. *Renew. Sustain. Energy Rev.* **25**, 420–430 (2013).

10. Aneke, M. & Wang, M. Energy storage technologies and real life applications – A state of the art review. *Appl. Energy* **179**, 350–377 (2016).

11. Blanco, H. & Faaij, A. A review at the role of storage in energy systems with a focus on Power to Gas and long-term storage. *Renew. Sustain. Energy Rev.* **81**, 1049–1086 (2018).

12. Wei, H. *et al.* Energy conversion technologies towards self-powered electrochemical energy storage systems: the state of the art and perspectives. *J. Mater. Chem. A* **5**, 1873–1894 (2017).

13. Li, M., Lu, J., Chen, Z. & Amine, K. 30 Years of Lithium-Ion Batteries. *Adv. Mater.* **30**, 1800561 (2018).

14. Champier, D. Thermoelectric generators: A review of applications. *Energy Convers. Manag.* **140**, 167–181 (2017).

15. He, R., Schierning, G. & Nielsch, K. Thermoelectric Devices: A Review of Devices, Architectures, and Contact Optimization. *Adv. Mater. Technol.* **3**, 1700256 (2018).

16. Pichanusakorn, P. & Bandaru, P. Nanostructured thermoelectrics. *Mater. Sci. Eng. R Reports* **67**, 19–63 (2010).

17. Snyder, G. J. & Toberer, E. S. Complex thermoelectric materials. *Nat. Mater.* **7**, 105–114 (2008).

18. Kim, F. *et al.* 3D printing of shape-conformable thermoelectric materials using all-

inorganic Bi2Te3-based inks. *Nat. Energy* **3**, 301–309 (2018).

19. Barako, M. T., Park, W., Marconnet, A. M., Asheghi, M. & Goodson, K. E. Thermal cycling, mechanical degradation, and the effective figure of merit of a thermoelectric module. *J. Electron. Mater.* **42**, 372–381 (2013).
20. Tritt, T. M., Böttner, H. & Chen, L. Thermoelectrics: Direct solar thermal energy conversion. *MRS Bull.* **33**, 366–368 (2008).
21. Heremans, J. P., Dresselhaus, M. S., Bell, L. E. & Morelli, D. T. When thermoelectrics reached the nanoscale. *Nat. Nanotechnol.* **8**, (2013).
22. Mehdizadeh Dehkordi, A., Zebarjadi, M., He, J. & Tritt, T. M. Thermoelectric power factor: Enhancement mechanisms and strategies for higher performance thermoelectric materials. *Mater. Sci. Eng. R Reports* **97**, 1–22 (2015).
23. He, J. & Tritt, T. M. Advances in thermoelectric materials research: Looking back and moving forward. *Science (80-.).* **357**, eaak9997 (2017).
24. Twaha, S., Zhu, J., Yan, Y. & Li, B. A comprehensive review of thermoelectric technology: Materials, applications, modelling and performance improvement. *Renew. Sustain. Energy Rev.* **65**, 698–726 (2016).
25. Zebarjadi, M., Esfarjani, K., Dresselhaus, M. S., Ren, Z. F. & Chen, G. Perspectives on thermoelectrics: from fundamentals to device applications. *Energy Environ. Sci.* **5**, 5147–5162 (2012).
26. Hicks, L. D. & Dresselhaus, M. S. Thermoelectric figure of merit of a one-dimensional conductor. *Phys. Rev. B* **47**, 16631–16634 (1993).
27. Hicks, L. D. & Dresselhaus, M. S. Effect of quantum-well structures on the

thermoelectric figure of merit. *Phys. Rev. B* **47**, 12727–12731 (1993).

28. Yin, Y., Baskaran, K. & Tiwari, A. A Review of Strategies for Developing Promising Thermoelectric Materials by Controlling Thermal Conduction. *Phys. Status Solidi Appl. Mater. Sci.* **216**, 1800904 (2019).

29. Jaziri, N. *et al.* A comprehensive review of Thermoelectric Generators: Technologies and common applications. *Energy Reports* (2019). doi:10.1016/j.egyr.2019.12.011

30. Enescu, D. Thermoelectric Energy Harvesting: Basic Principles and Applications. in *Green Energy Advances* (IntechOpen, 2019). doi:10.5772/intechopen.83495

31. Rafiee, M., Siadatan, A., Afjei, E. & Abadi, E. Z. A. Improving the efficiency of thermal power plant using thermoelectric material. in *ICIAS 2012 - 2012 4th International Conference on Intelligent and Advanced Systems: A Conference of World Engineering, Science and Technology Congress (ESTCON) - Conference Proceedings* **1**, 450–454 (2012).

32. Knox, A. R., Buckle, J., Siviter, J., Montecucco, A. & McCulloch, E. Megawatt-scale application of thermoelectric devices in thermal power plants. *J. Electron. Mater*. **42**, 1807–1813 (2013).

33. Fleurial, J. P. Thermoelectric power generation materials: Technology and application opportunities. *JOM* **61**, 79–85 (2009).

34. Yang, J. & Caillat, T. Thermoelectric materials for space and automotive power generation. *MRS Bull.* **31**, 224–229 (2006).

35. Zheng, X. F., Yan, Y. Y. & Simpson, K. A potential candidate for the sustainable

and reliable domestic energy generation-Thermoelectric cogeneration system. *Appl. Therm. Eng.* **53**, 305–311 (2013).

36. Petsagkourakis, I. *et al.* Thermoelectric materials and applications for energy harvesting power generation. *Sci. Technol. Adv. Mater.* **19**, 836–862 (2018).

37. Tan, G., Ohta, M. & Kanatzidis, M. G. Thermoelectric power generation: From new materials to devices. *Philos. Trans. R. Soc. A Math. Phys. Eng. Sci.* **377**, (2019).

38. Siddique, A. R. M., Mahmud, S. & Heyst, B. Van. A review of the state of the science on wearable thermoelectric power generators (TEGs) and their existing challenges. *Renew. Sustain. Energy Rev.* **73**, 730–744 (2017).

39. He, W., Su, Y., Riffat, S. B., Hou, J. & Ji, J. Parametrical analysis of the design and performance of a solar heat pipe thermoelectric generator unit. *Appl. Energy* **88**, 5083–5089 (2011).

40. Li, G. *et al.* A review of solar photovoltaic-thermoelectric hybrid system for electricity generation. *Energy* **158**, 41–58 (2018).

41. Wang, K., Yuan, B., Ji, G. & Wu, X. A comprehensive review of geothermal energy extraction and utilization in oilfields. *J. Pet. Sci. Eng.* **168**, 465–477 (2018).

42. Wang, H., Jasim, A. & Chen, X. Energy harvesting technologies in roadway and bridge for different applications – A comprehensive review. *Appl. Energy* **212**, 1083–1094 (2018).

43. Du, Y., Xu, J., Paul, B. & Eklund, P. Flexible thermoelectric materials and devices. *Appl. Mater. Today* **12**, 366–388 (2018).

44. Toshima, N. Recent progress of organic and hybrid thermoelectric materials. *Synth. Met.* **225**, 3–21 (2017).

45. Bashir, M. B. A., Mohd Said, S., Sabri, M. F. M., Shnawah, D. A. & Elsheikh, M. H. Recent advances on Mg2Si1-xSnx materials for thermoelectric generation. *Renew. Sustain. Energy Rev.* **37**, 569–584 (2014).

46. Patil, D. S., Arakerimath, R. R. & Walke, P. V. Thermoelectric materials and heat exchangers for power generation – A review. *Renew. Sustain. Energy Rev.* **95**, 1–22 (2018).

47. Rowe, D. M. Thermoelectrics, an environmentally-friendly source of electrical power. *Renew. Energy* **16**, 1251–1256 (1999).

48. Saniya LeBlanc. Thermoelectric generators: Linking material properties and systems engineering for waste heat recovery applications. *Sustain. Mater. Technol.* **1**–**2**, 26–35 (2014).

49. Leblanc, S., Yee, S. K., Scullin, M. L., Dames, C. & Goodson, K. E. Material and manufacturing cost considerations for thermoelectrics. *Renew. Sustain. Energy Rev.* **32**, 313–327 (2014).

50. Sakakibara. Supplier on thermoelectrics. (2019). Available at: http://www001.upp.so-net.ne.jp/Peltier/supplier_en.html. (Accessed: 5th November 2019)

51. Wang, Y., Dai, C. & Wang, S. Theoretical analysis of a thermoelectric generator using exhaust gas of vehicles as heat source. *Appl. Energy* **112**, 1171–1180 (2013).

52. Yadav, G. G., Susoreny, J. A., Zhang, G., Yang, H. & Wu, Y. Nanostructure-based

thermoelectric conversion: An insight into the feasibility and sustainability for large-scale deployment. *Nanoscale* **3**, 3555–3562 (2011).

53. Hatzikraniotis, E., Zorbas, K. T., Samaras, I., Kyratsi, T. & Paraskevopoulos, K. M. Efficiency study of a commercial thermoelectric power generator (TEG) under thermal cycling. *J. Electron. Mater.* **39**, 2112–2116 (2010).

54. Ochi, T. *et al.* Power-generation performance and durability of a skutterudite thermoelectric generator. *J. Electron. Mater.* **43**, 2344–2347 (2014).

55. Tritt, T. M. & Subramanian, M. A. Thermoelectric Materials , Phenomena, and Applications : A Bird's Eye View. *MRS Bull.* **31**, 188–198 (2006).

56. Rull-Bravo, M., Moure, A., Fernández, J. F. & Martín-González, M. Skutterudites as thermoelectric materials: revisited. *RSC Adv.* **5**, 41653–41667 (2015).

57. Kousaalya, A. B. *et al.* Polymer-Derived Silicon Oxycarbide Ceramics as Promising Next-Generation Sustainable Thermoelectrics. *ACS Appl. Mater. Interfaces* **10**, 2236–2241 (2018).

58. Amatya, R. & Ram, R. J. Trend for Thermoelectric Materials and Their Earth Abundance. *J. Electron. Mater.* **41**, 1011–1019 (2012).

59. Jeswani, H. K., Azapagic, A., Schepelmann, P. & Ritthoff, M. Options for broadening and deepening the LCA approaches. *J. Clean. Prod.* **18**, 120–127 (2010).

60. Yu, X., Nongaillard, A., Sekhari, A. & Bouras, A. An environmental burden shifting approach to re-evaluate the environmental impacts of products. in *IFIP Advances in Information and Communication Technology* **467**, 56–65 (Springer

New York LLC, 2016).

61. Hellweg, S. & Milà i Canals, L. Emerging approaches, challenges and opportunities in life cycle assessment. *Science* **344**, 1109–13 (2014).

62. Zhang, X. *et al.* A review on energy, environment and economic assessment in remanufacturing based on life cycle assessment method. *J. Clean. Prod.* **255**, 120160 (2020).

63. Cabeza, L. F., Rincón, L., Vilariño, V., Pérez, G. & Castell, A. Life cycle assessment (LCA) and life cycle energy analysis (LCEA) of buildings and the building sector: A review. *Renew. Sustain. Energy Rev.* **29**, 394–416 (2014).

64. Jolliet, O., Saadé-Sbeih, M., Shaked, S., Jolliet, A. & Crettaz, P. *Environmental Life Cycle Assessment*. **53**, (CRC Press, Taylor & Francis Group, 2016).

65. Rebitzer, G. *et al.* Life cycle assessment Part 1: Framework, goal and scope definition, inventory analysis, and applications. *Environ. Int.* **30**, 701–720 (2004).

66. Mattila, T., Lehtoranta, S., Sokka, L., Melanen, M. & Nissinen, A. Methodological Aspects of Applying Life Cycle Assessment to Industrial Symbioses. *J. Ind. Ecol.* **16**, 51–60 (2012).

67. ISO. ISO 14040:2006 - Environmental management - Life cycle assessment - Principles and framework. (2006). Available at: https://www.iso.org/standard/37456.html. (Accessed: 13th June 2018)

68. ISO. ISO 14044:2006 - Environmental management - Life cycle assessment - Requirements and guidelines. (2006). Available at: https://www.iso.org/standard/38498.html. (Accessed: 13th June 2018)

69. Anastas, P. T. & Zimmerman, J. B. Peer Reviewed: Design Through the 12 Principles of Green Engineering. *Environ. Sci. Technol.* **37**, 94A-101A (2003).

70. Anastas, P. & Eghbali, N. Green chemistry: Principles and practice. *Chem. Soc. Rev.* **39**, 301–312 (2010).

71. Nosonovsky, M. & Bhushan, B. Green tribology: Principles, research areas and challenges. *Philos. Trans. R. Soc. A Math. Phys. Eng. Sci.* **368**, 4677–4694 (2010).

72. Arbabzadeh, M., Johnson, J. X., Keoleian, G. A., Rasmussen, P. G. & Thompson, L. T. Twelve Principles for Green Energy Storage in Grid Applications. *Environ. Sci. Technol.* **50**, 1046–1055 (2016).

73. Arbabzadeh, M., Lewis, G. M. & Keoleian, G. A. Green principles for responsible battery management in mobile applications. *J. Energy Storage* **24**, 100779 (2019).

74. Prasad, S. *et al.* Sustainable utilization of crop residues for energy generation: A life cycle assessment (LCA) perspective. *Bioresour. Technol.* **303**, 122964 (2020).

75. Liu, H., Huang, Y., Yuan, H., Yin, X. & Wu, C. Life cycle assessment of biofuels in China: Status and challenges. *Renew. Sustain. Energy Rev.* **97**, 301–322 (2018).

76. Paredes, M., Padilla-Rivera, A. & Güereca, L. Life Cycle Assessment of Ocean Energy Technologies: A Systematic Review. *J. Mar. Sci. Eng.* **7**, 322 (2019).

77. Singlitico, A., Goggins, J. & Monaghan, R. F. D. The role of life cycle assessment in the sustainable transition to a decarbonised gas network through green gas production. *Renew. Sustain. Energy Rev.* **99**, 16–28 (2019).

78. Lijó, L. *et al.* Life Cycle Assessment of Renewable Energy Production from Biomass. in *Green Energy and Technology* 81–98 (Springer Verlag, 2019).

doi:10.1007/978-3-319-93740-3_6

79. Unterreiner, L., Jülch, V. & Reith, S. Recycling of Battery Technologies - Ecological Impact Analysis Using Life Cycle Assessment (LCA). in *Energy Procedia* **99**, 229–234 (Elsevier Ltd, 2016).

80. Nienborg, B. *et al.* Life cycle assessment of thermal energy storage materials and components. in *Energy Procedia* **155**, 111–120 (Elsevier Ltd, 2018).

81. Guney, M. S. & Tepe, Y. Classification and assessment of energy storage systems. *Renew. Sustain. Energy Rev.* **75**, 1187–1197 (2017).

82. Peng, J., Lu, L. & Yang, H. Review on life cycle assessment of energy payback and greenhouse gas emission of solar photovoltaic systems. *Renew. Sustain. Energy Rev.* **19**, 255–274 (2013).

83. Amponsah, N. Y., Troldborg, M., Kington, B., Aalders, I. & Hough, R. L. Greenhouse gas emissions from renewable energy sources: A review of lifecycle considerations. *Renew. Sustain. Energy Rev.* **39**, 461–475 (2014).

84. Ludin, N. A. *et al.* Prospects of life cycle assessment of renewable energy from solar photovoltaic technologies: A review. *Renew. Sustain. Energy Rev.* **96**, 11–28 (2018).

85. Longo, S. *et al.* Life Cycle Assessment of Solid Oxide Fuel Cells and Polymer Electrolyte Membrane Fuel Cells: A Review. in *Hydrogen Economy: Supply Chain, Life Cycle Analysis and Energy Transition for Sustainability* 139–169 (Elsevier Inc., 2017). doi:10.1016/B978-0-12-811132-1.00006-7

86. Zhou, Z., Tang, Y., Chi, Y., Ni, M. & Buekens, A. Waste-to-energy: A review of

life cycle assessment and its extension methods. *Waste Manag. Res.* **36**, 3–16 (2018).

87. Sherwani, A. F., Usmani, J. A. & Varun. Life cycle assessment of solar PV based electricity generation systems: A review. *Renew. Sustain. Energy Rev.* **14**, 540–544 (2010).

88. Asdrubali, F., Baldinelli, G., D'Alessandro, F. & Scrucca, F. Life cycle assessment of electricity production from renewable energies: Review and results harmonization. *Renew. Sustain. Energy Rev.* **42**, 1113–1122 (2015).

89. Astrup, T. F., Tonini, D., Turconi, R. & Boldrin, A. Life cycle assessment of thermal Waste-to-Energy technologies: Review and recommendations. *Waste Manag.* **37**, 104–115 (2015).

90. Turconi, R., Boldrin, A. & Astrup, T. Life cycle assessment (LCA) of electricity generation technologies: Overview, comparability and limitations. *Renew. Sustain. Energy Rev.* **28**, 555–565 (2013).

91. Varun, Bhat, I. K. & Prakash, R. LCA of renewable energy for electricity generation systems-A review. *Renew. Sustain. Energy Rev.* **13**, 1067–1073 (2009).

92. Dunn, J. B., Gaines, L., Kelly, J. C., James, C. & Gallagher, K. G. The significance of Li-ion batteries in electric vehicle life-cycle energy and emissions and recycling's role in its reduction. *Energy Environ. Sci.* **8**, 158–168 (2015).

93. Dunn, J. B. *et al. Material and Energy Flows in the Production of Cathode and Anode Materials for Lithium Ion Batteries.* (2015).

94. Gaines, L. The future of automotive lithium-ion battery recycling: Charting a

sustainable course. *Sustain. Mater. Technol.* **1**, 2–7 (2014).

95. Ghojel, J. I. Thermal and Environmental Assessment of a Conceptual Waste Heat Recovery System for Automotive Application. in *DS 35: Proceedings ICED 05, the 15th International Conference on Engineering Design, Melbourne, Australia, 15.-18.08.2005* (eds. Samuel, A. & Lewis, W.) DS35_31.61 (The Design Society, 2005).

96. Kishita, Y. *et al.* Evaluating the life cycle CO2 emissions and costs of thermoelectric generators for passenger automobiles: a scenario analysis. *J. Clean. Prod.* **126**, 607–619 (2016).

97. Patyk, A. Thermoelectrics: Impacts on the environment and sustainability. *J. Electron. Mater.* **39**, 2023–2028 (2010).

98. Patyk, A. Thermoelectric generators for efficiency improvement of power generation by motor generators – Environmental and economic perspectives. *Appl. Energy* **102**, 1448–1457 (2013).

99. Sergienko, O. I. *et al.* Environmental aspects of thermoelectric cooling. *J. Thermoelectr.* **4**, 5–10 (2010).

100. Bailey, L. G. G. Preparation and properties of silicon telluride. *J. Phys. Chem. Solids* **27**, 1593–1598 (1966).

101. Jawahir, I. S. & Bradley, R. Technological Elements of Circular Economy and the Principles of 6R-Based Closed-loop Material Flow in Sustainable Manufacturing. in *Procedia CIRP* **40**, 103–108 (Elsevier B.V., 2016).

102. Anastas, P. T. & Warner, J. C. *Green Chemistry: Theory and Practice*. (Oxford

University Press, 1998).

103. Kumar, S., Heister, S. D., Xu, X., Salvador, J. R. & Meisner, G. P. Thermoelectric Generators for Automotive Waste Heat Recovery Systems Part I: Numerical Modeling and Baseline Model Analysis. *J. Electron. Mater.* **42**, 665–674 (2013).

104. Kumar, S., Heister, S. D., Xu, X., Salvador, J. R. & Meisner, G. P. Thermoelectric Generators for Automotive Waste Heat Recovery Systems Part II: Parametric Evaluation and Topological Studies. *J. Electron. Mater.* **42**, 944–955 (2013).

105. II-VI Marlow. Technical Data Sheet for TG12-8 Single-Stage Thermoelectric Generator . (2019). Available at: www.marlow.com. (Accessed: 31st October 2019)

106. KELK. KELK Ltd. - High Performance Type/Multi Purpose Type. *Komatsu* (2019). Available at: https://www.kelk.co.jp/english/products/data_1.html#data_1_2. (Accessed: 12th October 2019)

107. Qin, Y. T. *et al.* High-performance bulk thermoelectric materials and devices. *Sci. Found. China* **24**, 67–80 (2016).

108. Zhang, Y. *et al.* High-temperature and high-power-density nanostructured thermoelectric generator for automotive waste heat recovery. *Energy Convers. Manag.* **105**, 946–950 (2015).

109. Joshi, G. R., Lan, Y., Ren, Z., Lan, Y. & Ren, Z. Half-Heusler Modules. in *Advanced Thermoelectrics* (eds. Ren, Z., Lan, Y. & Zhang, Q.) 683–696 (CRC Press, 2017). doi:10.1201/9781315153766-19

110. Mottainai Energy. Mottainai Energy Co., Ltd. (2018). Available at: http://mottainai-energy.com/. (Accessed: 6th November 2019)

111. Hu, X. *et al.* Power generation from nanostructured PbTe-based thermoelectrics: comprehensive development from materials to modules. *Energy Environ. Sci.* **9**, 517–529 (2016).

112. Kaibe, H. T. *et al.* Development of Thermoelectric Generating Cascading Modules using Silicide and Bi-Te. in (2004).

113. Aoyama, I. *et al.* Doping Effects on Thermoelectric Properties of Higher Manganese Silicides (HMSs, MnSi1.74) and Characterization of Thermoelectric Generating Module using p -Type (Al, Ge and Mo)-doped HMSs and n -Type Mg2Si0.4. *Jpn. J. Appl. Phys.* **44**, 4275–4281 (2005).

114. Kuroki, T. *et al.* Thermoelectric generation using waste heat in steel works. *J. Electron. Mater.* **43**, 2405–2410 (2014).

115. Salvador, J. R. *et al.* Conversion efficiency of skutterudite-based thermoelectric modules. *Phys. Chem. Chem. Phys.* **16**, 12510–12520 (2014).

116. Park, W., Barako, M. T., Marconnet, A. M., Asheghi, M. & Goodson, K. E. Effect of thermal cycling on commercial thermoelectric modules. in *InterSociety Conference on Thermal and Thermomechanical Phenomena in Electronic Systems, ITHERM* 107–112 (2012). doi:10.1109/ITHERM.2012.6231420

117. Gao, Y. *et al.* Nanostructured interfaces for thermoelectrics. *J. Electron. Mater.* **39**, 1456–1462 (2010).

118. Vizel, R., Bargig, T., Beeri, O. & Gelbstein, Y. Bonding of Bi2Te3-Based

Thermoelectric Legs to Metallic Contacts Using Bi0.82Sb0.18 Alloy. *J. Electron. Mater.* **45**, 1296–1300 (2016).

119. Kajihara, T., Fukuda, K., Sato, Y. & Kikuchi, M. Improvement of crystal orientation and thermoelectric properties for hot pressed n- and p-type Bi/sub 2/Te/sub 3/ compounds. in *Seventeenth International Conference on Thermoelectrics. Proceedings ICT98 (Cat. No.98TH8365)* 129–133 (IEEE, 1998). doi:10.1109/ICT.1998.740334

120. Rogl, G., Grytsiv, A., Bauer, E., Rogl, P. & Zehetbauer, M. Thermoelectric properties of novel skutterudites with didymium: DDy(Fe1−xCox)4Sb12 and DDy(Fe1−xNix)4Sb12. *Intermetallics* **18**, 57–64 (2010).

121. Shi, X. *et al.* Multiple-Filled Skutterudites: High Thermoelectric Figure of Merit through Separately Optimizing Electrical and Thermal Transports. *J. Am. Chem. Soc.* **133**, 7837–7846 (2011).

122. Tang, X., Chen, L., Goto, T. & Hirai, T. Effects of Ce filling fraction and Fe content on the thermoelectric properties of Co-rich $Ce_y Fe_x Co_{4-x} Sb_{12}$. *J. Mater. Res.* **16**, 837–843 (2001).

123. Bao, X. *et al.* Protective Properties of Electrochemically Deposited Al-Based Coatings on Yb0.3Co4Sb12 Skutterudite. *J. Electron. Mater.* **48**, 5523–5531 (2019).

124. Yan, X. *et al.* Stronger phonon scattering by larger differences in atomic mass and size in p-type half-Heuslers Hf1−xTixCoSb0.8Sn0.2. *Energy Environ. Sci.* **5**, 7543 (2012).

125. Joshi, G. *et al.* Enhancement of thermoelectric figure-of-merit at low temperatures by titanium substitution for hafnium in n-type half-Heuslers Hf0.75−xTixZr0.25NiSn0.99Sb0.01. *Nano Energy* **2**, 82–87 (2013).

126. Weera, S. L. L. Analytical Performance Evaluation of Thermoelectric Modules Using Effective Material Properties. (Western Michigan University, 2014).

127. Kaibe, H. T. *et al.* Development of thermoelectric generating cascade modules using silicide and Bi-Te. in *Proceedings of the 23rd International Conference on Thermoelectrics, ICT 2004* (ed. GoI, O.) (2004).

128. Industrial Process Heat Engineering Ltd. About - Inproheat. (2017). Available at: http://inproheat.com/about. (Accessed: 11th September 2017)

129. Inproheat Inc. Properties - Min-K Moldable. (2017). Available at: http://inproheat.com/sites/files/documents/Min-K_ Moldable.pdf. (Accessed: 11th September 2017)

130. Krez, J. *et al.* Long-term stability of phase-separated half-Heusler compounds. *Phys. Chem. Chem. Phys.* **17**, 29854–29858 (2015).

131. EIA. Natural gas generators make up the largest share of overall U.S. generation capacity . (2017). Available at: https://www.eia.gov/todayinenergy/detail.php?id=30872#tab2. (Accessed: 24th December 2019)

132. EIA. New U.S. power plants expected to be mostly natural gas combined-cycle and solar PV . (2019). Available at: https://www.eia.gov/todayinenergy/detail.php?id=38612. (Accessed: 24th

December 2019)

133. Spath, P. L. & Mann, M. K. *Life Cycle Assessment of a Natural Gas Combined Cycle Power Generation System*. (2000).

134. Raimi, D. *Decommissioning US Power Plants Decisions, Costs, and Key Issues Decommissioning US Power Plants: Decisions, Costs, and Key Issues*. (2017).

135. Duranceau, C. M. & Sawyer-Beaulieu, S. Vehicle recycling, reuse, and recovery: Material disposition from current end-of-life vehicles. in *SAE 2011 World Congress and Exhibition* (2011). doi:10.4271/2011-01-1151

136. Washington Mills. Washington Mills Recycling Services . (2019).

137. Ecoinvent. The Ecoinvent Database. *Ecoinvent* (2017). Available at: http://www.ecoinvent.org/database/database.html. (Accessed: 30th November 2017)

138. Papanikolaou, N., Maliaris, G., Loupis, M., Kyritsis, A. & Nikolaidis, V. Combination of building applied PV panels with thermoelectric generation and geothermal cooling. in *IET Conference Publications* **2014**, (Institution of Engineering and Technology, 2014).

139. PSI. HERMIGA 100/10 VI ATOMISER SIDEBAR TITLE. *Phoenix Scientific Industries* (2019). Available at: www.psiltd.co.uk. (Accessed: 22nd March 2020)

140. Kumar, S., Heister, S. D., Xu, X., Salvador, J. R. & Meisner, G. P. Thermal design of thermoelectric generators for automobile waste heat recovery. in *ASME 2012 Heat Transfer Summer Conf. Collocated with the ASME 2012 Fluids Engineering Div. Summer Meeting and the ASME 2012 10th Int. Conf. on Nanochannels,*

Microchannels and Minichannels, HT 2012 **1**, 67–77 (2012).

141. Tritt, T. M. Thermoelectric Phenomena, Materials, and Applications. *Annu. Rev. Mater. Res.* **41**, 433–448 (2011).

142. Huijbregts, M. A. J. *et al. ReCiPe 2016: A harmonized life cycle impact assessment method at midpoint and endpoint level - Report 1: Characterization*. *RIVM Report 2016-0104* (2016).

143. Classen, M. *et al. Life Cycle Inventories of Metals*. *Final report ecoinvent data v2.1, No. 10* (2009).

144. USGS. *Reserves & Production of Various Elements*. *USGS Mineral Resources Program* (2018). doi:10.3133/fs20143077

145. Ayres, R. U., Ayres, L. W. & Råde, I. *The Life Cycle of Copper, its Co-Products and By-Products*. (2002).

146. Kossoff, D. *et al.* Mine tailings dams: Characteristics, failure, environmental impacts, and remediation. *Appl. Geochemistry* **51**, 229–245 (2014).

147. Hong, J. *et al.* Life cycle assessment of copper production: a case study in China. *Int. J. Life Cycle Assess.* **23**, 1814–1824 (2017).

148. Beylot, A. & Villeneuve, J. Accounting for the environmental impacts of sulfidic tailings storage in the Life Cycle Assessment of copper production: A case study. *J. Clean. Prod.* **153**, 139–145 (2017).

149. Spath, P. L., Mann, M. K., Kerr, D. R., Marano, J. & Ramezan, M. *Life Cycle Assessment of Coal-fired Power Production*. (1999). doi:10.2172/12100

150. Atilgan, B. & Azapagic, A. Life cycle environmental impacts of electricity from

fossil fuels in Turkey. *J. Clean. Prod.* **106**, 555–564 (2015).

151. Atilgan, B., Azapagic, A., Atilgan, B. & Azapagic, A. Assessing the Environmental Sustainability of Electricity Generation in Turkey on a Life Cycle Basis. *Energies* **9**, 31 (2016).

152. Stamford, L. & Azapagic, A. Life cycle sustainability assessment of electricity options for the UK. *Int. J. Energy Res.* **36**, 1263–1290 (2012).

153. Molinaire, J. C. Sustainability analysis of copper extraction and processing using LCA methods. (Imperial College London, 2015).

154. Günkaya, Z., Özdemir, A., Özkan, A. & Banar, M. Environmental Performance of Electricity Generation Based on Resources: A Life Cycle Assessment Case Study in Turkey. *Sustainability* **8**, 1097 (2016).

155. Vieira, M. & Huijbregts, M. A. J. Mineral Resource Scarcity. in *LC-Impact Version 0.5: A spatially differentiated life cycle impact assessment approach* (eds. Verones, F. et al.) 136–142 (LC-Impact, 2016).

156. Nuss, P., Eckelman, M. J., Yamaguchi, H., Inaba, A. & Friedlander, E. Life Cycle Assessment of Metals: A Scientific Synthesis. *PLoS One* **9**, e101298 (2014).

157. Harper, E. M. *et al.* Criticality of the Geological Zinc, Tin, and Lead Family. *J. Ind. Ecol.* **19**, 628–644 (2015).

158. Iyer, R. K. & Pilla, S. Environmental profile of thermoelectrics for applications with continuous waste heat generation via life-cycle assessment. *Unpubl. results*

159. Bartholomé, K. *et al.* Thermoelectric Modules Based on Half-Heusler Materials Produced in Large Quantities. *J. Electron. Mater.* **43**, 1775–1781 (2014).

160. Brož, P. *et al.* Study of thermal stability of CoSb 3 skutterudite by Knudsen effusion mass spectrometry. *Calphad Comput. Coupling Phase Diagrams Thermochem.* **65**, 1–7 (2019).

161. Park, K. H. *et al.* High-temperature stability of thermoelectric skutterudite In 0.25Co 3FeSb 12. *J. Electron. Mater.* **41**, 1051–1056 (2012).

162. Hertwich, E. G. *et al.* Integrated life-cycle assessment of electricity-supply scenarios confirms global environmental benefit of low-carbon technologies. *Proc. Natl. Acad. Sci. U. S. A.* **112**, 6277–6282 (2015).

163. Lattanzio, R. K. *Life-Cycle Greenhouse Gas Assessment of Coal and Natural Gas in the Power Sector*. (2015).

164. Andrae, A. S. G., Itsubo, N., Yamaguchi, H. & Inaba, A. Life Cycle Assessment of Japanese High-Temperature Conductive Adhesives. *Environ. Sci. Technol.* **42**, 3084–3089 (2008).

165. Naumov, A. V. Selenium and tellurium: state of the markets, the crisis, and its consequences. *Metallurgist* **54**, 197–200 (2010).

166. USGS. *Tellurium*. (2018).

167. Koplow, M., Chen, A., Steingart, D., Wright, P. K. & Evans, J. W. Thick film thermoelectric energy harvesting systems for biomedical applications. in *Proc. 5th Int. Workshop on Wearable and Implantable Body Sensor Networks, BSN2008, in conjunction with the 5th Int. Summer School and Symp. on Medical Devices and Biosensors, ISSS-MDBS 2008* 322–325 (2008). doi:10.1109/ISSMDBS.2008.4575084

168. Hojas Baenas, J. M., De Castro, R., Gomes Battistelle, R. A. & Gobbo Junior, J. A. A study of reverse logistics flow management in vehicle battery industries in the midwest of the state of São Paulo (Brazil). *J. Clean. Prod.* **19**, 168–172 (2011).

169. Zhang, Q., Sun, Y., Xu, W. & Zhu, D. Organic Thermoelectric Materials: Emerging Green Energy Materials Converting Heat to Electricity Directly and Efficiently. *Adv. Mater.* **26**, 6829–6851 (2014).

170. Ge, Z. H. *et al*. Low-cost, abundant binary sulfides as promising thermoelectric materials. *Mater. Today* **19**, 227–239 (2016).

171. Van Der Kuijp, T. J., Huang, L. & Cherry, C. R. Health hazards of China's lead-acid battery industry: A review of its market drivers, production processes, and health impacts. *Environ. Heal. A Glob. Access Sci. Source* **12**, 61 (2013).

172. OSHA. Permissible Exposure Limits. (2018). Available at: https://www.osha.gov/dsg/annotated-pels/tablez-1.html#niosh_rel. (Accessed: 15th March 2020)

173. Cooper, W. C. Toxicology of selenium and tellurium and their compounds. *Arch. Environ. Health* **3**, 189–200 (1961).

174. Yang, J.-H. H., Yuan, Q., Deng, H., Wei, S.-H. H. & Yakobson, B. I. Earth-Abundant and Non-Toxic SiX (X = S, Se) Monolayers as Highly Efficient Thermoelectric Materials. *J. Phys. Chem. C* **121**, 123–128 (2017).

175. Yang, H., Jauregui, L. A., Zhang, G., Chen, Y. P. & Wu, Y. Nontoxic and abundant copper zinc tin sulfide nanocrystals for potential high-temperature thermoelectric energy harvesting. *Nano Lett.* **12**, 540–545 (2012).

176. Wei, T. R., Wu, C. F., Li, F. & Li, J. F. Low-cost and environmentally benign selenides as promising thermoelectric materials. *J. Mater.* **4**, 304–320 (2018).

177. Tang, Y. Q., Ge, Z. H. & Feng, J. Synthesis and Thermoelectric Properties of Copper Sulfides via Solution Phase Methods and Spark Plasma Sintering. *Crystals* **7**, 141 (2017).

178. Kirsanova, M. A., Reshetova, L. N., Olenev, A. V., Abakumov, A. M. & Shevelkov, A. V. Semiclathrates of the Ge-P-Te system: Synthesis and crystal structures. *Chem. - A Eur. J.* **17**, 5719–5726 (2011).

179. Kishlmoto, K., Koyanagi, T., Akai, K. & Matsuura, M. Synthesis and thermoelectric properties of type-I clathrate compounds Si46-xPxTe8. *Japanese J. Appl. Physics, Part 2 Lett.* **46**, L746 (2007).

180. Wang, H. *et al.* Beneficial Effect of S-Filling on Thermoelectric Properties of SxCo4Sb11.2Te0.8 Skutterudite. *J. Electron. Mater.* **47**, 3061–3066 (2018).

181. Fitriani *et al.* A review on nanostructures of high-temperature thermoelectric materials for waste heat recovery. *Renew. Sustain. Energy Rev.* **64**, 635–659 (2016).

182. Chen, Z. G., Hana, G., Yanga, L., Cheng, L. & Zou, J. Nanostructured thermoelectric materials: Current research and future challenge. *Prog. Nat. Sci. Mater. Int.* **22**, 535–549 (2012).

183. Iyer, R. K. & Pilla, S. Environmental profile of thermoelectrics for stationary applications with periodic waste heat generation via life-cycle assessment. *Unpubl. results*

184. Iyer, R. K., Kousaalya, A. B. & Pilla, S. Environmental life cycle assessment of thermoelectrics for automotive applications. *Unpubl. results*

185. Wang, H. & Yu, C. Organic Thermoelectrics: Materials Preparation, Performance Optimization, and Device Integration. *Joule* **3**, 53–80 (2019).

186. Saleemi, M. *et al.* Spark plasma sintering and thermoelectric evaluation of nanocrystalline magnesium silicide (Mg2Si). *J. Mater. Sci.* **48**, 1940–1946 (2013).

187. Katsuyama, S., Matsuo, R. & Ito, M. Thermoelectric properties of half-Heusler alloys Zr1-xYxNiSn1-ySby. *J. Alloys Compd.* **428**, 262–267 (2007).

188. Hooshmand Zaferani, S., Ghomashchi, R. & Vashaee, D. Strategies for engineering phonon transport in Heusler thermoelectric compounds. *Renew. Sustain. Energy Rev.* **112**, 158–169 (2019).

189. Singh, V., Pulikkotil, J. J. & Auluck, S. Mg9Si5: A potential non-toxic thermoelectric material for mid-temperature applications. *RSC Adv.* **6**, 62445–62450 (2016).

190. USGS. Minerals Yearbook - Metals and Minerals. *Minerals Yearbook - Volume I: Metals & Minerals* (2020). Available at: https://www.usgs.gov/centers/nmic/minerals-yearbook-metals-and-minerals. (Accessed: 28th April 2020)

191. Shedd, K. B., McCullough, E. A. & Bleiwas, D. L. Global trends affecting the supply security of cobalt. *Mining Engineering* 37–42 (2017).

192. US DoE. *Critical Materials Strategy*. (2011).

193. Graedel, T. E. *et al.* Criticality of metals and metalloids. *Proc. Natl. Acad. Sci. U.*

S. A. **112**, 4257–4262 (2015).

194. Basol, B. M. & McCandless, B. Brief review of cadmium telluride-based photovoltaic technologies. *J. Photonics Energy* **4**, 040996 (2014).

195. Lee, T. D. & Ebong, A. U. A review of thin film solar cell technologies and challenges. *Renew. Sustain. Energy Rev.* **70**, 1286–1297 (2017).

196. IEA. Data & Statistics - IEA. (2019). Available at: https://www.iea.org/data-and-statistics/?country=WORLD&fuel=Energy supply&indicator=Total primary energy supply (TPES) by source. (Accessed: 16th March 2020)

197. Gonzalez-Salazar, M. A., Kirsten, T. & Prchlik, L. Review of the operational flexibility and emissions of gas- and coal-fired power plants in a future with growing renewables. *Renew. Sustain. Energy Rev.* **82**, 1497–1513 (2018).

198. Stram, B. N. Key challenges to expanding renewable energy. *Energy Policy* **96**, 728–734 (2016).

199. Posada, J. O. G., Rivera, I., Berrio, J. G. R. & Hall, P. J. Towards the Development of Commercially Viable Grid Connected Batteries. in *10th International Conference on Sustainable Energy and Environmental Protection* (eds. Krope, J., Olabi, A. G., Goričanec, D. & Božičnik, S.) 23–34 (University of Maribor Press, 2017). doi:10.18690/978-961-286-064-6.11

200. Skomedal, G., Kristiansen, N. R., Sottong, R. & Middleton, H. Evaluation of Thermoelectric Performance and Durability of Functionalized Skutterudite Legs. *J. Electron. Mater.* **46**, 2438–2450 (2017).

201. Zhang, H., LeBlanc, S., Wang, S., Yang, J. & Taylor, P. Selective laser melting of

half-Heusler thermoelectric materials. in *Energy Harvesting and Storage: Materials, Devices, and Applications VIII* (eds. Dhar, N. K., Dutta, A. K. & Balaya, P.) **10663**, 12 (SPIE, 2018).

202. Carter, M. J., El-Desouky, A., Andre, M. A., Bardet, P. & LeBlanc, S. Pulsed laser melting of bismuth telluride thermoelectric materials. *J. Manuf. Process.* **43**, 35–46 (2019).

203. Gu, D. D., Meiners, W., Wissenbach, K. & Poprawe, R. Laser additive manufacturing of metallic components: materials, processes and mechanisms. *Int. Mater. Rev.* **57**, 133–164 (2012).

204. Sreenivasan, R. & Bourell, D. L. Sustainability Study in Selective Laser Sintering - An Energy Perspective. in *Proceedings of the Minerals, Metals and Materials Society/AIME* (2010).

205. Tele, C. & Seepersad, C. C. A Comparative Evaluation of Energy Consumption of Selective Laser Sintering and Injection Molding of Nylon Parts. in *Proceedings of the 22nd Annual International Solid Freeform Fabrication Symposium* 41–54 (1997).

206. Wang, P. *et al.* Lifetime prediction of thermoelectric devices under thermal cycling. *J. Power Sources* **437**, 226861 (2019).

207. Tarantik, K. R. *et al.* Thermoelectric Modules Based on Silicides - Development and Characterization. in *Materials Today: Proceedings* **2**, 588–595 (Elsevier Ltd, 2015).

208. Xing, Y. *et al.* High-efficiency half-Heusler thermoelectric modules enabled by

self-propagating synthesis and topologic structure optimization. *Energy Environ. Sci.* **12**, 3390–3399 (2019).

209. Barako, M. T., Park, W., Marconnet, A. M., Asheghi, M. & Goodson, K. E. A reliability study with infrared imaging of thermoelectric modules under thermal cycling. in *InterSociety Conference on Thermal and Thermomechanical Phenomena in Electronic Systems, ITHERM* 86–92 (2012). doi:10.1109/ITHERM.2012.6231417

210. Biswas, K., Subramanian, M. A., Good, M. S., Roberts, K. C. & Hendricks, T. J. Thermal cycling effects on the thermoelectric properties of n-type in,ce-based skutterudite compounds. *J. Electron. Mater.* **41**, 1615–1621 (2012).

211. Jaques, B., Zhang, Y. & Agarwal, V. *NanoStructured bulk thermoelectric generator for efficient power harvesting for self-powered sensor network.* (2018). doi:10.2172/1478227

212. Rausch, E., Balke, B., Ouardi, S. & Felser, C. Long-Term Stability of (Ti/Zr/Hf)CoSb $_{1-x}$ Sn $_{x}$ Thermoelectric p-Type Half-Heusler Compounds Upon Thermal Cycling. *Energy Technol.* **3**, 1217–1224 (2015).

213. Joshi, G. *et al.* NbFeSb-based p-type half-Heuslers for power generation applications. *Energy Environ. Sci.* **7**, 4070–4076 (2014).

214. Skomedal, G. *et al.* Design, assembly and characterization of silicide-based thermoelectric modules. *Energy Convers. Manag.* **110**, 13–21 (2016).

215. Volkov, M. P., Drabkin, I. A., Ershova, L. B. & Nazarenko, A. A. Miniature Thermoelectric Modules Developed for Cycling Applications. *Semiconductors* **53**,

599–602 (2019).

216. Fritsch. Planetary Mill Pulverisette 5/4. (2019). Available at: https://www.fritsch-international.com/sample-preparation/milling/planetary-mills/details/product/pulverisette-54-classic-line/technical-details/. (Accessed: 9th November 2019)

217. Lindberg/MPH. Lindberg/MPH Electric Box Furnaces. (2017). Available at: www.lindbergmph.com. (Accessed: 9th November 2019)

218. FCT Systeme GmbH. Spark plasma sintering furnace for field assisted sintering technique - FAST. (2017). Available at: http://www.fct-systeme.de/en/content/Spark_Plasma_Sinteranlage_Typ_HPD_HHPD/~nm.12~nc.32/Spark-Plasma-Sinteranlage-Typ-HP-D--HHP-D.html. (Accessed: 9th November 2019)

219. Quintus. Brochure - Quintus® Compact HIP Systems . (2019). Available at: https://quintustechnologies.com/knowledge-center/brochure-quintus-compact-hip-systems/. (Accessed: 9th November 2019)

220. Linn High Therm. IT-KTV-65/100/1650. (2019). Available at: https://www.linn-high-therm.de/products/induction-heating/laboratory-units/details/it-ktv-65-100-1650.html. (Accessed: 22nd March 2020)

221. Arcast. Arc 200 Cold Crucible Arc Melting Furnace. Available at: http://www.arcastinc.com/arc200.htm. (Accessed: 22nd March 2020)

222. Pace Technologies. NANO 1200 T Manual Polisher. (2019).

223. MTI. Precision CNC Dicing / Cutting Saw with Accessories & Laptop and

Software - SYJ-400. (2020). Available at: https://www.mtixtl.com/diamondsaw-SYJ-400.aspx. (Accessed: 18th March 2020)

224. US EPA. All EPA Emission Standards. (2020). Available at: https://www.epa.gov/emission-standards-reference-guide/all-epa-emission-standards. (Accessed: 6th February 2020)

225. Dieselnet. Emission Test Cycles. Available at: https://dieselnet.com/standards/cycles/index.php. (Accessed: 6th February 2020)

226. US EPA. 2017 Ratings Changes. (2020). Available at: https://www.fueleconomy.gov/feg/ratings.shtml. (Accessed: 6th February 2020)

227. US EPA. *Vehicle-specific 5-cycle fuel economy and carbon-related exhaust emission calculations*. 897–909 (2011).

228. US EPA. Derived 5-cycle coefficients for 2017 and later model years. (2015). Available at: https://iaspub.epa.gov/otaqpub/display_file.jsp?docid=35113&flag=1. (Accessed: 27th August 2019)

229. 2020 Chevy Suburban | Large SUV | 7, 8, or 9 Seat Options. *GM* (2019). Available at: https://www.chevrolet.com/suvs/suburban. (Accessed: 27th August 2019)

230. 2017 Chevrolet Suburban Dimensions. Available at: https://autotk.com/dimensions/chevrolet/suburban/2017/. (Accessed: 6th February 2020)

231. Engineering Toolbox. Air - Density at varying pressure and constant temperatures. (2004). Available at: https://www.engineeringtoolbox.com/air-temperature-

pressure-density-d_771.html. (Accessed: 6th February 2020)

232. Rolling Resistance. Available at: https://www.engineeringtoolbox.com/rolling-friction-resistance-d_1303.html. (Accessed: 6th February 2020)

233. Duralast Voltage Regulator VR781. Available at: https://www.autozone.com/batteries-starting-and-charging/voltage-regulator/duralast-voltage-regulator-vr781/31196_0_0. (Accessed: 6th February 2020)

234. U.S. DoE. Where the Energy Goes: Gasoline Vehicles. *US Department of Energy* (2010). Available at: https://www.fueleconomy.gov/feg/atv.shtml. (Accessed: 12th November 2016)

235. Menon, G. How many squares of size a×a can be packed into a circle of radius R? . *Quora* (2017). Available at: https://www.quora.com/How-many-squares-of-size-a×a-can-be-packed-into-a-circle-of-radius-R. (Accessed: 18th March 2020)

236. OSHA. Permissible Exposure Limits - Annotated Tables. (2017). Available at: https://www.osha.gov/dsg/annotated-pels/. (Accessed: 28th April 2020)